Cross Ventilation Using Wind Towers: How the position of a roof-top wind tower affects its ventilation effectiveness


Doctoral Dissertation
Doctoral Program in Production, Management, Design (32nd Cycle)

# Cross ventilation using wind towers

## How the position of a rooftop wind tower affects its ventilation effectiveness

**Mehrnoosh Ahmadi**
* * * * * *

**Supervisors**
Prof. Marco Simonetti, Supervisor
Prof. Mario Grosso, Co-Supervisor

**Doctoral Examination Committee:**
Prof. Ben Richard Hughes, Referee, University of Strathclyde
Prof. Guadalupe Huelsz Lesbros, Referee, National Autonomous University of Mexico
Prof. Abbas Elmualim, Referee, University of Sharjah
Prof. Ted Stathopoulos, Referee, Concordia University
Prof. Almerindo Ferreira, Referee, University of Coimbra

Politecnico di Torino
January 31, 2020

I hereby declare that, the contents and organisation of this dissertation constitute my own original work and does not compromise in any way the rights of third parties, including those relating to the security of personal data.

…….....

Mehrnoosh Ahmadi

Turin, January 31, 2020

# Abstract

During the 21st century, with the growing environmental concerns, the research on different innovative building systems has become of major significance as it can accelerate the transition toward sustainable building design. For this reason, natural ventilation solutions including the wind tower technology have been more and more contemplated as potential alternatives to the more energy-intensive air-conditioning systems.

In spite of the effectiveness of wind towers in providing an acceptable indoor air quality and cooling previously verified by several scholars and despite its satisfactory performance in providing natural ventilation in the handful of buildings utilizing this technology, its uptake in the sustainable building industry is rather slow. This hesitance on the one hand could be due to design issues related to the integration of this component in the architecture of mainly high-rise buildings and on the other hand highlights the necessity of proposing a clear architect-friendly guideline addressing seemingly basic questions regarding the wind towers such as: where to place it, what type of wind tower to choose, what advantage it has compared to a window, whether it is applicable in multi-zone spaces, etc.

This thesis aims to address some of these questions. For that, Computational Fluid Dynamics code ANSYS Fluent 18.0 has been employed. Verified and validated using pre-existing wind tunnel data, several steady-state RANS simulations have been done to predict cross-ventilation using a wind tower. The three-dimensional coupled simulations have been performed using realizable k-ε turbulence model in an isothermal condition and with an atmospheric boundary layer wind profile. In order to evaluate the cross-ventilation performance of wind towers, a one-sided and a four-sided rooftop wind tower have been joint each with a room window. Cross-ventilation using two windows, has been compared with cross-ventilation using a wind tower-window combination. The performance of four-sided wind towers in presence and absence of a window has been assessed. The effect of different rooftop positions of the wind towers on cross-ventilation at various wind incident angles has been determined. And, finally, the effect of

different placements of a room partition in cross-ventilation by a one-sided wind tower has been assessed.

The results of this thesis not only provide a knowledge about the airflow through wind towers and link some of the previous wind tower studies, but also point out to an important issue related to the ventilation assessment: the unpredictability of the variations of different ventilation indicators and thus the necessity to analyse them simultaneously.

# Acknowledgement

I would like to express my sincere gratitude to my supervisors. To Prof. Mario Grosso for believing in me, and for all the positive energy and support he has given me during the past 5 years that I know him. It was because of him that I ended up working on wind towers! To Prof. Marco Simonetti for following and supporting me during my third year as a PhD student. I am forever grateful to Prof. Jamileh Manoochehri from De Montfort University for her encouragements during these final months.

I am truly thankful to Dr. Hamid Montazeri from Technical University of Eindhoven for selflessly assisting me with CFD and for providing me some of the most applicable and interesting references.

A big thank you in advance to the examination committee, Professors Ben Richard Hughes, Guadalupe Huelsz, Abbas Emualim, Almerindo Ferreira, and Ted Stathopoulos, for taking their time to be present in my defence session. I look forward to hearing their remarks about my thesis.

Finally, I would like to extend my gratitude to my family. To mom, dad, and my sis that I owe much more than a thank you. To them I owe all the moments I was not there to make them happy. I owe them all the energy and care they invested in me hoping for my success. And, to Amir, a big thank you for all his unconditional support and love during these years we have been together.

*In wind towers, in CFD, I find three joys: One for home, Iran, the past, what is now part of my identity and my roots; one for the physics, the logic, the equations, the numbers, that I had a passion for when I was in high school; And one for the wind, for it makes me feel free.*

*I would like to dedicate this thesis to my younger self: the one I miss the most, the one that pushes me to try new things, the one who reminds me to keep seeking the enthusiasm for that is how I feel successful.*

# Contents

# List of Tables

# List of Figures

# Chapter 1

# Introduction

## 1.1 Background

Statistics show that in 2010, the buildings sector has used around one third of the final energy used in the world -24 percent in residential and 8 percent in commercial buildings (Lucon et al, 2014). IEA suggests that the households account for about 60 percent of the increase in energy demand majorly in form of electricity (International Energy Agency, 2013) and indeed in 2010, the building sector's emission of CO2 only represents one-third of the global CO2 emission (Lucon et al, 2014). Therefore, inevitably, part of the climate change mitigation policies is to impose higher energy performance standards for lighting, heating, and cooling appliances (International Energy Agency, 2013).

On the other hand, the unavoidable increase of cooling energy demand due to global warming, improving life standards (Kamal, 2012) and population growth associates with a higher electricity consumption and more CO2 emission.

Currently, 5 percent of the total energy consumption in buildings is due to space cooling facilities but this is the fastest growing end use in the sector (Kool, Jørgensen, Greisberger & Kurosawa, 2016). As IPCC suggests the global demand for the residential air-conditioning will rise from 300 TWh per year in 2000 to 4000 TWh in 2050 (Arent et al, 2014).

It is true that the introduction of mechanical air-conditioning not only increases the likelihood of achieving thermal comfort by controlling the temperature, moisture content, circulation and purity of air for more extended periods, but also permits a great deal of flexibility in building design, and simultaneously leads to changes in life style and work habits. However, the increasing level of damage to the environment has created greater awareness at the international level, and has resulted in the concept of green energy buildings.

For these reasons, the research on different innovative building systems has become of major importance as it can accelerate the transition toward sustainable building design (Loonen, Singaravel, Trčka, Cóstola & Hensen, 2014). In this

regard, assessing the possibility of implementing passive ventilation and cooling strategies as alternative solutions for providing human comfort can contribute in energy savings and address the climate change mitigation set by United Nations Environment Programme (UNEP).

Natural ventilation is, in fact, a sustainable solution for providing a good indoor air quality, improving thermal comfort and saving energy at the same time (Heiselberg, 2004). It is, actually, one of the passive alternatives for moderating the environmental impact of growing mechanical cooling systems (Chiesa & Grosso, 2016).

Figure 1.1. Malekzadeh House built during the Qajar dynasity (1794-1925) in Fahadan neighborhood of Yazd, known as city of wind towers, Iran

One of the natural ventilative cooling devices that despite its antiquity has only lately attracted attention of sustainable designers and engineers is the Iranian wind tower a.k.a. wind-catcher (figure 1.1) that was originally constructed in the Middle East over 2000 years ago (Vaziri & Bastani Parizi, 2006).

Previous parametrical analyses of a wind tower model using SPERAVent—a simplified thermal simulation tool for calculating the potential cooling energy reduction due to controlled natural ventilation (Grosso et al, 2011)— have shown promising results in different climatic conditions in Palermo (Grosso & Ahmadi, 2016), Milan and Rome (Ahmadi & Grosso, 2017).

Few examples of wind towers integrated in modern architecture can be seen in several buildings around the globe, as such are the Queen's Building at De Montfort University designed by Short and Associates in Leicester, UK (figure 1.2) built

between the years 1989-1993, Zion National Park Visitor Center designed by National Park Service-Denver Service Center in Utah, USA in 2000, and the 2006 public housing project (figure 1.3) jointly by Morphosis Architects and Begoña Diaz Urgorri Architect, in Carabanchel, Spain.

Figure 1.2. Naturally ventilated Queen's Building with its several wind towers at De Montfort University in Leicester, designed by Short and Associates

Figure. 1.3. Wind towers in 141 Housing project designed by Morphosis Architects & Begoña Diaz Urgorri Architect in Carabanchel, Spain (Halbe, 2007)

Despite the various studies on the conventional/traditional wind towers and the commercial ones such as those designed and marketed by Monodraught ltd (figure 1.4), all confirming the effectiveness of wind towers in providing natural ventilation, there is still no wide adoption of this technology in sustainable building industry.

Figure 1.4. Commercially produced Windcatcher$^{TM}$ Classic (Monodraught ltd, 2019)

This slow uptake of the wind tower technology on the one hand might be due to the design issues related to the integration of this element in the architecture of buildings especially the several-story ones, and on the other hand it emphasizes the need for further research about its performance and further clarification about its capabilities in providing acceptable indoor air quality and thermal comfort.

Providing design solutions about the integration of such building component is a difficult task as it is neither feasible to do full-scale experiments by constructing and monitoring several buildings with wind towers integrated in them, nor it is economically convenient to do several reduced-scale experiments in wind tunnel. Numerical assessments such as Computational Fluid Dynamics (CFD) simulations are good alternatives at the design stage, but their results are not valid if not compared with the experimental data. These issues illustrate why the majority of the natural ventilation studies using wind towers are performed on simplified models mainly composed of a room model and a wind tower that aim on providing a knowledge of the airflow.

Nevertheless, focusing on simplified models, there are still questions the answer of which can provide an insight at the design stage, too. For instance, understanding where to place a wind tower with respect to the lower space, what

wind tower size to use based on the room volume and the available wind conditions, what type of wind tower with how many openings to use based on the prevailing wind direction, whether to use a wind tower as an exhaust aperture or as an air inlet, and so on. The answer to these questions might not necessarily convince architects and building designers to employ a wind tower in their projects, but in case they decide to do so, this information will be very relevant and useful.

## 1.2 Problem definition

Understanding the real natural ventilation performance of a wind tower is a complicated task as it involves many variables ranging from the larger scale ones such as the transient solar radiation, temperature and wind conditions, the geographical and topographical features, the urban morphology, and the amount of outdoor air pollution, to the building scale variables such as the building dimension and geometry, building materials, the layout, the furniture, the indoor contamination sources, the number of occupants and the hours of occupancy, etc.

Nevertheless, parametrical assessments in which only few of the above variables are present can still be very useful as they can provide general information about the impact of the each parameter on the final performance.

The previous parametrical evaluations on wind towers have mainly focused on five aspects: understanding whether wind or buoyancy is the major force in providing greater airflow in or out of the wind tower; evaluating the wind towers' forms and understanding how a variation in wind towers' height, number of openings, internal partitions, roof shape, etc. can impact their performance and how addition of louvers and dampers can enhance the control of the airflow; assessing how the building connected to the wind tower can affect the ventilation by changing the size and position of the window and changing the building roof shape, among others; evaluating the possibility of integrating other passive solutions such as evaporative cooling, ground cooling, heat pipes and heat recovery systems in wind towers; and finally integrating wind towers in urban environment and using them to address ventilation issues in outdoor spaces.

The majority of these studies have compared the airflow rate values and temperature and velocity distribution in the space while other indicators such as mean age of air describing the freshness of the air have been utilized in fewer instances. The effectiveness of ventilation has been evaluated in a handful of the previous studies by assuming contaminant sources in the room which despite providing a useful insight, are not inclusive enough because the intensity and

position of the contamination sources in other configurations are usually neither known nor fixed.

The form of the wind towers in the previous studies can be classified into two general groups: tall tower-like wind towers placed next to the building and connected to it through an aperture on the wall, or shorter structures placed on the building roof. The position of these wind towers with respect to the building have been different in different studies but to date the effect to this variation has never been assessed. Furthermore, the wind direction variation has been ignored in some of the studies and the prevalent incident angle has been considered as zero.

## 1.3 Objectives and methodology

Through the literature review, CFD validated by experimental data was identified as one of the most utilized methods in assessing natural ventilation problems particularly concerning the wind towers. Therefore, in this thesis, it was employed in order to numerically evaluate how the change in the position of a rooftop wind tower affects its performance.

The thesis is composed of five case studies, four of which are investigated for seven wind directions ranging between zero and 180 degrees (30 degree intervals): case study I comprising 21 simulations on three positions of a one-sided wind tower working with a room window; case study II comprising 21 simulations on three positions of a four-sided wind tower working with a room window; case study III comprising 11 simulations (excluding symmetrical cases) on three positions of a four-sided wind tower when the lower room does not have any windows; case study IV comprising 4 simulations (excluding symmetrical cases) on a model having two windows on two opposite walls and no wind towers; and finally case study V comprising 6 simulations on a room model divided by three positions of an internal partition to two zones cross ventilated with a one-sided wind tower and a window each falling in one zone.

Each of the 63 cases where evaluated by comparing the results in terms of pressure coefficient, volume flow rate which corresponds to the number of air changes, velocity magnitude, mean age of air, and air change efficiency which gives a more general information about the ventilation effectiveness compared to the contamination removal index and is more relevant in design stage where the position and intensity of the contaminants are not known.

The questions that are answered by this thesis are therefore:

- At each specific wind direction and at variable wind directions 0-90 and 90-180, which wind tower type, one-sided or four-sided, can perform better in terms of cross ventilation;
- In a room ventilated by four-sided wind towers that can work as an air inlet and outlet simultaneously, how the presence or absence of another aperture such as a window can affect the cross ventilation performance;
- How the position of each of these wind tower cases on the roof of a building while the position of the window is fixed, can affect their performance at various wind directions;
- In what way the cross ventilation through two windows is different from cross ventilation through a combination of wind towers and windows.
- And finally, how the division of the room in two parts can affect the cross ventilation through the one-sided wind tower and a window.

## 1.4 Structure of the thesis

The thesis is composed of eight chapters.

Chapter 1 has been dedicated to explaining why natural ventilation is important and how wind towers can be utilized as alternative means of providing natural ventilation in buildings. The reasons behind not following other ideas related to the integration of wind towers in buildings have been mentioned. The problem which is going to be addressed in the thesis has been clarified and the objectives and methodology have been explained.

In Chapter 2 a brief introduction about natural ventilation is given. The principles thus the three modes of natural ventilation have been described. And the indicators and models that are commonly utilized for assessing its effectiveness in terms of indoor air quality and thermal comfort have been described. Furthermore, different methods and their advantage and disadvantages for studying natural ventilation in the built environment have been explained.

Chapter 3 provides a literature review on the wind towers, highlighting the research methods utilized in each study, their objectives, the wind characteristics, and the shape and position of the wind towers in each of the studies. At the end of the literature review, the gap in the literature is highlighted and duly the numerical CFD method as the most common method utilized in the literature has been selected for studying wind towers in this thesis.

As every CFD has to be validated by experimental data, Chapter 4 is dedicated to the validation study. It first gives a very brief insight into the theoretical background of CFD by explaining the governing equations, different discretization methods, the

various turbulence models, and near-wall modeling issues. Then, it validates the chosen CFD code ANSYS Fluent 18.0 and the selected solver settings in a comparison with the pre-existing wind tunnel data.

Chapter 5 is the main chapter of the thesis which includes the three case studies on two wind tower types at different rooftop positions. Each case study provides results in terms of volume flow rate, pressure coefficient, velocity magnitude, mean age of air, and air change efficiency for the selected type of wind tower. At the end of this chapter, the three case studies having wind towers are compared with one another.

In Chapter 6, the cross ventilation using two windows –i.e. no wind towers, has been assessed and the difference with the three cases in Chapter 5 has been outlined.

Chapter 7 is a brief introduction into a possible future project and investigates the cross-ventilation using wind tower in a two-zone space as opposed to all the previous assessments in one-zone rooms.

Finally Chapter 8 concludes the thesis by summarizing the outcomes of the case studies, highlighting the remaining unknowns about the wind tower performance and recommending future studies.

# Chapter 2

# Natural Ventilation

## 2.1 Introduction

Natural ventilation has been widely used throughout history as a means for improving indoor air quality and sometimes for cooling. Unfortunately, the application of natural ventilation techniques has been heavily restricted following the evolution of construction techniques and the emergence of mechanical cooling devices that are more flexibly fitted into densely populated buildings with higher internal heat loads and deeper plans. Followed by the energy crisis in 1973, modern architecture and the energy-conscious design has resulted in building envelopes being sealed from the outdoor environment in order to minimise the energy loss through air infiltration (Walker, 2006). The construction of large glass office buildings with non-operable windows has further eliminated the possibility of using natural ventilation with the belief that mechanical devices can more effectively provide a uniform yet controllable indoor air quality and thermal condition for occupants.

However, the growing overheating problem due to global warming, urban heat island phenomenon, increasing energy consumption caused by the overuse of electronic equipment, especially in airtight building retrofits during summer months on a global scale, together with smaller issues on building scale such as the noise produced by the mechanical ventilation devices, their ducting network, their maintenance cost considering their much shorter service life compared to the building itself, and their inadequacy in providing the desirable comfort condition for a diversity of occupants, have all encouraged architects and building engineers to rethink the traditional yet more sustainable design solution: the natural ventilation.

## 2.2 Principles of natural ventilation

Natural ventilation is the movement of air through buildings' openings caused by the pressure variance due to wind and/or temperature differences between the interior and exterior of the building. Equation 2.1, derived from the Navier-Stokes equation for a steady fully-developed flow (Allard & Ghiaus, 2006), is the general formula for calculating the air flow rate Q caused by the pressure difference across the building's larger openings ΔP (British Standards Institution, 1991). In this formula $C_d$ is the discharge coefficient, A is the opening area and ρ is the air density.

Eqn 2.1. $$Q=C_dA\sqrt{2\Delta P/\rho}$$

The main strategies for natural ventilation are therefore wind variation-induced single-sided ventilation, wind pressure-driven cross-ventilation, and buoyancy pressure-driven stack ventilation (Allard & Ghiaus, 2006). Even though more commonly all these types occur together in naturally ventilated buildings (Larsen, 2006) but usually one dominates the other.

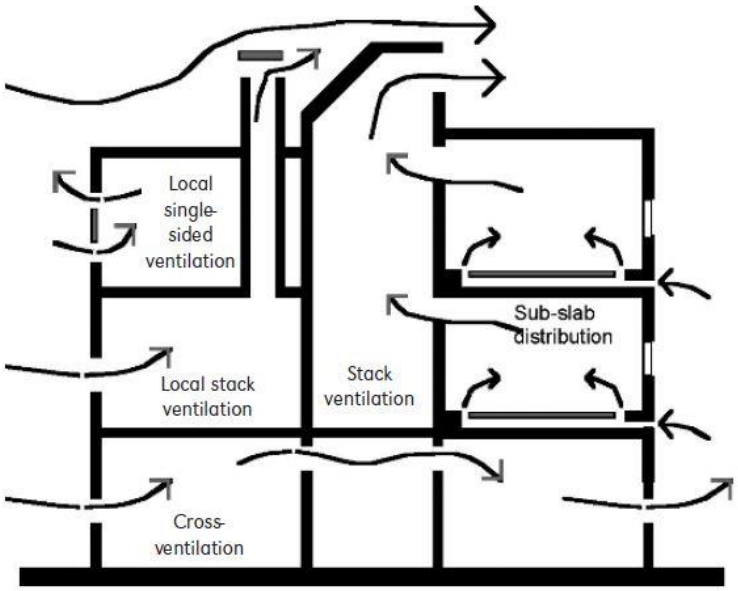


Figure 2.1. Different natural ventilation strategies in one building (Allard & Ghiaus, 2006)

### 2.2.1 Wind variation-induced single-sided ventilation

Single-sided ventilation is typical to most of our buildings today in which the rooms have only one operable window. The airflow through the window is due to the pressure variations caused by the turbulent nature of the wind and the temperature difference between inside and outside in addition to the room-scale

thermal stratification. For an effective ventilation using this method, it is recommended that the depth of the ventilated space should be less than 2.5 times the ceiling height (Building Research Establishment, 1994) (Klein & Schlenger, 2008).

### 2.2.2 The wind-driven cross-ventilation

In general, the wind induces positive pressure on windward side and negative pressure on leeward side of a building. These pressure differences are variable due to the turbulences in the wind airflow but are usually considered as averages in time.

The wind flow through the openings in a cross-ventilation is calculated by the equation 2.2:

Eqn 2.2. $$Q=C_d A U_o \sqrt{\Delta C_P/2}$$

In which the $C_d$ is the discharge coefficient, the $U_o$ is the reference wind velocity, and the $\Delta C_p$ is the difference between the windward and leeward pressure coefficients of the openings. The pressure coefficient $C_p$ on each point of the façade, usually determined through wind tunnel experiments (Orme, 1999), is calculated as (British Standards Institution, 1991):

Eqn 2.3. $$C_p=(p-p_o)(\frac{1}{2}\ \rho U_o^2)$$

In which, $\frac{1}{2}\ \rho U_o^2$ is the kinetic energy per unit volume of the reference wind velocity $U_o$, $\rho$ is the air density and $p_o$ is the free stream static pressure known as reference static pressure.

For an effective cross- or two-sided ventilation it is generally recommended that the distance between the two openings should not exceed 5 times ceiling height (Klein & Schlenger, 2008). Despite this recommendation, the critical inadequacy of this ventilation type, as evident in the former formula, is due to its substantial reliance on wind direction and wind speed which have variable values in time due to the turbulent nature of wind. Furthermore, assuming a time-averaged model, the pressure coefficient values on a building's envelope, in addition to the wind incident angle, depend on the building's geometry, façade details, and the surrounding obstacles especially the upstream terrain characteristics.

### 2.2.3 The buoyancy-driven stack-ventilation

Stack-ventilation occurs when the air pressure variation is caused by the air density gradient due to the temperature difference between the micro and macro

climate. In other words, the low pressure less dense warm air rises up and escapes from the aperture on the top while the new air is drawn into the space through lower apertures to replace the escaped air (Hughes, Calautit, & Ghani, 2012). Therefore, the greater the temperature variance between the building's openings, the bigger the buoyancy-driven airflow. The magnitude of this airflow is also directly affected by the height difference between the outlet and inlet openings.

However, it has been shown that the buoyancy can only provide acceptable ventilation rates if there is a wind forcing the airflow in the stack (Hughes & Mak, 2012).

## 2.3 Assessing ventilation effectiveness

Natural ventilation, as previously stated, can provide an acceptable indoor air quality and thermal comfort. Hence, the limitations and the effectiveness of natural ventilation systems can only be assessed considering the quality, quantity, controllability and desirability of the airflow they provide for the buildings' occupants (British Standards Institution, 1991).

The outdoor air is different from the indoor air in terms of quality and cleanliness. Where the outdoor air is particularly polluted, it has to be treated, even though the presence of the air filters resistant to the airflow can diminish the quantity of the air entering the building and thus the effectiveness of natural ventilation in terms of quantity. On the other hand, the variability of the meteorological conditions can affect the available airflow rate which means that the requirements for ventilation might not necessarily be met once the weather conditions changes. Natural ventilation on one hand can be handy when the number of occupants in a space changes greatly as it has the flexibility of changing the ventilation rate. On the other hand, compared to mechanical systems there are more fluctuations in the provided airflow rate due to the variation of the wind speed and direction. Finally, despite the more desirability of natural ventilation for the occupants in terms of thermal comfort, a mechanical system is a more appropriate option for industrial buildings or commercial kitchens where the contamination and need for fresh air is greater, the densely populated gathering halls and high-rise buildings where practicing natural ventilation solutions are not possible.

Below, several parameters for assessing the effectiveness of ventilation systems are presented. The indexes for assessing the indoor air quality which are more relevant to the current thesis have come first because in general the perception of IAQ by the occupants is less immediate than thermal comfort. In addition, the latter has been better-defined by the standards (Novoselac & Srebric, 2003).

### 2.3.1 Ventilation for indoor air quality

The primary reason for ventilation is to provide an acceptable indoor air quality by supplying clean air and removing contaminants effectively.

## Indoor vs. outdoor air quality

People spend most of their time indoors, therefore the quality of the indoor air and its impact on occupant's health is of major importance. Particularly in tightly insulated buildings aiming at a higher energy efficiency, the pollutants can get trapped inside the space resulting in a higher concentration and an increased exposure to the occupants. This highlights the role of ventilation in assuring an acceptable indoor air quality (Paraschiv & Paraschiv, 2017).

The main reason to ventilate a space is to eliminate the carbon dioxide resulting from the occupants' breathings and to provide oxygen by introducing fresh air. Other than the occupants, the major sources of the indoor air pollution are the outdoor air and the indoor air pollutants coming from the heating, cooking, molds, building materials, and household chemicals (Xueyan & Xinying, 2015) such as various cleansers, pesticides, paints, air fresheners, candles, etc. Therefore, according to the source location, the air pollutants are grouped into three categories (Yocom, 1982): group I are pollutants with sources located majorly outdoor including sulfur oxides, ozone, pollens, lead and manganese, calcium, chlorine, silicon and cadmium, and organic substances; group II are pollutants that their sources could be both indoor and outdoor, such as nitric oxide, nitrogen monoxide and carbon monoxide, carbon dioxide, particles, water vapor, organic substances, and spores; finally group II as pollutants which sources are predominantly indoors including radon, formaldehydes, asbestos, mineral and synthetic fibers, organic substances, ammonia, polycyclic hydrocarbons, arsenic, nicotine and acrolein, mercury, aerosols, viable organisms, and allergens.

Where the source of the pollutant is outdoor, often an indoor-outdoor (I/O) ratio is used to express the correlation for each pollutant. Even though any change in the outdoor concentration can directly affect that of the indoor, this correlation is shown to be not equal for different pollutants.

Another important issue to keep in mind is that the indoor concentration of some of the air pollutants such as ozone, nitrates, and carbon monoxide are independent of the choice of the ventilation system, whereas the concentration of particle matters can only be controlled effectively by filters of a mechanical system

and a natural ventilation system even at high ventilation rates is unable to manage the indoor concentration of such contaminant (Ben-David & Waring, 2016).

## Indicators for IAQ assessment

The most popularly used indicators for IAQ assessment are number of air changes, the contamination removal effectiveness and the air change efficiency (Novoselac & Srebric, 2003).

The air change number per time unit in a space $n_{AC}$ or the air change rate, which is the most widely used index in the standards, suggests the ventilation intensity and corresponds to the removal of air from the interior of a volume by a piston in an ideal fluid. It is usually expressed as volumetric airflow rate per person or per unit floor area depending on the space type and the activity happening there. It is calculated using the following formula 2.4 in which $Q_v$ represents the volumetric ventilation airflow rate and V is the room volume.

Eqn 2.4. $$n_{AC} = Q_v / V$$

Even though the air change rate value defines the total amount of supplied/fresh air into a space, it neither provides information on the distribution quality of this supplied/fresh air inside the space nor does it guarantee the effective removal of contaminants from the space.

The contamination removal effectiveness (CRE), $\bar{\varepsilon}$, as an indicator of a perceived air quality, is given as the ratio between the contaminant concentration in the exhaust and the mean concentration in the room (Mundt, Mathisen, Nielsen & Moser, 2004). For each point in the room, the local value, $\varepsilon_j$, is calculated using the equation 2.5 considering the contaminant concentration in different points $C_j$ and the supplied and exhausted contaminant concentrations, $C_s$ and $C_e$ respectively (Persily, 1985).

Eqn 2.5. $$\varepsilon_j = (C_e - C_s)/(C_j - C_s)$$

In the above formula, $C_j$ replaced by $\overline{C}$ can give the average contaminant removal effectiveness $\bar{\varepsilon}$ in the whole room. In the case of perfect mixing, the contaminant concentration is uniform in the room and equal to the exhaust concentration (Persily, 1985). The ideal result is achieved if the average contaminant concentration in the space is lower than the concentration in the exhaust. The latter depends on release rate of contaminant into to the space and the ventilation flow rate (Mundt et al, 2004).

While the objective of a ventilation system should be the removal of contaminants locally and preventing their further spread in the space, at the design stage when the use of the building and thus the placement and intensity of the contaminant sources are unknown, the efficiency of the ventilation system is evaluated using the air change efficiency index in order to ensure a rapid enough air exchange (Mundt et al, 2004). Using Sandberg's concept of mean age of air $\tau$ (Sandberg, 1981), the air change efficiency $\varepsilon_a$ is calculated as the ratio between the shortest possible air change time $\tau_n$ and the average time for exchanging room's air $\bar{\tau}_r$ (equation 2.6). While $\tau_n$, known as the nominal time constant, is the reverse value of number of air changes (Novoselac & Srebric, 2003), $\bar{\tau}_r$ also known as the actual air change time is double the spatial average of local mean ages of air, $\bar{\tau}$, in the whole room (Mundt et al, 2004).

Eqn 2.6. $$\varepsilon_a = \tau_n/\bar{\tau}_r = (V/Q_v)/2\bar{\tau}$$

In case the contaminant emission is uniform in the space, the absolute value of the air change efficiency is half the contaminant removal effectiveness.

### 2.3.2 Ventilation for thermal comfort

According to ASHRAE 55, thermal comfort is a person's subjective evaluation of his thermal environment and refers to a satisfactory condition of thermal neutrality for the person. Even though, there are studies arguing that thermal neutrality does not necessarily guarantee the thermal comfort of the occupants (Shahzad, Brennan, Theodossopoulos, Calautit & Hughes, 2018).

The concept of thermal comfort has been defined according to three different approaches. In the physiological approach the thermal perception of a human occurs due to the connection between the thermal receptors in the skin, the nervous sensors and the hypothalamus. The psychological approach believes that the thermal comfort is a "condition of mind which expresses satisfaction with the thermal environment". And in the rational approach thermal comfort depends on the heat balance of the human body (Attia, Carlucci, 2015).

There are six main factors influencing the thermal comfort grouped into personal factors such as metabolic rate (or activity level) and clothing insulation, and environmental factors such as air temperature, mean radiant temperature, air velocity and relative humidity.

## Thermal comfort models

Based on the three approaches mentioned above various mathematical models have been developed that simulate the occupants' thermal response to their environment using the personal and environmental variables depending on the steady or transient, uniform or non-uniform thermal conditions.

The most commonly used model for evaluating thermal comfort, especially in mechanically conditioned buildings is the PMV/PPD model proposed by Ole Fanger (Fanger, 1970).

PMV is the Predicted Mean Vote on thermal sensation scale of a large population of people exposed to a certain environment. It establishes a thermal strain based on steady-state heat transfer between the body and the environment and assigns a comfort vote to it. The PMV equation of Fanger only applies to humans exposed for a long period to constant conditions at a constant metabolic rate (Fountain & Huizenga, 1997).

The standard PMV surveys are based on seven-point scales and the votes vary between -3 for being cold and +3 for being hot and zero being the ideal value of thermal neutrality. As the PMV value changes away from the zero value, the PPD or Percentage of People Dissatisfied increases. The psychometric charts representing the comfort zone for PMV/PPD method, indicate the ranges of temperature and relative humidity that will be comfortable with the given values input for the remaining four parameters.

In addition to the static models such as the one by Fanger, for naturally ventilated buildings, there are adaptive models that can optionally be used (Linden, Loomans & Hensen, 2008). The adaptive comfort model assumes that humans' thermal perception differs due not only to the physics and physiology, but also by their gender, age, attitude, preferences, etc. (de Dear, Brager, & Cooper, 1997). People adapt to different thermal conditions in different times of the year and generally they adjust their behaviour or their environment, and act in a way that will restore their comfort. Such actions include taking off clothing, reducing activity or opening the windows (de Dear et al, 1997).

Numerous researchers have conducted field studies worldwide in which they survey building occupants about their thermal comfort while taking simultaneous environmental measurements. For instance, the occupants of naturally ventilated buildings accept and even prefer a wider range of temperatures (Moujalled, Cantin, & Guarracino, 2008) than their counterparts in sealed, air-conditioned buildings because their preferred temperature depends on outdoor conditions.

## American vs. European standards for thermal comfort

There are several standards developed based on the static and adaptive thermal comfort models. The figure below demonstrates the chronology of the standards integrating thermal comfort models.

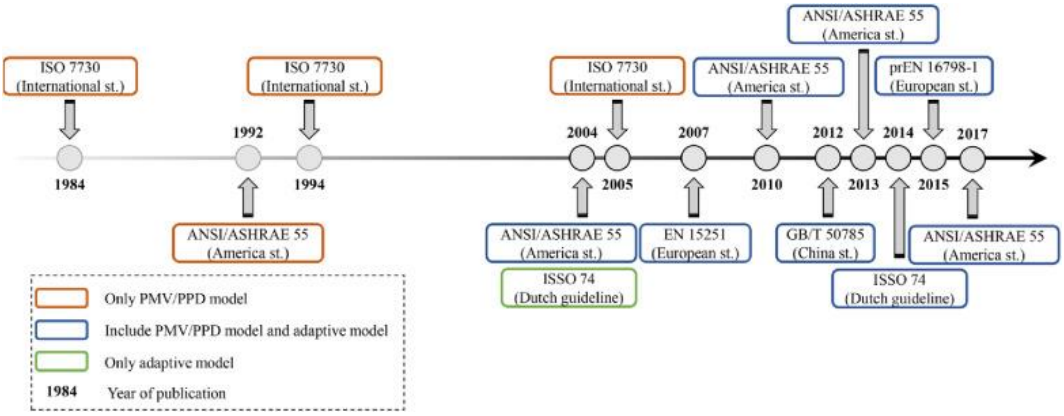


Figure 2.2. Chronology of standards integrating thermal comfort models (Carlucci, Bai, de Dear, & Yang, 2018)

Two of the most well-known standards that integrate both PMW/PPD and adaptive models are the American ASHRAE Standard 55 and European EN-16798 Standard which are included in the CBE Thermal Comfort Tool.

The PMV/PPD method in ASHRAE Standard 55 requires that at least 90% of the occupants of a space find the indoor thermal conditions satisfactory. It also recommends that the PMV limits for thermal comfort should fall between -0.5 and +0.5 (Grignon-Massé, Adnot, Rivière, 2008).

EN-16798 which is the updated version of EN-15251, on the other hand, defines four building categories and recommends the following PMV/PPD criteria for each of them:

- Category I PPD < 6% -0.2 < PMV < 0.2
- Category II PPD < 10% -0.5 < PMV < 0.5
- Category III PPD < 15% -0.7 < PMV < 0.7
- Category IV PPD > 15% PMV < -0.7, PMV > 0.7

These building categories are defined based on the occupants' expectation levels with Category I addressing the very sensitive and fragile people whose levels of expectation are high, Category II addressing the new and renovated buildings and occupants with a normal expectation level, Category III addressing

the existing buildings and occupants with an acceptable or moderate expectation level, and Category IV should be only accepted for a limited time of the year.

The adaptive comfort model has been added in ASHRAE 55-2004 considering the monthly mean outdoor temperature as the reference outdoor temperature. In 2013 version, the reference value was calculated by the prevailing mean outdoor temperature (Carlucci et al, 2018). The optimum indoor comfort temperature is then calculated as a function of this outdoor temperature and zones of 80% and 90% satisfaction are defined (Moujalled et al, 2008) (de Dear et al, 1997). In EN-16798, the comfort temperature is calculated as the approximate running mean outdoor temperature for Categories I, II and III with thermal acceptability limits of 90%, 80% and 65% respectively. (Moujalled et al., 2008).

According to ASHRAE 55 the adaptive comfort model may be applied to occupant-controlled naturally conditioned spaces, no matter the type of building, under the conditions that: there is no mechanical system installed and no heating system operated, the prevailing outdoor temperature must be between 10 and 33 °C, the occupants' metabolic rates are between 1 and 1.3 met, and the occupants are free to have a clothing resistance between 0.5 and 1.0 clo (Carlucci et al, 2018).

The EN-16798 adaptive approach may be applied to residential and office buildings and other similar building types. The upper limits of the running mean outdoor temperature ranges between 10 and 30 °C (Carlucci et al, 2018). Occupants can have quasi-sedentary activities, are free to adapt their clothing. The clothing resistance and the metabolic rates should have the same ranges as in ASHRAE 55. And, the rooms' operable windows, as the primary means of regulating thermal conditions, need to be under occupants' control (Moujalled et al., 2008). However, mechanical ventilation with unconditioned air is allowed (Carlucci et al, 2018).

The adaptive comfort approach in ASHRAE 55 and EN-16798 are developed based on different databases and different statistical methods. And they calculate the outdoor reference temperature by different approximations and different comfort equations. Though, their acceptable temperature ranges are comparable and their optimal comfort temperatures are similar. (Carlucci et al, 2018).

## 2.4 Methods of studying natural ventilation

Theoretical and experimental tools have been used for evaluating the ventilation performance in buildings ranging from analytical and empirical models, to small- and full-scale experimental models, and to numerical models as of

computational fluid dynamics (CFD) models, among others (Chen, 2009). Similarly, the performance of wind towers that are the main subject of analysis in this thesis has been assessed by these tools. In evaluating wind towers, analytical models were used in fewer instances compared to the experimental and numerical models.

In a study by Rezaeian, Montazeri & Loonen in 2017, the share of each of the different research methods used for assessing the wind towers has been mentioned. Among the 92 papers assessed, there were 20 wind tunnel tests, 21 full-scale experiments, 39 CFD studies, 6 papers using BPS & AFN (building performance simulation and air flow network) method, 24 analytical studies, and 14 literature reviews.

In this part of the thesis, a brief overview of different research methods used in assessing natural ventilation in wind towers is given as follows.

### 2.4.1 Theoretical models, pros and cons

Theoretical models can be grouped into analytical and numerical models. Analytical models are mainly derived from heat transfer and fluid dynamic equations such as those of conservation law (Chen, 2009). This method has been widely used for predicting ventilation because of its simplicity and little computational requirements. However, for complicated models and geometries, it might lack enough accuracy. These models have been majorly used to provide comparisons with results of the experimental and numerical models. In studying wind towers, a thorough analytical assessment was performed by Bahadori et al. estimating the air flow and temperature in conventional and evaporative wind towers (Bahadori, Dehghani & Sayigh, 2014).

In terms of numerical assessment, computational fluid dynamics is popularly used to mathematically model the fluid flow and heat transfer problems (Versteeg & Malalasekera, 1995). Finding its way in architecture, CFD allows one to evaluate the interaction between the building envelope and the indoor and outdoor environment. Therefore, it has been widely employed in studying the indoor air quality, thermal comfort, fire safety, HVAC system performance, among others, in various types of building models including those having wind towers.

While the advantage of a CFD analysis to a wind tunnel experiment is the lower cost, the accessibility, the wider range of result it can provide, and the irrelevance of the flow similarity constraints explained below, its drawback is the uncertainty of the numerical results. For this reason, CFD results must be validated by some experimental data derived from the wind tunnel and/or the in situ measurements.

### 2.4.2 Experimental studies, pros and cons

The experimental analysis on natural ventilation can be classified into laboratory experiments and in-situ measurements. In laboratory experiments, regardless of the scale of the model –i.e. full-scale or small-scale, a wind tunnel is utilised for simulating the outdoor wind (Chen, 2009). Sometimes, to observe the air flow pattern, smoke visualisation tests are carried out in the wind tunnel, too.

There are a few drawbacks in using wind tunnels which not only include the cost and time of setting up and running the test, but also, more importantly, are related to the dimension of the wind tunnel and the inlet boundary condition they provide. Since initially wind tunnels were constructed for aeronautical purposes, the majority of them can only provide uniform wind speeds with low turbulences. However, as the wind behaviour in buildings' scale in reality is completely different, eventually boundary layer wind tunnels were created for studying the building aerodynamics. Therefore, in studying the wind towers performance, the ABL wind tunnels are preferred.

Obviously, in wind tunnel tests, using small-scale models are less costly respect to full-scale ones. Reduced-scale models are frequently used in studying natural ventilation, especially as they provide the validation data for numerical studies.

It should be noted that for a valid wind tunnel experiment, the scale of the model to be tested should be small enough not to block more than 5% of the wind tunnel's volume (Campos-Arriaga, 2009), though, the model should not be too small to compromise the sensitivity of the measurements. The flow similarities in reduced-scale models and real-size ones have to be subsequently guaranteed by fixing airflow's dimensionless parameters such as Reynolds number, Grashof number, Prandtl number, etc. (Chen, 2009). Nevertheless, in aerodynamic studies, regardless of the price, size and the wind speed of the wind tunnel, in general it is not possible to achieve the similarity between the wind and turbulence Reynolds number for the simulated flow in wind tunnel tests and those of the real model. Yet, according to ASCE, for sharp edge structures, the equality of the model and full-scale Reynolds number is not necessary provided that the approach flow is independent of the Reynolds number. Thus, if the mean wind speed and a characteristic dimension of the tested structure are set in a way that the Reynolds number value becomes more than $10^4$, the distortion of the flow and the subsequent variation in pressure distributions will be negligible (ASCE, 1996) (Calautit & Hughes, 2014b).

The most realistic method of evaluating the ventilation is full-scale in-situ measurement. This method is generally expensive and time consuming and only

relevant for evaluating the exiting buildings' performance. In spite of the fact that the obtained data in this kind of assessment is highly affected by the unsteady meteorological conditions, they are usually, though less frequently compared to wind tunnel tests, utilised for validating the numerical simulations that are more convenient in doing design phase case studies.

# Chapter 3

# Wind towers for natural ventilation

## 3.1 Introduction

The old urban morphology and traditional architecture of the buildings in desert cities of Iran were influenced by harsh climatic conditions such as intensive solar radiation, substantial differences in diurnal temperature, little rain, very low air humidity and winds carrying sands from the nearby deserts (Zomarshidi, 1994). Therefore, the people living in these regions developed certain solutions to confront these harsh conditions.

For instance, in order to avoid sand storms and expose less surface to solar radiation, the buildings in these areas were constructed compactly with one another having tall and thick walls. This exaggerated density consequently prevented the air from reaching a human level. Therefore, to compensate, wind towers were built on top of almost all houses in these desert areas to convey the less sandy and fresher air of a higher altitude to the lower building (Ghobadian, 2008).

With the aim of having drinking water all year round, public cisterns were built where the water from the underground Qanat network was collected during the winter time. These public cisterns were equipped with several wind towers on their domed roofs, which had the task of maintaining an ongoing ventilation effect inside the cistern, preventing the formation of dew or humidity (Memarian, 1993) and at the same time keeping the water cool for summer use.

About the antiquity of wind towers, there is no precise information, even though according to several historians it was originated in Iran over 2000 years ago (Vaziri & Bastani Parizi, 2006) (Hodud al-Alam, 1983). Wind towers had still been constructed as one of the main elements in the Persian traditional architecture in many regions of Iran especially in Yazd during the Qajar dynasty (1794-1925) (Bolouhari, 2017) but were eventually abandoned with the morphological evolution of the cities during the 20th century. The so-called modern cities and their buildings were designed so to host a larger and denser population, and the bulky wind towers that were function- and form-wise more suited to the precedent architecture style

were substituted by the mechanically conditioning devices that were more flexibly fit in the smaller modern buildings. What remains from the traditional Persian architecture and the wind towers are now part of the heritage and they continue to fascinate many travellers, architects and engineers visiting the historical parts of desert cities of Iran.

## 3.2 Effective elements in wind towers' performance

There are several review studies on the wind towers that very well gather the various assessments on this building element (Hughes et al, 2012) (Saadatian, Haw, Sopian & Sulaiman, 2012) (Jomehzadeh et al, 2017). In all these assessments, wind towers have been investigated either for their ventilation performance or for their cooling effect. In the latter case, other cooling systems such as evaporative cooling, ground cooling, heat pipes, solar chimneys, etc. have been joint with them, too. This literature review provides yet another summary of various studies on wind towers and then gives an overview on the position of the wind towers in these studies.

According to Bahadori et al, the temperature and mass flow rate of the air entering to a building equipped with a wind tower depend on either the climatic and environmental factors such as ambient temperature, solar radiation, the difference between diurnal and nocturnal temperatures and of course the wind direction and speed, and on the geometrical factors of the wind tower and the building including the shape, position, height, cross section, internal partitions, number of wind tower's opening, and the building's layout, materials, dimensions, windows size and position, etc. (Bahadori et al, 2014).

All these elements affecting either the temperature or the wind flow, would change the pressure distribution around the building and the wind tower and subsequently alters the wind tower's efficiency.

### 3.2.1 Buoyancy vs wind

In 2002, Awbi and Elmulaim have done a wind tunnel test on a full-scale louvered four-sided wind tower installed on top of a test room. Their objective was to understand how the performance of wind tower is affected if a change in wind speed and direction occurs, if a heat source is present in the system, and if dampers and egg-crate grille is added to the outlet of the wind tower. The wind simulated in the wind tunnel had a uniform profile, its direction had a range between 0 and 45 degrees with 15 degree intervals, and the wind speed range was set between 0.5 and 6 m/s. Their results show that the increase in wind velocity increases the airflow rate through the wind tower, the deviation toward 45 degrees reduces the airflow

particularly at lower velocities, the installation of dampers and egg-crate grille reduces the airflow, and finally the introduction of a heat source in the room, improves the airflow rate at lower wind speeds (Awbi & Elmualim, 2002). This test was replicated by the same authors during the same year in CFD (Elmualim & Awbi, 2002). In 2003, they tested a full-scale seminar room in UK equipped with a wind tower. Their monitoring results confirm that the ventilation rate provided by the wind tower depends on the indoor and outdoor temperature, wind velocity and direction (Elmualim & Awbi, 2003). They have also highlighted the effectiveness of wind towers in removing the daytime heat gains through nocturnal ventilation. According to Elmualim, a wind tower is able to offer a substantially greater ventilation rate compared to a window with an equivalent area (Elmualim, 2006). The other advantage of the wind towers is that they can provide natural ventilation with increased control and reliability compared to windows (Elmualim, 2006).

The efficiency of wind towers in night-time ventilation has been verified by other scholars, Bahadori et al., who have focused on conventional wind towers and have theoretically proved that a wind tower alone is not able to cool the air entering the building. They confirm that solely during the night time when the outdoor air is cooler than the indoor air, and if the outside air is provided through a secondary aperture such as a window, the rise and extraction of the solar heat stored in the wind tower and the building during the day could create an upward airflow which is able to cool down the building (Bahadori et al, 2014).

Through a CFD analysis, a similar observation has been noted by Hughes et al. Their study highlights that the wind, in comparison with buoyancy, is the main factor influencing natural ventilation performance of the wind towers (Hughes et al, 2012). In fact, in providing natural ventilation, the wind is 76% more effective than the buoyancy resulted by internal heat generated by occupants, computers and lighting facilities. The result of their simulation also shows that for the buoyancy to have a significant effect on the internal ventilation, an airflow passage other than that of the wind tower, such as that of a window, is required. In fact, introducing a window is shown to increase the internal air speed by 47% (Hughes & Mak, 2011).

A similar result has been derived by Kirk and Kolokotroni who have employed the tracer gas decay method in three buildings with wind towers. Their experimental analysis confirms that the air exchange rates are related to the wind speed and only at low wind speeds the correlation between the air exchange rates and the buoyancy force becomes evident (Kirk & Kolokotroni, 2004).

Li & Mak through a CFD analysis show that the airflow rate through a wind tower is mainly dependant on the wind direction. Especially when the external wind

speed is less than 3 m/s, the increase in wind incident angle toward 45 degrees, affects the ventilation performance negatively, whereas with wind speeds higher than 4 m/s, a wind tower at 15 degrees wind direction performs better compared to the wind directions 0, 30 and 45 degrees (Li & Mak, 2007).

### 3.2.2 Wind tower geometry

Montazeri & Azizian have used a wind tunnel to study the performance of a one-sided (Montazeri & Azizian, 2008) and a two-sided (Montazeri & Azizian, 2009) wind tower in various wind directions by measuring the pressure coefficient values on the internal walls of the wind tower and calculating the natural ventilation efficiency. In 2013, Ghadiri et al have employed CFD to simulate Montazeri's two-sided wind tower. They have assessed the sensitivity of computational choices such as the structured vs unstructured meshes, grid resolution, turbulence models, full-scale vs reduced-scale simulations, size of the computational domain, and discretization order, on the accuracy of the numerical results compared to the experimental data from the wind tunnel (Ghadiri, Lukman, Ibrahim & Mohamed, 2013).

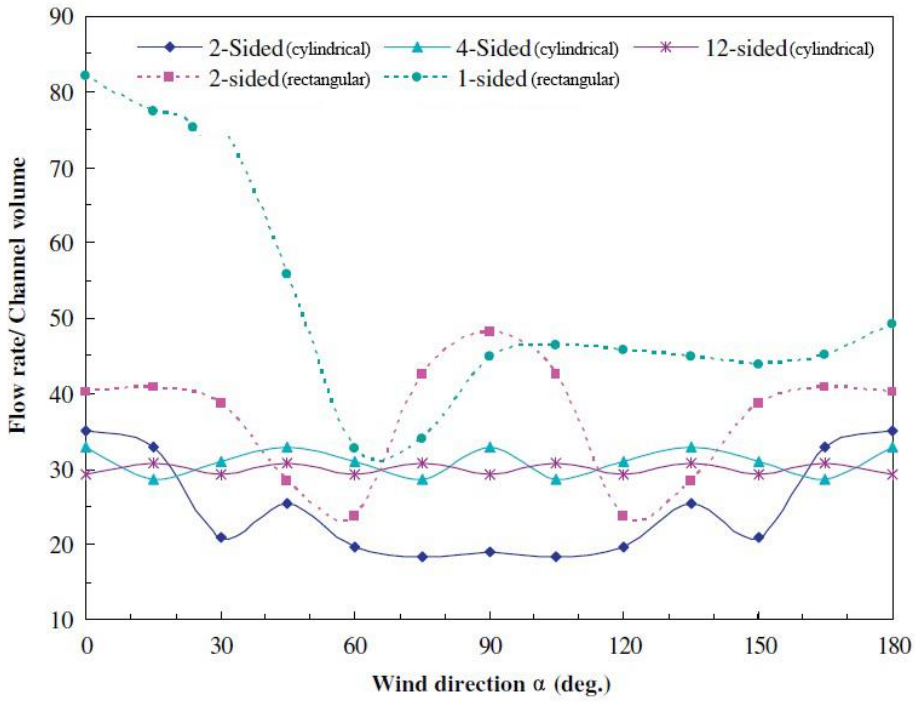


Figure 3.1. Difference between the airflow rates induced by cylindrical wind towers with different numbers of openings (Montazeri, 2011)

Montazeri has, furthermore, studied cylindrical wind towers with different numbers of opening –i.e. two, three, four, six and twelve in another wind tunnel assessment and a further CFD analysis (figure 3.1). He has shown that in general, the wind towers' sensitivity against wind angle decreases by increasing the number of openings and the natural ventilation performance of those with less number of openings drops more considerably by increasing the wind angle (Montazeri, 2011).

Moreover, Montazeri has compared the air flow rates induced by rectangular two-sided wind towers that were measured in a previous wind tunnel test (Montazeri & Azizian, 2009) with the air flow rates generated by cylindrical two-sided wind towers. His comparison shows that a rectangular wind tower is 13% more efficient than the cylindrical one (Montazeri, 2011).

A similar assessment has been done by Elmualim who has evaluated the performance of a cylindrical and a cubical wind tower and has identified that the sharp edges of the latter create a better flow separation and thus a higher pressure difference around the tower which consequently increases the induced airflow rate (Elmualim, 2006).

Mahdavinejad & Javanroodi have used Vasari software to simulate one-sided, two-sided and four-sided wind tower in various wind direction and temperatures representing an average one-year period. They have compared the three wind towers by measuring the airflow rate and air velocity at the apertures and the average pressure coefficient values at wind tower openings, window, and inside the building. They have concluded that the two-sided and four-sided wind towers are more efficient than the one-sided one (Mahdavinejad & Javanroodi, 2014).

Mahyari was one of the first scholars who performed a wind tunnel test on wind towers of Yazd, Iran. His has experimentally investigated various four-sided wind towers with different internal divisions and a two-sided wind tower, that were placed beside an Iwan (a rectangular room with one of four walls entirely open) and a basement connected to a courtyard, representing the desert houses of Iran. He has explained how the internal partitions of the wind tower which were designed to exploit the winds from different directions, can actually increase the exhaust air through the leeward sides for 50 to 100 per cent while decreasing the inflow. The induced flow patterns by the wind tower are highly affected by the arrangement of the Iwan and courtyard. The thermal performance of the wind tower becomes negligible during the afternoon and the comfort of the occupants will depend only on the thermal mass of the building structure (Mahyari, 1996).

A similar assessment on wind tower partitions has been done by Cruz-Salas et al. The experimental results are obtained from an open-water channel and a particle

image velocimetry measurement. The model was composed of a square room with a windward window and a rooftop wind tower divided by partitions into one, two and four internal channels. Their experiment shows that when the window acts as the windward aperture, the wind tower with no internal partitions but with two opposite openings parallel to the wind direction generates the highest airflow rate (Cruz-Salas, Castillo & Huelsz, 2014).

The effect of different partitioning of the wind tower was also investigated by Hosseinnia et al. They have used CFD in order to simulate five common partitioning of wind tower and have shown that the induced air velocity from the room to the tower can increase from 1 m/s to 1.53 m/s only by changing the internal arrangement of the wind tower partitions. As part of their assessment, they have monitored the average inlet velocity, the inlet mass flow rate, and the percentage of the wind tower induced airflow rate that enters the room (Hosseinnia, Saffari & Abdous, 2013).

Ghadiri has also utilised CFD to compare four-sided wind towers with different internal divisions and has realized that the towers with + shaped cross section perform relatively better than H-, X-, I- and K-shaped ones (Ghadiri, Ibrahim & Mohamed, 2013).

The performance of four-sided wind tower connected with Iwan and courtyard at various wind directions has been numerically and experimentally assessed by Dehghani Mohamadabadi et al. The model was inspired by the compact desert cities of Iran in which the roof levels of the buildings were quasi uniformly integrated with each other and courtyards were the only perforations in this dense morphology. The wind tower in the majority of the desert houses of Iran is placed on the roof slightly behind the Iwan space which from the open side connects to the courtyard. The wind tower used in this assessment had a rectangular cross section and was divided into six identical smaller rectangles by internal partitions. The author highlight that wind directions between 0-30 and 120-180, the dominant function of the wind tower is extracting the air out of the building, and in incident angles between 45-105, they function as air exchangers as the supply and extract air flows have equal amounts. Their observations are contrary to the general perception of wind towers as catchers of the cool air and therefore they highlight the importance of assessing this architectural component within a building context (Dehghani Mohamadabadi, Dehghan, Ghanbaran, Movahedi & Dehghani Mohamadabadi, 2018).

In two complementary studies, using smoke visualization in a wind tunnel and a semi-analytical model, Kazemi et al and Dehghan et al have visualised the flow

in one-sided wind towers with flat, inclined and curved roofs (figure 3.2). They have measured the pressure coefficients around all external and internal surfaces of the tower and the induced airflow rates at wind speeds of 10, 15 and 20 m/s and wind incident angles of 0, 15, 30 and 60 degrees. Their experiments demonstrate that at zero incident angle curved roof one-sided wind tower performs 10% and 4.5% better than those with flat and inclined roofs respectively (Kazemi, Dehghan, Manshadi & Mohagheghian, 2012). The wind tower with inclined roof compared to the other two captures more airflow at higher wind incident angles and is the least sensitive one to the change in wind direction (Dehghan, Kazemi & Manshadi, 2013). In fact, changing the wind direction from 0 to 60 degrees, the flat, curved and inclined roof towers induce less airflow rates for 63%, 54% and 35% correspondingly (Dehghan et al, 2013). The authors investigating wind towers with 15°, 30° and 45° degrees of roof inclination, have identified that the steeper roof causes smaller vortices inside the tower and thus this smaller separation zone allows a larger effective airflow passage that consequently results in a better ventilation performance (Kazemi et al, 2012).

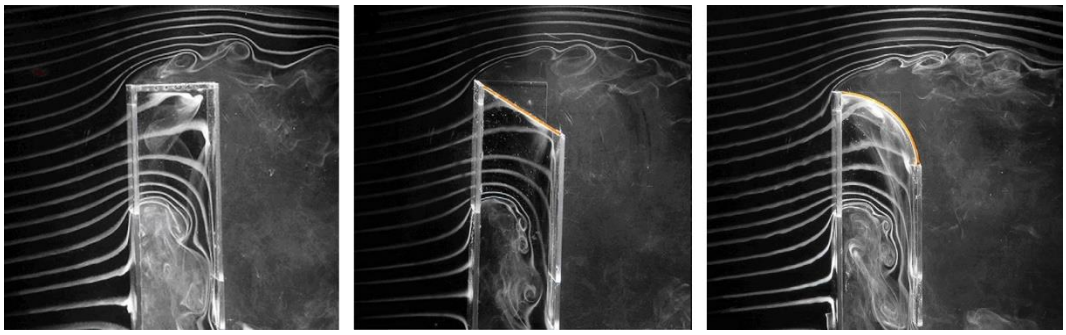

Figure 3.2. Smoke visualization test demonstrating how a curved roof one-sided wind tower can perform better than the ones with inclined roof and flat roof respectively (Kazemi et al, 2012)

In another CFD study, Ghadiri et al have assessed how the height of a four-sided wind tower can affect its performance. The square plan wind towers' heights ranged between 3.5 and 10.5 meters (Ghadiri, Ibrahim & Dehnavi, 2011) while those with rectangular cross section had a height variation between 4.5 and 18.5 meters (Ghadiri, Lukman & Mohamed, 2014). These studies show that with heights greater than 6 meters, the wind tower becomes unable to further reduce the temperature of the induced airflow. Furthermore, the ventilation performance of the taller towers is worse than the shorter ones even though the wind velocity on the windward side of the tower increases with height.

The performance of wind towers in providing thermal comfort has been investigated in 2D simulations by Reyes et al and Hosseini et al. Reyes et al have

majorly focused on the intersecting aperture between the tower and the room (Reyes, Moya, Morales & Sierra Espinosa, 2013). Their results show how different configurations can change the direction and magnitude of the induced airflow in room and those of the leeward tower channel. Hosseini et al have instead studied the effect of height, width (cross section area), roof detail and tower outlet detail (Hosseini, Shokry, Ahmadian Hosseini, Ahmadi & Calautit, 2016). Their CFD analysis show that the increase in height of the wind tower reduces the ventilation airflow in the lower room; tightening the wind tower channel can majorly affect the induced airflow velocity; the addition of a curve roof to the opening of the tower can improve the entrance of the flow in the wind tower channel, even though this does not impact the airflow distribution in the room significantly; a curved detail at the outlet of the wind tower, on the other hand, can direct the airflow to the room more effectively. A bigger induced airflow can create a higher velocity in the lower parts of the room causing discomfort to the occupants (Hosseini et al 2016).

In order to assess thermal comfort, in both studies, to each wall surface of the model a specific temperature has been assigned. The internal space of the room has been divided into 15 parts and the temperature and velocity of each part have been measured. Finally, using Olgyay diagram (Reyes et al, 2013) and CBE tool for calculating thermal comfort based on PMV method (Hosseini et al 2016), the comfort of the occupants has been assessed in each of these 15 regions. Their overall observation is that with a wind velocity of 4 m/s at the wind tower entrance, this architectural component is able to provide moderate to high thermal comfort level for the occupants and any slight variation in the design details of this structure, affecting the induced airflow in terms of velocity, can change the comfort condition.

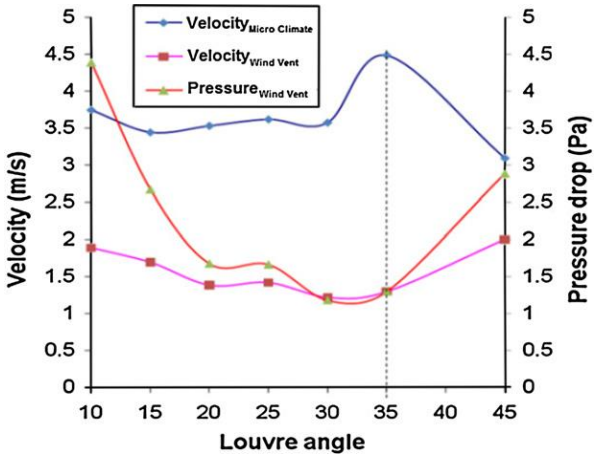


Figure 3.3. Effect of louver angle on the velocity and pressure drop in a wind tower (Hughes & Ghani, 2010) (Hughes, Calautit & Ghani, 2012)

Hughes & Ghani have employed CFD and wind tunnel to investigate the effect of louvers and its inclination on the performance of a four-sided wind tower in terms of air velocity and pressure (figure 3.3). The louver angles ranged between 10°-45° with 5° degree increments and the external wind velocity was set at 4.5 m/s representing the average speed in UK. His study shows that the optimum louver inclination is 35° which improves the occupants' comfort level by 45% (Hughes & Ghani, 2010). In another CFD study using the same wind condition and wind tower as before, Hughes & Ghani have examined the effect of damper angles (figure 3.4). Their investigation using four dampers with angles ranging between 0 and 90 degrees shows that the optimum damper angles that are able to reduce the ventilation flow in compatibility with the British standards are those between 45 and 55 degrees (Hughes & Ghani, 2009).

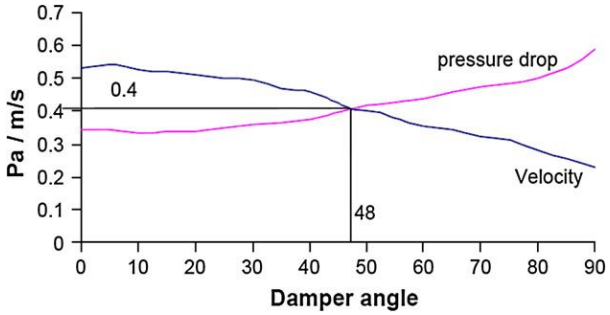


Figure 3.4. Effect of damper angle on velocity and pressure drop in a wind tower (Hughes & Ghani, 2009) (Hughes et al, 2012)

Effect of louvers has been assessed also by Liu et al. Validated by the wind tunnel data provided by Elmualim (Elmualim, 2006), they have employed CFD in order to understand how the length and the number of louver layers affect the performance of wind towers (Liu, Mak & Niu, 2011). Their study shows that with a wind velocity of 3 m/s and a zero wind incident angle, the airflow rate provided by a four-sided wind tower enhances when the number of louvers increases even though the improvement intensity reduces after a certain limit. It is important to note that in this parametrical assessment, the gap between the louvers were kept constant so any increase in the number of louvers resulted in a taller wind tower with a taller aperture. On the other hand, they have shown that the optimum louver length for louver angle of 45 degrees, providing the maximum air flow rate, is $\sqrt{2}$ times the gap between the two louver layers.

Nejat et al have experimentally and numerically studied a two-sided wind tower with wing walls and have compared it with a conventional wind tower in Malaysia (Nejat et al, 2016). A boundary layer wind tunnel test has been done with wind

velocity of 10 m/s on three wind towers with wing wall angles of 30, 45 and 60 degrees, then, a similar CFD analysis was performed on wind towers having wing wall angles ranging between 5 and 70 degrees at 5 degree increments in a 2.5 m/s wind speed representing the average velocity in Malaysia. The results of the analyses show that the optimum wing wall angle inducing the greatest inflow velocity is 30 degrees while the worst is 70. The supply air's average velocity by these two angles are 0.735 m/s and 0.675 m/s respectively.

### 3.2.3 Building and window configuration

There have been studies focusing on the effect of building's window size and position on cross ventilation using wind towers. For instance, Ghadiri et al observing the contours of velocity magnitude in CFD have found that the best window position in a room ventilated by a four-sided wind tower is down the leeward wall opposite the wind tower (Ghadiri et al, 2013).

Montazeri & Montazeri in 2018 studying one-sided wind-towers and zero wind incident angle, have compared the effect of window size. Their CFD analysis has proven that as long as the window is smaller than the wind tower's opening, the increase in window size improves the cross ventilation. Whereas, when the outlet window is larger than the wind tower's inlet, the increase in window size does not affect the performance considerably.

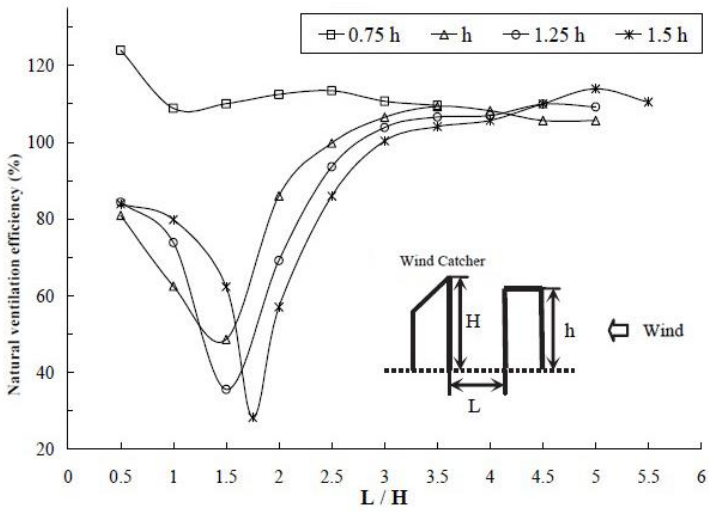


Figure 3.5. How placing an object upstream of a one-sided wind tower affects its natural ventilation efficiency (Montazeri & Azizian, 2008)

Placing an upstream object –e.g. a building or another wind tower among others, can affect a wind tower's performance. This has been studied by Montazeri

for one-sided (Montazeri & Azizian, 2008) (figure 3.5) and two sided wind towers (Montazeri & Azizian, 2009) (figure 3.6) and by Dehghan et al for one-sided wind towers (Dehghan et al, 2013).

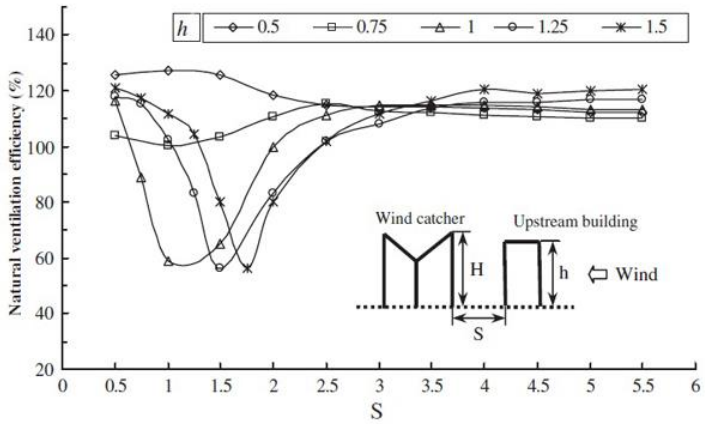


Figure 3.6. How placing an object upstream of a one-sided wind tower affects its natural ventilation efficiency (Montazeri & Azizian, 2009)

Su et al have studied the ventilation behaviour of Monodraught commercial wind towers experimentally and numerically in various wind speeds and directions. They have used a cone flow meter and a blower fan in order to measure the ventilation flow rate induced by the wind tower into its lower test chamber. They have done several CFD assessments for wind directions 0, 45 and 90. At 0 incident angle, different inlet pressures were set to assess the pressure sensitivity of their monitoring. Additionally, using CFD they have installed the same cylindrical four-sided louvered wind tower on flat-roof and pitched-roof buildings in far-field wind conditions in order to measure the ventilation flow rate in each building type. They conclude that the wind direction has a small effect of less than 20% on the extract flow rate. However, the wind direction is more pronounced when the supply air flow rates are small. A pitched-roof is shown to perform better especially if the building does not contain any other aperture than the wind tower. Furthermore, they confirm that the temperature difference between outdoor and indoor has a limited positive effect which is especially negligible when the wind speed is larger than 3 m/s (Su, Riffat, Lin & Khan, 2008).

Ameer et al have investigated the effect of roof typology of building on performance of wind towers using CFD (Ameer, Chaudhry & Agha, 2016). They have compared models with flat roof, 90-degree pitched roof, narrow roof inspired

by Venturi effect, curved roof, and tilted curved roof, all having a commercial wind tower on the roof center while the wind incident angle is 0, 45 and 90. Their study shows that the model with narrow roof has the highest air flow rate, lowest mean age of air, highest indoor velocity, and highest air change efficiency at wind angles 0 and 45.

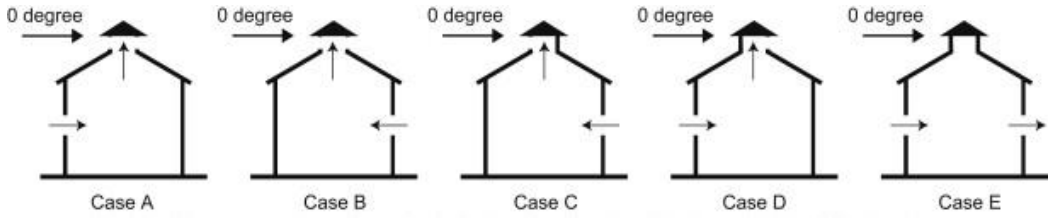


Figure 3.7. The cases in the monitor roof assessment by Kobayashi et al, 2013

Another CFD assessment on pitched roofs has been done by Kobayashi et al on buildings having monitor roofs which act similarly to the wind towers (figure 3.7) (Kobayashi, Chikamoto & Osada, 2013). Their study shows that a monitor roof can majorly enhance the ventilation airflow rate inside the building compared to buildings with windows only. However, the distance between the neighboring buildings and the target building with a monitor roof does not significantly affect the performance of the latter. Moreover, they have compared the cases where the monitor roof has two openings on opposite sides and where either the leeward or the windward opening is closed. Their study shows that in zero wind incident angle there is not a major difference between one-sided and two-sided monitor roofs but when the wind direction deviates to 45 and then 90 degrees, the two-sided monitor roof performs much better.

Calautit et al have investigated how the arrangement and spacing of multiple louvered four-sided wind towers on top of a single building can affect the ventilation airflow, its indoor distribution and the CO2 concentration as the indicator of indoor air quality (Calautit, O'Connor & Hughes, 2014). Their wind tunnel and CFD assessment have shown that in a test room representing a classroom of 30 students, a parallel arrangement of wind towers, i.e. positioning one in the wake of the other at zero wind incident angle, can cause the leeward wind tower let in the exhaust airflow of the windward wind tower into the building and thus re-increasing the CO2 concentration. Increasing the distance between parallel wind towers, however, can improve this condition by augmenting the air velocity in the inlet opening of the leeward wind tower. A staggered arrangement can significantly perform better in this regard. Moreover, in staggered arrangement a larger area of negative pressure is created behind the leeward side of the wind tower which results

in a higher exhaust air speed. Of course, any change in the wind direction can deviate the wake region and affect the above-mentioned result.

Using a CFD with RNG k-ε turbulence model and a Lagrangian particle tracking model, Liu et al have analysed the air flow pattern and the particle dispersion in four different layouts with different placements of windows and heat sources, in a constant wind velocity and direction (Liu et al, 2011). The have concluded that the best side of the room for a window placement is the leeward side. This position guarantees a better air velocity and contaminant concentration uniformity in the room.

Asfour & Gadi have integrated three wind tower configurations with building having domes or vaults (Asfour & Gadi, 2006). They have employed CFD to simulate 8 models at wind velocities of 1 and 3 m/s and wind directions of 0, 45 and 90 degrees. They have concluded that for deep plan buildings, using curved roofs and wind tower is an effective strategy especially for low wind velocities and have proposed a series of guidelines based on the results of their experiment which are as follows: the wind tower acting as an air supply increases the outflow rate through windows which consequently improves the internal airflow distribution; a wind tower acting as an exhaust works better when the building plan is not very deep; and the windward wind tower increases the air suction through roof openings.

Heidari et al have used CFD to study the vernacular homes of Sistan, Iran, where the most predominant climatic feature is the north-western wind blowing during summer between June and September. The authors have chosen the most popular architectural elements such as the Sistani type of roof, the short one-sided wind tower typical of that region known as Kolak, and the two façade openings called Dariche and Surak. Finally, they have simulated three building layouts at a wind speed of 9 m/s. Their overall observation is that despite the strong wind entering from the various narrow openings of the buildings, the indoor airflow is very calm. In cases where the main façade is perpendicular to the wind direction, the rooms act separately in terms of ventilation. Only when the shorter façade faces the wind, there is an airflow between the upstream and downstream rooms. However, orienting buildings of the last type in a scale of a village, could create very windy alleyways causing discomfort for the citizens. The results of this computational assessment have been validated with in-situ measurements (Heidari, Sahebzadeh & Dalvand, 2017).

Benkari et al have compared two types of wind towers in a semi-enclosed courtyard in Sultan Qaboos University, Oman. The objective of their study was to improve the indoor air quality in the courtyard because the current design of the

yard's roof as a thin layer lifted by several truss structures on each side prevented the wind from circulating inside the yard (Benkari, Fazil & Husain, 2017). They have placed a 26-meter wind tower inside the courtyard with its outlet distant from the yard floor as the roof structure was unable to support the weight of the wind tower. Their proposed wind tower had a cross section area equal to a quarter of the yard. Their first wind tower model increased the ventilation airflow in the yard, however the distribution of this airflow was uneven. Therefore, in the second model, they added a cone structure underneath the wind tower outlet which comparatively improved the airflow distribution. The airflow rate achieved by the second model at a wind velocity of 4 m/s was at least 100 per cent higher than ASHRAE standard.

### 3.2.4 Integration of other passive systems

Due to the inadequacies of conventional wind towers in reducing the air temperature, Bahadori has suggested their combination with evaporative effect (Bahadori, 1994). His new designs (figure 3.8) include a wind tower with a wetted column which employs clay conduits or cloth curtains within the wind tower, and the other with wetted surface which uses evaporative cooling pads at the opening of the tower and has experimentally and theoretically assessed them (Bahadori, Mazidi & Dehghani, 2008). His evaluations of the two systems show that the wetted column wind tower is more suitable when the wind velocity is high, whereas the tower with wetted surfaces is more effective with low wind speeds. The highest temperature reduction can be achieved with wetted surface wind tower (Hughes, Calautit & Ghani, 2012).

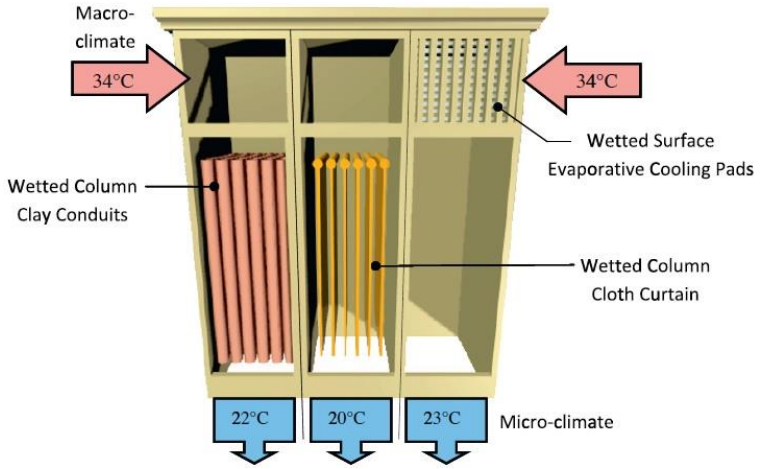


Figure 3.8. The evaporative wind towers designed and experimentally tested by Bahadori et al in 2008 (Hughes et al, 2012)

Kalantar has done a CFD test on an evaporative wind tower having water sprays on top. His experiment in a dry climate representing the desert cities of Iran (36 degrees of ambient temperature, 10% of relative humidity and a wind velocity of 3 m/s) shows that the water sprays are able to decrease the air temperature for a maximum of 10-15° degrees. Furthermore, the majority of this decline (8-12 degrees) happen at the top 2 meter of the 10-meter-tall wind tower even when the water sprays are spread evenly throughout the tower's height (Kalantar, 2009).

A similar CFD assessment has been done by Saffari & Hosseinnia. They have shown that the variation in air temperature has a greater impact on the temperature of the entering air through an evaporative wind tower compared to any change in the air velocity and relative humidity. They suggest that the size of the water droplets and their temperature have an impact on the performance of the evaporative wind tower, affirming that the water droplets with a higher temperature induce an air with higher temperature and lower relative humidity into the lower building. Furthermore, the higher the total surface area of all water droplets, the higher the exchange of mass and heat between the air and water and thus the cooler the air (Saffari & Hosseinnia, 2009).

In a study by Spentzou et al, several natural ventilation strategies have been implemented in one building in a small urban area represented by nine building blocks. These strategies include single-sided ventilation through windows and open internal doors, cross ventilation through windows and an airshaft on the roof, ventilation through a four-sided wind tower on the roof, ventilation through the wind tower combined with a dynamic façade, and finally combining the evaporative effect with the two latter ventilation types. The simulations have been done in CFD Phoenics code for three wind velocities and three wind directions. Their observations show that even though cross ventilation improves the very low ventilation conditions provided by single-sided model, the addition of wind tower can still enhance it substantially for around 76% which could further increase for 40% in addition of dynamic façade. In low wind speeds, the passive downdraught evaporative cooling reduces the indoor air temperature by 5 degrees. Lastly, the most suitable solution for Mediterranean region is recommended as a combination of wind tower, evaporative cooling and dynamic façade (Spentzou, Cook & Emmitt, 2017).

There are several other studies on evaporative wind towers such as those of Bowman et al, 1997, Belarbi, Ghiaus & Allard, 2006, Bouchahm, Bourbia & Belhamri, 2011, Ahmadikia, Moradi & Hojjati, 2012, Soutullo, Olmedo, Sanchez & Heras, 2011, Soutullo, Sanjuan & Heras, 2012, Kang & Strand, 2013, Haghighi

& Mohabbati, 2017, among others. The following picture (3.9) demonstrate the 14000 square meter laboratory building in Ahmadabad, India with its downdraft evaporative wind towers. Monitoring the building in its first 12-month period shown that the internal temperature was around 10-15 degrees lowers than the external one and no complaint was made by the staff about the comfort conditions (Ford, Patel, Zaveri & Hewitt, 1998).

Figure 3.9. Evaporative downdraft wind towers in Torrent Research Center in Ahmadabad, India (Torrent Pharmaceuticals ltd, n.d.)

Calautiti et al have done a wind tunnel test and a CFD analysis on louvered one-sided wind towers integrated with a heat pipes. In this study, the outdoor air temperature was assumed as 318 K and the temperature of the heat transfer device was set as 293 K. This study shows that with approaching wind velocities between 0.5 to 5 m/s, the integration of the heat transfer device in the wind tower will decrease the indoor air speed by a value ranging between 28% and 52%. However, using this device, the temperature can reduce between 5 to 12 degrees Celsius for approaching wind velocities of 5 and 1 m/s (Calautit, Hughes & Shahzad, 2015). They have compared the results of this study with a field test in Emirates, too (Calautit & Hughes, 2016).

Calautit and his team have done another experiment using wind tunnel and CFD on a louvered four-sided wind tower integrated with a heat pipes as a heat recovery system on the wind tower's roof in order to ensure the thermal comfort of the occupants in winter time in UK. The wind in their assessment has a zero incident angle and a uniform speed. However, as part of their experiment, the wind velocity varies between 1 and 5 m/s. Their experiment shows that the integration of the heat pipes can reduce the airflow rate between 8% and 17%. However, at a wind velocity

over 1 m/s, the induced ventilation range complies with the standards when the occupancy is 1.7 $m^2$ per person. Obviously, the heat pipes on wind tower's roof increased the temperature of the air entering and the room. This increase was measured as 4.5 K with the incoming outdoor air of 283 K and a heat pipe surface temperature of 293 K (Calautit, O'Connor & Hughes, 2016).

O'Connor et al have used CFD and wind tunnel to assess the integration of a rotary thermal wheel in a four-sided wind tower. They set the rotation speed of the rotary wheel at its maximum of 115 rpm causing the maximum blockage to the airflow. Their study shows that for a wind tower integrated rotary wheel to be able to provide the required ventilation rate in a classroom with 13 students and an occupancy of 1.8 $m^2$ per person, an inlet air velocity of 3 m/s is needed. Furthermore, they have observed that the outlet stream of the wheel has a higher air temperature than the inlet stream (set as 23.2 °C) by 3 °C. This temperature difference, in case of recovery can create an energy saving of 20% (O'Connor, Calautit & Hughes, 2014).

Nouanégué et al have combined a solar chimney with a wind tower in order to enhance its stack effect (Nouanégué, Alandji & Bilgen, 2008). This stack airflow is a combination of buoyancy-driven airflow due to the accumulated solar heat in the tower and an upward wind-driven airflow generated by placing the wind tower's aperture on the leeward side of it which creates a negative pressure at this outlet. The authors employed Simpler (semi-implicit method for pressure linked equations revised) algorithm for this two-dimensional assessment and have concluded that among others the wall thickness has a negligible effect on the ventilation performance when the Reynolds number is low, and that the aspect ratio of the wind tower has a direct effect on its ventilation performance.

In a CFD study by Haghighi, Pakdel & Jafari (2016), a wind tower has been combined with a solar adsorption cooling system composed of a solar collector, a hot water tank and a two-bed silica gel-water adsorption chiller. The wind tower in this study is connected to a two-storey building and the effect of wind tower's height, the aperture size and the number and length of the cooling plates on the performance of the system has been investigated. The results show that the shorter wind towers provide slightly less number of air change. This, however, can be beneficial as the room's temperature declines more at lower air change rates. The length of the plates has a direct impact on the cooling of air, whereas any increase in the number of plates results in less cooling in low ACH values and more cooling in high ACH values. The system is proved to be able to cool the air between 10-20

degrees at various climatic conditions. Lower relative humidity provides the chance for a more pronounced cooling effect of the proposed system.

Sadeghi & Kalantar have employed CFD in order to assess the combination of wind towers and underground cooling (Sadeghi & Kalantar, 2018). Their model is inspired by some of the desert houses of Iran that had direct access to the underground Qanat network. The water from the Qanat in these houses would increase the humidity in basements of these houses. Occasionally, if wind towers were present, they helped in distributing this humidified cooler air of the basement in upper rooms. Sadeghi & Kalantar have performed their analysis on two models one in presence of underground water and the other in absence of it. Their leeward one-sided wind towers in these conditions were able to reduce the temperature in the underground channel by 15.4 and 7.6 degrees Celsius so that the final temperature in the basement was lowered from the initial value of 42 °C to 34.4 ° and 26.6 °C respectively. Their assumed underground temperature was 15 degrees Celsius at a 5-meter depth from the earth surface.

### 3.2.5 Wind towers in urban scale

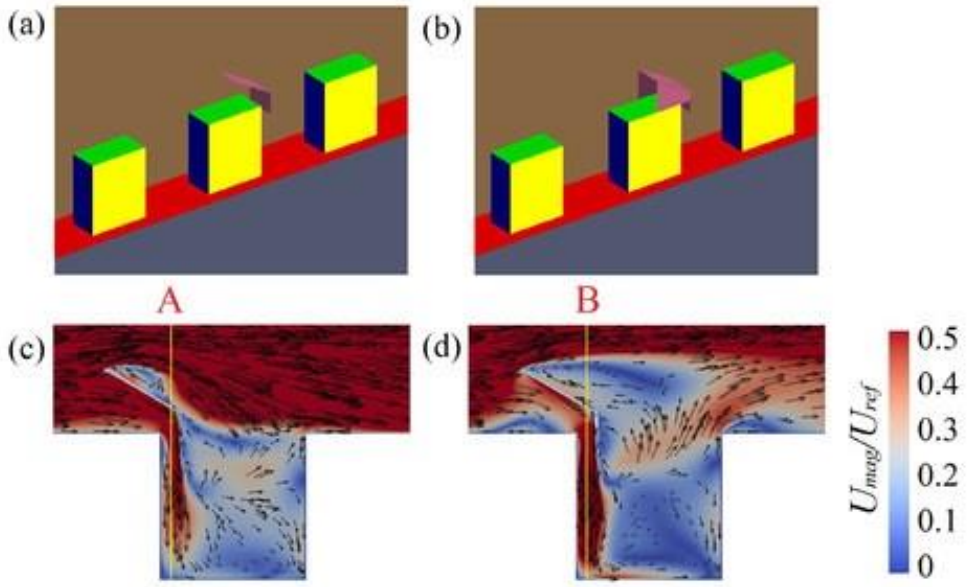


Figure 3.10. Wind towers with (a) an without (b) side walls can enhance the velocity of the airflow in street canyons (Chew et al, 2017)

Chew et al, have experimentally and numerically evaluated whether or not the addition of wind towers to buildings can improve the limited air flow in street canyons (Chew, Nazarian & Norford, 2017). Their two-dimensional assessment

shows that a wind tower facing the wind direction can enhance the near-ground wind velocity by 2.5 times in street canyons having aspect ratio of 1. However, a leeward wind tower acts as a tall building and decreases the downstream air velocity. Their three-dimensional simulations confirm the 2D results with lower values. In fact, the near-ground air velocity in 3D urban canyons increases by only 15% using a wind tower with no side walls. Adding wall to the wind tower improves the air channeling and increases the air velocity by 30% in vicinity of the ground (see figure 3.10).

## 3.3 Wind towers' shapes and positions in literature

Table 3.1 summarizes the wind towers studied in the literature review with a focus on their form characteristics including their position with respect to the building, shape and number of openings, and the wind direction and the inlet profile utilized. Finally, this table provides an overview of the methods of assessing wind towers and highlights the gap this thesis aims to fulfill.

The popularity of CFD validated by the experimental data obtained from wind tunnel tests in studying wind towers is evidently seen in the table. The majority of the wind towers used in these studies are three dimensional structures coupled either with a room or a building. However, in terms of shape and position of the wind tower with respect to the building, there is not much consistency. There are many articles considering a tall tower with its outlet aperture on the wall of the lower space, and there are many others considering a short structure on rooftop of the space. Those towers placed on the roof, are either commercial louvered wind towers positioned on the roof center or there are simplified structures on the roof edge at the farthest distance from the lower room's window. In addition, few articles use an atmospheric boundary layer wind profile and not many of them alter the wind direction in their assessments.

Therefore, in order to fill in such a gap, this thesis aim to assess different positions of short cuboid rooftop one-sided and four-sided wind towers performance, in different atmospheric wind directions. Moreover, since the performance evaluation of wind towers in majority of the previous studies were done by comparing airflow rate values, pressure coefficients, thermal comfort, and internal velocity, in this thesis two other parameters of mean age of air and air change efficiency are assessed, too. The simulations in this thesis have been performed in isothermal conditions.

Table 3.1. Literature review on wind towers

| authors | research method | opening | shape | position | wind or stack | inlet profile | wind direction | aim of study |
|---|---|---|---|---|---|---|---|---|
| Mahyari 1996 | wind tunnel | 2, 4 | 3D tower | beside the building | w & s | ABL | 0, 90, 180 | effect of internal divisions of the wind tower |
| Awbi et al 2002 | wind tunnel full scale | 4 | 3D cuboid/ louvered | roof centre | w & s | uniform | 0, 15, 30, 45 | wind tower performance under various wind speeds and directions, wind tower performance with dampers |
| Asfour et al 2006 | CFD | 1 | 3D tower | beside the building, leeward and windward | w | ABL | 1, 45, 90 | wind tower and curved roof buildings |
| Li et al 2007 | CFD | 4 | 3D cuboid/ louvered | not coupled with a building | w | uniform | 0, 15, 30, 45 | wind tower performance under various wind speeds and directions |
| Montazeri & Azizian 2008 | wind tunnel | 1 | 3D cuboid | roof edge | w | uniform | 0-180 at 15 | wind tower performance |
| Nouanegue et al 2008 | N.A. | 1 | 2D tower | Not coupled with a building | w & s | uniform | N.G. | stack wind tower with solar chimney |
| Bahadori et al 2008 | full-scale experiment, analytical model | 1 | 3D tower | beside the building | w & s | ABL | varied | integration of evaporative cooling |

| | | | | | | | | |
|---|---|---|---|---|---|---|---|---|
| Su et al 2008 | CFD, cone flow meter & blower fan | 4 | 3D cylinder | roof centre | w & s | uniform | 0, 45, 90 | pitched roof vs flat roof, effect of wind direction, wind vs buoyancy |
| Saffari et al 2009 | CFD | 1 | 3D tower | beside the building | w & s | uniform | 0 | evaporation effect |
| Kalantar 2009 | CFD | 1 | 3D tower | not coupled with a building | w & s | uniform | 0 | evaporation effect |
| Montazeri et al 2009 | CFD, wind tunnel | 2 | 3D cuboid | roof edge | w | uniform | 0-180 at 15 | wind tower performance |
| Hughes et al 2009 | CFD | 4 | 3D cuboid/ louvered | roof centre | w | uniform | 0 | effect of damper angle |
| Hughes et al 2010 | CFD, wind tunnel | 4 | 3D cuboid/ louvered | roof centre | w | uniform | 0 | effect of louver angle |
| Hughes et al 2011 | CFD | 4 | 3D cuboid/ louvered | roof centre | w & s | uniform | 0 | wind vs buoyancy |
| Liu & Mak 2011 | CFD | 4 | 3D cuboid/ louvered | roof centre | w & s | uniform | 0 | louver numbers and their length |
| Bouchahm 2011 | full-scale experiment, analytical model | 1 | 3D tower | beside the building | w & s | ABL | varied | integration of evaporative cooling |
| Montazeri 2011 | CFD, wind tunnel | 2, 3, 4, 6, 12 | 3D cylinder | roof edge | w | uniform | 0-180 at 15 | effect of number of opening |
| Ghadiri et al 2011 | CFD | 4 | 3D tower | beside the building | w & s | uniform | 0 | effect of wind tower height on the induced temperature |

| | | | | | | | | |
|---|---|---|---|---|---|---|---|---|
| Soutullo et al 2012 | CFD | 3 | 3D cylinder tower | not coupled with a building | w & s | uniform | varied | evaporation effect |
| Ahmadikia et al 2012 | CFD | 1 | 2D tower | beside the building | w & s | uniform | 0 | evaporation effect |
| Kazemi et al 2012, Dehghan et al 2013 | CFD, wind tunnel, semi-analytical model | 1 | 3D cuboid | roof edge | w | uniform | 0, 15, 30, 45, 60 | effect of wind tower roof shape and inclination |
| Ghadiri et al 2013 | CFD | 4 | 3D tower | beside the building | w | uniform | 0 | effect of wind tower internal partitions/best placement of window |
| Ghadiri et al 2013 | CFD | 2 | 3D cuboid | roof edge | w | uniform | 0-90 at 15 | wind tower performance, effect of computational parameters |
| Reyes et al 2013 | CFD | 2 | 2D tower | beside the building | w & s | uniform | 0 | thermal comfort, effect of outlet opening |
| Kang el al 2013 | CFD | 1 | 2D tower | not coupled with a building | w & s | uniform | 0 | evaporation effect |
| Hosseinnia et al 2013 | CFD | 4 | 3D tower | beside the building | w & s | ABL | 0 | effect of internal partitions of the wind tower |
| Kobayashi et al 2013 | CFD, wind tunnel | 1, 2 | 3D cuboid | roof centre | w | ABL | 0, 45, 90 | monitor roofs |
| Cruz-Salas et al 2014 | open water channel | 1, 2, 4 | 3D cuboid | roof centre | w | uniform | 0, 90 | windward window and wind tower with different partitions |
| Ghadiri et al 2014 | CFD | 4 | 3D tower | beside the building | w | uniform | 0 | effect of wind tower height on the induced airflow rate |

| | | | | | | | | |
|---|---|---|---|---|---|---|---|---|
| Mahdavinejad 2014 | Vasari | 1, 2, 4 | 3D tower | beside the building | w & s | N.A. | varied | wind tower performance |
| Calautit & Hughes 2014a | CFD, wind tunnel | 4 | 3D cuboid, louvered | roof centre | w | uniform | 0, 30, 45, 60, 90 | wind tower performance |
| Calautit et al 2014 | CFD, wind tunnel | 1 | 3D cuboid/ louvered | roof centre | w & s | uniform | 0, 30, 60, 90 | integration of heat transfer device for cooling |
| Calautit el al 2014 | CFD, wind tunnel | 4 | 3D cuboid, louvered | roof centre | w | uniform | 0, 30, 45, 60, 90 | arrangement of multiple wind tower on the roof |
| Calautit et al 2015 | CFD, wind tunnel | 1 | 3D cuboid/ louvered | roof centre | w & s | uniform | 0, 30, 60, 90 | wind towers integrated with heat transfer device |
| Calautit et al 2016 | CFD, wind tunnel | 4 | 3D cuboid, louvered | roof centre | w & s | uniform | 0 | wind towers integrated with heat recovery systems |
| Ameer er al 2016 | CFD, wind tunnel | 4 | 3D cuboid, louvered | roof centre | w | uniform | 0, 45, 90 | wind towers on different building roof configurations |
| Hosseini et al 2016 | CFD | 2 | 2D tower | beside the building | w & s | uniform | 0 | thermal comfort, effect of height, width, outlet and inlet detail |
| Nejat et al 2016 | CFD, wind tunnel | 2 | 3D cuboid | roof centre | w | ABL | 0 | wind tower with wing walls |
| Haghighi et al 2016 | CFD | 1 | 3D tower | beside the building | w & s | ABL | 0 | wind tower combined with solar adsorption cooling |
| Benkari et al 2017 | CFD | 1 | 3D tower | within the yard | w | ABL | 0 | IAQ in semi-enclosed courtyard |
| Chew et al 2017 | CFD, wind tunnel | 1 | 2D/ 3D cuboid | roof edge | w | ABL | 0, 180 | wind towers in urban canyons |

| | | | | | | | | |
|---|---|---|---|---|---|---|---|---|
| Sadeghi et al 2017 | CFD | 1 | 3D tower | room floor centre by underground channel | w & s | ABL | 0 | underground cooling with and without water in the underground channel |
| Heidari et al 2017 | CFD | 1 | 3D cuboid | roof centre | w | uniform | 0 | compound rooms in Sistani architecture |
| Dehghani Mohamadabadi et al 2018 | CFD, wind tunnel | 4 | 3D tower | roof, beside a courtyard | w | uniform | 0-180 at 15 | wind tower performance, connected to a courtyard and an Iwan |
| Spenzou et al 2019 | CFD | 4 | 3D tower | beside the building | w & s | ABL | N.G. | comparison between various natural ventilation strategies |

# Chapter 4

# CFD Validation study

## 4.1 Introduction

Computational Fluid Dynamics is an ideal tool for parametric studies related to fluid flows. It can be used to generate quantitative predictions of fluid flows by numerically solving the mathematical equations following the three fundamental principles of fluid motion: mass is conserved, energy is conserved, and momentum is conserved (Hoffmann & Chiang, 2000).

The continuing improvement of computers has made CFD a much more economical tool compared to wind tunnel experiments. However, despite offering more detailed information about the flow-field, CFD results especially for turbulent flows are subject to error and therefore they have to be validated by physical models (Anderson, 2009). This inaccuracy in turbulent flows is due to the fact that the CFD solutions used in various turbulence models are all approximations of the real physics because the various constants used in these turbulence models depend on the empirical data.

Every CFD code consist of three main elements: pre-processor step for problem formulation and geometry/mesh construction, solver step for numerically solving the fluid flow equations in the computational domain, and post-processor step for analyzing and representing the results of the simulations.

### 4.1.1 Governing equations and their discretization

In CFD, the fundamental fluid physics principles are addressed by a set of governing equations that can be stated in integral or differential forms if applied to an extended region or to a point/fluid particle.

Mass conservation or continuity equation is a scalar equation based on the principle that a specific collection of neighboring fluid particles moves and deforms in terms of volume but its mass remains constant (equation 4.1).

The scalar energy equation is based on the first law of thermodynamics that the thermal energy cannot be created or destroyed and it can transfer from one place to the other or convert into other forms of energy (equation 4.2).

Momentum is a vector quantity as the product of the mass and velocity of a particle and its conservation addresses Newton's second law. For a three dimensional problem of an incompressible isothermal fluid with constant viscosity such as the air, the conservation of the momentum is expressed using three scalar (equations 4.3) or one vector equations (equation 4.4) and which are known as Navier-Stokes equations (Sert, n.d.) (Ramponi, 2014).

Eqn 4.1: $$\text{div}\,\vec{V} = 0$$

Eqn 4.2: $$\rho\, C_p \left[\frac{\partial T}{\partial t} + \vec{V}.\,\text{grad}\, T\right] = k\,\text{grad}^2\, T + \phi$$

Eqn 4.3a: $$\rho\,\frac{\partial u}{\partial t} + \rho\,\text{div}(u\vec{V}) = -\,\frac{\partial P}{\partial x} + \text{div}(\mu\,\text{grad}\, u)$$

Eqn 4.3b: $$\rho\,\frac{\partial v}{\partial t} + \rho\,\text{div}(v\vec{V}) = -\,\frac{\partial P}{\partial y} + \text{div}(\mu\,\text{grad}\, u)$$

Eqn 4.3c: $$\rho\,\frac{\partial w}{\partial t} + \rho\,\text{div}(w\vec{V}) = -\,\frac{\partial P}{\partial z} + \text{div}(\mu\,\text{grad}\, u)$$

Eqn 4.4: $$\rho\left[\frac{\partial \vec{V}}{\partial t} + \vec{V}.\,\text{grad}\,\vec{V}\right] = -\,\text{grad}\, p + \mu\,\text{grad}^2\,\vec{V} + \rho\,\vec{f}$$

In the above equations, $\vec{V}$ is the instantaneous velocity vector. u, v and w are the x, y and z components of the instantaneous velocity vector. div and grad are the divergence and gradient operators, $\rho$ the fluid density, $C_p$ the specific heat at constant pressure, t the time coordinate, T the temperature, k the thermal conductivity, $\phi$ the dissipation rate, p the instantaneous pressure, $\mu$ the dynamic viscosity, and $\vec{f}$ is the body force per unit of mass.

The above partial differential equations cannot be solved analytically except in special cases. Therefore, discretization methods are employed to approximate the solution numerically by a system of algebraic equations. A CFD calculation is usually performed using one of the following three discretization methods: the finite-difference method, the finite-element method and finite-volume method.

In the finite-difference method, which is suitable for simple geometries and not for complex flow problems, the differential equations are approximated by nodal values of the functions at each grid point of the solution domain (Ferziger & Perić, 2002).

In finite element method, the equations are multiplied by a weight function and then they are integrated over the domain which is divided into a set of elements approximated by triangles in 2D and tetrahedrons or hexahedrons in 3D (Ferziger & Perić, 2002). This method is suitable for arbitrary geometries because the grids can be easily refined.

The control-volume or the finite-volume method is a special case of finite difference methods and is the one employed in CFD code Fluent utilized in this thesis. In this method, the domain is discretized into a finite set of control volumes or cells and the general conservation or transport equations are solved as surface and volume integrals on the surfaces and the volumes of each of these cells (Ferziger & Perić, 2002). This method has the broadest applicability in CFD. In finite-volume method, the results of the solver step at the center of all cells are the numerical values of the three velocity components, the pressure and the turbulence quantities.

### 4.1.2 Turbulence models

Predicting turbulent flows is a very important issue when modeling natural ventilation in buildings. Turbulence is one of the unsolved problems in physics. Even though there is no accurate definition for turbulent flows, they have a number of common properties: they are irregular and highly unsteady, they have a high diffusivity, they are three-dimensional and dissipative, their fluctuations have a broad range of length and time scales, and they have high Reynolds number. Reynolds number as the ratio between inertial and viscous forces is used to describe turbulent vs laminar flows (equation 4.5).

Eq 4.5: $$\mathrm{Re}=\frac{UL}{\upsilon}$$

In which U is the characteristic velocity, L the characteristic length of the flow and $\upsilon$ the kinematic viscosity of the fluid.

The three main methods for predicting turbulent flows are Direct Numerical Simulation (DNS), Large Eddy Simulation (LES), and Reynolds-Averaged Navier-Stokes equation (RANS) which is divided into two principle types: Reynolds-stress model and eddy-viscosity model (Teodosiu, Ilie & Teodosiu, 2014) (Ferziger & Perić, 2002).

In DNS, the Navier-Stokes equations are solved for all scales of the motion in turbulent flow. For this reason, this method has a high accuracy and an extremely high computational cost. Therefore, the application of this method is limited to low Reynolds numbers and simple geometries.

In LES, the Navier-Stokes equations are solved for a filtered velocity field. Meaning that the turbulent eddies that are larger than the filter's size are solved while those smaller are modelled using subgrid-scale models. In order to resolve the eddies LES requires an accurate spatial and temporal discretization. Though this accuracy and thus the computational requirements in LES are less than those in DNS. This method is used for simulating the wind flow around buildings.

With RANS, which is the most commonly applied and validated method in numerical assessment of airflow in and around the buildings, the mean flow is solved and all the scales of the turbulence are modelled, i.e. the solution variables of the Navier-Stokes equations are decomposed into a mean (either time-averaged if the flow is statistically steady or ensemble-averaged if the flow is time-dependent) and a fluctuating component. This averaging creates Reynolds stresses as additional unknowns which have to be computed either using Reynolds-stress transport equations or through application of various turbulence models.

Therefore, the momentum conservation equations for RANS are as expressed in equations 4.6, with the terms in brackets representing the Reynolds stresses. The U, V and W are the x, y and z values for mean wind velocity.

Eqn 4.6a: $$\rho \frac{\partial u}{\partial t} + \rho \, \mathrm{div}(U\vec{V}) = - \frac{\partial P}{\partial x} + \mathrm{div}(\mu \, \mathrm{grad} \, u) + [- \frac{\partial \overline{\rho u'^2}}{\partial x} - \frac{\partial \overline{\rho v' u'}}{\partial y} - \frac{\partial \overline{\rho w' u'}}{\partial z}]$$

Eqn 4.6b: $$\rho \frac{\partial v}{\partial t} + \rho \, \mathrm{div}(V\vec{V}) = - \frac{\partial P}{\partial y} + \mathrm{div}(\mu \, \mathrm{grad} \, u) + [- \frac{\partial \overline{\rho u' v'}}{\partial x} - \frac{\partial \overline{\rho v'^2}}{\partial y} - \frac{\partial \overline{\rho w' v'}}{\partial z}]$$

Eqn 4.6c: $$\rho \frac{\partial w}{\partial t} + \rho \, \mathrm{div}(W\vec{V}) = - \frac{\partial P}{\partial z} + \mathrm{div}(\mu \, \mathrm{grad} \, u) + [- \frac{\partial \overline{\rho u' w'}}{\partial u} - \frac{\partial \overline{\rho v' w'}}{\partial y} - \frac{\partial \overline{\rho w'^2}}{\partial z}]$$

The most common turbulence models for approximating all the scales of turbulence in RANS equations are the k-ε models, the mixing-length model, the Reynolds stress equation model (RSM) and the algebraic stress model (ASM), among which the k- ε is the most used one.

The effect of turbulence can be represented as an increased viscosity (Ferziger & Peric, 2002). This assumption is the basis of the k- ε turbulence model. The eddy viscosity distribution in Boussinesq hypothesis (equations 4.7) that relates the stresses to the mean deformation rate is obtained through one or more transport equation. In k-ε model and its three variants, these transport equations are for turbulent kinetic energy (k) (equation 4.8) and turbulent dissipation rate (ε) (equation 4.9).

Eqn 4.7a: $$- \rho \overline{u_i' u_j'} = 2\mu_t S_{ij} - \frac{2}{3} \rho k \delta_{ij}$$

Eqn 4.7b: $\mu_t = \rho C_\mu \frac{k^2}{\varepsilon}$

Eqn 4.7c: $S_{ij} = \frac{1}{2}\left(\frac{\partial U_i}{\partial x_j} + \frac{\partial U_j}{\partial x_i}\right)$

Eqn 4.8: $k = \frac{1}{2}\overline{u_i' u_i'}$

Eqn 4.9: $\varepsilon = \upsilon \overline{\frac{\partial u_i'}{\partial x_j}\frac{\partial u_i'}{\partial x_j}}$

In the above equations, $\mu_t$ is the turbulent viscosity, $S_{ij}$ the mean strain rate, and $\delta_{ij}$ the Kronecker delta. $C_{\mu\ is}$ an empirical constant and $\upsilon$ the kinematic viscosity.

Standard, Realizable and RNG k-ε all share the transport equations for k and ε. Their difference is in the calculation method of the turbulent viscosity, the turbulent Prandtl number, and in the generation and destruction terms in the ε equation (ANSYS, 2009).

The standard k-ε model was developed by Jones & Launder in 1972 for fully turbulent flows with negligible effects of molecular viscosity. It is a semi-empirical model based on model transport equations for k and ε, in which the model transport equation for k is derived from the exact equation but the model transport equation for ε is obtained using physical reasoning and thus is not similar to its exact mathematical equation (ANSYS, 2009). The two equations are expressed as follows:

Eqn 4.10a: $\rho\frac{\partial k}{\partial t} + \rho\ \mathrm{div}(k\vec{V}) = \mathrm{div}(\frac{\mu_t}{\sigma_k}\ \mathrm{grad}\ k) + 2\mu_t S_{ij}S_{ij} - \rho\varepsilon$

Eqn 4.10b: $\rho\frac{\partial \varepsilon}{\partial t} + \rho\ \mathrm{div}(\varepsilon\vec{V}) = \mathrm{div}(\frac{\mu_t}{\sigma_\varepsilon}\ \mathrm{grad}\ \varepsilon) + C_{1\varepsilon}\frac{\varepsilon}{k}2\mu_t S_{ij}S_{ij} - \rho C_{2\varepsilon}\frac{\varepsilon^2}{k}$

In which σ is the turbulent Prandtl number recommended as 1.00 for $\sigma_k$ and 1.30 for $\sigma_\varepsilon$. $G_k$, the turbulent kinetic energy produced by the mean velocity gradients is expressed as $2\mu_t S_{ij}S_{ij}$. For $C_\mu$ in equation 4.7b, and $C_{1\varepsilon}$ and $C_{2\varepsilon}$ in equation 4.10b the values of 0.09, 1.44 and 1.92 are recommended respectively (ANSYS, 2009).

In realizable k-ε model proposed by Shih, Liou, Shabbir, Yang & Zhu in 1995, the Schwarz inequality for the Reynolds shear stresses and the positivity of the normal Reynolds stresses are satisfied differently than in the standard k-ε model. In the new formulation for realizable eddy viscosity, $C_\mu$ is made sensitive to the mean flow and the turbulence (k, ε). And a new equation for dissipation rate has been proposed which is based on the dynamic equation for fluctuating vorticity. Therefore, in the realizable model, while the transport equation 4.10a in the

standard model is maintained, the equation 4.10b is varied to equation 4.11 as following:

Eqn 4.11: $$\rho\frac{\partial\varepsilon}{\partial t} + \rho\ \mathrm{div}\ (\varepsilon\vec{V}) = \mathrm{div}(\frac{\mu_t}{\sigma_\varepsilon}\ \mathrm{grad}\ \varepsilon) + \rho C_{1\varepsilon}\sqrt{2\mu_t S_{ij}S_{ij}}\ \varepsilon - \rho C_{2\varepsilon}\frac{\varepsilon^2}{k+\sqrt{\upsilon\varepsilon}}$$

While the constants $C_\mu$ and $C_{1\varepsilon}$ are calculated using formulas explained in Shih et al 1995, the values for $C_{2\varepsilon}$, $\sigma_k$ and $\sigma_\varepsilon$ are recommended as 1.9, 1.0 and 1.2 respectively.

The renormalization group (RNG) k-ε model was developed in 1992 by Yakhot, Orszag, Thangam, Gatski & Speziale. In this method, a statistical technique called renormalization group is applied to the instantaneous Navier-Stokes equations. Contrary to the standard and realizable models in which the constant values were derived from the experimental data, in RNG these values such as that of Prandtl number are explicitly computed. Moreover, a modified transport equation for the dissipation rate (ε) is utilized in order to increase the accuracy for the rapidly strained flows. The effect of swirl on the turbulence is also included in this model.

For the flows with high Reynolds number, the k-ε transport equations are expressed as:

Eqn 4.12a: $$\rho\frac{\partial k}{\partial t} + \rho\ \mathrm{div}(k\vec{V}) = \mathrm{div}(\alpha_k\ \mu_{eff}\ \mathrm{grad}\ k) + \tau_{ij}S_{ij} - \rho\varepsilon$$

Eqn 4.12b: $$\rho\frac{\partial\varepsilon}{\partial t} + \rho\ \mathrm{div}(\varepsilon\vec{V}) = \mathrm{div}(\alpha_\varepsilon\ \mu_{eff}\ \mathrm{grad}\ \varepsilon) + C^*_{1\varepsilon}\frac{\varepsilon}{k}\tau_{ij}S_{ij} - \rho C_{2\varepsilon}\frac{\varepsilon^2}{k}$$

The $\mu_{eff}$ as the effective viscosity and the $C^*_{1\varepsilon}$ as the strain-dependent correction term are calculated by equations 4.13 and 4.14.

Eqn. 4.13: $$\mu_{eff} = \mu + \rho C_\mu\frac{k^2}{\varepsilon}$$

Eqn. 4.14: $$C^*_{1\varepsilon} = C_{1\varepsilon} - \frac{\eta\ (1-\eta/\eta_0)}{1+\beta\eta^3}$$

In the above equations, η is calculated as $\frac{k}{\varepsilon}\sqrt{2S_{ij}S_{ij}}$ and the values 1.42, 1.68, 0.0845, 4.377 and 0.012 are used for constants $C_{1\varepsilon}$, $C_{2\varepsilon}$, $C_\mu$, $\eta_0$ and β respectively. Furthermore, $\alpha_k = \alpha_\varepsilon = 1.39$.

### 4.1.3 Near-wall treatment

In vicinity of the solid walls, the viscosity effect becomes more considerable. In these regions the flow has a low Reynolds number thus the turbulence models will be no longer valid. In fact, a near-wall flow has four layers: in the fourth and

the most outer layer, the flow is turbulent even though its velocity is affected by the wall shear stress; in the third layer the inertial effects are greater compared to viscous ones and the velocity profile is logarithmic, therefore, this layer is called the log-law layer; the second layer known as buffer layer is where the viscous and turbulent forces are almost equal; and finally in adjacency of the wall, there is the linear sub-layer where the viscosity effects are dominant and the velocity profile becomes linear.

Wall functions and low Reynolds number modelling are the two methods used for modelling the flow near the walls. In the low Reynolds number modelling, the three inner layers are solved following a modification to the turbulent model applied to the core flow. While, in wall-function method, employed in this thesis, the three inner layers are not numerically assessed. Instead, semi-empirical functions link the turbulent outer layer, the wall and the turbulence model in order to predict the flow in near-wall region.

The most common wall-functions are proposed by Launder and Spalding in 1974 and are known as standard wall functions which are applicable for smooth walls. For rough walls, an empirical model was developed by Schlichting named the equivalent sand-grain roughness model which predicts the skin friction and hear transfer between the turbulent flows and the rough wall surface (Schlichting, 1937).

In simulating the atmospheric boundary layer flows over a rough terrain surface described by an equivalent sand-grain roughness $k_s$, there are four requirements that have be satisfied simultaneously (Blocken, Stathopoulos & Carmeliet, 2007). One requirement is that the sand-grain roughness height $k_s$ of the terrain has to be smaller than half height of the first cell adjacent to the domain floor. At the same time, the following relationship between the three roughness parameters has to be valid in simulations done by ANSYS Fluent. In this equation, $y_o$ is the aerodynamic roughness length and $C_s$ is the roughness constant.

Eqn. 4.15: $$k_{s,ABL} = \frac{9.793\, y_0}{C_s}$$

## 4.2 Validation of the one-sided wind tower

In order to achieve reliable results, every CFD simulation has to be validated. The objective is to verify the validity of the applied CFD code, to assess the solution's numerical uncertainty, and to evaluate how accurately the physical or experimental situations are reproduced in the numerical assessment by CFD.

### 4.2.1 Experimental analysis

The reference experimental study on a one-sided wind tower model connected to a room with a window has been done in 2009 by Montazeri & Azizian. The wind tunnel used in this experiment had a square cross section of 46 cm sides and a length of 3.6 m. As shown in figure 4.1, the model in this analysis had been placed in the wind tunnel such that the room fell under the tunnel and the wind tower only was causing a maximum blockage of around 5 per cent.

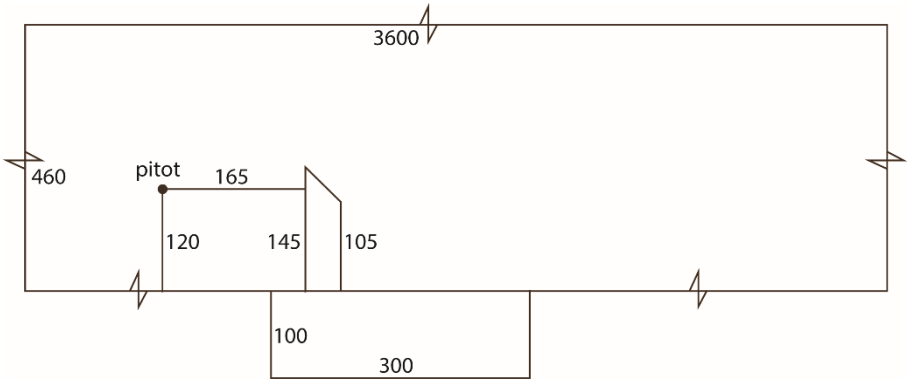


Figure 4.1. The wind tower and the room's placement in the wind tunnel and their respective dimensions in millimeter

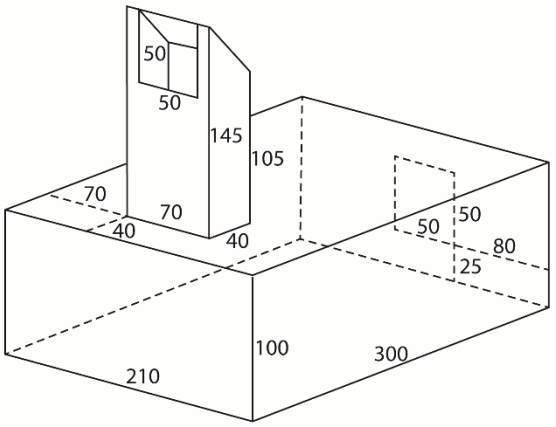


Figure 4.2. Dimensions of the room and the one-sided wind tower model in millimeter

As part of the analysis the static pressures on different internal surfaces of the wind tower had been measured using 23 pressure taps. In order to calculate the pressure coefficients at these 23 points, the reference static pressure was determined using a pitot tube placed at a 16.5 cm distance upstream of the wind tower at the height of 12 cm from the wind tunnel floor. The wind tower was then rotated by 15 degrees intervals to see how different wind incident angles affect the pressure

distribution inside the wind tower. The wind tower model's dimensions are reported in figure 4.2. The experiment had been done with a wind velocity of 20 m/s in order to guarantee the independence of the airflow from the Reynolds number calculated as about 198000 (Montazeri & Montazeri, 2018) according to the equation 4.5 and considering the height of wind tower 0.145 m and air's kinematic viscosity of $1.47 \times 10^{-5}$ $m^2/s$ at a temperature of 15° C.

### 4.2.2 CFD analysis

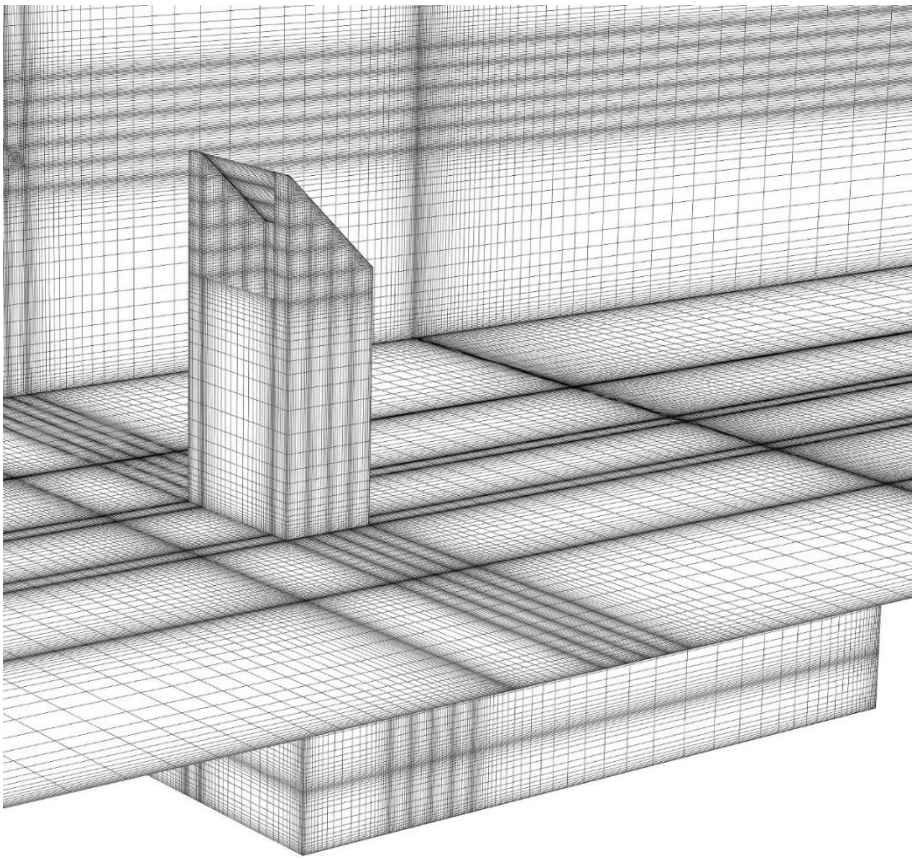

Figure 4.3. The medium mesh quality of one-sided wind tower at wind incident angle zero

The software Gambit 2.4.6 was used to create four structured meshes of circa four million hexahedral cells for four wind tower directions of 0 (figure 4.3), 30, 150 and 180 degrees. The dimensions of the model and the wind tunnel were the same as the experimental data as shown in figures 4.1 and 4.2. The boundary conditions considered as part of this study include a uniform 20 m/s velocity with a 3% turbulence intensity as the velocity inlet of the tunnel, and a zero gauge pressure of similar turbulence intensity at its outlet. The window of the room fallen out of the wind tunnel section is given a zero gauge pressure, too. The hydraulic

diameter of the turbulent flow is 0.46 m considering the square cross section of the wind tunnel. All walls of the model and the wind tunnel have been considered as no slip with zero roughness height.

Steady state RANS equations were solved in ANSYS Fluent 18 with a standard wall function and realizable k-ε turbulence model. The SIMPLE scheme has been considered as the pressure-velocity coupling and the second order discretization has been selected for pressure, momentum, turbulent kinetic energy and turbulent dissipation rate.

The solution convergence was observed by controlling the residual levels and the parity of the mass flow rate values at the inlets and outlets of the model.

### 4.2.3 Comparison between CFD and wind tunnel results

The comparison between CFD and experimental pressure coefficients have been done on the middle vertical line of each internal wall of the wind tower assuming a clockwise rotation of the tower with respect to the wind –i.e. green represents the middle vertical line on the left wall, black on the central wall, and red on the right one. In order to calculate the pressure coefficients, the reference static pressure $P_0$ has been taken from the pitot tube, upstream of the wind tower, the reference velocity was set as 20 m/s similar to the wind tunnel test, and the air density is considered as $\rho$=1.225 kg/m$^3$.

As shown in figures 4.4 to 4.7, when the wind incident angle is 0 and 30 degrees, the pressure coefficients produced inside the tower are close to those of wind tunnel test. Contrarily, when the wind tower is leeward to the airflow, as in 150 and 180 wind incident angles, the numerical and experimental values differ more considerably. This is in line with a previous sensitivity analysis by Montazeri et al who have noted that the Realizable k-ε model compared to the Standard k-ε model, Renormalization Group k-ε model, Standard k-ω model, Shear-stress transport k-ω model and the Reynolds Stress model, is able to better reproduce the surface static pressure and indoor air speed at wind incident angle 0, while at wind incident angle 180 all turbulence models reproduce the surface static pressure with the same quality and none predict the mean indoor air speed accurately (Montazeri & Montazeri, 2018).

For wind direction 0, the Realizable k-ε turbulence model has reproduced the pressure coefficient values with error percentages of 13%, 16% and 18% respectively on the left, middle and right walls of the wind tower. These values change correspondingly to 25%, 24% and 27% at 180 degrees wind direction.

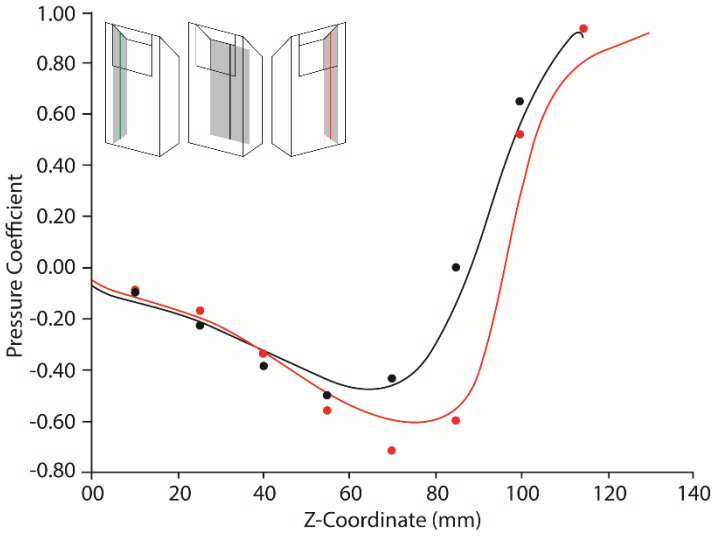


Figure 4.4. Comparison between the pressure coefficients on the mid (black) and right wall (red) of the wind tower derived from the CFD (lines) and the experiment (dots) at wind tower direction 0 degrees

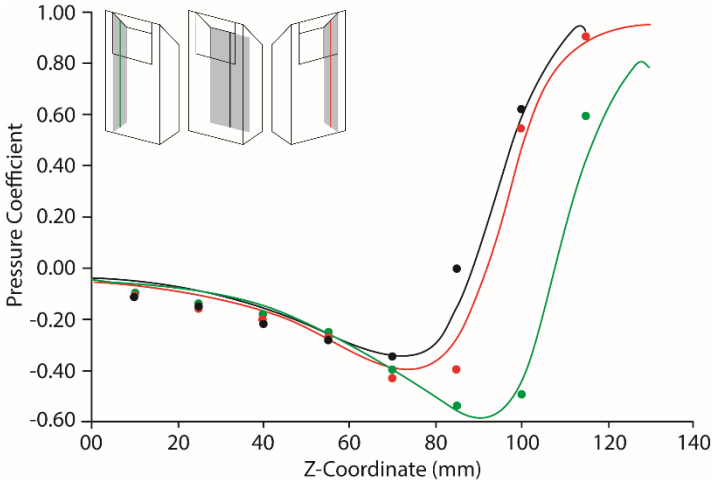


Figure 4.5. Comparison between the pressure coefficients on the mid (black), left (green) and right wall (red) of the wind tower derived from the CFD (lines) and the experiment (dots) at wind tower direction 30 degrees

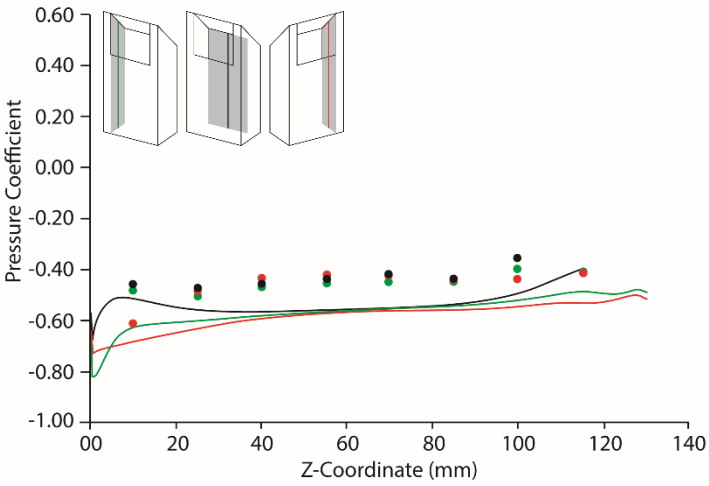


Figure 4.6. Comparison between the pressure coefficients on the mid (black), left (green) and right wall (red) of the wind tower derived from the CFD (lines) and the experiment (dots) at wind tower direction 150 degrees

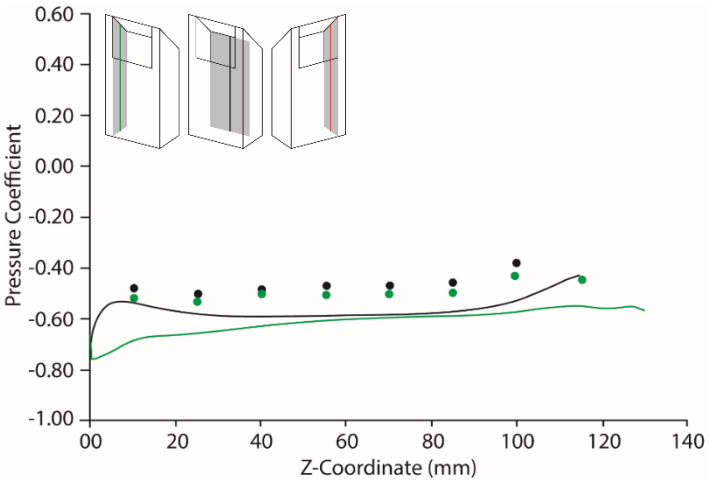


Figure 4.7. Comparison between the pressure coefficients on the mid (black) and right wall (red) of the wind tower derived from the CFD (lines) and the experiment (dots) at wind tower direction 180 degrees

### 4.2.4 Grid independence analysis

In order to make sure the solution is independent of the grid resolution, a grid sensitivity analysis has been done on the cases with zero and 180 degree wind incident angles by coarsening and refining their meshes with a factor of $2^{1/2}$. The original grids contained 4,132,254 cells while the reproduced coarser and finer ones have respectively 1,391,827 and 11,134,616 cells. Figures 4.8 and 4.9 represent the difference between the three grid qualities for these wind directions.

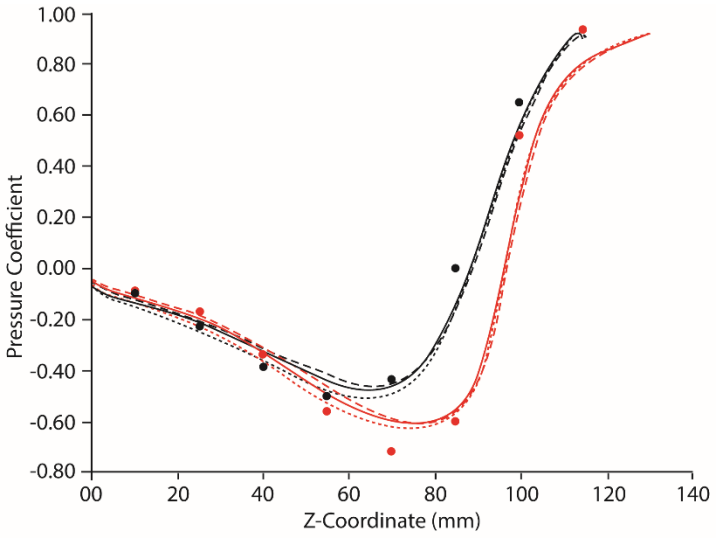


Figure 4.8. Comparison between the pressure coefficients on the mid (black) and right wall (red) resulted from the wind tunnel test (dots) and those of CFD derived from the coarse (dashed line), medium (full line) and fine (dotted line) meshes for wind incident angle 0.

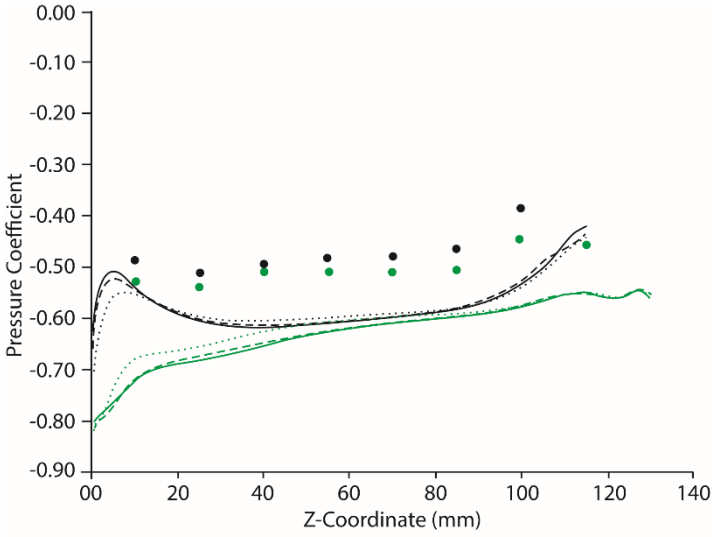


Figure 4.9. Comparison between the pressure coefficients on the mid (black) and left wall (green) resulted from the wind tunnel test (dots) and those of CFD derived from the coarse (dashed line), medium (full line) and fine (dotted line) meshes for wind incident angle 180.

As demonstrated in figure 4.8, at zero incident angle, the finer grid quality better matches the wind tunnel data, especially at the heights lower than 60 mm. At heights above 80 mm, the three grids reproduce the pressure coefficient values almost with the same quality but the difference with the experimental data is more

pronounced. The biggest difference between the wind tunnel and CFD is observed at mid height (z=70 mm).

At wind incident angle 180 degrees (figure 4.9) the fine and the coarse grid reproduce closer values to each other compare to the grid with medium resolution. On the mid wall of the tower, the main difference between the three grids is seen in the lowest part of the tower at its intersection to the underneath room. The pressure coefficients in this part of the tower are reproduced better by fine and coarse grids as they have closer values to the wind tunnel data. On the left wall of the wind tower, however, the difference in the Cp values produced by fine and coarse vs medium quality grid is more evident as latter shows improved values for at least the lower 80 mm height of the wind tower.

The grid resolution can minimize the difference between CFD and wind tunnel. At wind incident angle 0, the coarse grid reproduces the Cp with errors of 14%, 17% and 19% on left, middle and right walls of the wind tower, while these values improve to 9%, 15% and 18% by using the fine grid. At wind angle 180, the Cp errors by the coarse grid are 25%, 23% and 26% which improve to 21%, 22% and 25% using the fine grid.

## 4.3 Validation of the four-sided wind tower

Validation of the four-sided wind tower model was done very briefly based on the available experimental data published by Montazeri previously in 2011.

### 4.3.1 Experimental analysis

The experiment on various multi-opening wind tower models was done in the same wind tunnel that was used for testing the one-sided wind tower. The placement of the wind tower and the room in this test was also identical with the previous study.

The wind tower tested in this experiment had a circular cross section with a diameter of 9 cm and a height of 13 cm from which the upper 5.2 centimeters were left open as wind tower's apertures (figure 4.10). The model caused a blockage of 5.5% in the wind tunnel. The cross section of the wind tower was divided into 2, 3, 4, 6 and 12 parts in order to study how the sensitivity of the wind tower changes with the increase in internal divisions.

The study was done using a uniform wind velocity of 19.5 m/s rotating the wind tower at 15 degree intervals, thus simulating wind incident angles of 0, 15, 30 and 45 degrees for the four-sided wind tower model. The airflow rates passing through

each of the four wind tower internal divisions had been measured using 28 pitot tubes and 8 static tubes mounted half on the top and half on the bottom surfaces of the wind tower model.

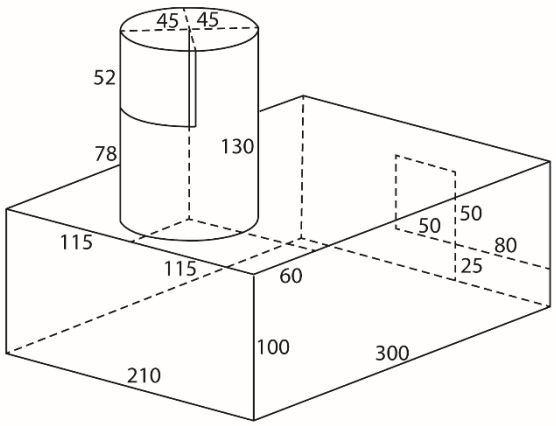


Figure 4.10. Dimensions of the room and the one-sided wind tower model in millimeter

### 4.3.2 CFD analysis

Gambit 2.4.6 was employed to construct one structured mesh of about 2.3 million cells representing the four-sided wind tower and zero degree wind direction (figure 4.11). The uniform wind velocity of 19.5 m/s and a turbulence intensity of 3% were utilized as the boundary conditions of wind tunnel's inlet. The outlet was given a zero gauge pressure and the same turbulence intensity. The room's window placed underneath the wind tunnel section was given a zero gauge pressure, too. Similar to the one-sided model, all walls of the wind tower, room and the wind tunnel have been considered as no slip with zero roughness height.

The rest of the simulation settings in Fluent such as the turbulence model, the pressure-velocity coupling scheme and the discretization orders have been set matching the one-sided model explained in section 3.2.2.

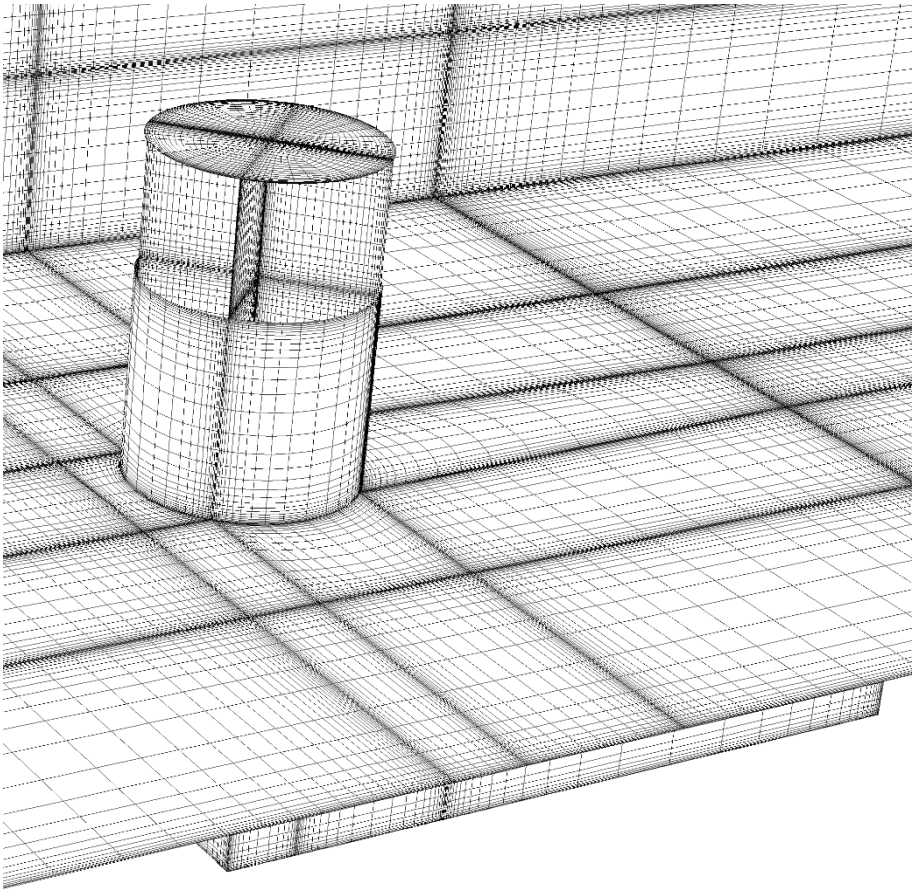

Figure 4.11. The medium mesh quality of four-sided wind tower at wind incident angle zero

### 4.3.3 Comparison between CFD and wind tunnel results

The only variable that was evaluated in both CFD and wind tunnel, was the entering air flow rate value. The experimental net air flow rate entering the room through the windward aperture of the wind tower and the room's window had a value of 0.024 m3/s while a value of 0.029 m3/s was observed by the same author in his CFD analysis published together with the experimental results (Montazeri, 2011).

The CFD simulation that was performed in this thesis similarly shows a value of 0.029 m3/s combining the inward airflow rates of 0.018 m3/s through the windward wind tower aperture and 0.011 m3/s through the room's window.

# Chapter 5

# Cross ventilation by wind towers

## 5.1 Introduction

In order to evaluate how the position of a rooftop wind tower affects its cross ventilation performance at various wind incident angles, 53 simulations have been done. Three groups of simulations are done on room models having wind towers on the roof which consist of: 21 cases for three positions of a one-sided wind tower working with a window simulated for seven wind directions between 0 and 180 (figure 5.1), 21 cases for three positions of a four-sided wind tower working with a window simulated for seven wind directions between 0 and 180 (figure 5.3), and 11 cases for two positions of a four-sided wind tower working alone simulated for wind directions between 0 and 180 (figure 5.5).

Despite the difference between the geometries of the one-sided and four-sided wind towers, all the remaining parts of the models are constructed similarly in terms of meshing. Therefore, the domain is identical for all of them. The solver settings and the boundary conditions set in Fluent are also equal in all cases.

In this chapter, after explaining the geometries of the models and the CFD settings, the results of each group of cases in terms of air flow rate, velocity magnitude, mean age of air, air change efficiency, and pressure coefficient are reported in separate sections. And in the conclusion, the three groups are compared with each other. It is to be noted that since the pressure coefficient values are not a proper means for explaining the cross ventilation quality, they have been explained for each group of cases but are not included in the ventilation comparisons.

## 5.2 Description of the geometries and domain

Three groups of simulations have been performed in a single domain for wind directions varying between 0 and 180 degrees at 30 degree intervals.

In group 1, a one-sided wind tower with a square cross section of 1 $m^2$ and a height of 1.5 m having an aperture of 1x1 m was placed on the rooftop of a room

with length, width and height of 8, 6 and 3 meters respectively. The room has a window placed in the center of one of the smaller walls having a square cross section of 1 $m^2$. The window would provide a cross-ventilation flow together with the wind tower.

In terms of position, the wind towers were placed along the longer symmetry axis of the roof at the farthest, central and closest distance from the window and as shown in figure 5.1, they are nominated as T4, T5 and T6, respectively.

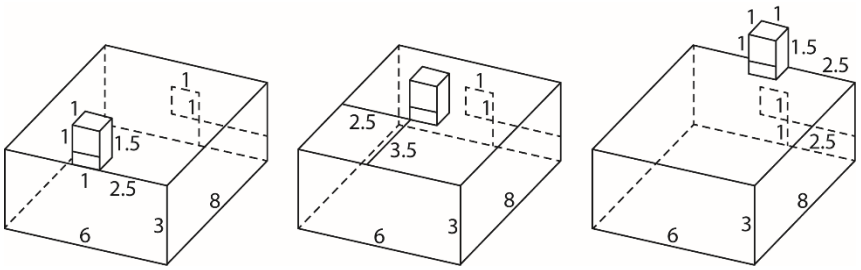


Figure 5.1. The room with three wind tower positions T4 (left), T5 (center) and T6 (right), and their relative dimensions in meters.

The three models are made with structured meshes of 3,447,444 (T4 and T6) and 4,098,360 (T5) cells (figure 5.2).

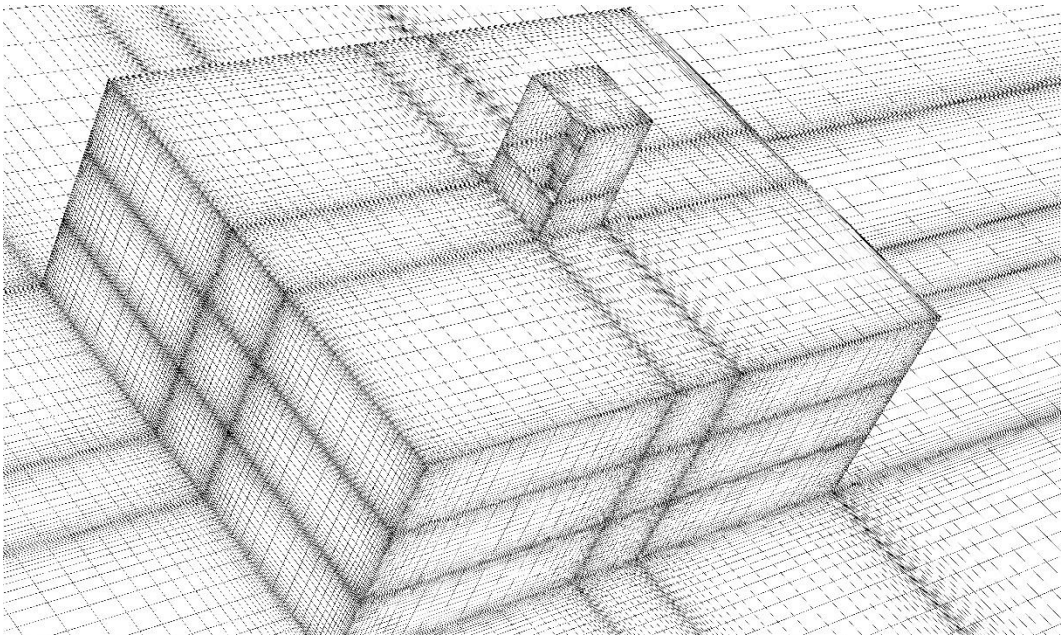

Figure 5.2. The mesh structure of the one-sided wind tower T5

In group 2, the same tower as in study 1 has been divided by two vertical blades into 4 identical parts. Each triangular opening at the intersection of the room and tower has 0.25 square meters of area and there are four apertures of 1x1 m on each side of the wind tower. The tower has been placed at the three previously-specified positions on the roof of the room. As shown in figure 5.3, the tower at the farthest, central and closest distance from the window are nominated as M4, M5 and M6, respectively and are made with structured meshes of 3,560,340 (M4 and M6) and 4,211,256 (M5) cells (figure 5.4).

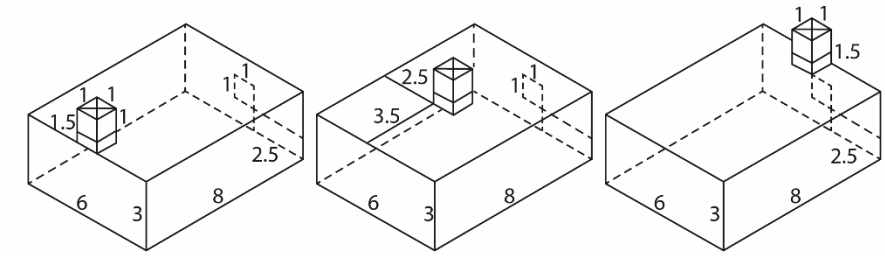


Figure 5.3. The room with three wind tower positions M4 (left), M5 (center) and M6 (right), and their relative dimensions in meters.

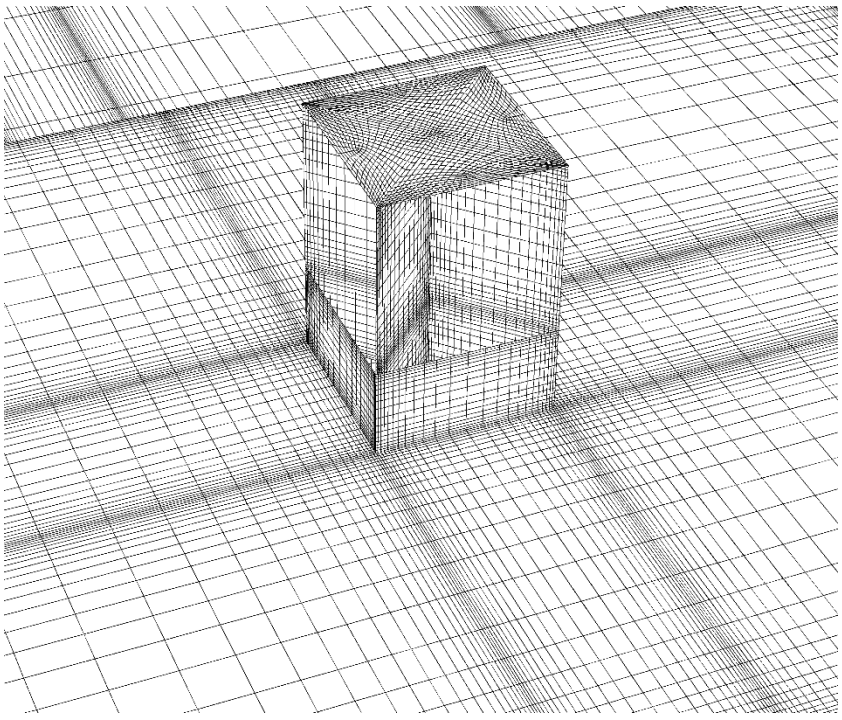

Figure 5.4. The mesh structure of the four-sided wind tower M5 and M5W

The models in group 3 are identical as those in group 2. The only difference is that the room's window has been closed (figure 5.5). In these cases, the wind towers

act both as inlets and outlets of ventilation air flow. Therefore, M4W, M5W and M6W have the same number of cells as M4, M5 and M6: 3,560,340 (M4 and M6) and 4,211,256 (M5) cells.

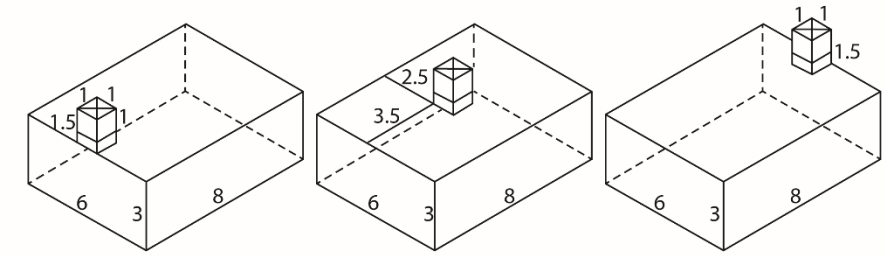


Figure 5.5. The windowless room with three wind tower positions M4W (left), M5W (center) and M6W (right), and their relative dimensions in meters.

It should be noted that due to the symmetry of M4W and M6W in group 3, the simulations have been performed only on one of them. The results are however accordingly attributed to the abandoned case, in order to make comparisons more meaningful.

The domain in which all the wind tower models have been simulated has corresponding measurements of 98, 96 and 27 m (figure 5.6) respecting the CFD guidelines for domain size (Franke, Hellsten, Schlünzen, & Carissimo, 2007).

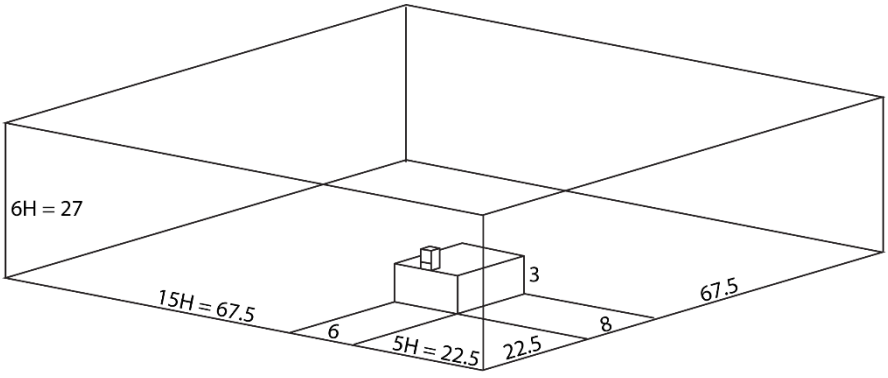


Figure 5.6. View of the domain, its measurements in meters, and the placement of the model in it.

## 5.3 Boundary conditions and solver settings

The dimensions of the model with one-sided wind tower and the solver settings are identical with those utilized in a 2018 paper by Montazeri & Montazeri with the latter being similar to the validation study as well.

An atmospheric boundary layer (equation 5.1) with a wind speed of U=3 m/s at a height of 10 m is imposed using a user defined function (UDF) applied to the domain's inlet. The reference velocity magnitude utilized for calculating the pressure coefficient values is measured as 2.59 m/s at a height of 4.5 m corresponding to the model's height from the domain floor. The turbulent kinetic energy k(z) and turbulence dissipation rate ε(z) both at the inlet and the outlet are calculated using the same UDF in accordance with the equations 5.2 and 5.3 respectively (Tominaga et al, 2008).

Eqn 5.1: $$U(z) = \frac{u^*_{ABL}}{\kappa} \ln\left(\frac{z+z_0}{z_0}\right)$$

Eqn 5.2: $$k(z) = 3.3\, u^{*2}_{ABL}$$

Eqn 5.3: $$\varepsilon(z) = \frac{u^{*3}_{ABL}}{\kappa(z+z_0)}$$

where U(z) is the mean wind speed, $u^*_{ABL}$ is the atmospheric boundary layer friction velocity, κ is the von Karman constant (0.42), and $z_o$ is the aerodynamic roughness length.

Standard wall functions are used for domain's floor which is assumed to be a terrain covered by large grass with the aerodynamic roughness length of $z_0$=0.03 m. The sand-grain roughness height $k_s$ which has to be smaller than half height of the first cell adjacent to the domain floor is considered as $k_s$ =0.006 m based on the relevant grid measurements (the height of the first cell above the domain floor is about 0.012 m). Furthermore, following the roughness equation in ANSYS Fluent, explained in the previous chapter (equation 4.15), $C_s$ value of the domain floor is set to a maximum allowed number 7 using the previously mentioned UDF.

For all other wall surfaces, the standard wall functions, with $C_s$ value of 0.5 and $k_s$ of 0 have been utilized. A constant zero gauge pressure has been considered for the outlet of the domain and the lateral sides of the domain, at wind incident angles 0, 90 and 180, have a symmetry boundary condition.

Furthermore, in computing the mean age of air, another user-defined function was applied to the room volume solely, solving the user-defined scalar (UDS) equation below (see Equation 5.4) in which $\mu_{eff}$ is the effective air viscosity and $Sc_t$ is the Turbulent Schmidt number set in Fluent's viscosity model settings as 1.2 for the Realizable k-ε turbulence model.

Eqn 5.4: $$(2.88*10^{-5})\rho+\mu_{eff}/Sc_t$$

Residuals of continuity and epsilon levelled off around $10^{-6}$, k and x-velocity around $10^{-7}$, and y-velocity and z-velocity around $10^{-8}$. In some cases, especially for the wind tower placement on the centre of the roof such as T5, M5 and M5W at 0 wind incident angle, oscillatory convergence was observed. This is often due to the fact that the flow is unsteady but it is being solved by steady RANS approach (Ramponi & Blocken, 2012). For this reason, in addition to controlling the mass flow rate values through different apertures of the model, the velocity magnitude values were monitored for several points in the room, too. The figure 5.7 shows the variation of velocity in 5 different points in the model over 8000 iterations.

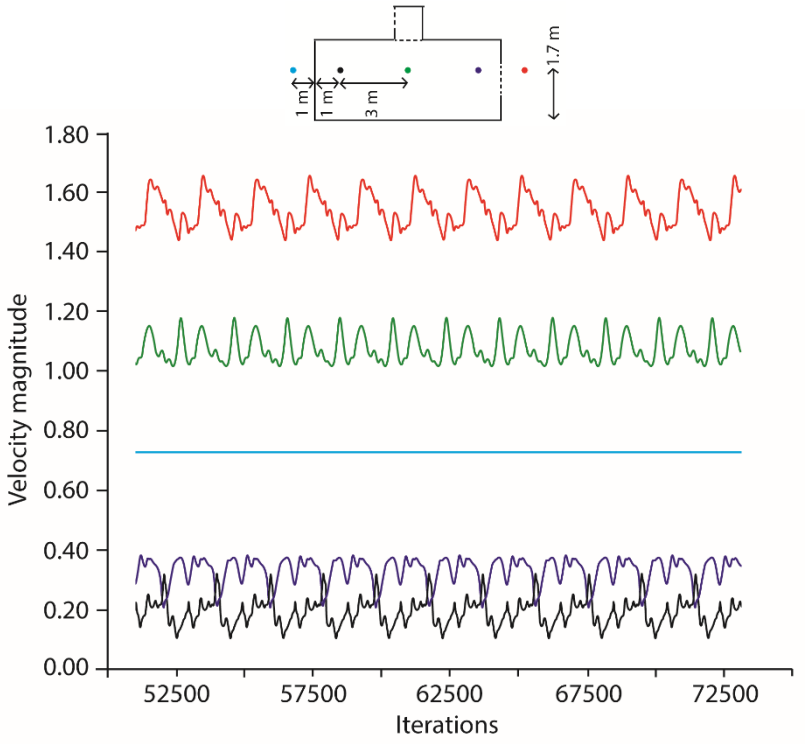


Figure 5.7. Velocity magnitude variation at different points in model T5.

## 5.4 Group I: one-sided wind tower model with a window

### 5.4.1 Grid independence analysis

The resolution of the grid T4 has been refined and coarsened by a factor of $2^{1/2}$ (figure 5.8). The coarse, fine and reference medium grid qualities have respectively 1218464, 9747712 and 3216217 cells.

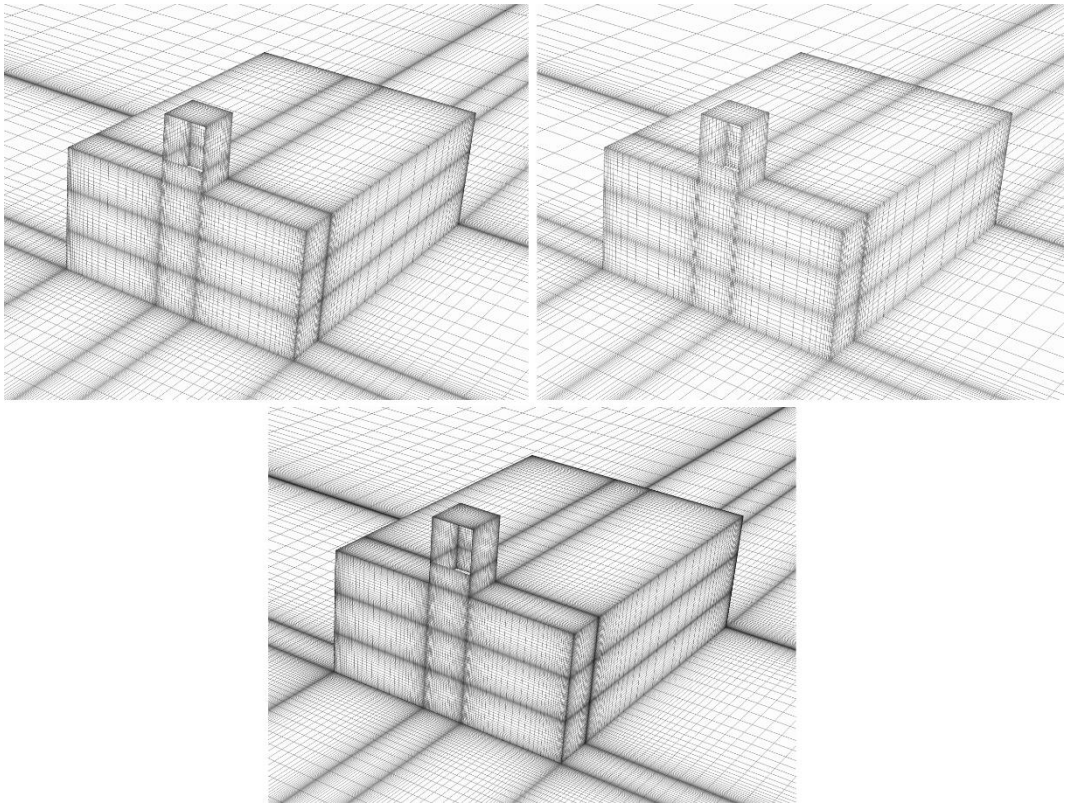

Figure 5.8. The coarse (above right), medium (above left) and fine (below) grids for the wind tower model T4

In order to make sure the solutions are not affected by the grid quality, the three grid were simulated at wind incident angle 0 and the velocity magnitude values were controlled for the three mesh qualities on two lines in the room as shown in figure 5.9: one 8-meter-long horizontal line placed at mid height of the room, and a 3-meter-long vertical line placed underneath the wind tower.

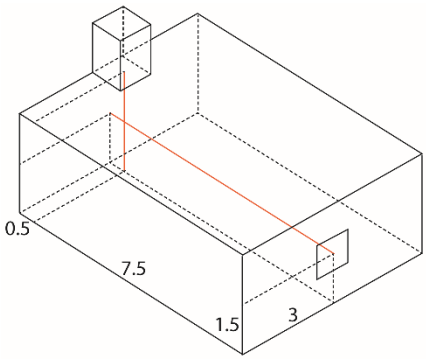


Figure 5.9. The vertical and horizontal lines on which the velocity magnitude has been controlled

As evident in both figures 5.10 and 5.11, the quality of the grid has a minimal effect on the velocity magnitude in the room ventilated by tower T4.

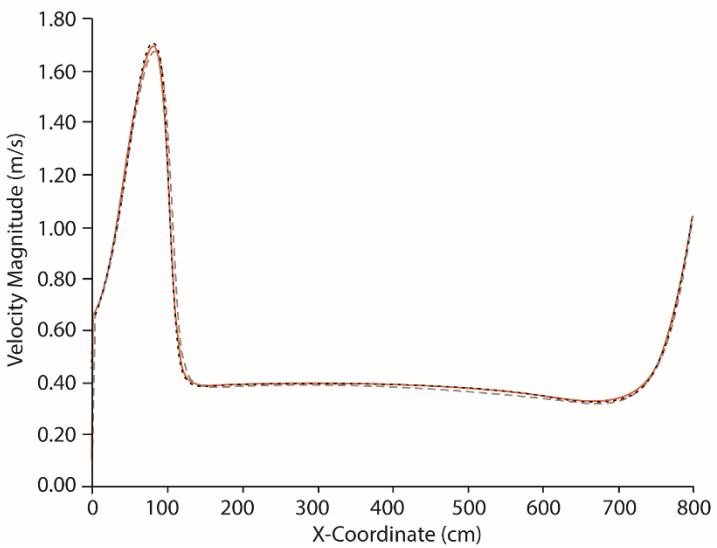


Figure 5.10. Velocity magnitude (m/s) on the horizontal line for three grid qualities

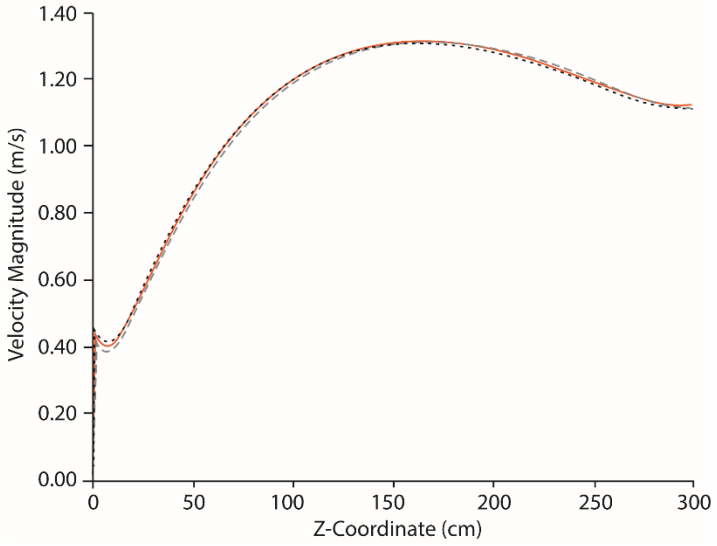


Figure 5.11. Velocity magnitude (m/s) on the vertical line for three grid qualities

## 5.4.2 Reference values at zero incident angle

The reference contours of pressure coefficient, velocity magnitude and mean age of air have been represented for zero wind incident angle on two vertical planes and three horizontal ones as demonstrated in the figure below. The vertical plane 1 is placed at the longer symmetry axis of the room cutting the window and the towers

in the middle. The distance between plane 1 and 2 is 1.5 meters. Horizontal planes 3, 4 and 5 are 0.65, 1.3 and 1.7 meters above the ground representing the breathing heights of a person lying-on-bed, seated and standing (figure 5.12).

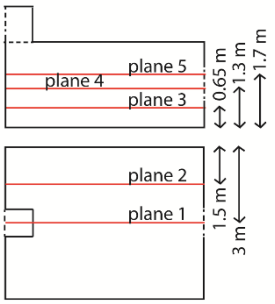


Figure 5.12. The vertical and horizontal planes on which the contours of pressure coefficient, velocity magnitude and mean age of air have been reproduced

Comparing the pressure coefficient contours reproduced on the vertical plane 1 in the middle of the room (table 5.1), it is noted that the presence of the wind tower at the upstream side of the model (T4) is linked with higher Cp values on the upstream façade and soon inside the wind tower channel. The Cp values in the wind tower channel decrease as the wind tower is moved away from the upstream edge of the roof.

The room, in all the three tower positions experiences similar Cp values. In fact, the average Cp values in the rooms having T4, T5 and T6 are respectively 0.24, 0.27 and 0.26. On the room floor, underneath the wind tower the Cp values are higher than the rest of the room, but this is only limited to a small area.

What is further interesting to observe is the separation between the negative and positive Cp values produced around the wind tower. While the two areas have been formed easily around the T4 case, in T5 the negative values on the room's roof upstream edge are affected by the positive Cp values in front of the wind tower aperture. Increasing the distance of the wind tower from the upstream roof edge and placing it at position T6 would minimise the effect of the positive and negative Cps on one another. This is understandable also looking at the average Cp values on the wind tower apertures which for T4 is 0.55, while for T5 and T6 is 0.28 and 0.34.

The position of the wind tower on the roof at zero incident angle does not have any impact on the Cp of the window as this value is around 0.02 for the three cases.

Table 5.1. Contours of pressure coefficient (-) on the central vertical surface

| plane | T4 | T5 | T6 |
|---|---|---|---|
| Cp (-) | 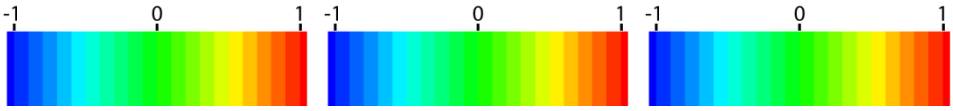 | | |
| 1 | 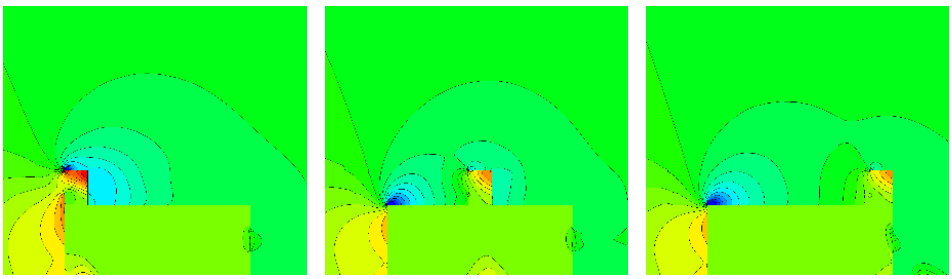 | | |



The table 5.2 demonstrates the contours of velocity magnitude for the three positions at wind incident angle 0 on the vertical and horizontal surfaces indicated above.

As shown in table 5.2, on plane 1, it is evident that in T4, the jet of air entering from the tower hits the floor and spreads along both x and y directions (the y directions not shown in the table). Compared to other positions, in T4, the internal wind speed is higher according to the velocity contours on the symmetry plane 1. In T5, too, the jet of air arrives to and spreads on the floor in x and y direction though the distribution of it in y axis is less pronounced compared to T4. In T5, the portion of the room volume where the wind speed is null is greater than T4. In T6 position, there is almost no velocity distribution inside the room and because of the tower being right on top on the window, the jet of air is majorly deviated to outside and hardly hits the room floor.

In fact, the average volumetric velocity magnitude in T4, T5 and T6 at zero wind incident angle are respectively 0.29, 0.26 and 0.13 m/s.

Among all three position, the wind velocity inside the tower T4 is the greatest and likewise, there is a greater velocity variation inside the tower. In T5 and T6 the airflows inside the tower is more uniformly and calmly distributed as a result of the bigger distance between the tower and the roof's windward edge.

The velocity distribution behind the tower is likewise different in the three models. In T4, there is a bigger and stronger velocity alteration on the roof behind the tower.

In T6, the other interesting point is how the exhausting airflow from the window is deviated downwards influenced by the wind entering from the tower. This is evident in the velocity contours on plane 3 and plane 5.

Table 5.2. Contours of velocity magnitude (m/s) on different horizontal and vertical surfaces

| **plane** | **T4** | **T5** | **T6** |
|---|---|---|---|
| U (m/s) | 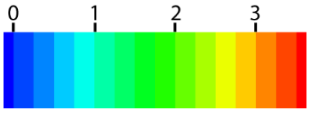  | 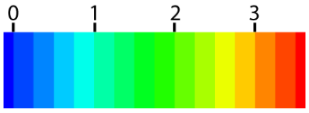  | 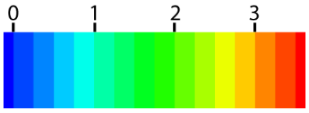  |
| 1 | 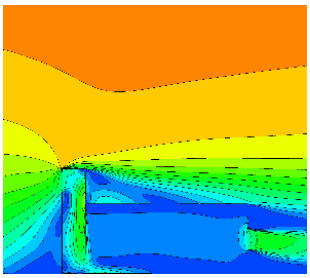 | 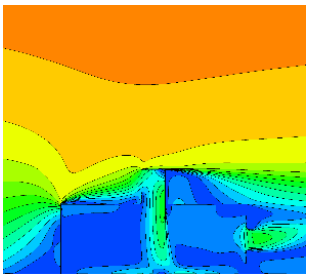 | 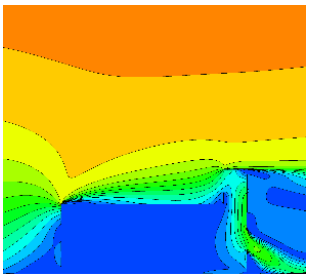 |
| 2 | 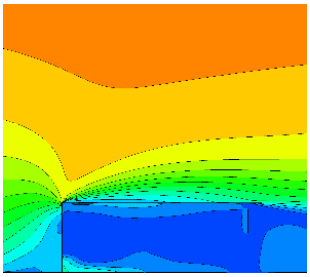 | 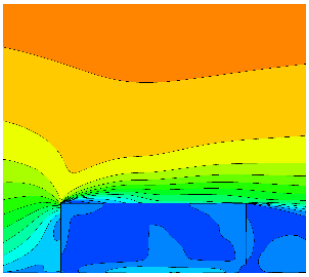 | 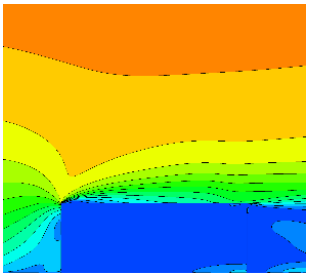 |
| 3 | 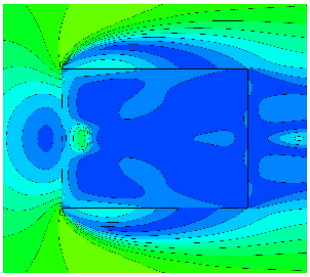 | 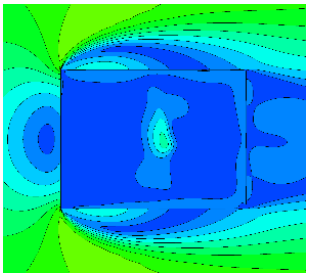 | 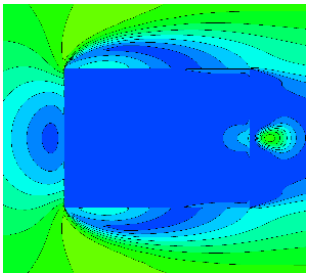 |

| | | | |
|---|---|---|---|
| 4 | 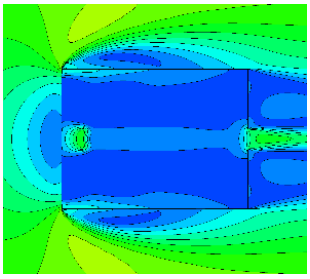 | 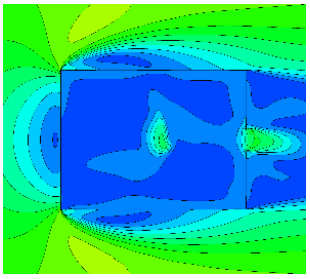 | 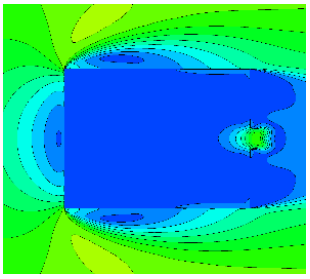 |
| 5 | 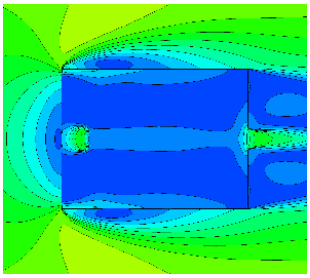 | 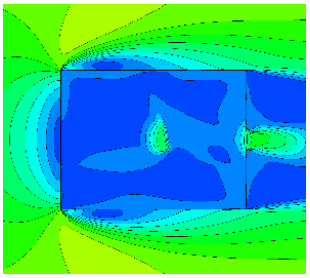 | 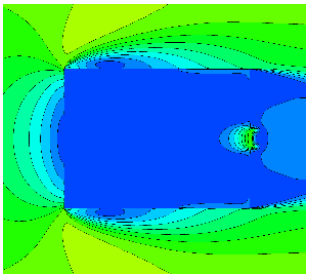 |

The contours of mean age of air (table 5.3) show how the freshness of air is distributed in the rooms ventilated by wind towers. Looking at the contours at zero incident angle, it is noticeable how the fresh air enters from the wind tower and how it is distributed in the room. T5 shows slightly better air age compared to T4 while the two have much better performance compared to T6 wind towers. The average mean age of air in the room having T4 is 107 seconds, while in T5 it is 6 seconds fresher. In T6 this average is about 378 seconds.

T4 shows how the jet of fresh air into the room is wider compared to T5 in which the colour representing the freshest air narrows as it gets close to the room's floor. And, in T6 this only arrives below the window.

T4 and T6 both show a symmetrical distribution of the mean air age in the room while in T5 the symmetry is not observed due to the periodic oscillations in the residual values.

In general, the air is fresher near the walls, floor, roof, and corners of the room. Comparing the contours on the plane 3 and those on planes 4 and 5, the effect of window presence in distribution of the freshness is evident. The flow is in general fresher in front of the window compared to other parts of the room. This is visible especially on the y direction i.e. on horizontal planes rather than on z direction i.e. on vertical planes.

Table 5.3. Contours of mean age of air (s) on different horizontal and vertical surfaces

| plane | T4 | T5 | T6 |
|---|---|---|---|
| τ (s) | 0 300 600 900 | 0 300 600 900 | 0 300 600 900 |
| 1 |  | 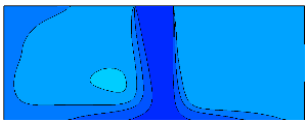 | 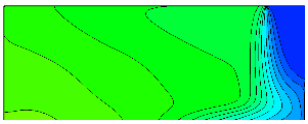 |
| 2 | 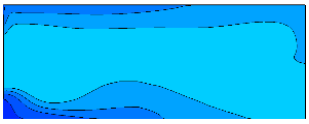 | 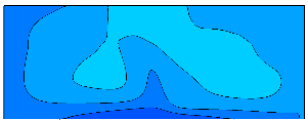 | 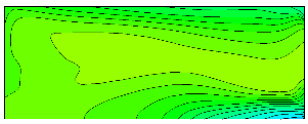 |
| 3 | 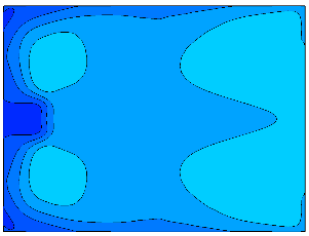 | 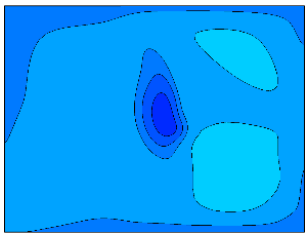 | 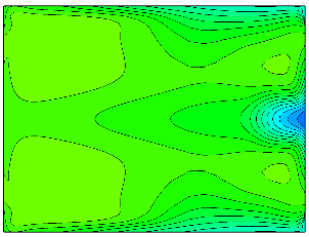 |
| 4 | 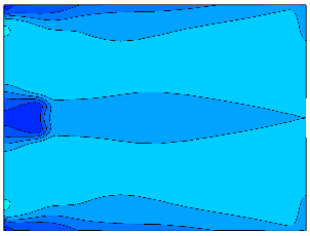 | 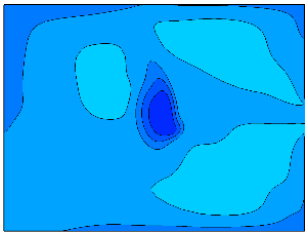 | 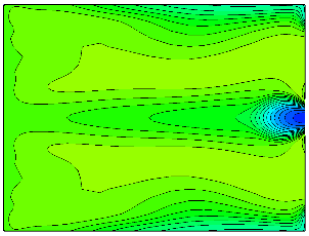 |
| 5 | 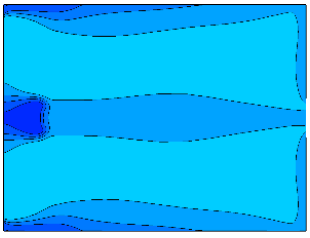 | 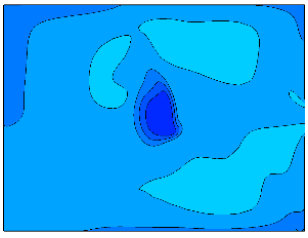 | 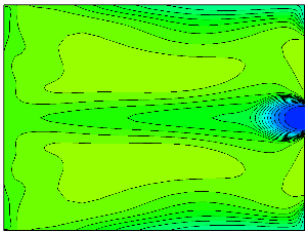 |

### 5.4.3 Volume flow rate and air change number

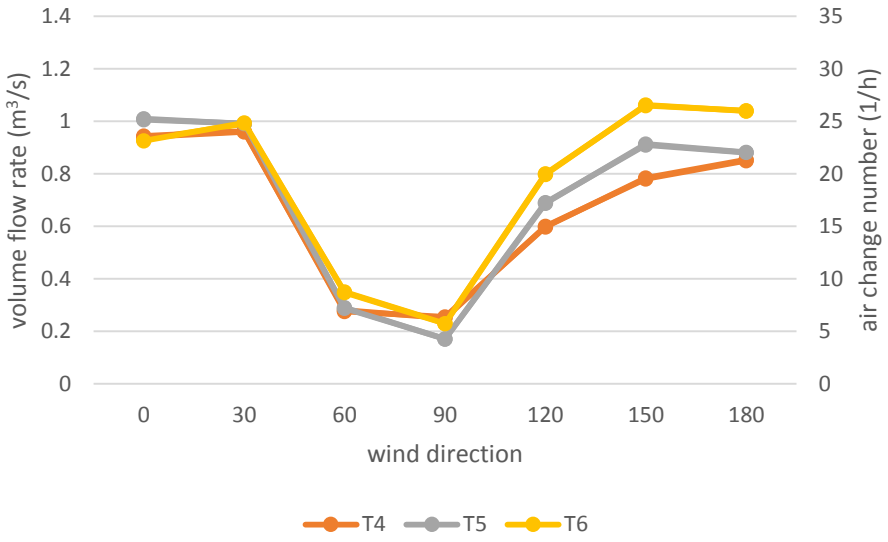


Figure 5.13. Absolute volume flow rate ($m^3/s$) and air change number (1/h) by each one-sided tower at different wind directions

According to the figure 5.13, it is evident that at windward wind incident angles, the position of the wind tower does not have a major effect on the induced volume flow rate ($m^3/s$) and number of air changes. However, at leeward incident angles, especially at 180 degrees, the wind tower placed on top of the window (T6) provides a higher flow rate and air change compared to the centrally placed wind tower (T5) and the farthest wind tower (T4). In fact, T6 and T4 are providing respectively higher and lower air flow rates than T5 in five out of seven wind directions.

The highest volumetric air flow rates and consequently the greatest air change numbers are induced by T5 at 0 and 30 incident angle and T6 at 30, 150 and 180 degrees which are all providing a volume flow rate of around 1 $m^3/s$ and an ACH of 25.5 on average. While, the worst wind directions are 60 and 90. In fact the lowest airflow rate of all is provided by T5 at 90 degrees arriving to a value of 0.17 $m^3/s$ which corresponds to 4.2 ACH. Interestingly, the wind angle 120 provides almost double times more air flow rate than the wind angle 60 degrees which on average in three tower positions is 0.69 $m^3/s$.

The air goes out of the wind tower aperture in wind angles 90, 120, 150, and 180 degrees. These are observable as negative values in the chart of volume flow rate.

## 5.4.4 Pressure coefficient

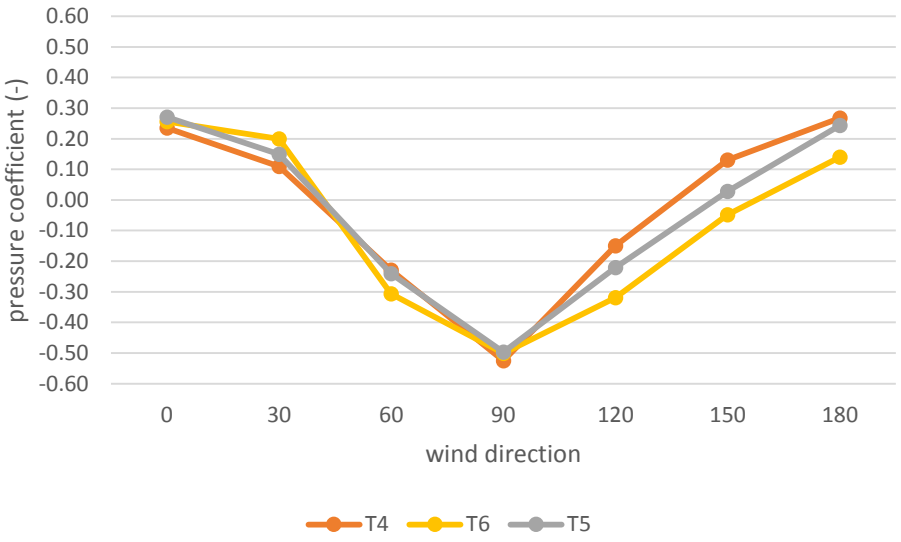


Figure 5.14. Volume-weighted average pressure coefficient (-) in the room

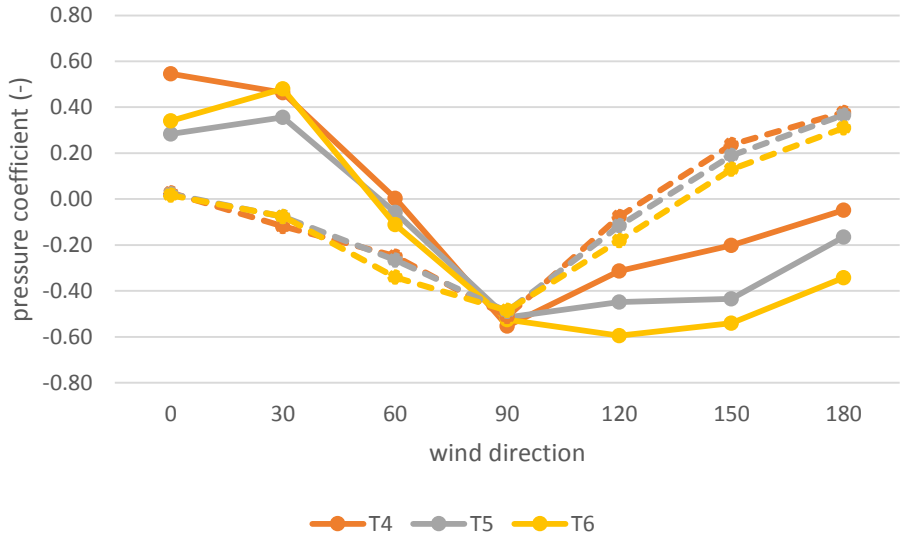


Figure 5.15. Area-weighted average pressure coefficient on the wind tower aperture (full line) and the window (dashed line)

The average volume-weighted Cp values in the room are represented for each wind direction in the graph 5.14. The Cp values for the three wind tower positions, despite the minor differences show a similar pattern by the change in the wind

direction. The effect of position is more evident as the wind incident angle goes beyond 90 degrees.

The lowest Cp values for the three models is observed at 90 degrees where wind towers T4, T5 and T6 provide mean Cp values of -0.53, -0.50 and -0.50 respectively. While, the highest values are observed at wind direction 0 and 180.

The Cp values reproduced on the wind tower aperture and the window are shown in figure 5.15. The dashed lines representing the Cp values on the window demonstrate the negligible effect of wind tower position. The major effect of wind tower displacement is on the wind tower aperture which is more pronounced for wind direction 0 and wind directions over 90 degrees. In fact, over 90 degrees, as the wind tower is put closer to the window, the Cp value decreases.

### 5.4.5 Velocity magnitude

Table 5.4 summarises the velocity magnitude contours on a horizontal plane placed at a height of 1.7 m. The area-averaged velocity magnitude on wind tower aperture and on intersecting aperture are given in figure 5.16. While the area-averaged velocity on the window and the volume-averaged velocity magnitude in the room are shown in figures 5.17 and 5.18 respectively. The velocity contours on vertical and/or horizontal surfaces other than the one in table 5.4 are explained but not shown in the thesis.

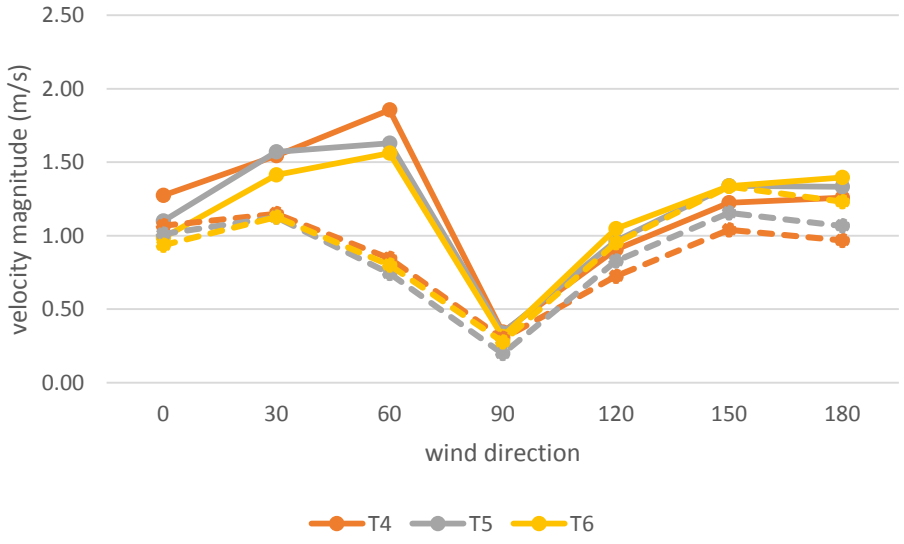


Figure 5.16. Area-averaged velocity magnitude (m/s) on wind tower aperture (full line) and the intersecting aperture (dashed line)

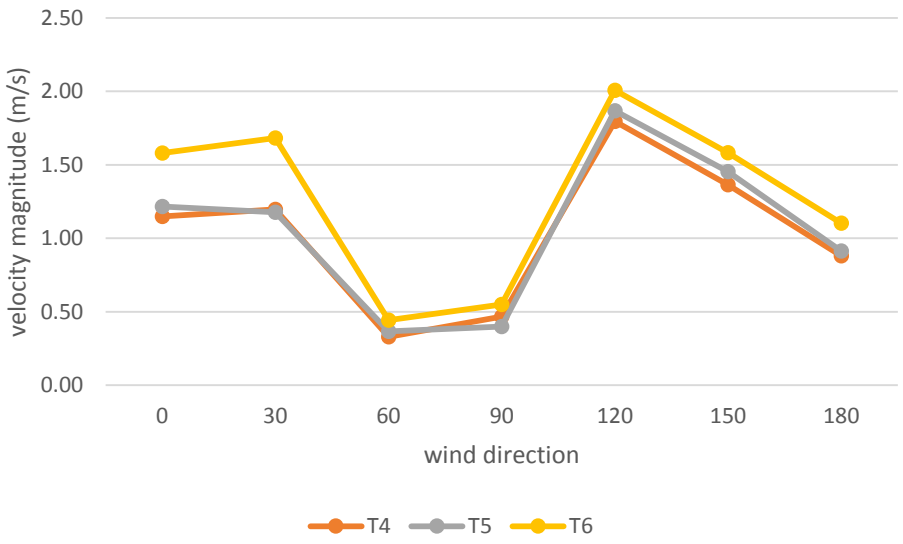


Figure 5.17. Area-averaged velocity magnitude (m/s) on the window

According to table 5.4 showing the contours of velocity magnitude at a height of 1.7 m from the ground, it is noted that similar to wind angle 0, at 30 degrees, the tower T4 shows a better velocity distribution inside the room compared to T5 and T6 despite the fact that there are more parts of the room having zero air movement with wind direction 30 compared to wind direction 0. The major impact of this change in wind direction is, as evident on plane 2 (not shown in the table), the null air velocity on one side of the window. In T5, the wind direction change results in the air jet not hitting the room floor completely and a greater portion of the room having zero air movement. T6 is the case which is least affected by the wind direction alteration. In this position, there is a subtle deviation in the perpendicularity of the air jet entering from the tower which results in asymmetric distribution of the flow on the ground.

At 30 degrees, the velocity magnitude on the tower aperture and that on the intersecting aperture is higher compared to the zero incident angle. At 30 degrees, similar to other wind directions, the speed on the intersecting aperture is almost equal for the three tower positions and is about 1.13 m/s which, compared to the other windward angles, is the pick velocity magnitude on this surface (see figure 5.16).

On the window surface at 30 degrees, the wind speed is 0.5 m/s higher in case T6 compare to T4 and T5 which experience identical values. This pattern is seen also at zero incident angle though the difference between the velocity figures is 0.43

m/s. At other incident angles also T6 case window is speedier but the difference with T4 and T5 is much less (figure 5.17).

Considering the airflow inside the tower, it was observed that the increase in the wind angle results in a bigger flow separation inside the tower. This was especially pronounced in T5. T5 also showed a more inclined air jet compared to T4 and T6 (velocity magnitude contours on vertical planes are not included in the thesis).

At wind direction 60 degrees, there is almost no airflow inside the room for all three tower positions (table 5.4). This is despite the fact that the velocity magnitude on the wind tower aperture is highest compared to other wind directions, respectively 1.86, 1.63 and 1.56 m/s in T4, T5 and T6 cases (see figure 5.16). In T5, only underneath the tower there is a slight air movement. In T4 an air movement is also seen along the windward wall of the room. The airflow velocity inside the tower is almost identically formed in the three positions. In fact, on the intersecting aperture, the velocity magnitude values are close, ranging between 0.74 and 0.85 m/s for the three cases (figure 5.16).

At wind angle 90 degrees also there is almost no air movement inside the room according to table 5.4. The speed on the wind towers openings and on the intersecting aperture are both at their minimum values ranging respectively ranging between 0.31-0.34 m/s and 0.20-0.30 m/s (figure 5.16). At this direction, in all cases there is a small downward airflow in the vicinity of the window. The velocity magnitude on the window surface is respectively 0.47, 0.40 and 0.55 m/s for T4, T5 and T6 (figure 5.17). In case T4 the airflow through the window spreads towards the room floor centre while the cases T5 and T6 show much less of such behaviour.

As the wind surpasses 90 degrees and the window falls on the windward side, there is a major change in the airflow distribution inside the room. In all three positions, the wind enters the room through the window and exits from the tower. At 120 degrees, the case with the optimal velocity distribution is T5, in which in almost all parts of the room the velocity is non-zero and in the mid-height of the room, there is a higher velocity. Contrarily, the worst velocity distribution is provided by T4 in which the only air movement is felt along the walls, floor and ceiling and there is a minimal distribution in vicinity of the window, toward the leeward side (plane 2). In case T6, the room core is majorly experiencing zero air movement (see table 5.4).

Furthermore, at 120 degrees, the area-average velocity magnitude on the window surface is at its pick value for the three wind tower positions. This value is 2.01 m/s for wind tower T6 which is slightly higher than 1.87 in T5 and 1.79 in T4

cases (figure 5.17). The case T6 provides a higher velocity magnitude also on the intersecting aperture and wind tower aperture with corresponding values of 0.95 and 1.05 m/s (figure 5.16).

At 150 degrees, the T5 positioning of the tower provides a higher velocity inside the room and more parts of the room experience air movement. In fact, in this position, only at the room corners in adjacency of the window, the air speed is zero. Similarly, T6 provides a good distribution of velocity, however, in this case, at the room centre there is a low speed zone. Respect to other positions, at this wind angle, case T6 allows a speedier wind inside the room through the window and likewise the exhaust air through the tower has a higher speed as well (table 5.4). In fact, the window, intersecting aperture and wind tower aperture in case T6 has velocity magnitudes of 1.58, 1.34 and 1.34 m/s which is between 0.12 and 0.30 m/s higher than the values for T4 and T5. The wind velocity on the intersecting aperture of T6 wind tower is higher than all other cases and all other wind directions.

At wind incident angle 150, as the tower is placed more distant from the window, the speed of the incoming air decreases. However, it is notable that even though in T6 the air velocity entering the room is greater, the distribution of this velocity inside the space is more uniform in case T5. Case T4 provides the least velocity spreading inside the room, with a considerable portion in the centre having no air movement at all.

Finally, when the wind blows perpendicularly to the window and the wind tower is at its more leeward condition, the model that provides a better-spread air movement inside the room is T6. In this case the wind enters the window with a higher speed and arrives almost to the room's opposite side. Even though the major air movement is at the central plane of the room and the lateral sides of the window do not benefit from this velocity spreading, but T6 is the one in which these still zones are minimal. Case T4 is the one that has large parts of the room especially parallel to the air jet experiencing no air movement. The more the tower is close to the window, the higher the speed of air exiting from the tower. The former statement is also observable through the graphs of velocity magnitude on intersecting aperture and wind tower aperture. In T4, the intersecting aperture has a speed of 0.97 m/s while this value for T5 and T6 is 1.07 and 1.23 m/s. The same figures on the aperture of the wind tower correspond to 1.26, 1.33 and 1.40 m/s.

Table 5.4. Contours of velocity magnitude (m/s) on a horizontal surface placed 1.7 m above the ground

| wind angle | T4 | T5 | T6 |
|---|---|---|---|
| U (m/s) | 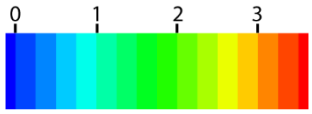  | 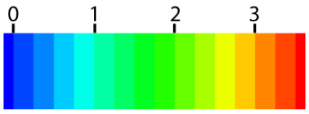  | 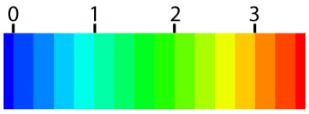  |
| 0 | 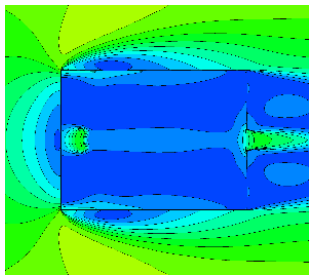 | 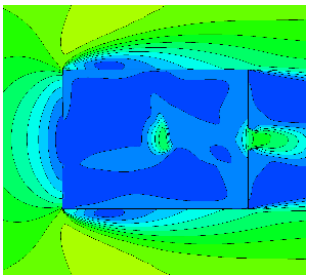 | 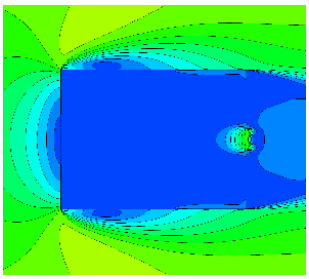 |
| 30 | 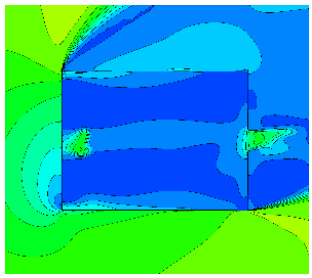 | 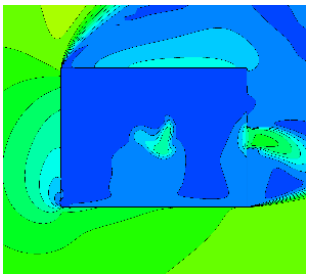 | 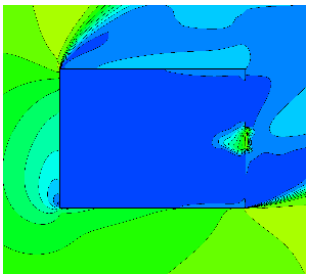 |
| 60 | 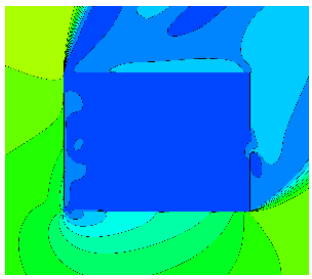 | 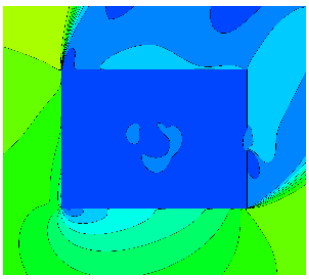 | 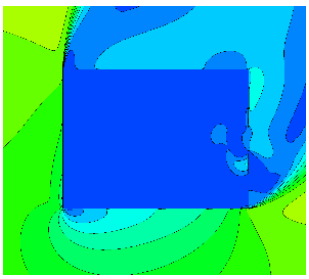 |
| 90 | 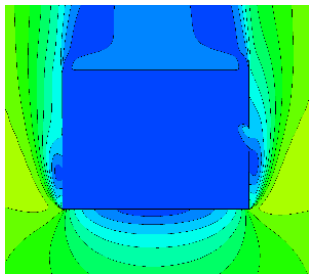 | 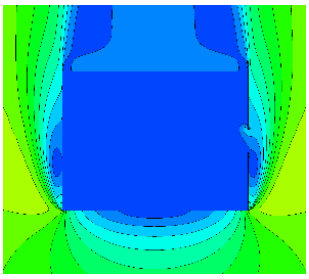 | 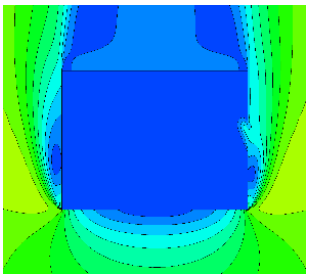 |

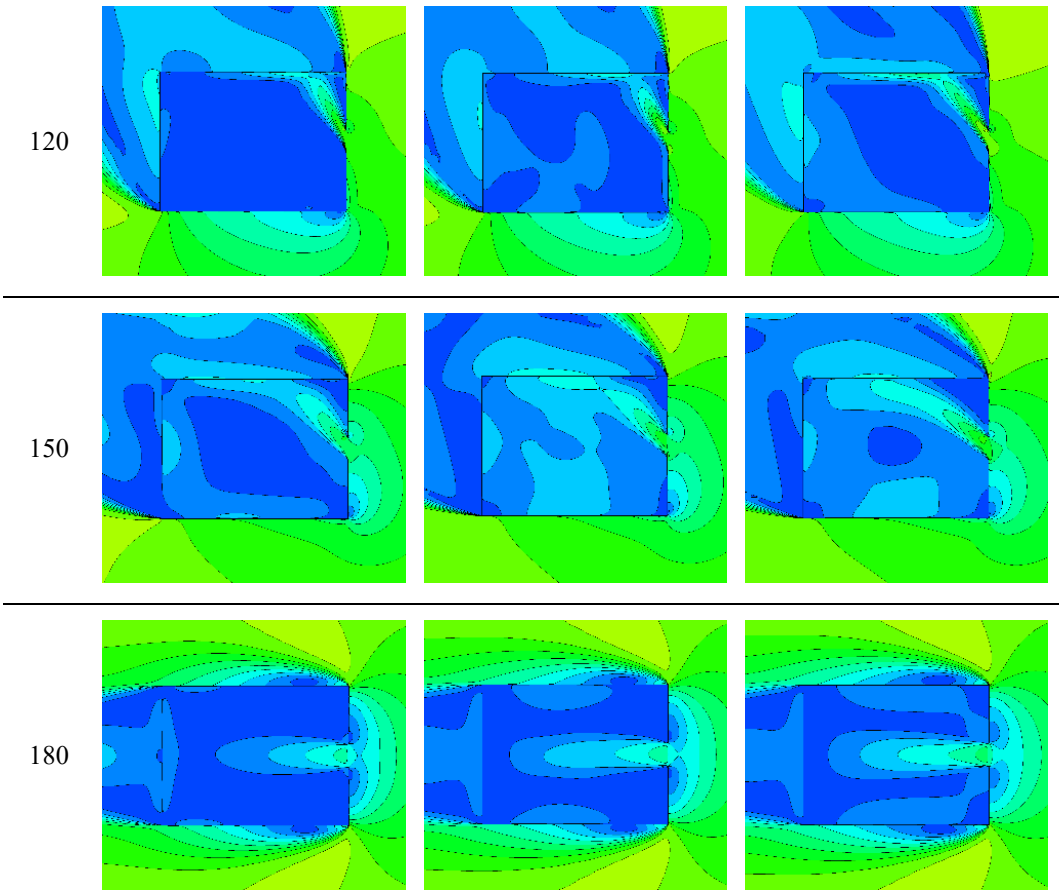


Generally, the velocity contours in table 5.4 show that in cases where the window acts as the air inlet, there is a more considerable air movement with a superior distribution inside the room. Contrarily, when the tower acts as the air supplier, the downward jet of air seems not to spread evenly enough. Corresponding to the volume flow rate values shown in figure 5.13, at 150 degrees incident angle, the velocity contours demonstrate a better performance for the case T6. However, in the cases T5 and T4 the highest mass/volume flow rate values do not necessarily indicate a better velocity distribution inside the room.

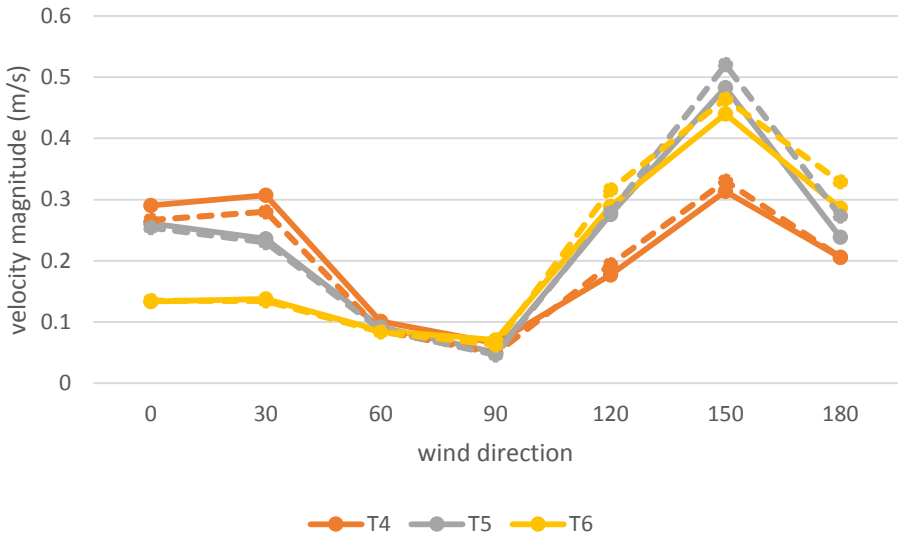


Figure 5.18. Volume-weighted (full-line) and area-weighted (dashed line) average velocity magnitude (m/s) at different wind tower positions

Looking at the volume-weighted average velocity magnitude (m/s) in the room in figure 5.18, it is evident that for wind directions 0 to 60 degrees, and for those between 120 and 180, respectively T6 and T4 wind towers have the poorest performance in terms of velocity magnitude provision in the room. This is valid both for volume-weighted average values in the room and for area-weighted average values on a horizontal surface at a height of 1.7 m. Although, the highest and lowest values of wind speed, corresponding to 0.48 and 0.05 m/s as a volume-average and 0.52 and 0.04 m/s as a surface-average, occur both in T5 wind tower, at 150 and 90 degrees wind angles respectively.

In more details, at wind directions 0 and 30, the farthest the wind tower is from the window (T4), the higher is the velocity magnitude in the room. In fact, at incident angle 0 the wind tower T4 is providing an average wind speed of 0.29 m/s while this value for T5 and T6 are 0.26 m/s and 0.13 m/s.

The wind angles 60 and 90 degrees generate the lowest air speed in the room, regardless of the position of the tower. At wind direction 90 representing the worst wind direction, the volume-weighted average air velocity in the room is 0.1, 0.09 and 0.08 m/s for wind tower positions T4, T5 and T6 respectively. These values correspondingly reduce to 0.05, 0.05 and 0.06 m/s at a height of 1.7 m.

As the wind deviates towards 180, the induced wind speed greatly improves with 150 degrees providing the pick value of 0.48 m/s as a volume-average and

0.52 m/s as a surface-average for the standing person. Contrary to the windward wind towers, in wind directions 120, 150 and 180, when the window is the supplier of the air flow, the T4 position underperforms compared to T5 and T6, this is especially notable in wind directions 120 and 150 degrees, when T4 provides 0.1 m/s less air speed in the room than T5 and T6 which perform similarly better.

Comparing the performance of the three wind tower positions at wind incident angles 120 and 180, it is observable that while the volume-weighted average velocity values are quite similar in both wind angles, the distribution of this velocity is notably better at 180 on the considered surface at 1.7 m.

### 5.4.6 Mean age of air

According to table 5.5, at 0 wind incident angle, the tower positions T4 and T5 provide much better air age distribution in the room respect to T6 position. The major portion of the room in T4 has an air age of 120 seconds while the room in T5 is 30 seconds fresher. In T6 position, the contours of the mean age of air has a wider range of values in the room and it varies between 390 and 450 seconds. At this angle, and similarly at 30 and 60 degrees, all three towers act as the source of fresh air.

At 30 degrees, similar to 0 degrees, the mean age of air in the rooms ventilated by towers T4 and T5 is much less compared to the one working with T6. At this incident angle, the air age in T5 case is still 30 seconds better than T4, for the latter containing a portion with air age of 150 seconds. T6 at this angle has a fresher air respect to the previous wind direction.

At 60 degrees, the air age increases considerably for all three tower positions with T6 being the worst case (highest air age) and T5 the best (lowest air age). At T6 position, the air age arrives to more than 840 seconds. At T5 the highest air age at a seated person's height is around 420 seconds (figure 5.19) and the major portion of the room has a mean age of air of between 360 and 420. At T4 almost one third of the room at a standing human height has an air age of 450 seconds while in the other parts of the room the air age is between 360 and 450 seconds.

When the wind direction is 90, the T5 has the worst performance as it causes the highest mean age of air in the room (figure 5.19). At this position T4 works better than T6. While in T4 the highest mean age of air hits 570-600 seconds, at T6 this value is between 600-630 seconds. T5 at this direction has the worst performance compared to the other cases at other wind incident angles. In fact, at a height of about 60 cm, the air age in vicinity of one of room corners arrives to 950 seconds. For a standing person in the left half of the room the freshness ranges

between 630 and 720 seconds while on the right half this ranges between 510 and 600. At this angle and the followings where the window falls on the windward facade, the contribution of the window in lowering the air age starts and the towers cease to provide any fresh air.

At wind direction 120, T6 works better than T5 and T4 respectively, providing a mean age of air about 120 seconds in almost the entire part of the room. At T5, almost the entire room at a standing human height has a mean age of air of 150 seconds. In T4 position having the worst air quality, the air age ranges between 180 and 270 seconds.

At 150 degrees, the flow of air entering through the window, hits the inner wall and whirls in the middle of the room. This swirl though causes different distribution of air age in the room for the three tower positions. T5 has a better performance respect to T6 and T4 respectively. While at T5 the central portion of the room has a freshness of 120 seconds, at T6 this value hits 180 and at T4 240 seconds.

At 180 which is the optimum wind direction for the least air age, T6 provides the least mean age of air respect to T5 and T4 correspondingly. At T6, at least half of the room has an air age of between 60 and 90 seconds and on the downstream part of the room on both sides of the window this value is 90 seconds. At T5, however, almost 75 percent of the room has a mean age of between 90 and 120 seconds. Finally, at T4, there is a greater variation in the room's air age with the maximum figure arriving to 210 seconds. In fact, the maximum value for the air age in case T4 is 245 seconds (see figure 5.19).

In general, it is possible to conclude that for the wind angles between 00 and 90, the tower T6 provides the least favourable condition in terms of air age while for the wind directions between 90 and 180, when the window is the major source of fresh air, the tower T4 which is the farthest from the window has the worst performance. At 90 degrees, however, T5 has the least efficiency of all cases collectively. Looking at the maximum values of air age in the whole room shown in figure 5.19, only at 120 degrees wind incident angle, when T5 provides lower maximum than T6, the T6 position has a better distribution of air age and thus provides a better air quality. In all other cases, where the maximum mean of air is lower, the distribution of the air age in the room is better too.

Table 5.5. Contours of mean age of air (s) on a horizontal surface placed at 1.7 m above the ground

| wind angle | T4 | T5 | T6 |
|---|---|---|---|
| τ (s) | 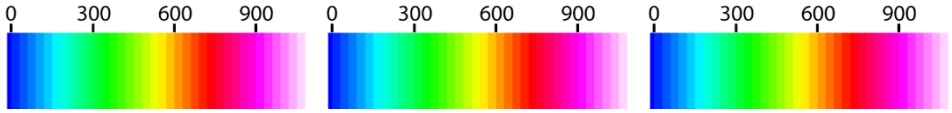  | | |
| 0 | 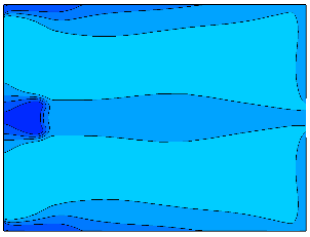 | 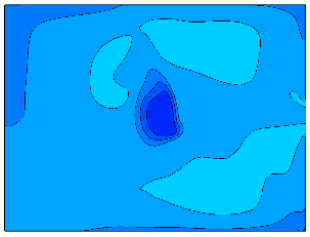 | 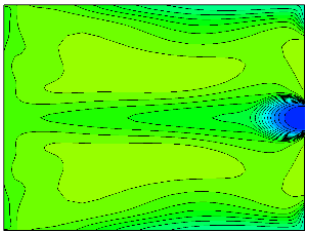 |
| 30 | 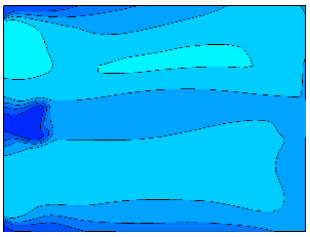 | 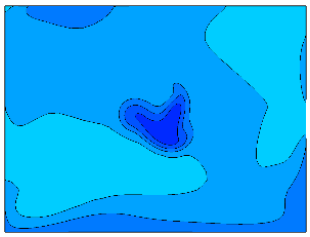 | 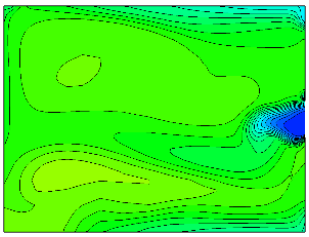 |
| 60 | 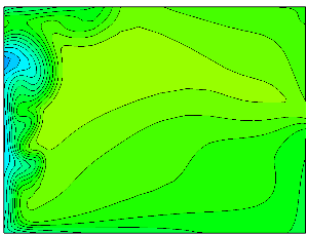 | 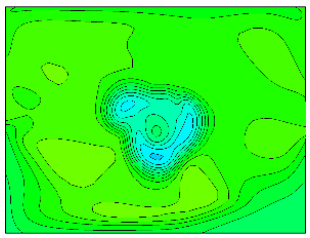 | 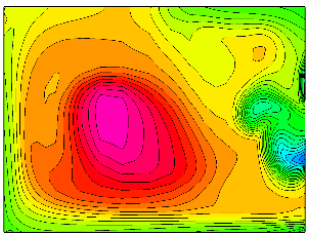 |
| 90 | 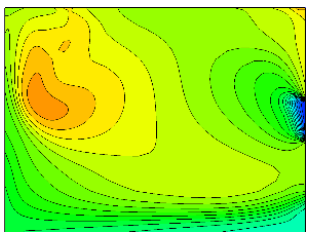 | 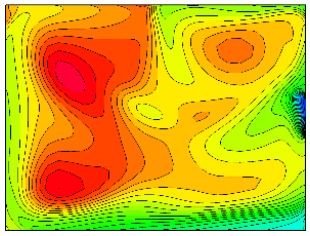 | 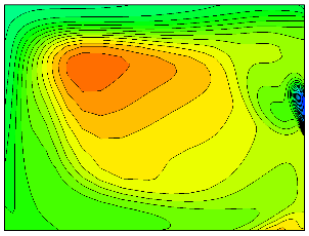 |

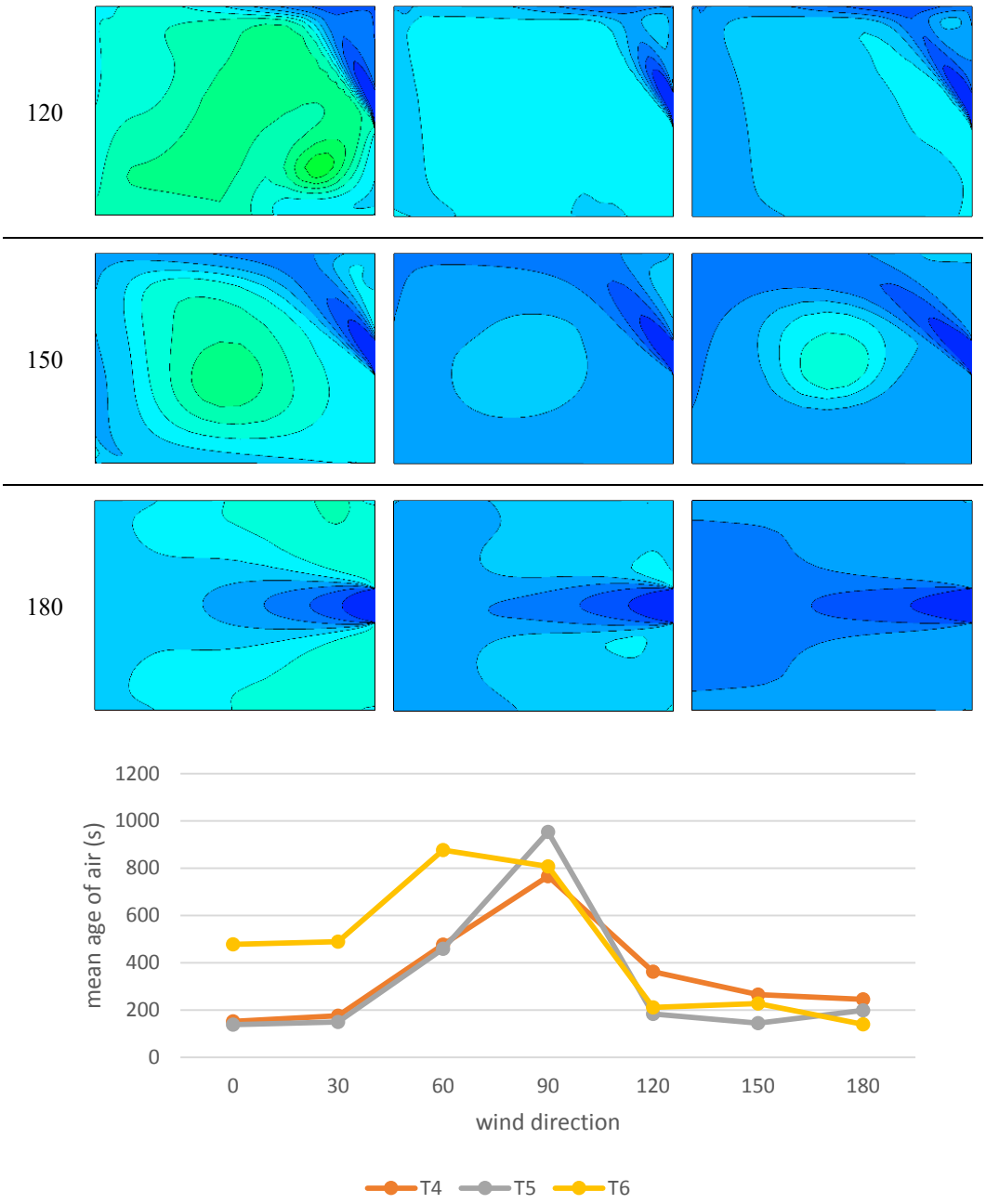


Figure 5.19. Maximum value of mean air age (s) in the room

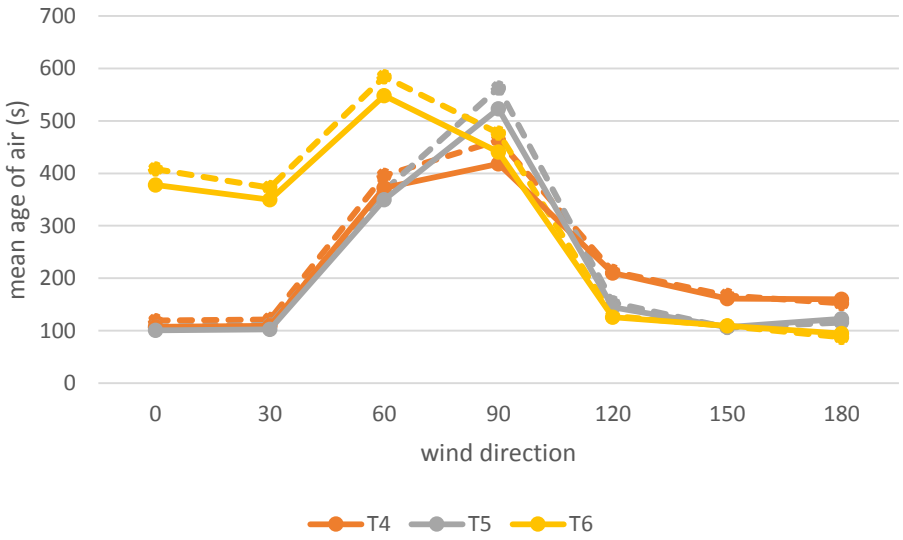


Figure 5.20. Volume-weighted (full-line) and area-weighted (dashed line) average mean age of air (s) at different wind tower positions

The volume-weighted average mean age of air values are summarised in the graph 5.20. According to the graph, in wind direction 0, 30 and 60 when the wind tower is windward, the wind tower T6 considerably underperforms compared to wind towers T4 and T5 which provide similar mean age of air values. This is also notable in the contours of mean age of air at a height of 1.7 m. In fact, at incident angles 0 and 30, the area-weighted average mean age of air on this surface has a range between 107 and 121 seconds for T4 and T5 while for it arrives to 408 and 372 respectively. These values increase to 396, 366 and 584 seconds for T4, T5 and T6 at wind direction 60.

As predicted, the mean age of air values at 90 degrees are higher than all other wind directions. At this angle, the wind tower T5 provides the least fresh air inside the room followed by T6 and T4. The maximum value of mean age of air in a room ventilated by a centrally positioned wind tower is 952 seconds. In the whole room volume and on the surface at a height of 1.7 m this value is 522 and 562 seconds respectively. It is notable that while the point having the maximum mean age of air is found in T5 at 90 degrees wind angle, the distribution of the air age is worse for a standing person in a room ventilated by T6 at 60 degrees wind incident angle. When the window acts as the air supply, at wind directions 120, 150 and 180 degrees, the wind tower T5 and T6 provide a fresher air compared to T4.

For a standing person, T6 at 180 degrees is the optimum combination able to provide a fresh air with age of 87 seconds which increases to 95 seconds considering

the whole room volume. The stalest point in a room ventilated by T6 at 180 degrees has an air age of 139 seconds.

### 5.4.7 Air change efficiency

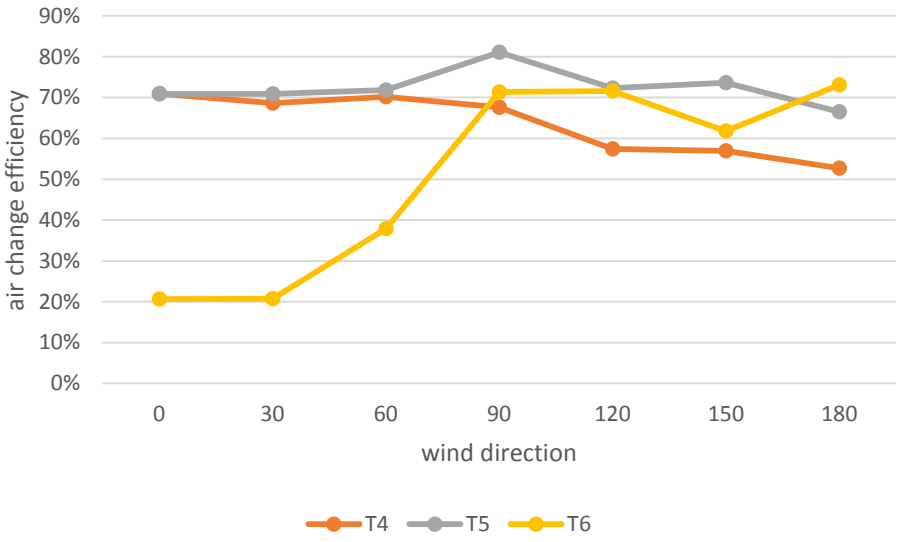


Figure 5.21. Air change efficiency (%)

The graph 5.21 shows the air change efficiency values. It is easily notable how the T6 wind tower has the worst performance compared to T4 and T5 which have similar efficiencies at wind directions 0, 30 and 60 degrees. In fact, at 0 degrees, both T4 and T5 have an efficiency of 71 per cent while this value for T6 is only 21 per cent which the lowest value compared to all other combinations, too. At 90 degrees, T4 and T6 has almost similar values which is about 10 per cent lower than T5's efficiency. When the window is windward, there is more fluctuation in the values of efficiency index, however, evidently the wind tower T4 underperforms respect to the other two wind tower positions. T4 has its worst efficiency of 53 per cent at 180 degrees.

Excluding T6 at 180 degrees, in all other wind directions the wind tower T5 has the highest air change efficiency compared to T4 and T6. However, T5 shares almost the same efficiency with T4 at 0, 30 and 60 and with T6 at 120 degrees. Comparing all configurations, T5 at 90 degrees has the highest air change efficiency of 81 per cent.

## 5.4.8 Conclusion

The results of the simulations in terms of air change efficiency ($\varepsilon^a$), volume-average mean age of air ($\bar{\tau}$), volume-average velocity magnitude ($\bar{U}$) and volume flow rate ($Q_v$) are summarized in the table 5.6, in which the colour blue is the best case (higher velocity, higher flow rate, higher efficiency and lower mean age of air) while red is the worst case. Where the wind towers in two positions had the same value, half of one cell is coloured.

Table 5.6. Best (blue) and worst (red) performances comparing different positions of a one-sided wind tower working with a window

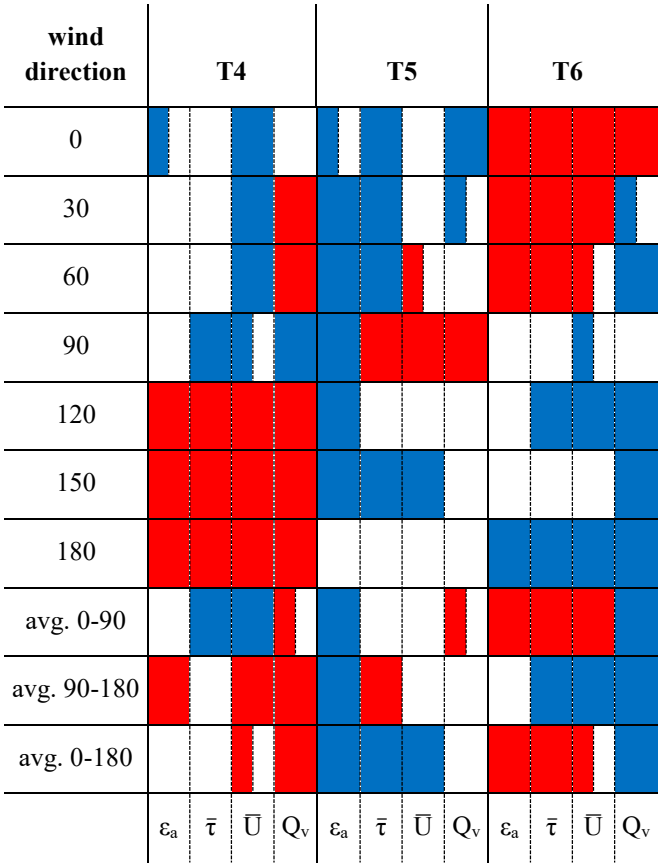


It is notable that the wind tower which has most of the worst values (more cells coloured red) is T6 in wind directions 0, 30, and 60, T5 in wind direction 90, and T4 in wind directions 120, 150, and 180.

Comparing the cases in each wind direction, it is notable that the four indicators do not necessarily follow the same pattern. For instance, while T5 at 90 degrees incident angle, has worse values for velocity, age of air and air flow rate than the other two wind towers, the air change efficiency of T5 is higher than both T4 and

T6. Or, in wind direction 60, while T6 has the worst velocity, air age and air change efficiency than T4 and T5, its volume flow rate is higher than both of them.

The values of each of the four indicators have been averaged for wind direction ranges of 0-90, 90-180 and 0-180 for the three wind tower positions. There are, however, some inconsistencies between these average values and the individual values at specific wind directions. To be more precise, for instance, despite the fact that T5 compared to T4 is showing better values of mean age of air in 0, 30 and 60 degrees and only a worse value in 90 degrees, the average air age of T4 in wind variation 0-90 is better. Or, looking at the velocity figures for T5, it is noticeable that T5 has the highest velocity only at one wind direction (150 degrees), but the average velocity provided by T5 in wind variation 0-180 is better than T4 and T6.

## 5.5 Group II: four-sided wind tower model with a window

### 5.5.1 Reference values at zero incident angle

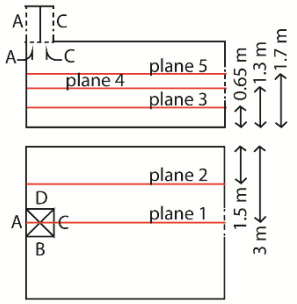


Figure 5.22. The vertical and horizontal planes on which the contours of pressure coefficient, velocity magnitude and mean age of air have been reproduced

The pressure coefficient contours on central vertical plane 1 are represented in table 5.7. Similar to the one-sided wind tower, inside the windward channel of the wind tower (channel A) the Cp values are higher for the wind tower M4. The more the wind tower gets distant from the windward edge of the roof, the more the Cp values in the tower reduce. This is slightly different from what happens on the wind tower aperture. In fact, correspondingly in M4, M5 and M6 the Cp values reproduced on the aperture A (the windward wind tower aperture) are 0.79, 0.48, and 0.51.

In the leeward channel of the wind tower (channel C), the Cp figures with negative values are visible. As the wind tower gets closer to the window and the leeward edge of the roof, the Cp values get closer to zero and their absolute value

decreases. The mean Cp values on the leeward aperture of the wind towers M4, M5 and M6 at zero wind direction are -0.51, -0.34 and -0.18 respectively.

The average Cp in the room are similar in the three cases. In M5 and M6, the volume-average Cp is -0.13, while for the M4 this figure is -0.19.

Table 5.7. Contours of pressure coefficient (-) on the central vertical surface

| plane | M4 | M5 | M6 |
|---|---|---|---|
| Cp (-) | 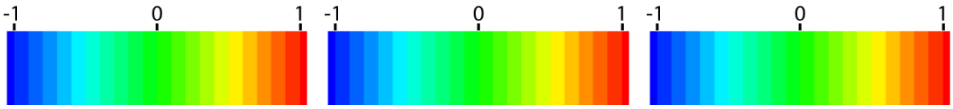  | | |
| 1 | 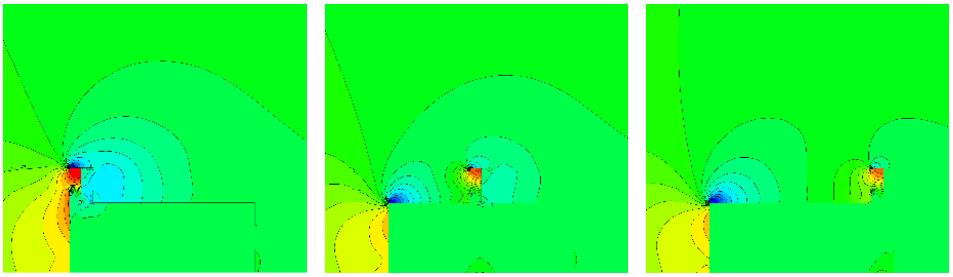 | | |

Comparing the velocity magnitude contours at wind incident angle 0 shown in table 5.8, it is evident that in M4 position, the wind entering the windward aperture A, has a lower velocity both near the roof of the tower and at the intersection between the tower and the room. The velocity magnitude on the aperture A is 0.68, 0.89 and 0.71 m/s in cases M4, M5 and M6, while the figures respectively change to 1.59, 1.88 and 1.72 m/s on the intersection surface of aperture A with the room. The air jet through aperture A in this position reduces speed at a slightly higher distance from the floor compared to the other positions.

At leeward apertures B, C and D (B & D not shown in the figures) in position M4 the extracting air is speedier compared to M5 and M6 correspondingly. For instance, the corresponding velocity magnitude on the aperture C in M4, M5 and M6 are 0.64, 0.43 and 0.39 m/s.

Inside the room in M4 case, there is a distribution of the velocity in ceiling adjacency (see plane 1 in table 5.8), while in the major portion of the room the air remains still. As the tower's position gets closer to the window, the extraction of air from aperture C decreases and the internal air movement increases. In fact, on plane 5, the area-average velocity in case M6 is 0.16 m/s, while it is 0.157 m/s in M5 and 0.14 m/s for M4.

The speed of the air through the window reduces as the tower gets close to the window. In cases M4, M5 and M6 the area-average velocity magnitude on the window is 0.55, 0.32, and 0.07 m/s.

Table 5.8. Contours of velocity magnitude (m/s) on different horizontal and vertical surfaces

| plane | M4 | M5 | M6 |
|---|---|---|---|
| U (m/s) | 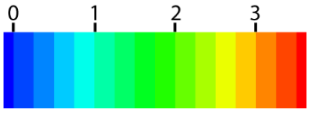  | 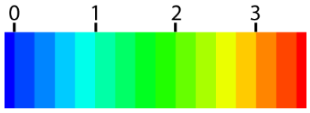  | 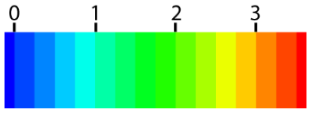  |
| 1 | 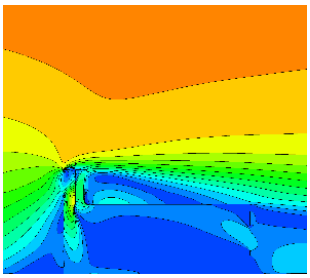 | 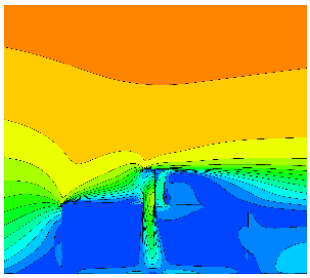 | 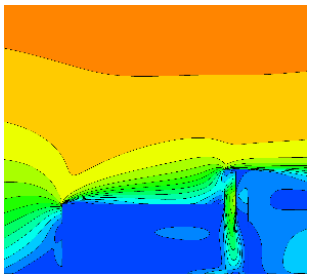 |
| 2 | 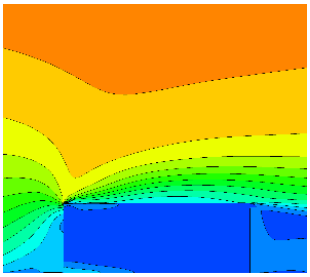 | 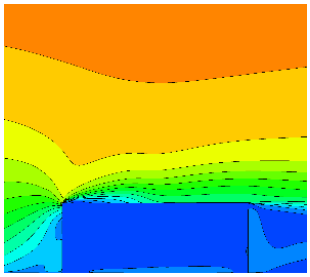 | 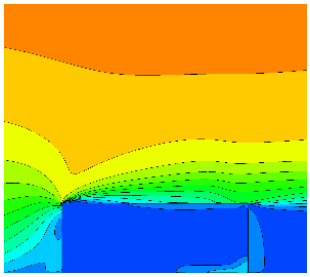 |
| 3 | 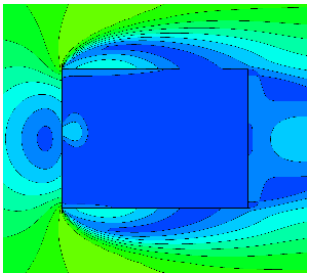 | 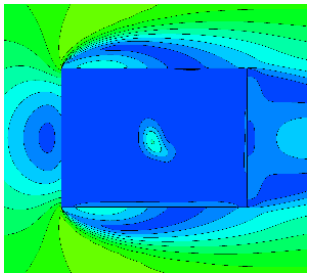 | 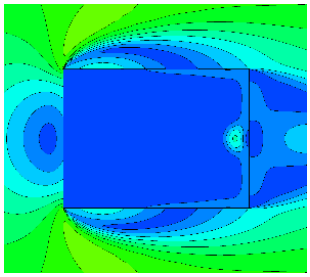 |

| | | | |
|---|---|---|---|
| 4 | 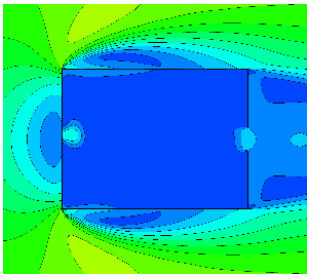 | 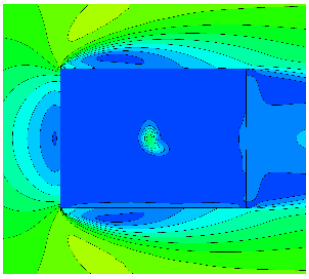 | 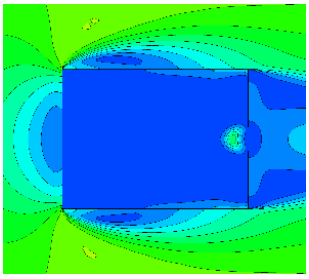 |
| 5 | 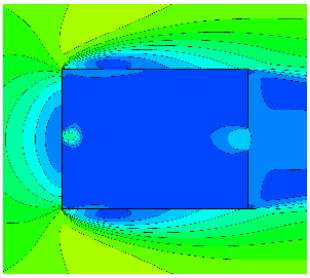 | 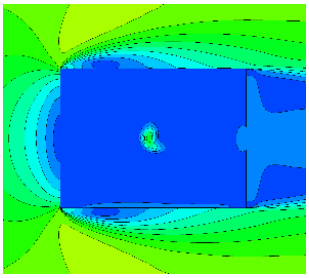 | 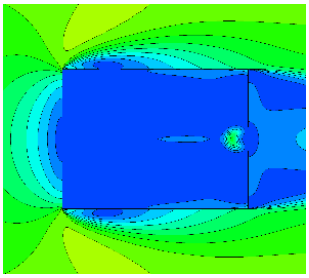 |

Table 5.9. Contours of mean age of air (s) on different horizontal and vertical surfaces

| **plane** | **M4** | **M5** | **M6** |
|---|---|---|---|
| τ (s) | 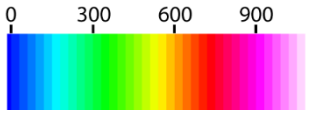 | 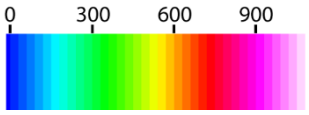 | 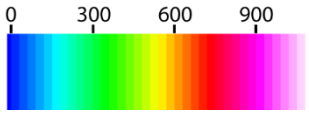 |
| 1 | 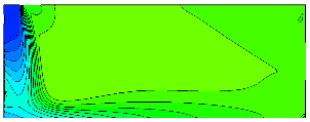 | 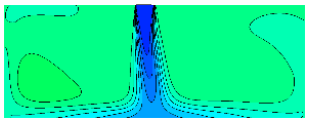 | 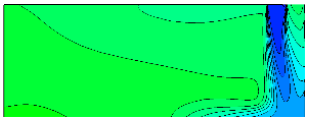 |
| 2 | 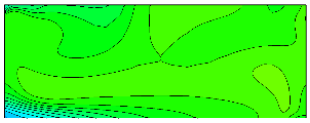 | 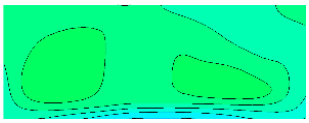 | 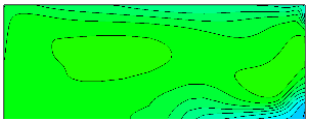 |
| 3 | 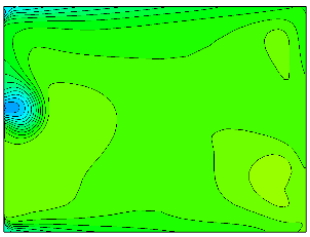 | 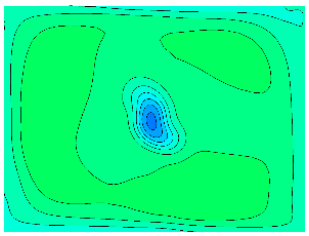 | 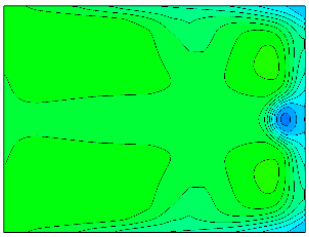 |

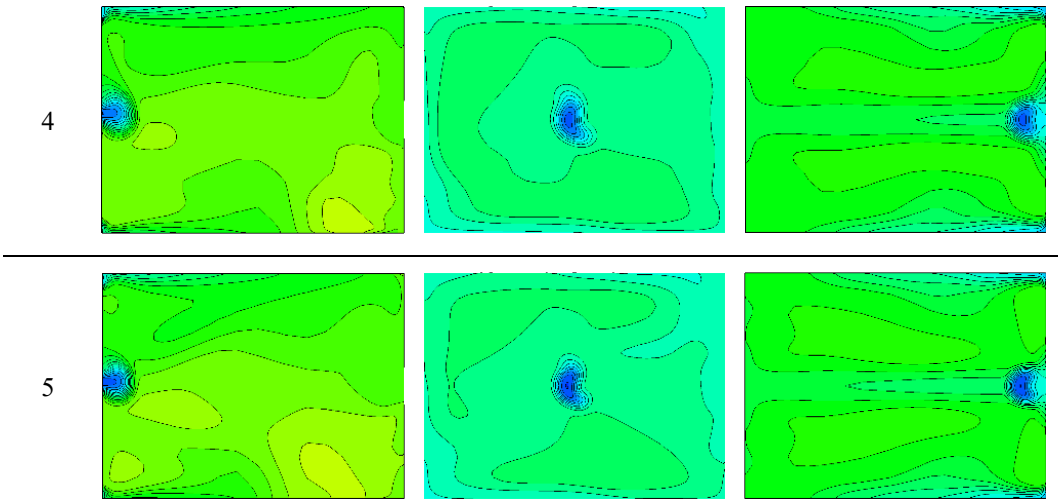


A general observation of contours of mean age of air shown in table 5.9 indicates that at 00 wind incident angle, the room's air is fresher in case the tower is placed at M5 position. In this case, even though that the air has a better quality in adjacency of the walls, but the freshness of the air is almost homogenously distributed through the room and it ranges between 240 and 270 seconds. Case M4 is the one with the worst air quality at 00 incident angle in which at some points the mean age of air arrives to around 480 seconds. Case M6 shows how air is fresher around the walls and in the room central axis. Similarly, the air is fresher in vicinity of the floor and the roof while at a seated or standing human height the age of air is between 330 and 360 seconds.

The average air age in the room volume is 395, 247 and 313 seconds respectively in M4, M5 and M6. The correspondingly value on plane 5 representing a standing human is 409, 254 and 334 seconds.

## 5.5.2 Volume flow rate and air change number

The volume flow rate values through different apertures of the wind tower are shown in figures 5.23 (aperture A & C) and 5.24 (apertures B & D), while the air flow rate through the window is shown in figure 5.25.

In all three tower positions, at 0 incident angle, obviously the only wind tower aperture through which the airflow goes in is aperture A. However, comparing the volume flow rate of the three positions, it is evident that in case the tower is placed in the center of the room (case M5-00) this airflow is bigger (0.47 $m^3/s$ in M5 compared to 0.43 in M6 and 0.39 in M4), while at M4 position, the three apertures B, C and D which are positioned on the leeward side are more efficient in extracting

the air from the room (figures 5.23 and 5.24). Interestingly, at this angle the window is working as an air inlet in wind towers M4 and M5, while it works as an outlet in M6 (see figure 5.25).

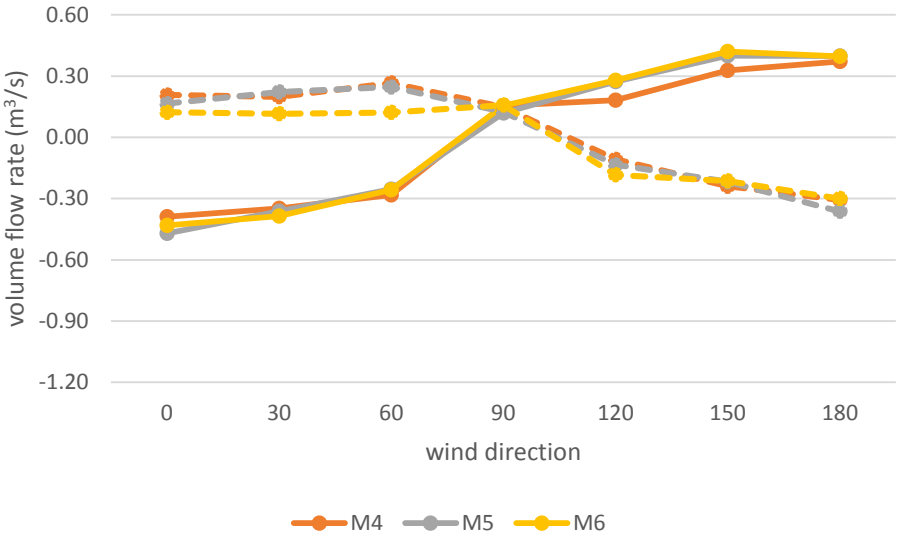


Figure 5.23. Volume flow rate ($m^3/s$) through apertures A (full line) and C (dashed line) at different wind directions

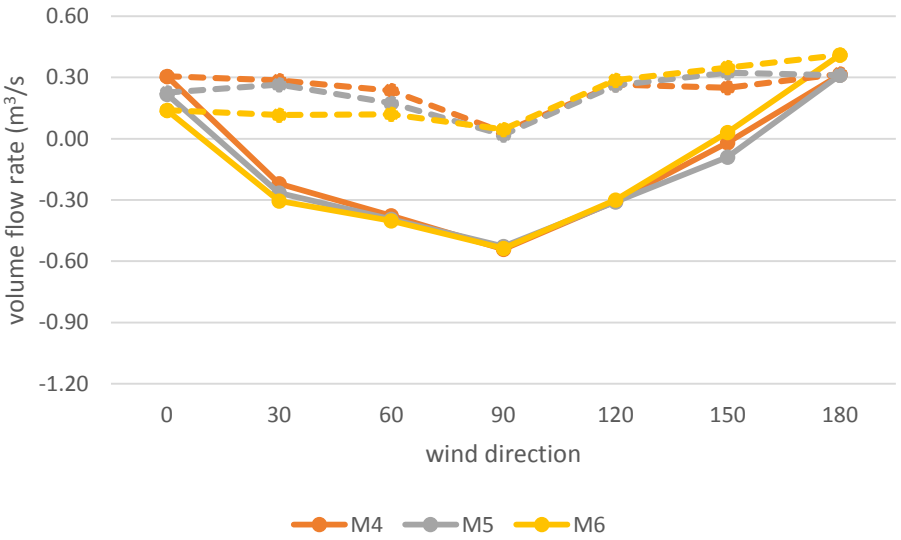


Figure 5.24. Volume flow rate ($m^3/s$) through apertures B (full line) and D (dashed line) at different wind directions

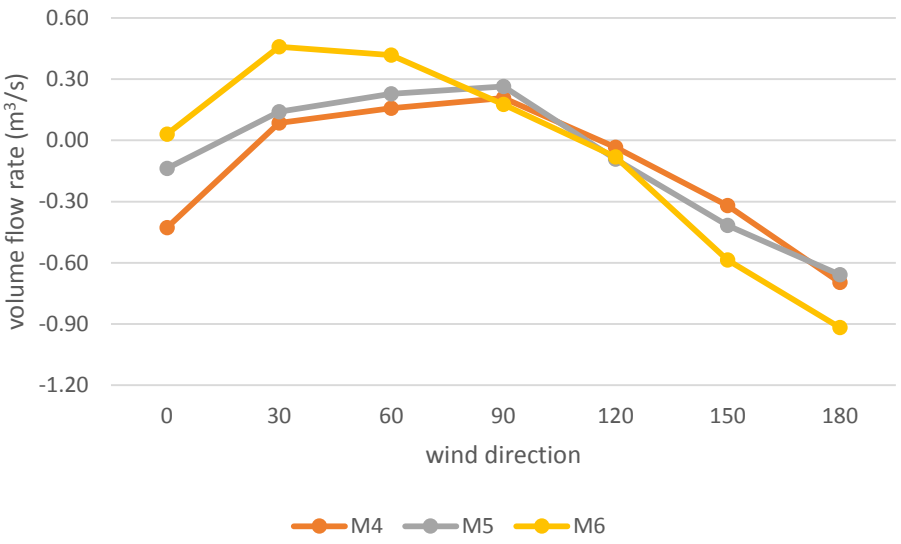


Figure 5.25. Volume flow rate ($m^3/s$) through the window at different wind directions

At 30 and 60 degrees, apertures A and B work as inlets in all three tower positions. At incident angle 30, M6 position is the one that maintains a greater inward air flow collectively with a volume flow rate of 0.69 $m^3/s$ compared to 0.62 in M5 and 0.57 in M4. At this angle, M5 and M4 are more efficient than M6 and provide the same amount of air exhaustion equal to about 0.48 $m^3/s$ as a sum through the two apertures C and D. At 60 degrees, the three tower positions provide almost the same amount of inward airflow. However, M4 has the best extracting performance.

At 90 degrees, evidently, the main inlet aperture is B for all three positions. At this incident angle, all three towers M4, M5 and M6 have almost the same efficiency in letting 0.53 $m^3/s$ of air through. Though, the tower M6 is the one that provides the most outward airflow through its leeward apertures.

At 120 degrees, the M6 position shows a generally better performance comparing the volume flow rate through its 4 apertures, regardless of the direction of the airflow -i.e. it is the tower position providing the most inward and outward airflows.

At 150 degrees angle, M5 is the tower position providing a better inlet air flow of 0.31 $m^3/s$ through its apertures B and C, while M6 maintains the most extraction with the sum value of 0.77 $m^3/s$ through apertures A and D. Aperture B in M6 in this wind angle, contrary to the same aperture in M4 and M5, work as an air outlet rather than an inlet, even though this value is a very small value of 0.03 $m^3/s$.

Finally at 180 degrees where aperture C is the only inward airflow provider, M5 works better than the other two as an inlet as it lets in an air flow of 0.36 $m^3/s$ while the outlet air flow through the three apertures A, B and D is greatest at M6 with a sum of 1.62 $m^3/s$.

To summarize, concerning the inward airflow, M6 and M5 has the best performance at three angles while M4 at one angle. Concerning the outward airflow, however, M6 has the best efficiency at four angles while M4 and M5 at one angle solely.

Contrarily, considering the least flow rates, M4 is the one providing the smallest inward airflows at three angles while M5 and M6 at two. On the other hand, M6 and M4 provide the lowest outward airflow at three directions while this number is one for M5.

Concerning the air flow rate through the window of the room, the highest value is observed in wind direction 180 for all the wind towers. The wind tower M6 provide the value of 0.92 $m^3/s$ while this value for M4 and M5 are 0.70 and 0.66 $m^3/s$ respectively. The lowest air flow rates through the window for the three wind towers are at 120 degrees incident angle when M4, M5 and M6 show values of 0.03, 0.09 and 0.08 $m^3/s$ respectively. Additionally, the wind tower M6 at 0 incident angle has an airflow rate of 0.03 $m^3/s$ which is considerably lower than that in M4 case with corresponding value of 0.43 $m^3/s$.

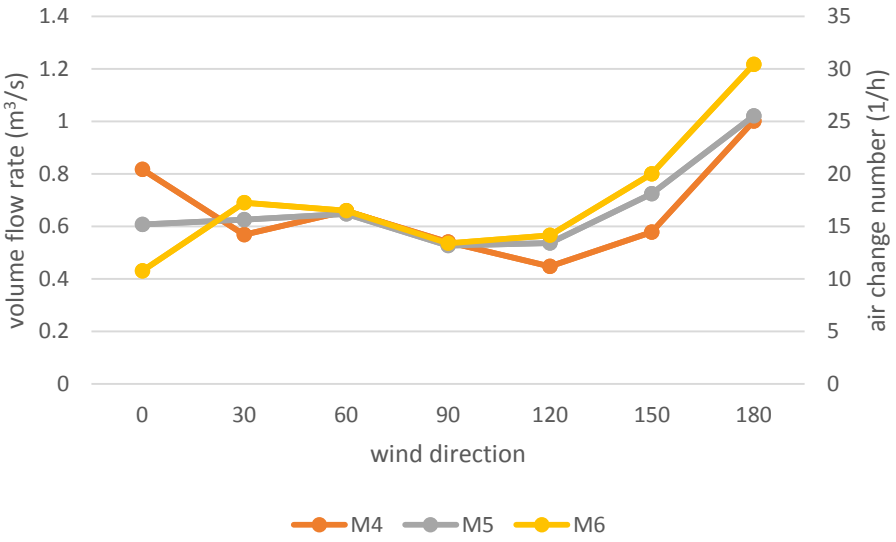


Figure 5.26. Volume flow rate (m3/s) and air change number (1/h) by each four-sided tower at different wind directions

According to the graph 5.26 summarising the total volumetric air flow rate values and air change numbers provided by the four-sided wind tower that works with the room window, it is noticeable that the tower position M6 provides the highest airflow rate and a corresponding air change number in all wind directions except 0 and 90 degrees. In these incident angles, M4 induces more airflow rates and thus guarantees a higher air change in the room compared to M5 and M6. In fact, M6 at 0 wind direction provides the least air flow rate of 0.43 m3/s and an ACH of 10.7. At 60 and 90 degrees, the three tower positions perform similar to one another providing 0.65 and 0.53 volumetric airflow rates which correspond to 16 and 13 ACH. At wind angles over 90 degrees, T6 performs better than T5 and T4 respectively. The highest airflow rate of 1.2 and 30 air change per hour is provided by T6 at 180 degrees.

### 5.5.3 Pressure coefficient

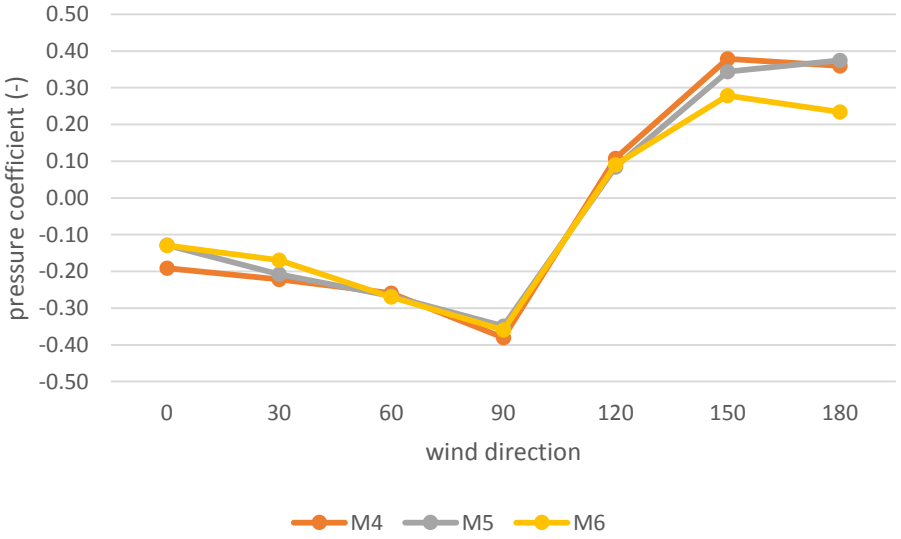


Figure 5.27. Volume-weighted average pressure coefficient (-) in the room

The graph 5.27 demonstrates the average pressure coefficient values inside the room at various wind directions. As it is evident in the graph, for the three wind directions 60, 90 and 120, the change in the position of the wind tower shows no impact on the average Cp in the room. At these wind incident angles, the average Cp values in the room are around -0.27, -0.36 and 0.09 respectively.

The most notable difference between the Cp values by the three wind tower positions is visible in 180 degrees when the room's Cp in case M6 is around 0.14 less than those of M4 and M5.

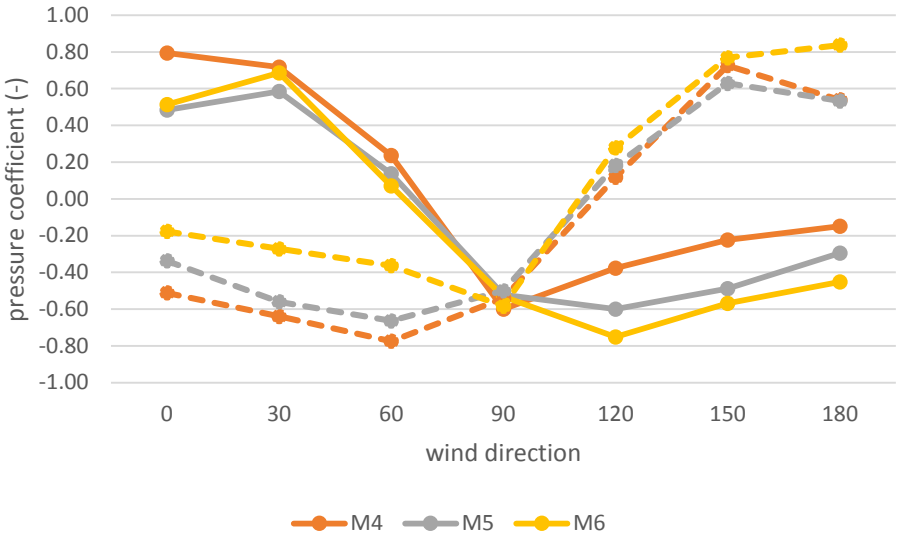


Figure 5.28. Area-weighted average pressure coefficient (-) on wind tower apertures A (full line) and C (dashed line)

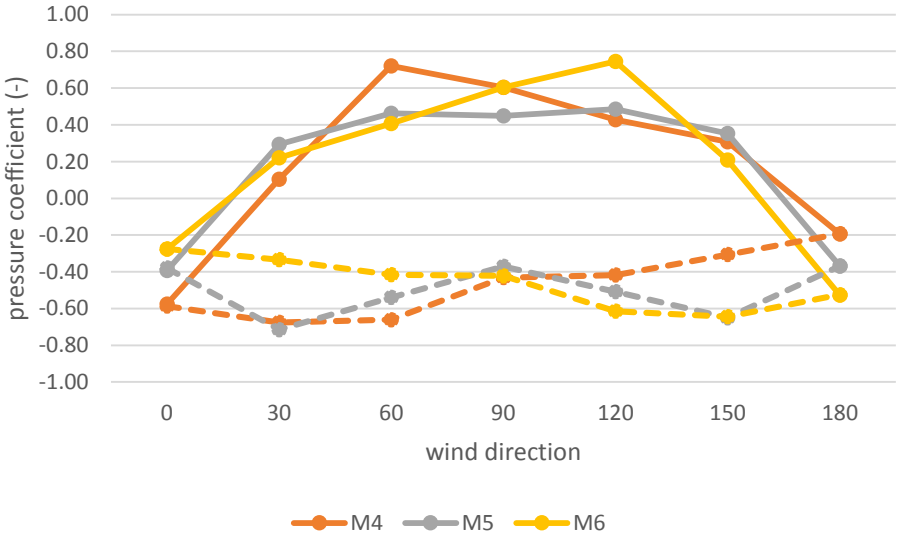


Figure 5.29. Area-weighted average pressure coefficient (-) on wind tower apertures B (full line) and D (dashed line)

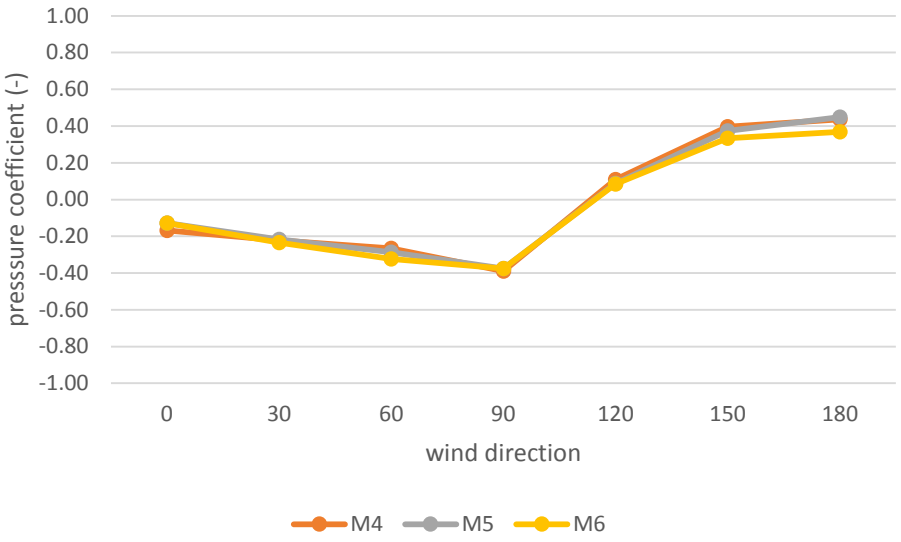


Figure 5.30. Area-weighted average pressure coefficient (-) on the window

The variation of the pressure coefficient values on different wind tower apertures and the window are presented in the graphs 5.28, 5.29 and 5.30. It is noted in figure 5.30 that the effect of wind tower position on the Cp value of the window is negligible. The highest variation in the window's average Cp value occurs at 180 degrees when the window of the model M6 has a Cp value of only 0.08 less compared to M4 and M5.

Wind tower apertures (figures 5.28 and 5.29), contrary to the window, experience more alteration in Cp values by a change in position of the wind tower. All apertures in M5 position show symmetrical behaviour in terms of Cp by the change in wind direction. While M4 and M6 seem to be a reflection of one another with 90 degrees being the reflection axis.

M4's Cp values on aperture A except for the wind direction 90 show a higher mean value compared to M5 and M6. M6 has the identical behaviour in aperture C. The difference between the pressure coefficients on aperture A in three wind tower cases is greater with wind directions over 90, while the same pattern is seen on aperture C with wind directions 0-90. On these apertures, the maximum difference between the Cp values arrive to 0.41 which is the difference between Cp value on aperture C of the cases M4 and M6 at 60 degrees.

### 5.5.4 Velocity magnitude

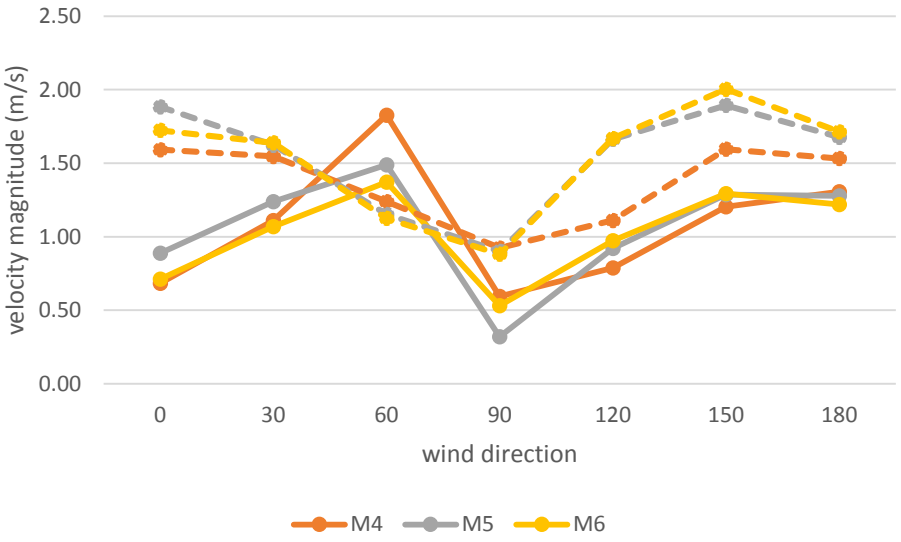


Figure 5.31. Area-averaged velocity magnitude (m/s) on wind tower aperture A (full line) and the intersecting aperture A (dashed line)

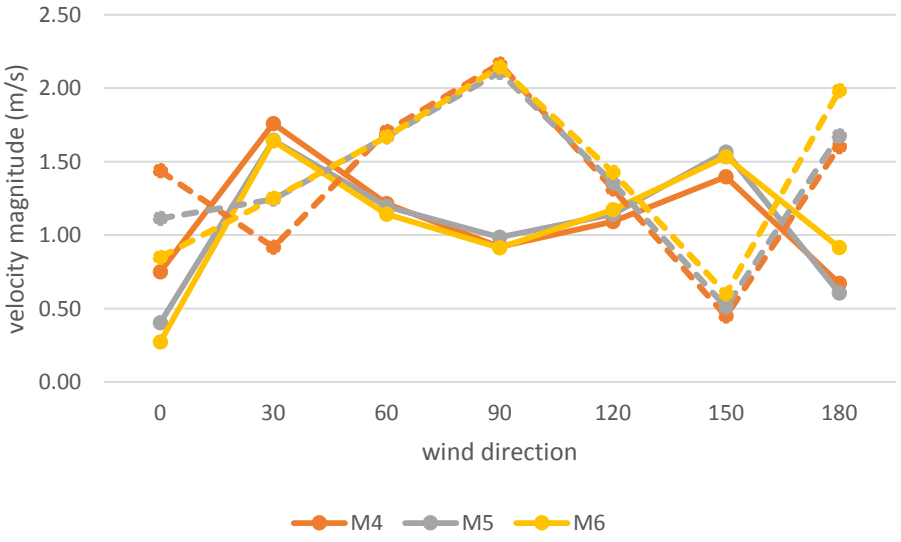


Figure 5.32. Area-averaged velocity magnitude (m/s) on wind tower aperture B (full line) and the intersecting aperture B (dashed line)

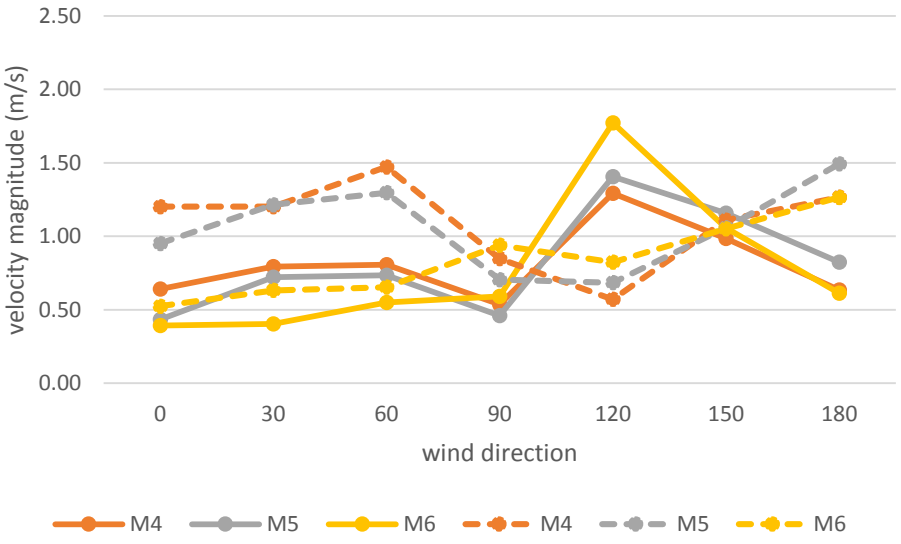


Figure 5.33. Area-averaged velocity magnitude (m/s) on wind tower aperture C (full line) and the intersecting aperture C (dashed line)

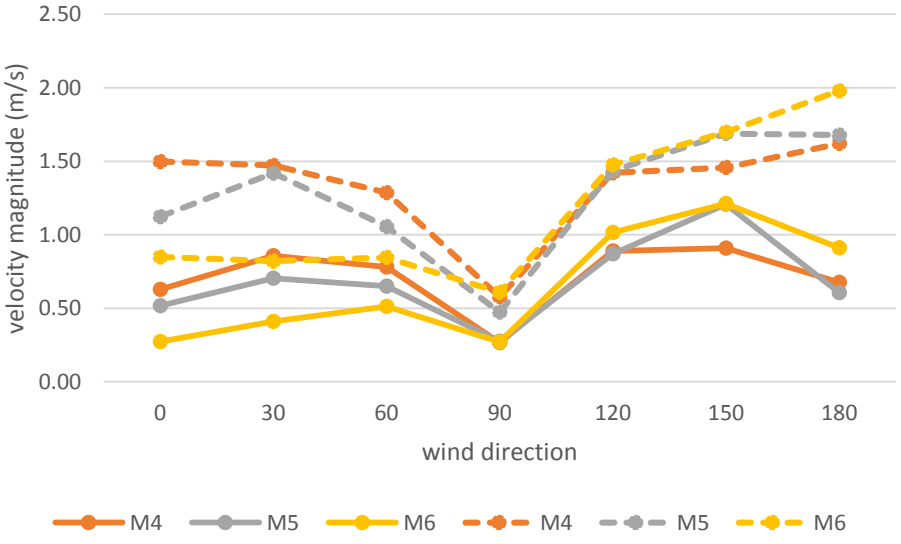


Figure 5.34. Area-averaged velocity magnitude (m/s) on wind tower aperture D (full line) and the intersecting aperture D (dashed line)

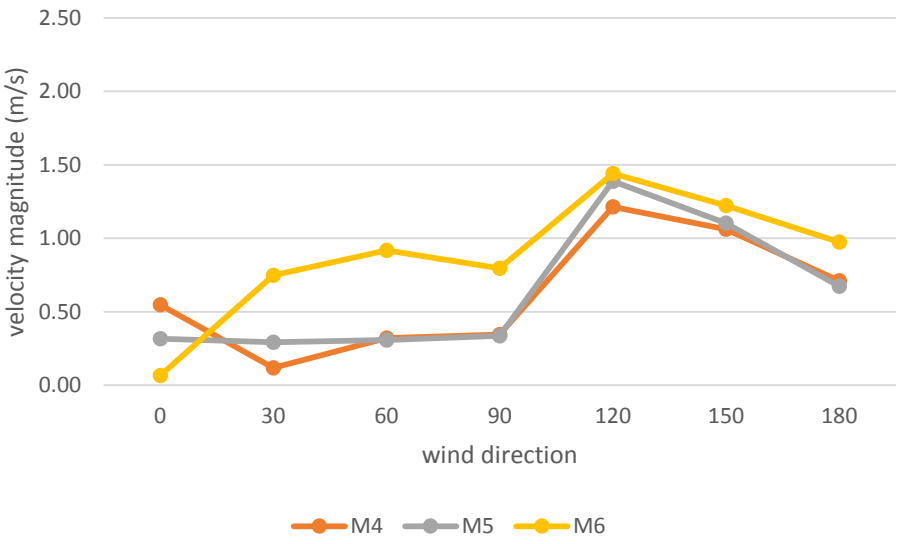


Figure 5.35. Area-averaged velocity magnitude (m/s) on the window

The figures 5.31 to 5.34 demonstrate the velocity magnitude values on each of the wind towers apertures and their corresponding intersecting apertures, while figure 5.35 shows the same value on the window.

According to table 5.10, at wind incident angle 30 degrees, the distribution of velocity inside the room is better in cases M5 and M6 compared to M4. In Case M4, there is almost no air movement in any part of the room other than the left hand side of the tower. The air jet in this case is less speedy compared to the other two positions and it barely reaches the floor. Comparing the area-average velocity magnitude on tower apertures and intersecting apertures at this angle, what is notable between the three wind towers positions is the difference between the speed in leeward apertures B and D (figures 5.32 and 5.34) in which the M6 case shows less speedy air movement while the M4 and M5 are similar. Contrary to the 0 wind direction, the speed on the window is much greater in case M6 compared to M5 and M4 where this figure is 0.75, 0.29 and 0.12 m/s respectively (see figure 5.35).

At 60 degrees, the closer the tower is to the window, the less speedy is the air jet entering the room. This is because while the air through aperture B is almost equally speedy in the three cases, the M4 provides a higher velocity through aperture A. The same applies to the leeward airflow extracting from apertures C and D. However, there is not a notable difference in the distribution of air movement comparing the three tower positions shown in table 5.10. In fact, the average velocity felt by a standing person in M4, M5 and M6 cases are 0.19, 0.22 and 0.20

m/s (figure 5.36). At this angle, the air speed on the window surface is around 0.31 m/s for M4 and M5 while for M6 is 0.92 m/s (figure 5.35).

At 90 degrees, the aperture B which is perpendicular to the wind direction, conveys almost the same velocity of air to the room in all three tower positions. The velocity magnitude on the opening of this aperture is 0.92, 0.98 and 0.91 m/s for M4, M5 and M6 while it arrives to around 2.16, 2.1 and 2.14 m/s on the room and tower intersecting surface (see figure 5.32). The leeward apertures also show similar air speeds either on the wind tower opening or on the intersecting aperture. The variation between the air speed in these apertures is no greater than 0.037 m/s which is the difference between M4 and M5 wind speeds on aperture A (figure 5.31). The air movement distribution inside the room shown in table 5.10 varies in the three cases but the M4 case seems to have a better circulation.

As the wind incident angle reaches 120, in all three tower positions, the efficiency of the tower in providing air movement decreases greatly. However, the M6 case shows speedier velocity contours in all its four apertures. Apart from the tower underneath, in the other parts of the room the air is still. The average air speed in the room volume for the three cases is around 0.13 m/s which is slightly (0.2 m/s) more than the velocity felt by a standing person (figure 5.36). At this angle, even though the windward aperture C show velocity values of between 1.29 and 1.77 m/s, the entering air through this channel to the room is not similarly speedy and its value reduces to a value between 0.57 and 0.82 m/s respectively (figure 5.33). This happens in the reversed way in the other windward aperture B in which the velocity on the intersecting surface is higher than that on the wind tower aperture (figure 5.32). Furthermore, from this direction until 180 degrees, where the window is windward too, the effect of wind tower position on the velocity on the window reduces. The highest velocity on the window happens at wind direction 120 when the M6 case provides a value of 1.44 m/s (figure 5.35).

At 150 incident angle, similar to 120 degrees, the distribution of air movement inside the room is poor but better than the 120 degrees. M6 works better than M5 and M4 in this regard because there is an inward airflow from the window which has a greater velocity in M6 compared to M5 and M4 respectively (table 5.10). The average velocity magnitude on the window surface is 1.22, 1.10 and 1.06 m/s in the three cases (see figure 5.35), which are values less than those in wind direction 120, however, the contours of velocity magnitude show that at 150 degrees, the air movement through the window is greater (see table 5.10).

Finally, at 180 degrees, the window has an evident impact on the air distribution inside the room shown in table 5.10 even though the speed on its surface (figure

5.35) is less than 120 and 150 degrees. M6 position shows a better velocity distribution in all levels and directions compared to M5 and M4. The average speed in the room volume is 0.25, 0.18, 0.16 m/s respectively (figure 5.36). This is despite the fact that the windward aperture C in M6 has a lower velocity compared to M5 (figure 5.33). In M6, the leeward apertures B and D extract the air with 0.38 m/s higher speed compared to M4 and M5.

Table 5.10. Contours of velocity magnitude (m/s) on a horizontal surface placed 1.7 m above the ground

| **wind angle** | **M4** | **M5** | **M6** |
|---|---|---|---|
| U (m/s) | 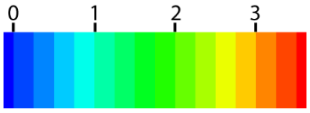 | 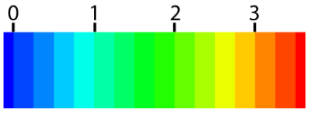 | 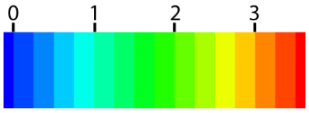 |
| 0 | 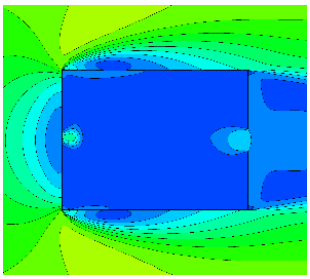 | 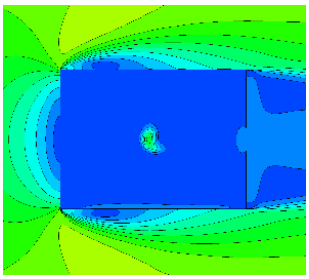 | 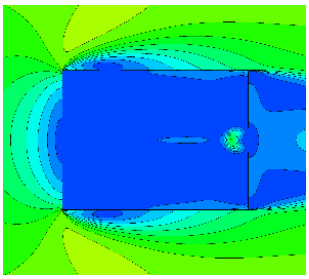 |
| 30 | 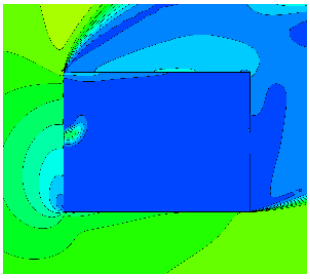 | 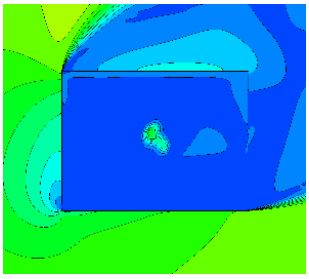 | 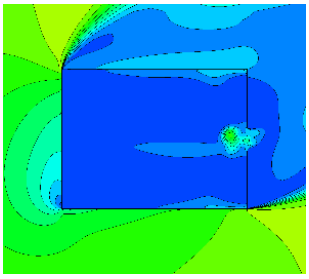 |
| 60 | 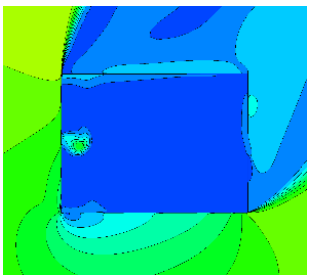 | 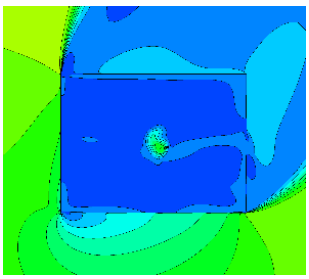 | 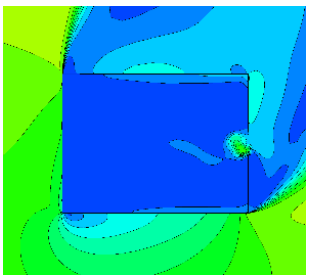 |

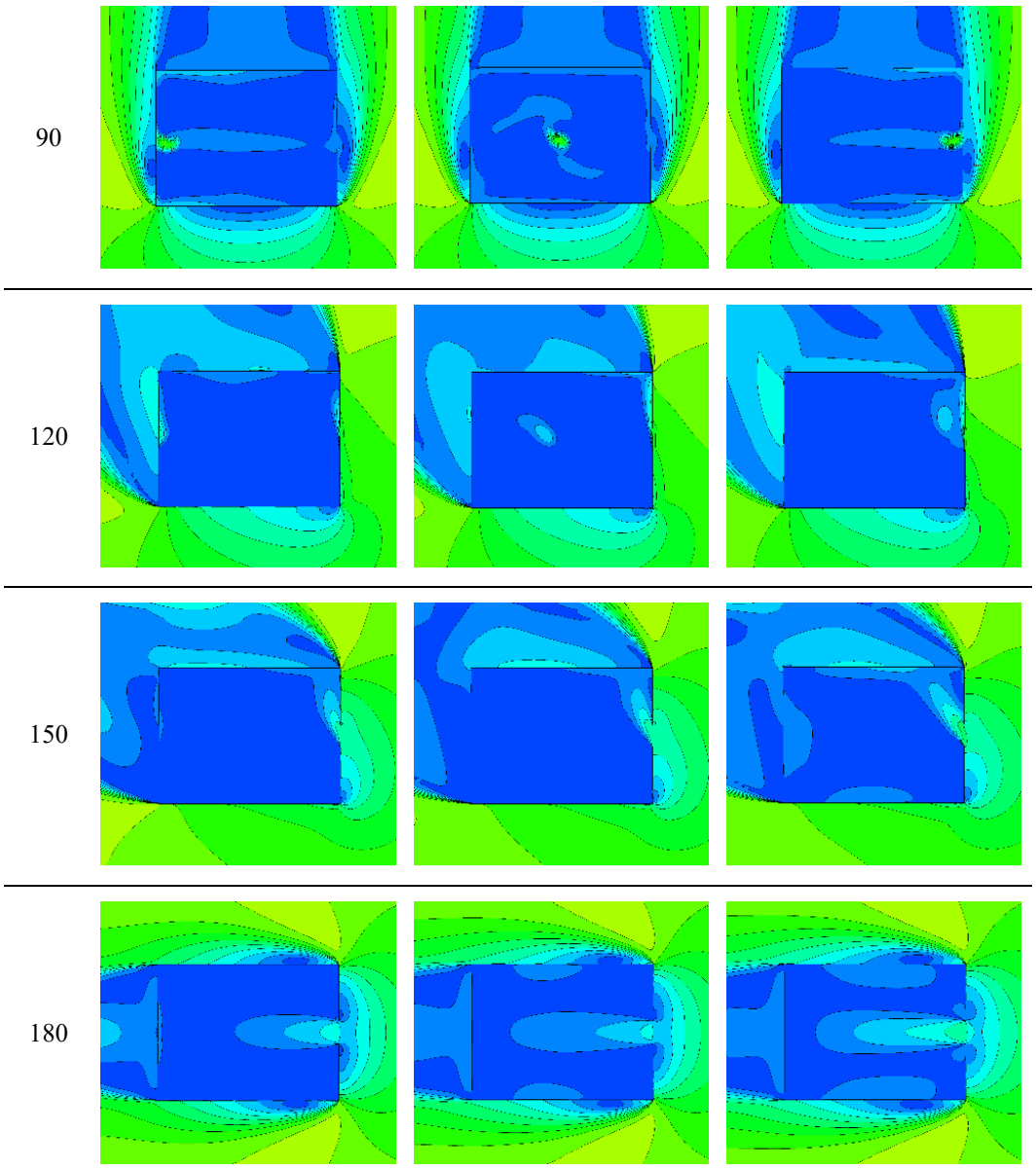


The graph of average volume-weighted velocity magnitude provided by the three wind tower positions and shown in figure 5.36 has several fluctuations. The room volume at wind incidents 0 and 30, experiences similar air movement in M5 and M6 that generate 0.03 m/s and 0.07 m/s more air speed than M4. Between 30 and 90 degrees the air speed provided by M5 remains stable in the room. Actually, this wind tower position, provides a volume-weighted air velocity of 0.21 m/s from which on average 0.19 m/s is felt by a standing person at a height of 1.7 m. At 90 degrees, the wind tower M4 provides a relatively high air movement which arrives to 0.24 m/s, which is the second highest air speed in the room volume. At 120

degrees, the three wind towers generate similar air movement in the room which is about 0.12 m/s. At 150 and 180 when the window, too, acts as the air supply, the closer the wind tower is to the window, the higher is the induced air velocity. In fact, the highest air speed of all is provided by M6 wind tower at 180 degrees providing 0.25 m/s which increases to an average of 0.28 m/s on a horizontal surface at a height of 1.7 m from the room floor, while the lowest velocity of all is provided by T4 at 150 degrees having an average value of 0.1 m/s.

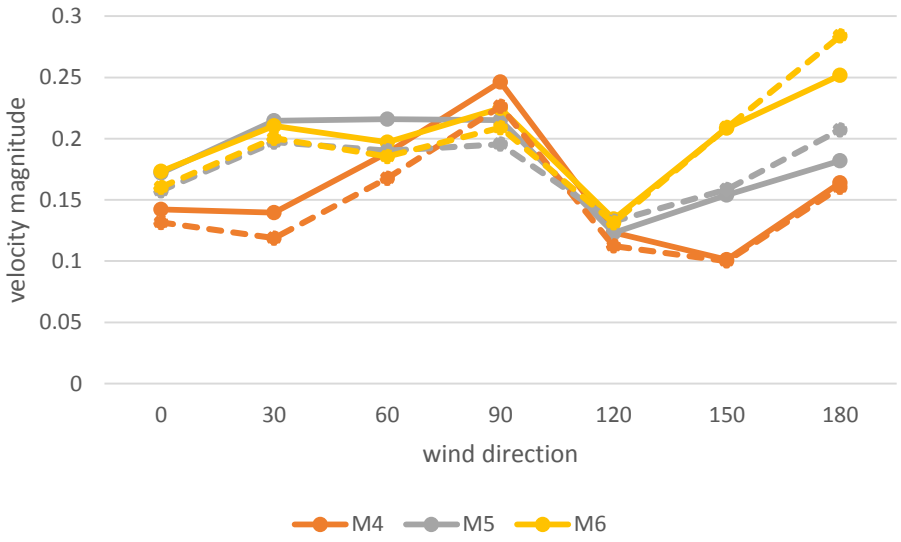


Figure 5.36. Volume-weighted (full-line) and area-weighted (dashed line) average velocity magnitude (m/s) at different wind tower positions

What is additionally noticeable comparing the graph 5.36 with the contours of velocity magnitude at the height of interest (table 5.10), is that the despite the contours showing less air movement in the room at 90 degrees by the three wind towers, the graph demonstrate that the average velocity provided at this angle is in fact greater than what M4 and M5 induced at 180 degrees. Or, for instance, the average velocity on the height of 1,7 m provided by M6 at 30 degrees, is almost equal to that provided by M5 at 180 degrees.

### 5.5.5. Mean age of air

According to table 5.11, at 30 degrees wind incident angle, similar to 0 incident angle, the best to worst air quality is seen respectively in M4, M5 and M6. At this angle, the air quality shows an evident improvement in all three positions, though in case M4 it is much more notable than the other two. M5 having the least age of

air at this wind angle, provides a quasi-constant age of air of around 210 seconds at the height of a seated or standing human.

At 60 degrees, M4 and M5 provide quasi similar air freshness inside the room. Their main difference is that in case M5 at a human height and in the vicinity of the window the air has a lower mean age with respect to M4. In M6 as the worst case at this wind angle and M5, the air is older at the right hand side of the room, while in case M4 this old air is mainly accumulated in front of the window.

At 90 degrees, similar to the previous wind incident angles, the room's air travels for less time and so it is fresher in case M5. At this position, the air in the room is almost homogenously 210 second old. The only places of the room where the air is fresher in this position are the adjacency of the downstream wall of the room and beneath the tower where the air jet comes in. Cases M4 and M6, despite the latter being the worst condition, provide a similarly symmetrical distribution of mean age of air inside the room and in both the accumulation of the air with highest age is the farthest side of the room from the tower.

At 120 degrees, in which the window can operate as an air inlet, M6 provides the lowest and M4 the highest age of air in the room. In M6, on left hand side of the window the age of air abruptly changes while in the other cases this change is much more gradual. In case M5 and M6 the freshest air is accumulated in vicinity of the wall on the opposite side of the window. While in case M4, a narrow portion of the room on the left side of the window has a fresh air. In this case, the age of air in the middle of the room varies between 360 and 420. In case M5 this value is between 300 and 360 and in case M6 is averagely 300 seconds.

At 150 and 180 degrees, in which the window's performance in letting the air through the room becomes more efficient, the M6 provides a considerably better air quality compared to the other two tower positions.

At 150 degrees, in all cases, the left side of the window is the freshest part of the room. In case M6, in a circular area with a diameter of 4.5 meters approx. the air is least fresh with a local age of air of between 210 and 240 seconds. In M5 position, only in 1/3 length in vicinity of the window, the freshest and stalest air could be found, while in the remaining 2/3 portion of the room farther from the window, the age of air has a constant range of between 240 and 270 seconds.

At 180, the air age in the middle of the room being fully affected by the window ranges between 60 and 90 seconds in case M6, while on the lateral portions of the room this value has a maximum of 120 seconds. The same form of air age distribution is seen in case M5 with the mean age of air values ranging between 120

and 180 seconds. In the worst position, M4, the 2/3 length of the room lateral to the window has an air age of between 210 and 240 seconds while the rest of the room has an average freshness of between 120 and 210 seconds.

Table 5.11. Contours of mean age of air (s) on a horizontal surface placed 1.7 m above the ground

| **wind angle** | **M4** | **M5** | **M6** |
|---|---|---|---|
| τ (s) | 0 300 600 900 | 0 300 600 900 | 0 300 600 900 |
| 0 | 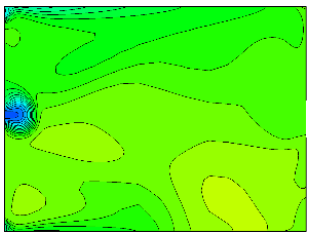 | 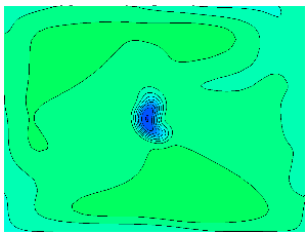 | 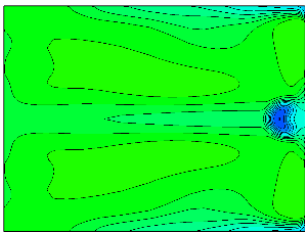 |
| 30 |  | 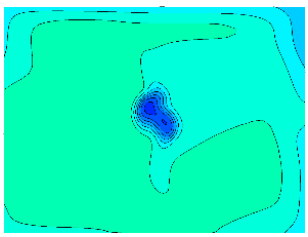 | 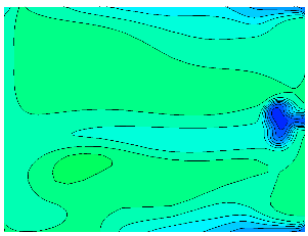 |
| 60 | 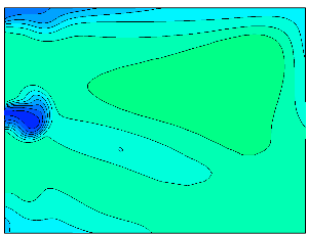 | 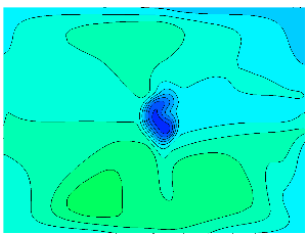 | 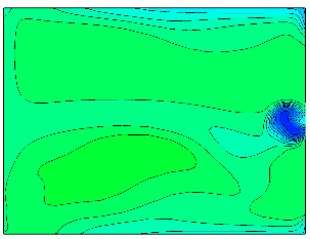 |
| 90 | 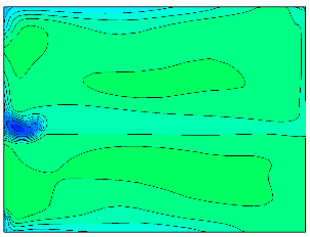 | 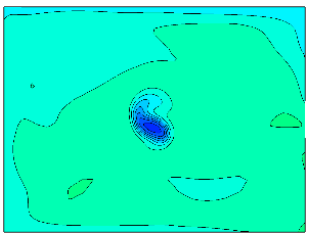 | 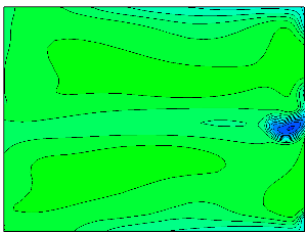 |

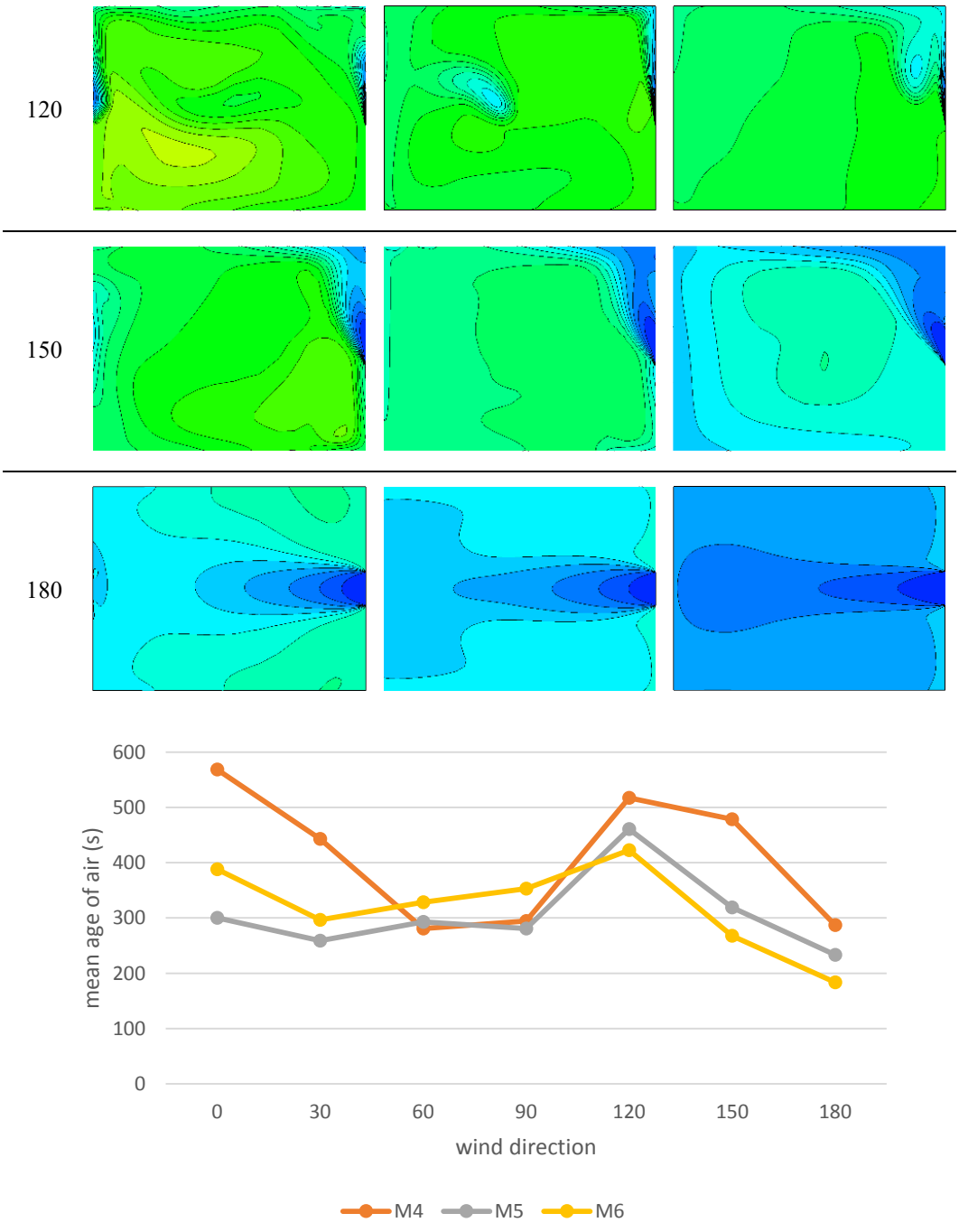


Figure 5.37. Maximum value of mean air age (s) in the room

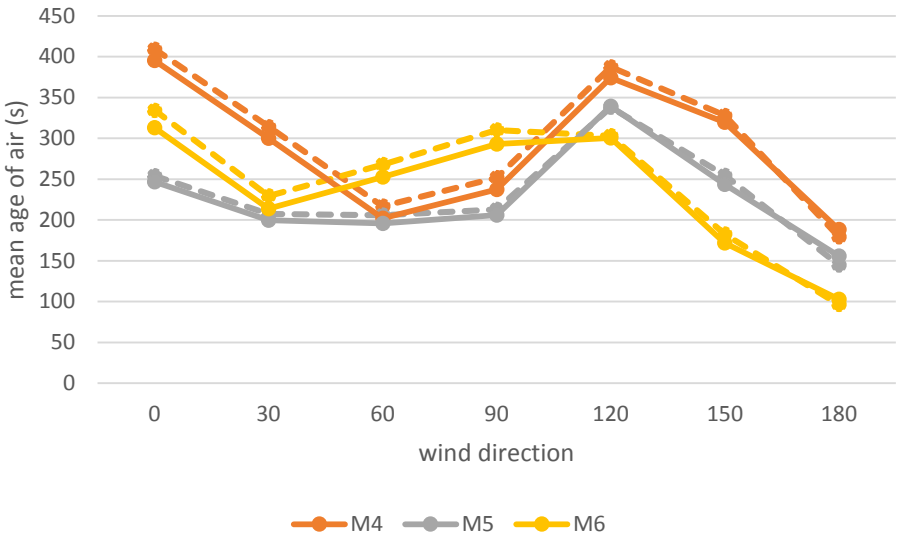


Figure 5.38. Volume-weighted (full-line) and area-weighted (dashed line) average mean age of air (s) at different wind tower positions

According to the graph 5.38 demonstrating the average freshness of the air in the room, it is clear that except for the wind directions 60 and 90 degree in which M6 underperforms compared to the other two wind tower positions, in all other wind directions M4 wind tower is the one taking more time to change the room's air. This is visible also in the contours of mean age of air. The stalest room is in fact the room ventilated by M4 and a wind direction of 0 degrees in which the mean age of air has a maximum value of 568 seconds (see graph 5.37). In this case, the average air age in the room is 395 seconds and 409 seconds on a breathing height of an average standing person.

In wind angles between 0 and 90, M5 is the one providing the freshest air which is also the least sensitive to the change in wind angle (see figure 5.38). In fact, the mean age of air in the room provided by M5 ranges between 196 and 206 seconds in wind directions 30, 60 and 90 degrees when the standing person breathes in an air with an average age of 208 seconds.

After 90 degrees, the closer the wind tower to the window, the fresher the air. According to the contours of mean age of air, at 180 degrees, M4, M5, and M6 and at 150 degrees, M6 are the combinations providing the freshest air of all in the room. M6 at 180 degrees, as the optimal configuration, is able to provide an air age of 103 seconds averaged in the whole room volume. For a standing person, the area-weighted average of mean age of air is 96 seconds. And the stalest point in the room according to figure 5.37 has an age of 183 seconds.

## 5.5.6 Air change efficiency

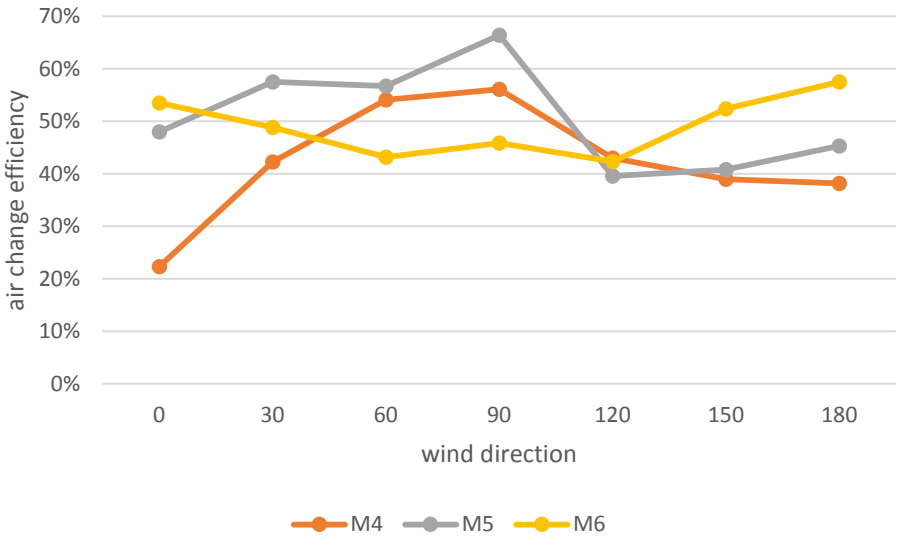


Figure 5.39. Air change efficiency (%)

The pick value in the graph of air change efficiency (figure 5.39) is 66 per cent which corresponds to wind tower M5 and wind direction 90 degrees. This wind tower outperforms the other two in two other wind directions of 30 and 60 degrees. The lowest air change efficiency, on the other hand, attributes to M4 at 0 incident angle with a value of 22 per cent. M4 is the wind tower position having the least efficiency in four wind directions of 0, 30, 150 and 180 degrees.

M6 compared to the other two wind towers seem to be less sensitive to the change in wind direction and has an air change efficiency range between 42 and 58 per cent. The air change efficiency of M4 increases as the air deviates from zero toward 90 degrees and then gradually declines until it arrives to 38 per cent at 180 wind angle. M5 has more fluctuations and soon after having its pick value at 90, with a 30 degree deviation, it has its least efficiency of 40 per cent.

## 5.5.7 Conclusion

Table 5.12 demonstrates how different positions of four-sided wind towers working with a window can affect the ventilation performance, comparing different indicators of air change efficiency ($\varepsilon^a$), volume-average mean age of air ($\bar{\tau}$), volume-average velocity magnitude ($\bar{U}$) and volume flow rate ($Q_v$). The colour blue represents the best case while red is the worst one. Where the wind towers in two positions show the same value, half of one cell is coloured.

Table 5.12. Best (blue) and worst (red) performances comparing different positions of a four-sided wind tower working with a window

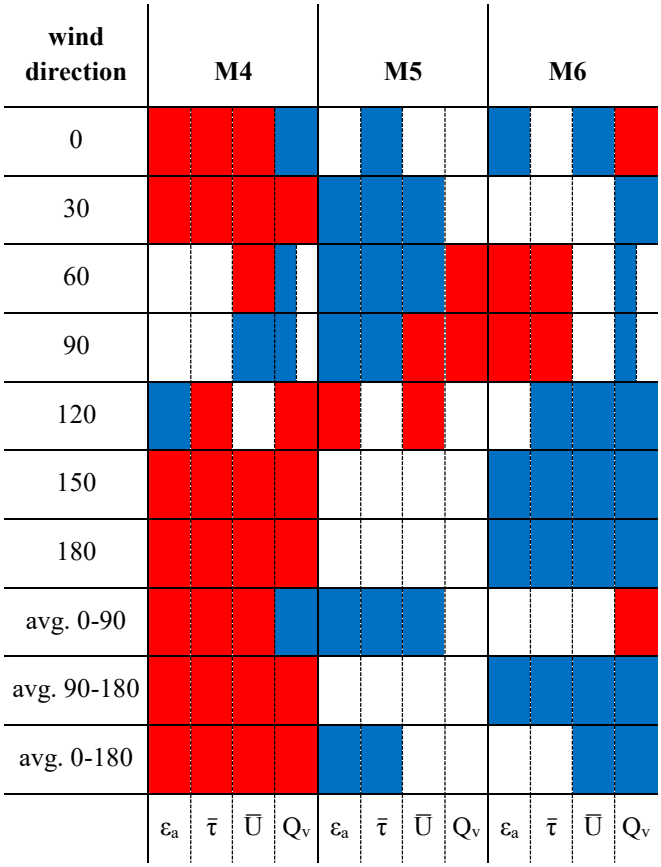


The many red cells on M4 columns demonstrate that in majority of wind directions this wind tower has the worst performance compared to M5 and M6.

In wind directions between 0 and 90, the M5 wind tower provides the best air change efficiency and air age figures. Though, at 60 and 90 degrees, it has the worst air flow rate and at 90, the worst velocity values.

The wind tower M6, despite having the best performance in terms of volume flow rate, velocity magnitude and mean age of air, does not have the highest air change efficiency in wind direction 120 degrees. In wind incident angles 60 and 90, M6 has the poorest performance in terms of air change efficiency and air freshness. These two indicators in their best condition together with highest volume-average velocity and highest air flow rate, happen in M6 in wind directions 150 and 180. In fact, averaging the wind directions 90-180, M6 provides the highest values for all indicators.

## 5.6 Group III: four-sided wind tower without a window

### 5.6.1 Reference values at zero incident angle

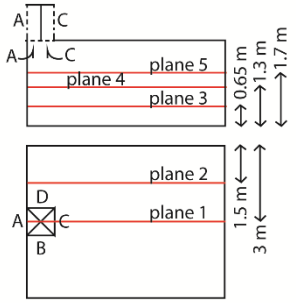


Figure 5.40. The vertical and horizontal planes on which the contours of pressure coefficient, velocity magnitude and mean age of air have been reproduced

Table 5.13. Contours of pressure coefficient (-) on the central vertical surface

| plane | M4W | M5W | M6W |
|---|---|---|---|
| Cp (-) | -1 0 1 | -1 0 1 | -1 0 1 |
| 1 | 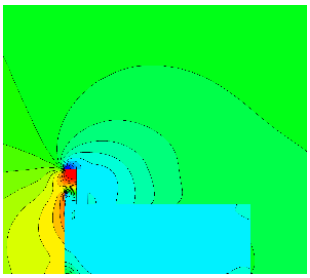 | 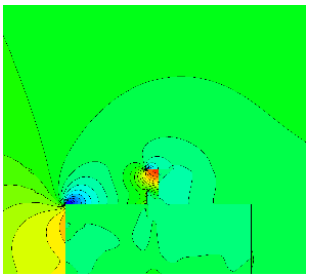 | 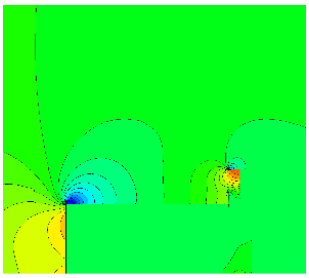 |

The pressure coefficient distribution on plane 1 is demonstrated in the table 5.13 for the three wind tower positions at wind incident angle 0. In the case M4W, the room has a Cp value of -0.5 while in M5W this value ranges between -0.1 and -0.2 and in M6W is -0.1.

Inside the wind tower channel A, where the Cps are positive, the M4W has the highest Cp values which diminishes as the wind tower's distance with the roof's windward edge increases. The leeward side of the wind tower, channel C, has Cp values close to that of the room. In M5W case, it is however slightly lower and has a value of -0.3.

The impact of the wind tower position on the distribution of the Cp above the roof and around the wind tower is similar to the previous case studies.

Table 5.14. Contours of velocity magnitude (m/s) on different horizontal and vertical surfaces

| plane | M4W | M5W | M6W |
|---|---|---|---|
| U (m/s) | 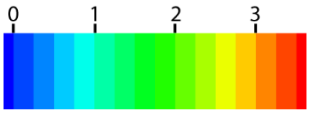  | 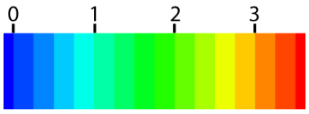  | 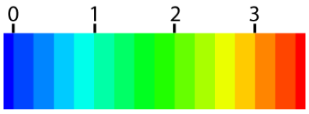  |
| 1 | 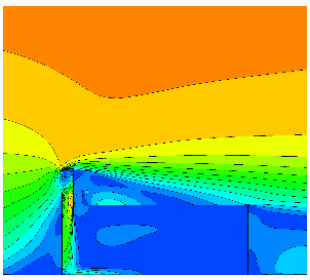 | 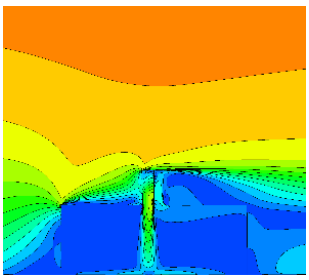 | 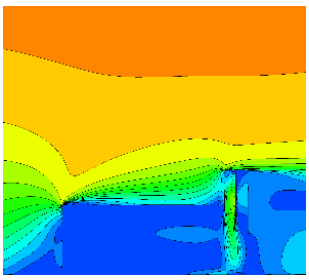 |
| 2 | 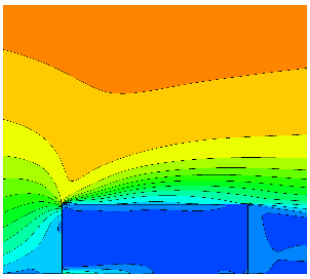 | 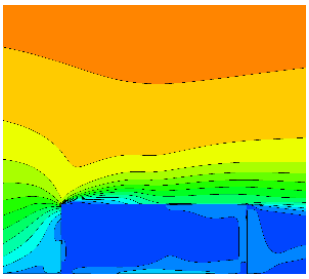 | 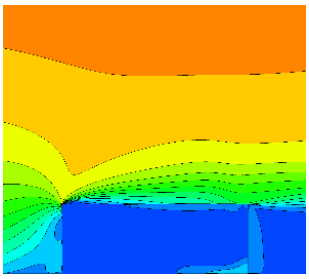 |
| 3 | 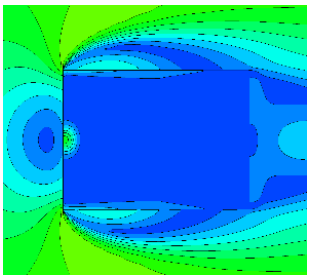 | 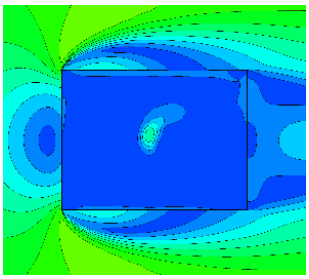 | 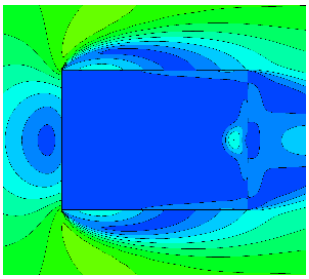 |
| 4 | 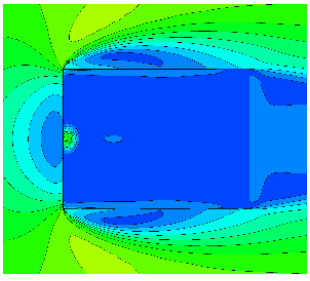 | 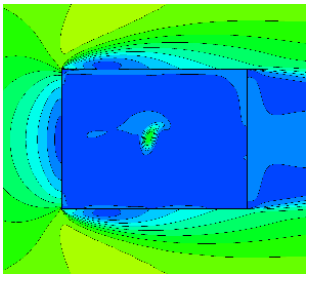 | 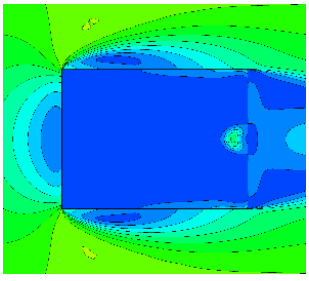 |

5

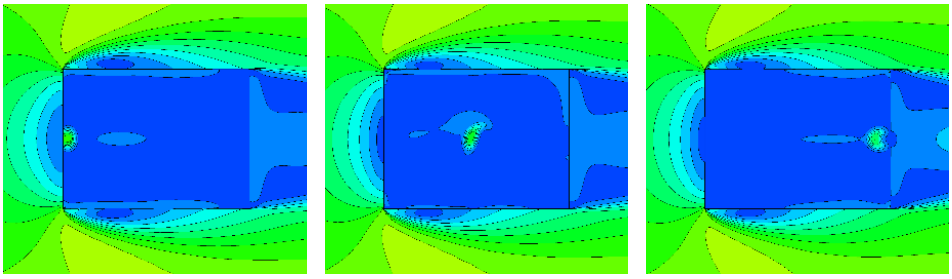

Table 5.14 demonstrates the variation in the velocity magnitude values in wind incident angle 0. It is observed that at this angle there is a subtle air movement inside the room in all three cases. And only by looking at the contours it is difficult to conclude which tower position is providing better velocities in the room.

Looking at the wind tower itself, the velocity of the wind is higher in case M4W, compared to M5W and M6W, where the wind hits the internal wall of the wind tower. The jet of air through the wind tower is also speedier in the same order.

The distribution of the velocity magnitude on the room's floor after the air jet arrives to this level, is smallest in M6W case. While in M4W a bigger velocity magnitude spreads on a small surface on the floor, in M5W the surface on which this spreading happens in wider and thus the air speed is lower.

In the leeward channel of the wind tower (channel C) the air velocity is higher in M5W compared to M6W and M4W respectively.

Apart from the area underneath the wind tower and the symmetry axis between the wind tower and the window on which some air movement is observed, the only other areas of the room that experience some velocity are the adjacencies of the ceiling, the floor and the four walls.

Table 5.15. Contours of mean age of air (m/s) on different horizontal and vertical surfaces

| **plane** | **M4W** | **M5W** | **M6W** |
|---|---|---|---|
| τ (s) | 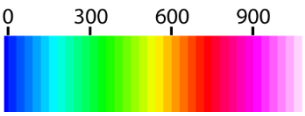  | 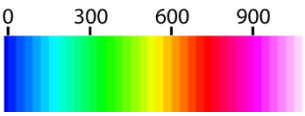  | 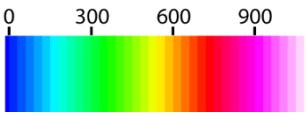  |
| 1 | 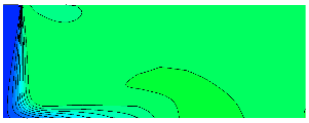 | 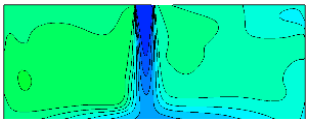 | 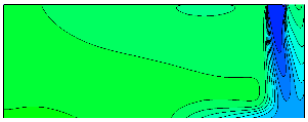 |

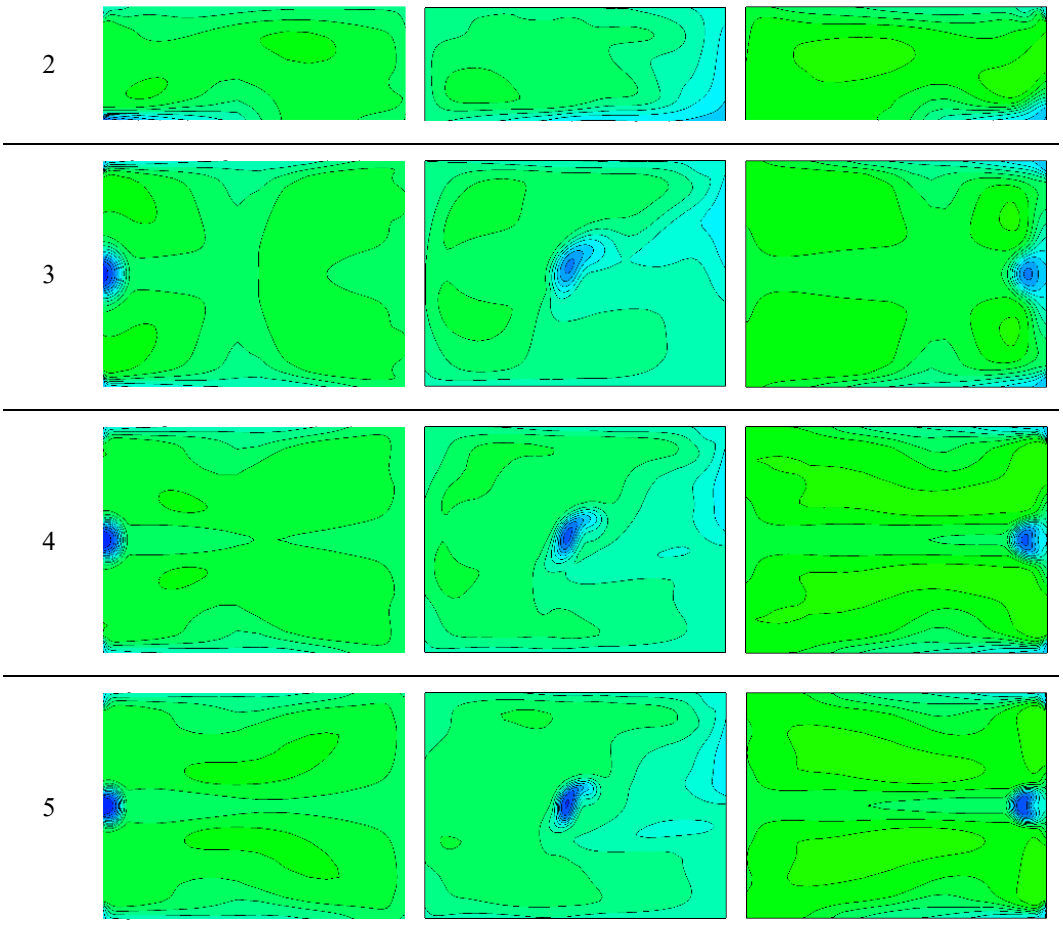


Comparing the mean age of air 00 wind incident angle (table 5.15), it is noted that the tower position which provides a fresher air inside the room is the one placed in the center of the roof (M5W). Contrarily, the tower placed on the leeward edge of the building (M6W) has the least efficiency in which the air age ranges between 300 and 360 in a major portion of the room. In M4W, which is about 30 seconds fresher than M6W, and M6W positions, in almost all parts of the room the air age is constant, while in M5W the downstream part of the room has a 60-seconds-fresher accumulation of air respect to its upstream part.

## 5.6.2 Volume flow rate and air change number

The variation of the volume flow rate through different wind tower apertures are shown in the following two graphs (5.41 & 5.42) that resemble those of the previous cases study (M cases).

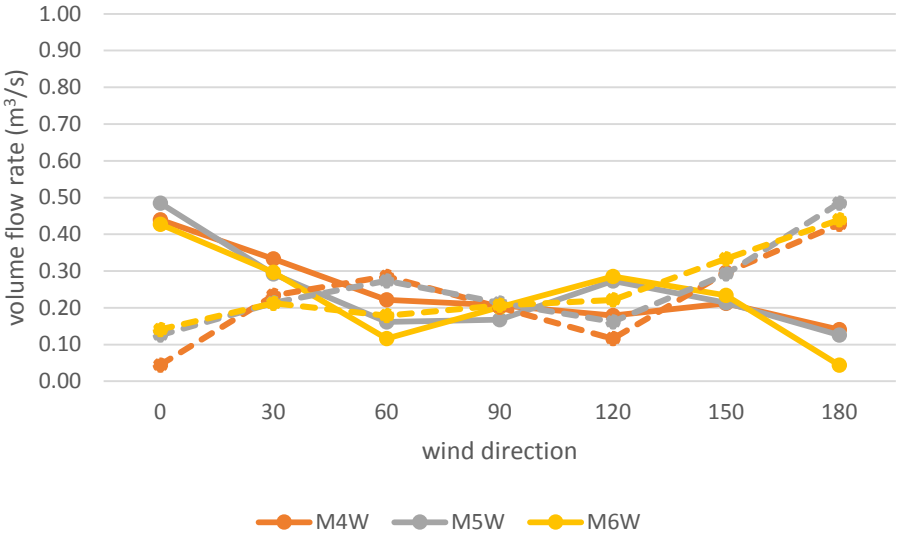


Figure 5.41. Volume flow rate ($m^3/s$) through apertures A (full line) and C (dashed line) at different wind directions

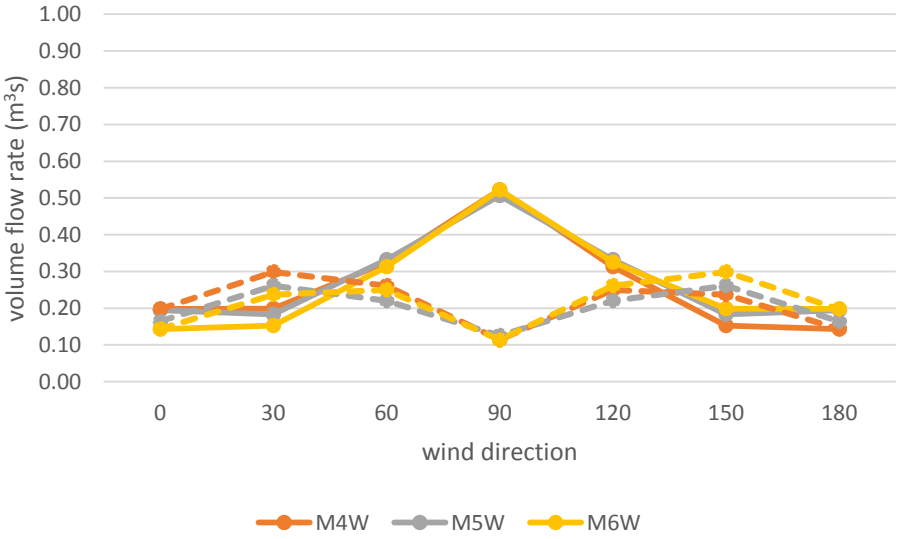


Figure 5.42. Volume flow rate ($m^3/s$) through apertures B (full line) and D (dashed line) at different wind directions

According to the graphs, the highest absolute volume flow rate through aperture B in all three wind towers when the wind direction is 90 degrees when the airflow rate through this aperture is about 0.52 $m^3/s$ (see figure 5.42). This is followed by aperture A in wind direction 0 and aperture C in wind direction 180, which induce 0.48 $m^3/s$ in M5W and about 0.43 $m^3/s$ in M4W and M6W cases (both apertures

shown in figure 5.41). In all these cases, the air is entering through the aperture. On the other hand, the highest outgoing air flow rate occurs in aperture D in wind direction 30 for M4W and in wind direction 150 for M6W when the air flow rate value stands at 0.30 $m^3/s$ (figure 5.42).

The lowest volume flow rates with a value of 0.04 $m^3/s$ is provided by aperture A of wind tower M6W in wind angle 180 corresponding to aperture C in wind tower M4W in wind angle 0 (figure 5.41).

Comparing the total volumetric flow rate (figure 5.43) of the cases where the four-sided tower is placed on the center of a roof (M5W) with the ones on the building edge (M4W and M6W) while the lower space does not have any windows, it is evident that at incident angles 00 and 180, the tower placed in the center works better while contrarily at 90 degrees, it works only subtly worse.

At angles between 00 and 90 and similarly between 90 and 180, the towers placed on the roof edge work better on the condition that the wind blows close to the tower i.e. the wind travels less on the roof surface.

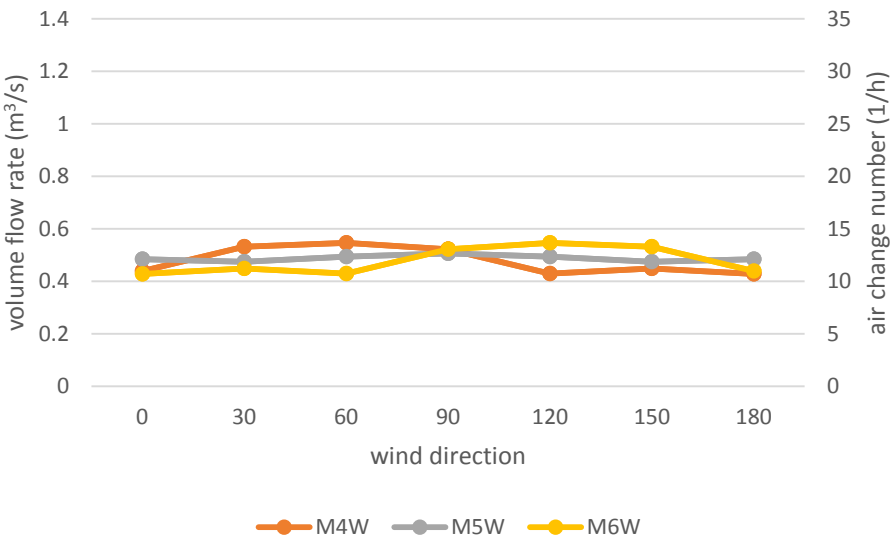


Figure 5.43. Volume flow rate ($m^3/s$) and air change number (1/h) by each four-sided tower at different wind directions

According to the chart 5.43 which summarizes the volume flow rate and number of air changes for four-sided wind towers working alone when the room does not have a window, the highest induced air flow rate of 0.54 $m^3/s$ and ACH of 13.6 is through wind towers M4W and M6W at 60 and 120 wind incident angles

respectively. The lowest values correspond to the same wind towers at 180 and 0 wind directions with volumetric air flow rate of 0.43 $m^3/s$ and an ACH of 10.7.

Generally speaking, the tower placed on the roof center has the better performance compared to the edge-placed wind towers only at 0 and 180 degrees. For wind directions between 0 and 60, and those between 120 and 180 degrees, the wind towers M6W and M4W induce the lowest air flow rates respectively.

### 5.6.3 Pressure coefficient

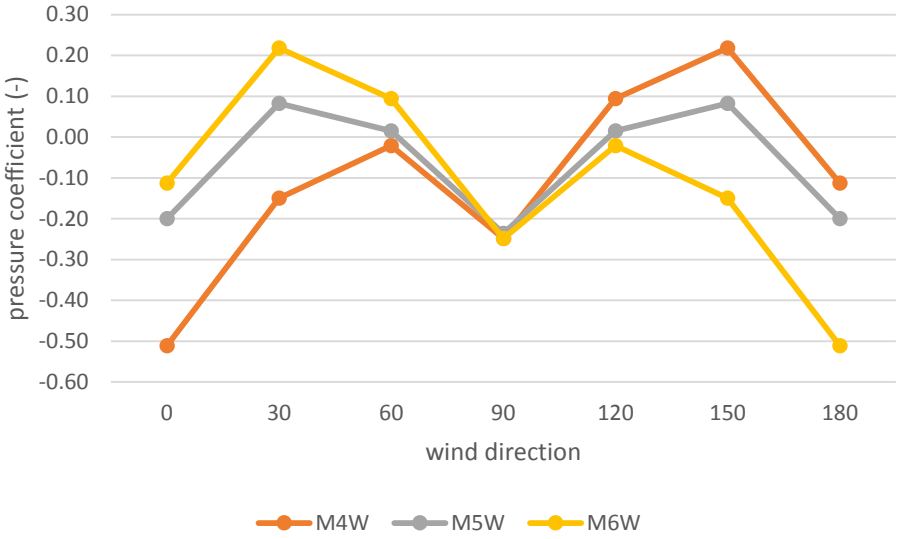


Figure 5.44. Volume-weighted average pressure coefficient (-) in the room

The average Cp value in the room volume for the cases with four-sided wind towers and no windows are represented in the graph 5.44. The lowest pressure coefficient values of -0.51 is observed in case M4W at 0 wind incident angle which is identical as the case M6W at 180 degrees. The second lowest Cp value is shared between the three wind towers at 90 degrees when the mean Cp is -0.25. The highest Cp on the other hand is observed in M4 at wind direction 150 which is identical to M6 at 30 degrees.

The variations of the pressure coefficient on different wind tower apertures are summarized in the two graphs 5.45 and 5.46. Even though the average Cp value in the room is heavily affected by the absence of window in MW cases, the variation of the Cp around wind tower apertures are identical with that in M cases.

The apertures B and D in M5W position show symmetrical behaviour in terms of Cp by the change in wind direction (figure 5.46). The aperture A shows the mirrored behaviour of aperture C in M5W (figure 5.45) while this reflection is seen between M4W and M6W in all the apertures in M4W and M6W, with 90 degrees being the reflection axis.

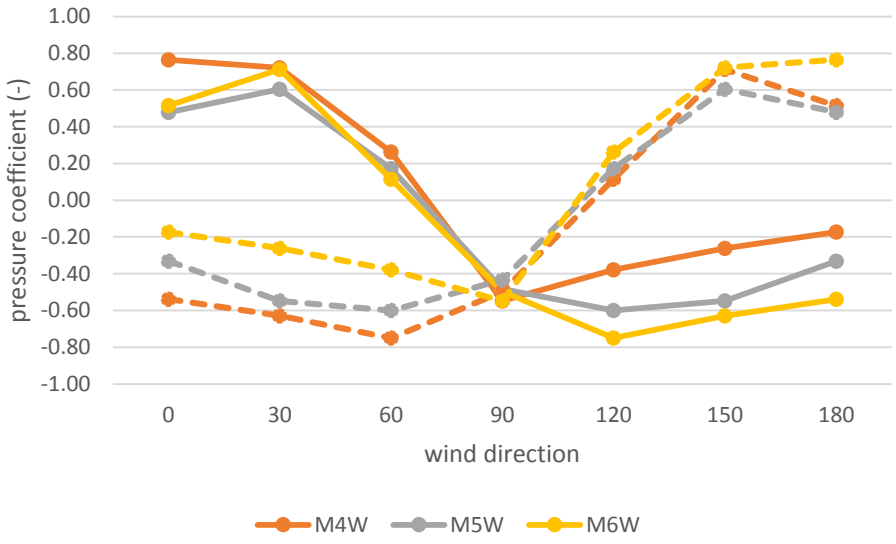


Figure 5.45. Area-weighted average pressure coefficient (-) on wind tower apertures A (full line) and C (dashed line)

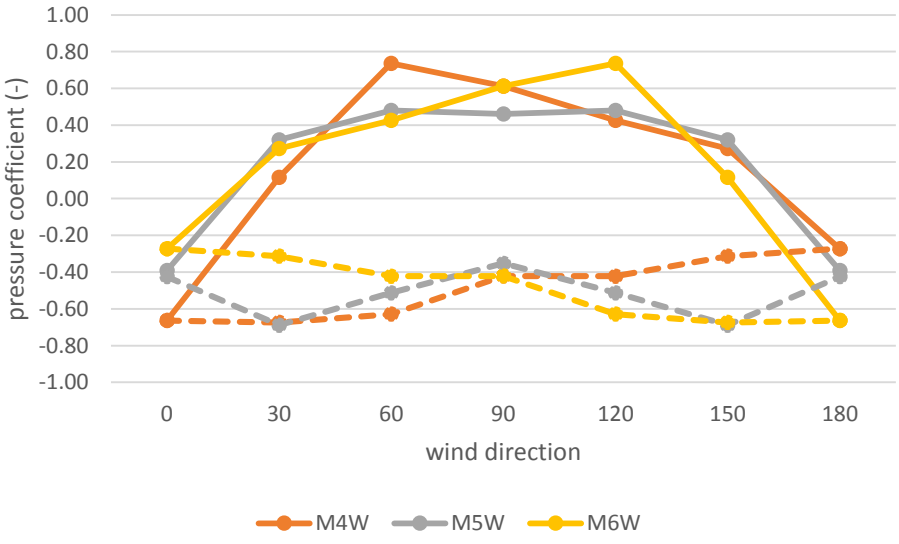


Figure 5.46. Area-weighted average pressure coefficient (-) on wind tower apertures B (full line) and D (dashed line)

M4W's Cp values on aperture A corresponding to M6W's Cps on aperture C, except for the wind direction 90 show higher mean values compared to M5. The difference between the pressure coefficients on aperture A in three wind tower cases is greater with wind directions over 90, while the same pattern is seen on aperture C with wind directions 0-90. On these apertures, the maximum difference between the Cp values arrive to around 0.37 which is the difference between Cp values on aperture C of the cases M4 and M6 at 0, 30 and 60 degrees (corresponding to aperture A in the same cases at wind angles 120, 150 and 180).

### 5.6.4 Velocity magnitude

The following four graphs (5.47 to 5.50) represent the area-average velocity magnitude on the four wind tower apertures and on the intersecting openings between the wind tower and the room. It is interesting to note that the fluctuations of these figures do not necessarily correspond to each other meaning that a lower velocity on the tower aperture does not result in a lower velocity on the intersecting aperture.

Contrary to apertures B (shown in figure 5.48) and D (shown in figure 5.50) which have a completely symmetrical behavior by the change in wind direction, the fluctuations of the velocity magnitude values on tower apertures A (figure 5.47) and C (figure 5.49) in different wind directions are numerous and it is generally not possible to say which wind tower position is better or worse in this regard. The variation on the intersecting apertures A and C have a sinusoidal form while this is not the case on the tower aperture. In general, the wind towers M5W and M6W show closer values on both surfaces while the M4W has more abrupt variations in 60 and 120 degrees.

The most notable points on the graph of aperture A are attributed to wind direction 60 degrees where M4W, M5W and M6W respectively experience highest velocity magnitudes. M4W has the highest velocity of 1.79 m/s which also corresponds to aperture C of M6W case at 120 degrees. The lowest values on aperture A are observed in wind incident angles 90 and 180, where the M5W case has particularly lower velocities than the other two wind towers that are 0.32 and 0.37 m/s respectively (see figure 5.47).

Considering the intersecting aperture A, the highest velocity magnitudes are observed in wind direction 0 with M5W having 1.94 m/s and the lowest figures in 180 degrees with M6W having 0.48 m/s. These values are correspondingly observed also in aperture C, in M5W at 180, and M4W at 0 incident angles (see figures 5.47 and 5.49).

The pick velocity values on wind tower aperture B (figure 5.48) happen at 30 degrees in M4W, M5W and M6W and at 150 degrees in M6W, M5W and M4W, respectively having velocities of 1.75, 1.61 and 1.53 m/s. The lowest velocity magnitude on the wind tower aperture B is in M6W at 0 and M4W at 180 degrees with magnitude of 0.27 m/s. The pick velocity magnitude on the intersecting apertures instead is seen at 90 degrees when the three positions show similar values of between 2.03 and 2.09 m/s.

On aperture D which in all the 21 cases has an air extraction performance (see figure 5.50), the variation of the velocities has an orderly pattern. The intersecting aperture D in all wind directions experience a velocity of on average 0.57 m/s higher than the tower aperture D. Thus the maximum and minimum values for both surfaces occur simultaneously. The lowest velocities are observed at 0, 90 and 180 degrees while the highest are at 30 and 150. The lowest velocity magnitude of 0.27 m/s occurs at 180 degrees in M4W followed by 0.33 m/s at the same wind angle in M5W on wind tower aperture D. These correspond to the same aperture on M6W and M5W at 0 incident angle too. The pick value of 0.93 m/s on this wind tower aperture associates with M5W in wind directions 30 and 150. Similarly, on the intersecting aperture D, the pick velocity values are observed on M5W in wind directions 30 and 150 when the magnitude is 1.62 m/s. This indicates the highest difference between the velocities on tower aperture and intersecting aperture D. The lowest velocity on the intersecting aperture D occurs at 90 degrees in M5W with a value of 0.74 m/s.

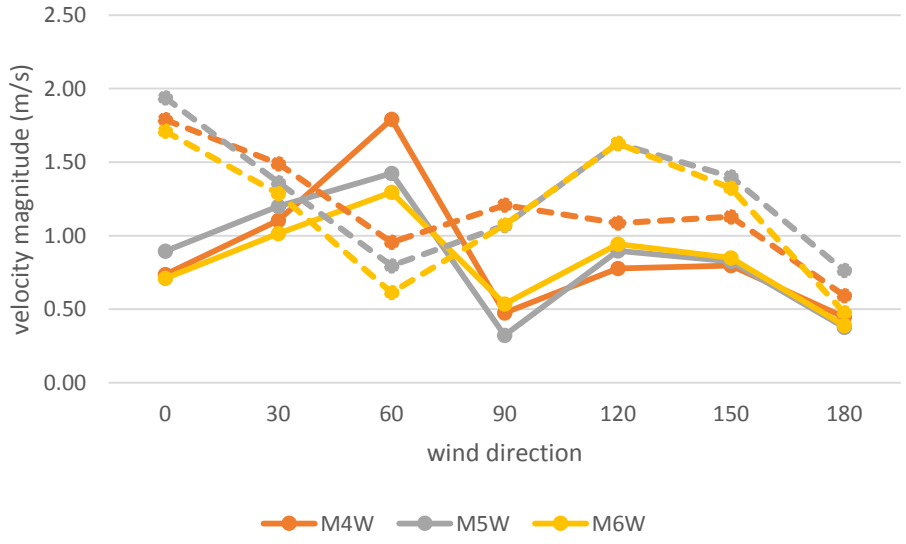


Figure 5.47. Area-averaged velocity magnitude (m/s) on wind tower aperture A (full line) and the intersecting aperture A (dashed line)

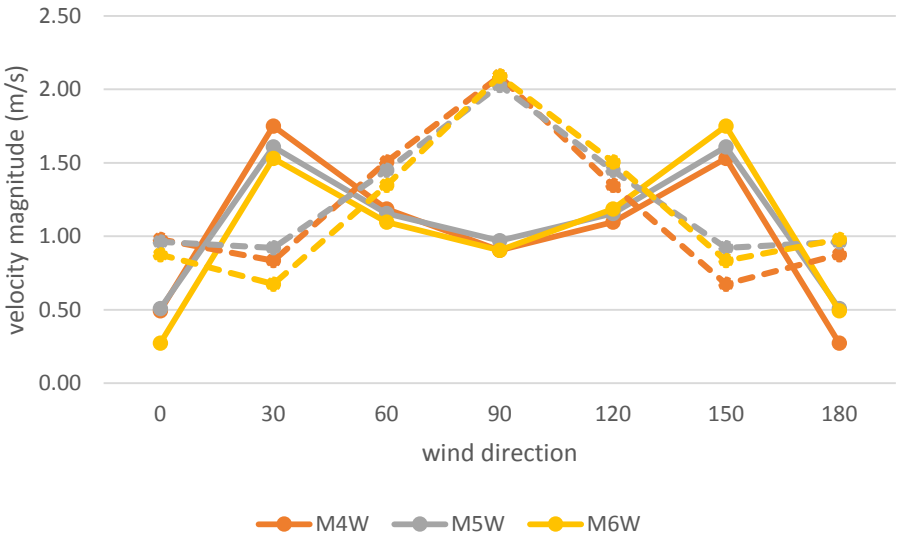


Figure 5.48. Area-averaged velocity magnitude (m/s) on wind tower aperture B (full line) and the intersecting aperture B (dashed line)

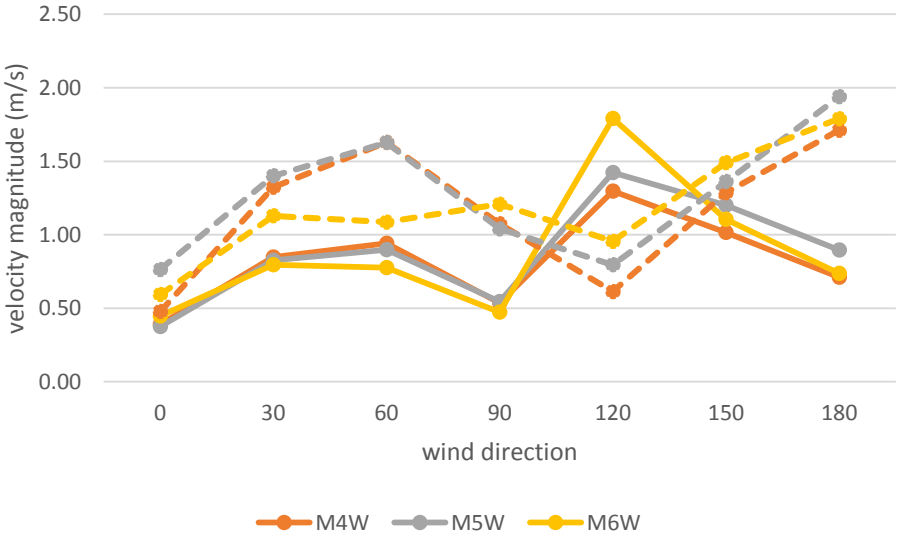


Figure 5.49. Area-averaged velocity magnitude (m/s) on wind tower aperture C (full line) and the intersecting aperture C (dashed line)

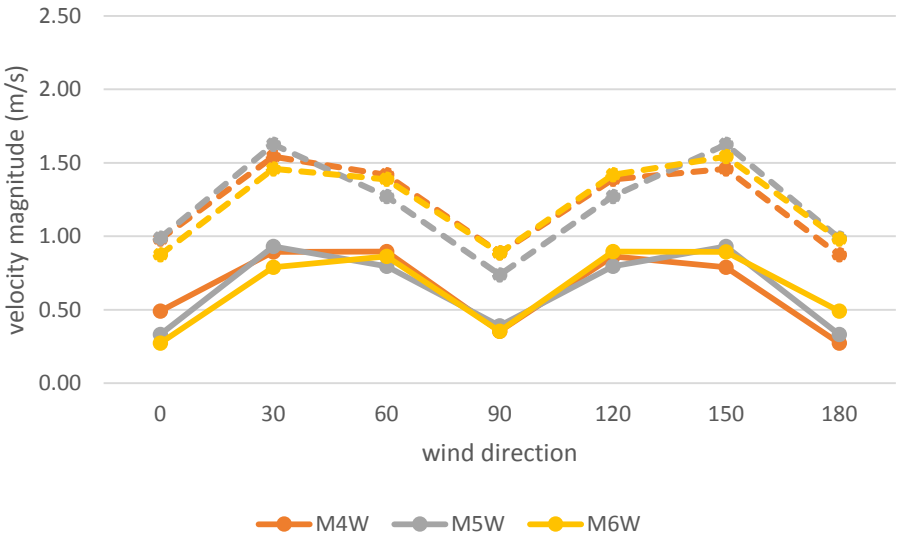


Figure 5.50. Area-averaged velocity magnitude (m/s) on wind tower aperture D (full line) and the intersecting aperture D (dashed line)

Comparing the window-less spaces ventilated by four-sided wind towers, and looking at the distribution of velocity inside the space shown in table 5.16, it is observed that as the wind angle deviates to 30 degrees, the air jet from the tower becomes noticeably weaker than 00 degrees. At this angle the tower placed on the windward side of the building creates a bigger air jet and the weakest one is provided by M5W. In fact in case M5W only in a tiny portion under the tower there is non-zero air velocity while such an air movement is seen beside the walls in case M6W. Case M4W which shows a bigger mass/volume flow rate at this angle and also a longer and stronger air jet, however, shows the weakest air distribution inside the room.

At 60 degrees, similar to the previous incident angle, the distribution of velocity is scarce inside the room. However, M6W and M4W both seem to be a bit more efficient in distributing the air speed at a seated or standing human height. While in M6W this non-zero air movement in seen in adjacency of the walls, in M4W it is mainly accumulated underneath the tower. At this angle, the air jet is quite short. In M4W, the wind hits the internal blades of the tower more strongly than M5W and M6W respectively.

At 90 degrees, there is a quite good air circulation inside the room. The jet of air from aperture B reaches the ground at all three cases. The velocity inside the edge-placed towers, M4W and M6W, is higher than M5W but the distribution of this velocity inside the room seems to be similarly good.

At 120 and 150 degrees in M6W position, similar to 60 and 30 degrees, the air movement is limited to the tower underneath while the major portion of the room remains still.

At 180 degrees, similar to 00 degrees, the air jet is speedy and reaches the floor. At this angle, the velocity is more effectively spread in the room in the case the tower is placed on the windward edge of the building –i.e. M6W, while the least velocity distribution is seen of the tower being on the leeward side, M4W. This observation also matches the mass/volume flow rate results.

Table 5.16. Contours of velocity magnitude (m/s) on a horizontal surface placed 1.7 m above the ground

| **wind angle** | **M4W** | **M5W** | **M6W** |
|---|---|---|---|
| U (m/s) | 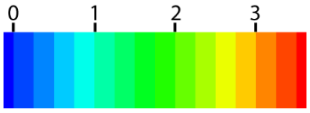 | 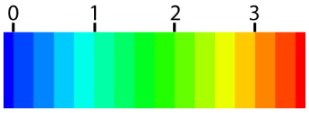 | 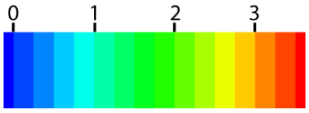 |
| 0 | 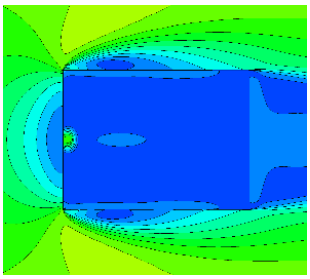 | 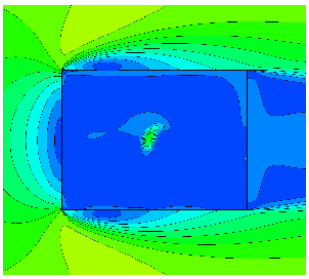 | 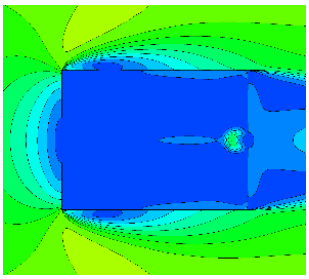 |
| 30 | 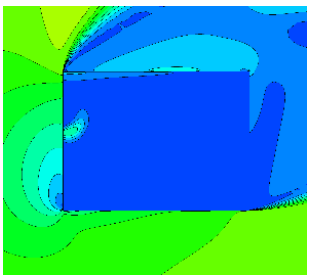 | 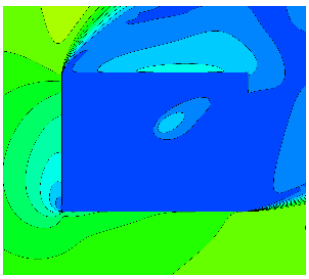 | 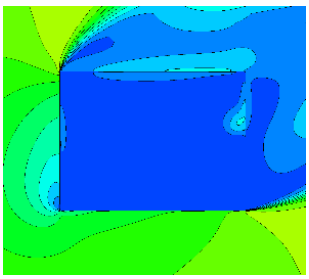 |

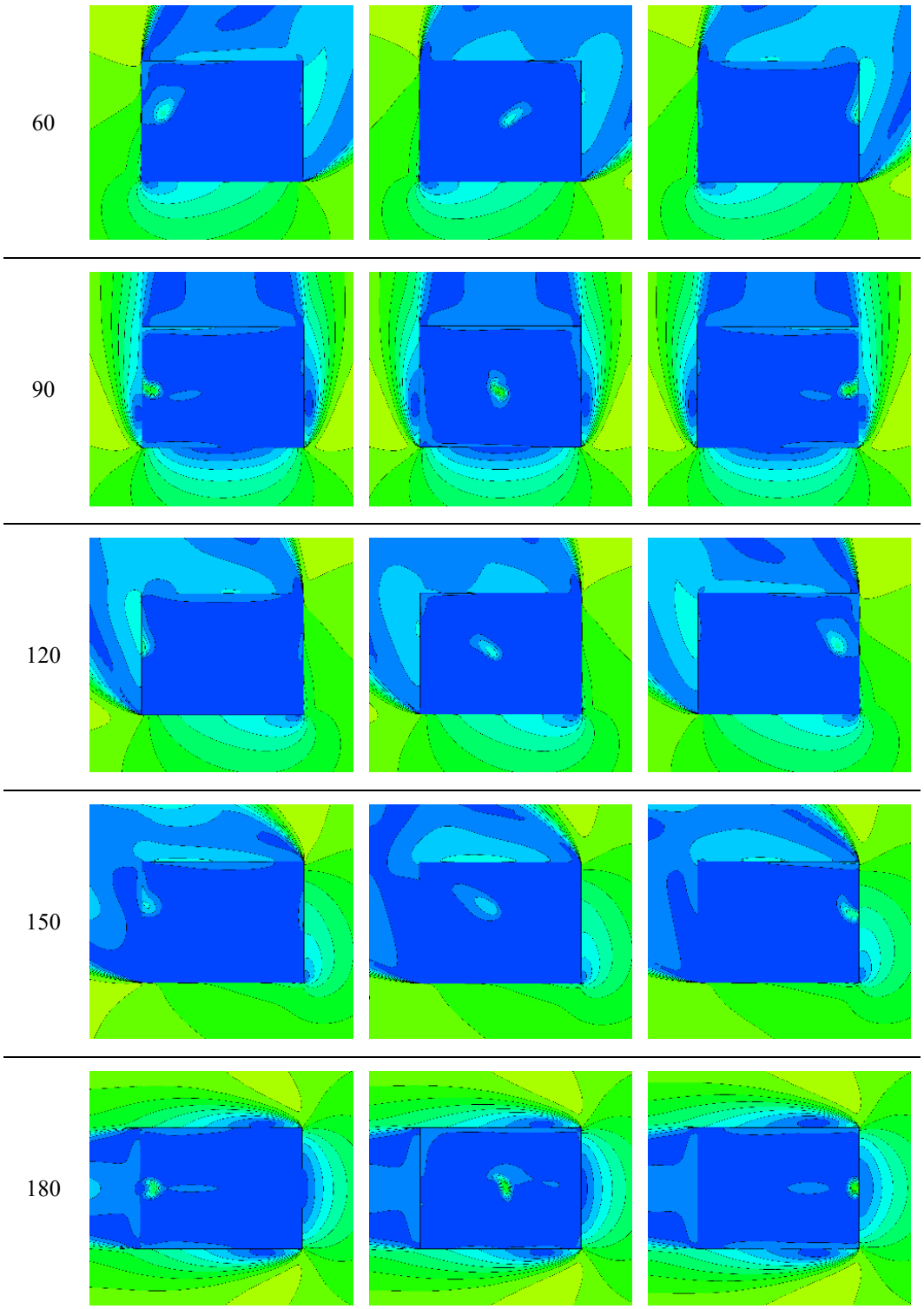
60
90
120
150
180

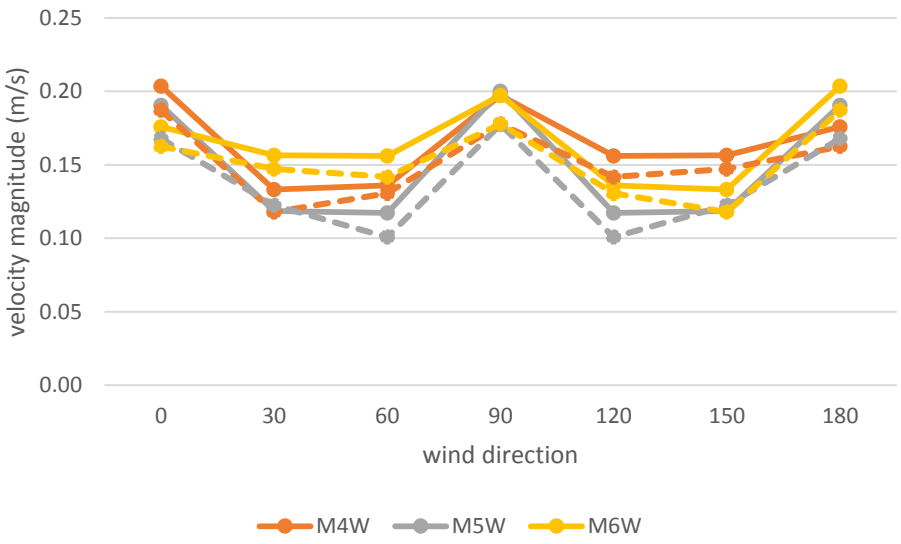


Figure 5.51. Volume-weighted (full-line) and area-weighted (dashed line) average velocity magnitude (m/s) at different wind tower positions

The maximum velocity magnitude induced averagely in the room volume (shown in graph 5.51) has a value of 0.2 m/s and is provided by the wind towers M4W at 0 and M6W at 180 degrees. This value is 0.01 m/s higher than the velocity averaged on the surface placed at a height of 1.7 m above the room floor. The wind tower position M5W at wind incident angles 60 and 120, on the other hand, is the one providing the lowest velocities of 0.12 m/s and 0.1 m/s respectively as volume-weighted and area-weighted averages.

In general, since in all cases with all wind incident angles, the air movement inside the room is commonly small, it is concluded that the position of tower is not an influential parameter in improving the velocity distribution inside the room when there is no window.

### 5.6.5 Mean age of air

Looking at the contours of mean age of air on a horizontal surface at a height of 1.7 m, shown in table 5.17, it is noted that at 30 degrees, the M4W position is the one providing a fresher air inside the room compared to M5W and M6W respectively. In M6W, the central part of the room has an air age of between 570 and 630 seconds. In M5W as opposed to the other two positions, central part of the room has the lowest age of air. In M4W the freshest air is mainly seen beside the walls and the stalest air in the room center has an age of between 390 and 420 seconds.

Compared to 30 degrees, the 60 degree incident angle provides an even worse condition regarding the age of air in the same order as in 30 degrees. Similarly at this angle, M6W is worse than M5W and M4W respectively. At M6W the central part of the room experiences an air ages that arrive up to 690 seconds. Whereas in M5W a major portion of the room has an air age of between 450 and 510 seconds.

At 90 degrees, the situation drastically improves compared to previous incident angles and M5W provides a better air quality in the room compared to when the tower is placed on the building edge. In this position, while beside the walls the air age value is between 210 and 240 seconds, in the middle of the room it is almost uniformly spread between 240 and 270 seconds. In M4W and M6W cases, the mean age of air in most parts of the room is between 270 and 330 seconds.

Thanks to symmetry, the models M4W at 120, 150 and 180 degrees show the same behavior as that of M6W at 60, 30 and 00 degrees respectively.

Table 5.17. Contours of mean age of air (s) on a horizontal surface placed 1.7 m above the ground

| **wind angle** | **M4W** | **M5W** | **M6W** |
|---|---|---|---|
| τ (s) | 0 300 600 900 | 0 300 600 900 | 0 300 600 900 |
| 0 | 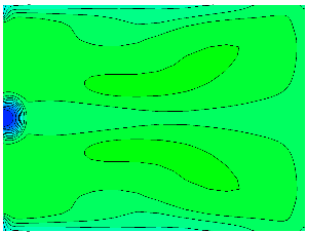 | 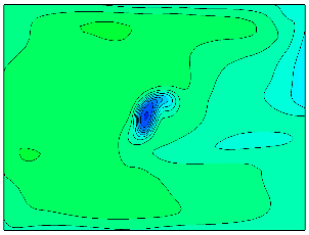 | 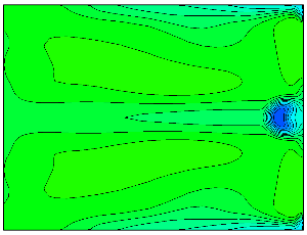 |
| 30 | 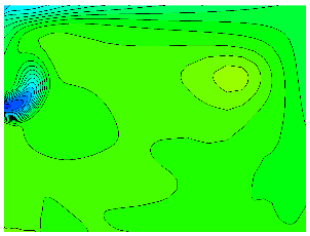 | 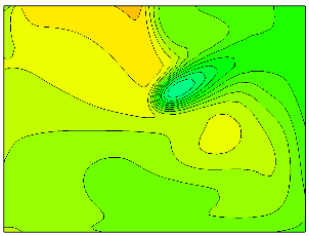 | 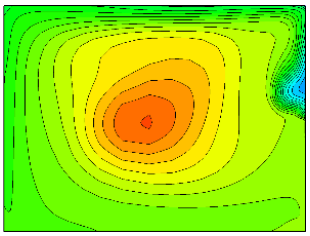 |

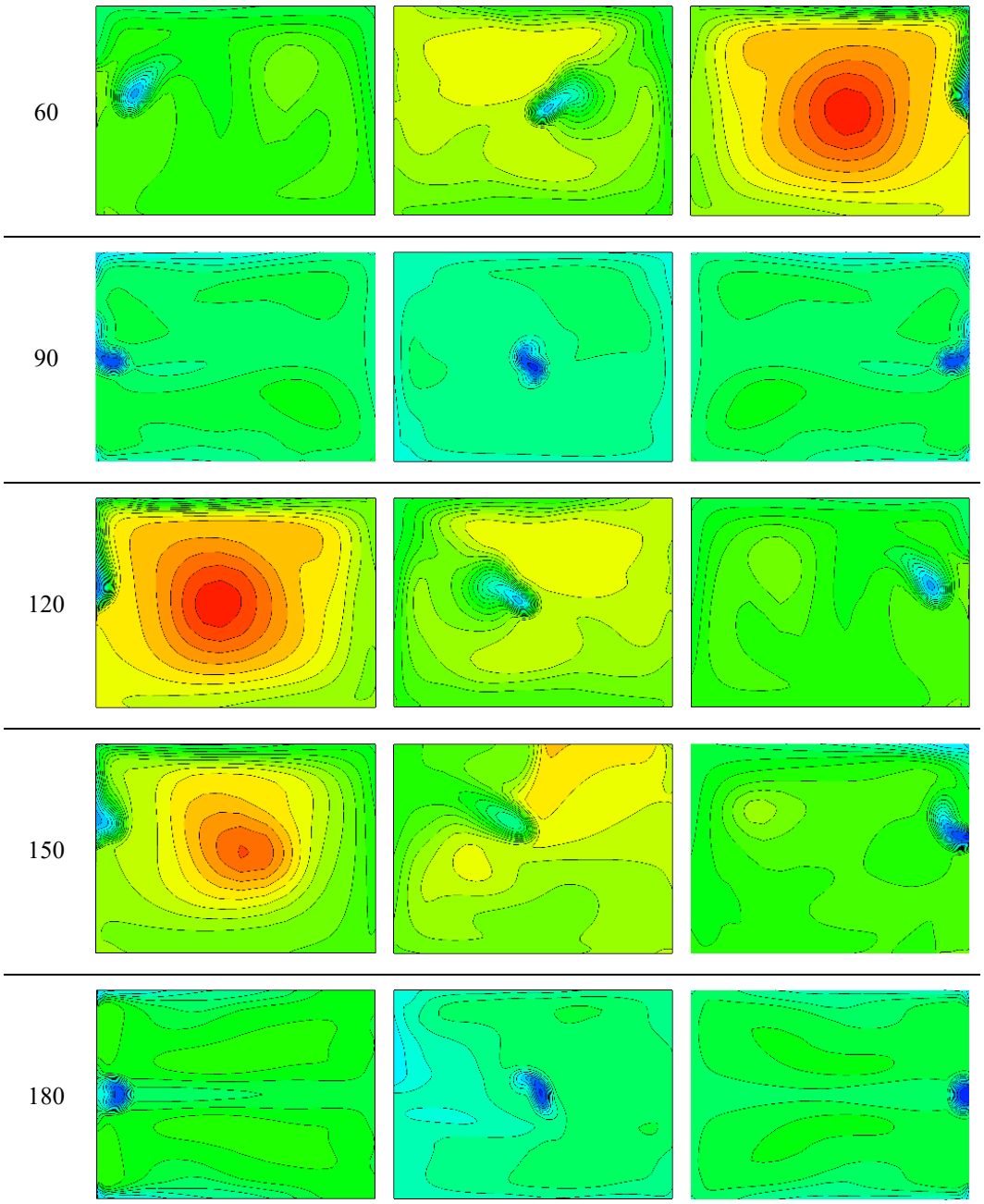
60
90
120
150
180

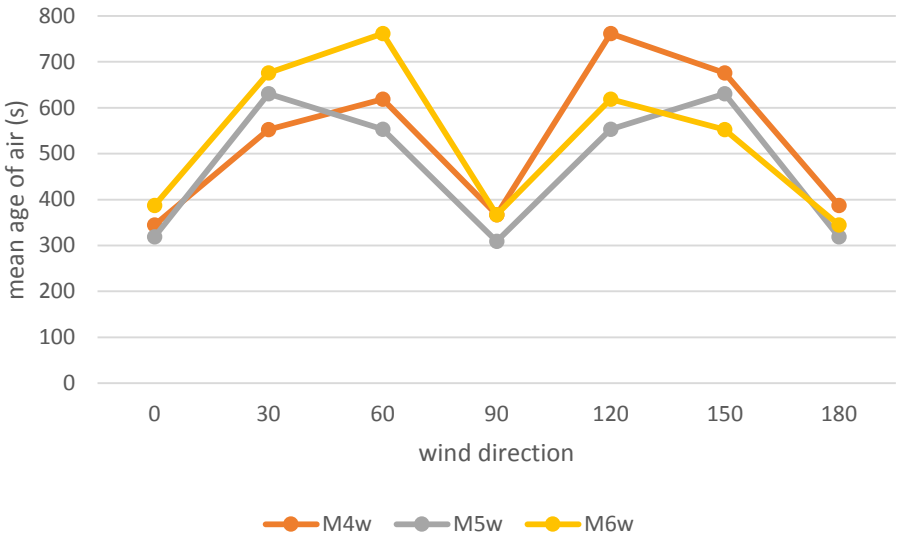


Figure 5.52. Maximum value of mean age of air (s) in the room

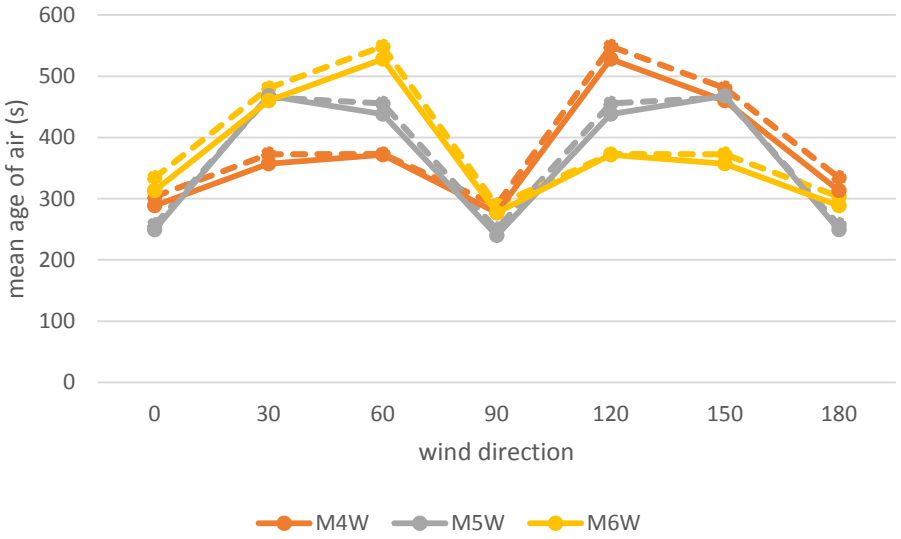


Figure 5.53. Volume-weighted (full-line) and area-weighted (dashed line) average mean age of air (s) at different wind tower positions

The average freshness of air inside the room is deducible from the graph 5.53. In general, the air in the room is freshest at wind directions 0, 90 and 180 regardless of the wind tower position. According to the graph, age of air in the central wind tower M5W at 90 degrees has the lowest value of 240 seconds compared to the other configurations. In this case, the stalest point in the room has an air age of 309

seconds (see figure 5.52) and a standing person the age of air is averagely 250 seconds (see dashed lines in figure 5.53).

On the other hand, the least fresh rooms are the rooms working by M4W and M6W respectively at wind directions 120 and 60 degrees, in which the volume-weighted average mean age of air arrive to a value of 528 seconds. At a room height of 1.7 m, the area-weighted freshness value is 548 seconds on average (figure 5.53). The oldest point in these two configurations has an air age of 761 seconds (figure 5.52). It is noticeable from the mean age of air contours that the same wind towers at wind directions 150 and 30 degrees provide the second least fresh air of all. The oldest point of the room in these two configurations has an air age of 676 seconds (fig 5.52) and a standing person breathes an air of 480 seconds old on average (figure 5.53). Interestingly, in the room ventilated by these two wind tower positions, the volume-weighted average value of air age is 8 seconds lower than the age of air provided by M5W in these wind directions.

### 5.6.6 Air change efficiency

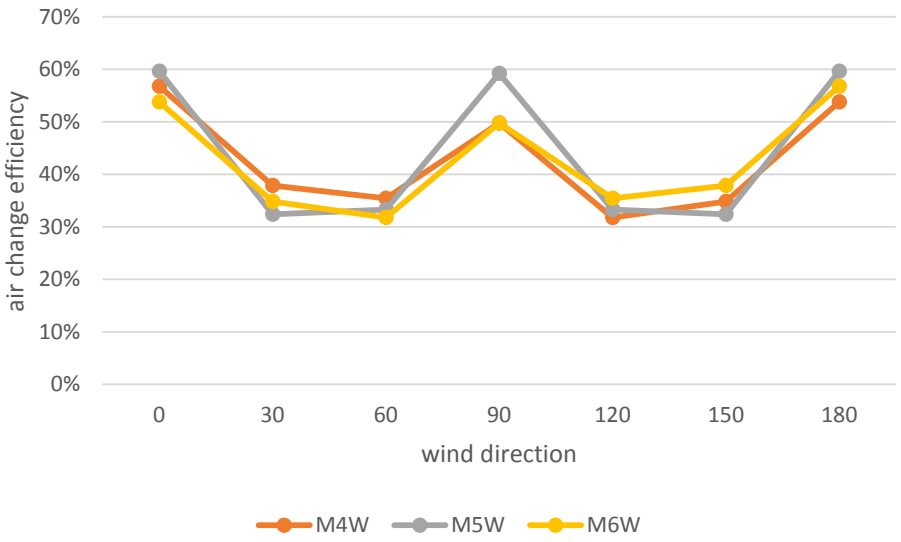


Figure 5.54. Air change efficiency (%)

The air change efficiency (graph 5.54) contrary to the age of air graphs has its pick values at wind directions 0, 90 and 180. In fact, at these wind direction, the central wind tower M5W has an efficiency of 59-60 per cent. The lowest air change efficiencies reaching 32 per cent are seen in M4W at 120 degrees, M6W at 60 degrees, and M5W at 30 and 150 degrees. Despite the slight variation, the air change efficiency does not seem to be very sensitive to the wind tower position.

### 5.6.3 Conclusion

Table 5.18 demonstrates which four-sided wind tower working on its own can perform better or worse when different indicators are considered. The colour blue represents the highest air change efficiency($\varepsilon^a$), the lowest volume-average mean age of air ($\bar{\tau}$), the highest volume-average velocity magnitude ($\bar{U}$), and the highest volume flow rate ($Q_v$), whereas red represents the contrary. Wherever half a cell is coloured, it means another wind tower position has the same performance.

Table 5.18. Best (blue) and worst (red) performances comparing different positions of a four-sided wind tower working alone

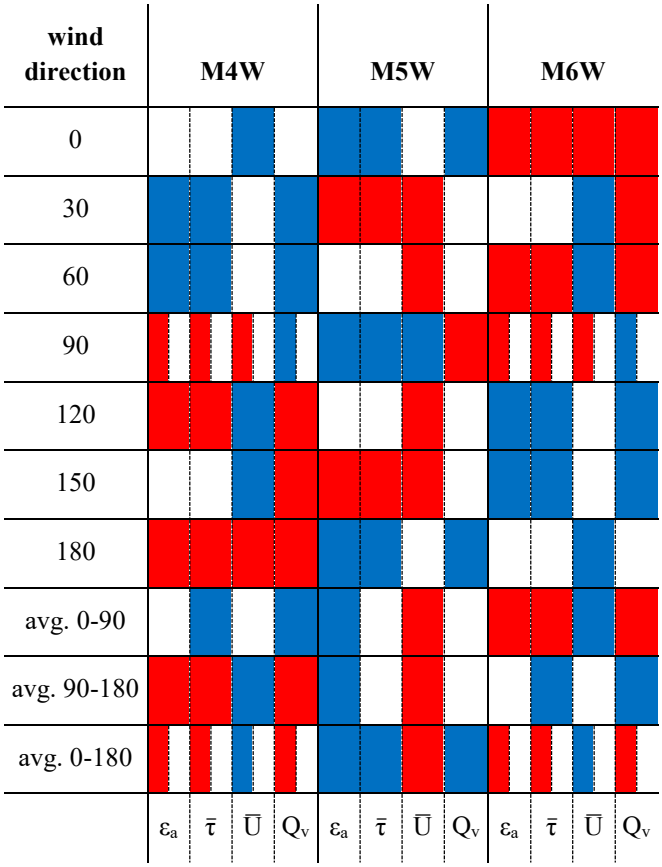


Even though it is possible to observe certain general patterns about the variation of each indicator, it is difficult to derive an inclusive conclusion about the optimum or poorest case considering all indicators together. For instance, while concerning air change efficiency, mean age of air, and volume flow rate, M4W is the optimal case in wind directions 30 and 60, the highest velocity is observed in M6W which has the worst performance with the other indicators. As the two cases are symmetrical, this behaviour is seen in wind directions 120 and 150 in reverse order,

too. Similarly, in wind direction 0, while the air change efficiency, air age and volume flow rate are better in M5W, the M4W is the one providing the highest velocity.

Taking an average between various wind directions, the wind tower M5W is the one that has highest air change efficiency in wind angles 0-90, 90-180, and 0-180. While in all these directions, its velocity values are lower than the other two wind tower positions.

Considering only the mean age of air and air change efficiency, the position 6 is the worst in wind directions 0, 30, 60 and 90. While in wind angles 90, 120, 150, and 180, the position 4 becomes the worst placement for a four-sided wind tower on the roof of a windowless room. When the wind blows perpendicularly to the wind tower, in angles 0, 90, and 180, the optimum placement that provides highest air change efficiency and freshest air is the central position 5.

## 5.7 Comparison between the case studies

In order to compare the nine models, the maximum and minimum values of volume flow rate (figure 5.55), area- and volume-averaged velocity magnitude (5.56), area- and volume-averaged mean age of air (figure 5.57), and air change efficiency (5.58) have been selected regardless of the wind direction. Moreover, the average value for each indicator was calculated for three wind variations of 0-90, 90-180 and 0-180 (same figures).

### 5.7.1 Volume flow rate and air change number

Looking at the graph 5.55, averaging the performance of the wind towers in wind directions between 0-90, 90-180 and 0-180 and comparing their performance in terms of volumetric air flow rate and number of air changes, it is evident that in wind directions between 0-90, the T group wind towers operate similarly, while in M group the induced airflow decreases as the wind towers is placed closer to the window. When the wind angle is in 90-180 range, the performance of the T and M groups wind towers are similar. While, considering the wind directions 0-180, the average performance of the T group is higher than the M group despite the fact that the M group wind towers show larger minimum and maximum values.

Considering the average performances in 90-180 and 0-180 wind directions, it is possible to state that the closer wind towers to the window (position 6) are able to induce more air changes and higher air flow rates compared to the central wind towers (position 5) and the farthest wind towers (position 4). This is however not

true when the wind is in 0-90 range. In these wind directions, the T wind towers perform similarly, while the performance of M and MW wind towers decrease as they are placed closer to the window. The MW group show a much more limited variation and their average performance is less than the other wind towers groups working in connection with a window.

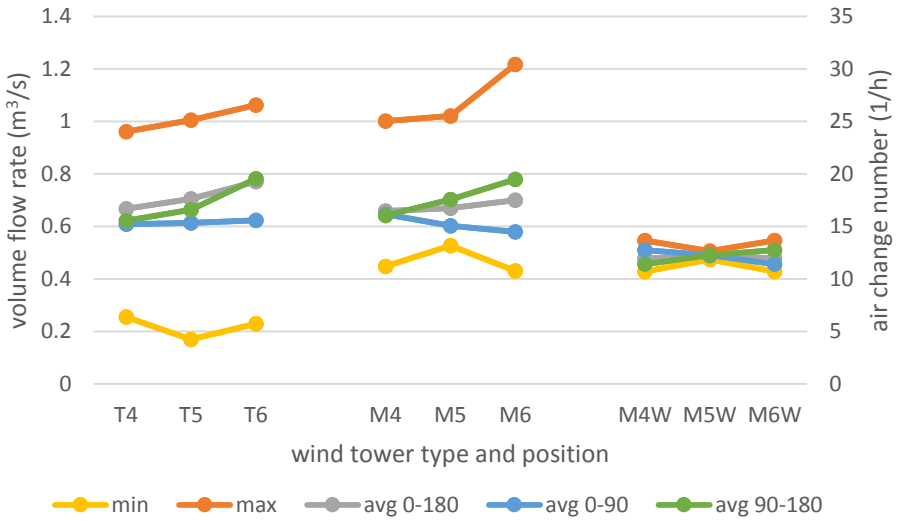


Figure 5.55. Volume flow rate ($m^3/s$) and air change number (1/h) at different wind tower positions

## 5.7.2 Velocity magnitude

Comparing different wind tower groups in terms of induced velocity magnitude (in figure 5.56), it is visible that the one-sided wind tower (group T) despite having the lowest minimum wind speed, is able to generate bigger maximum and bigger averages in the room in wind directions 90-180 and 0-180 followed by four sided wind towers (group M and group MW respectively). In wind directions 0-90, the M group perform better than the other two groups. The velocity magnitude values averaged on a surface at a height of 1.7 m from the room floor are also close to the volume-average values and show the same trend. Similar to the air flow rate values, the air speed figures induced by the MW groups have a limited range and the difference between the minimum and maximum velocities in those rooms are less than 0.1 m/s.

The T wind towers (T group) can induce higher velocities in 0-90 wind direction when placed on the roof position 4 while this the worst position when the wind direction is 90-180. Position 5 is the therefore preferred when the wind

direction ranges between 0-180. The M group in all wind directions should be positioned on top of the window (position 6) in order to induce bigger velocities. When a four-sided wind tower is supposed to ventilate a room individually (MW), it is more suitable to be positioned on the roof edge (4 or 6 position).

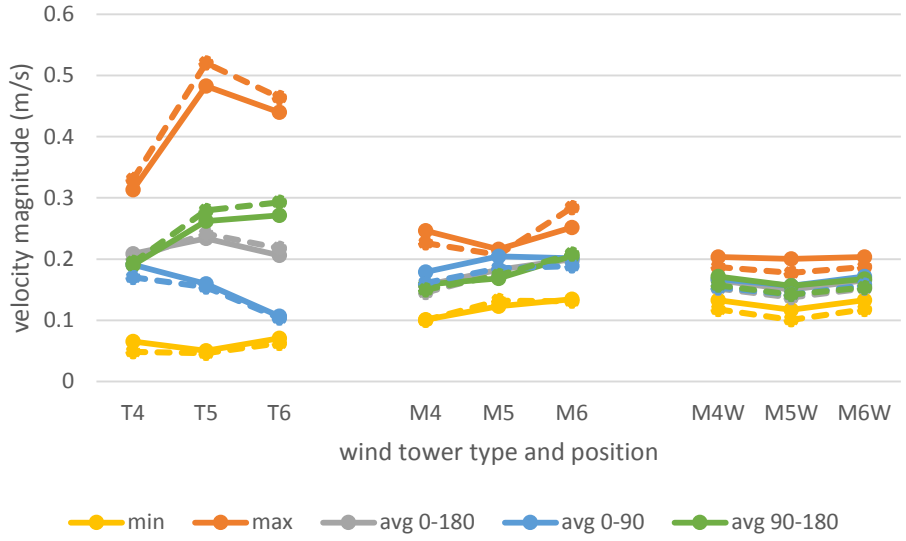


Figure 5.56. Volume-weighted (full-line) and area-weighted (dashed line) average velocity magnitude (m/s) at different wind tower positions

## 5.7.3 Mean age of air

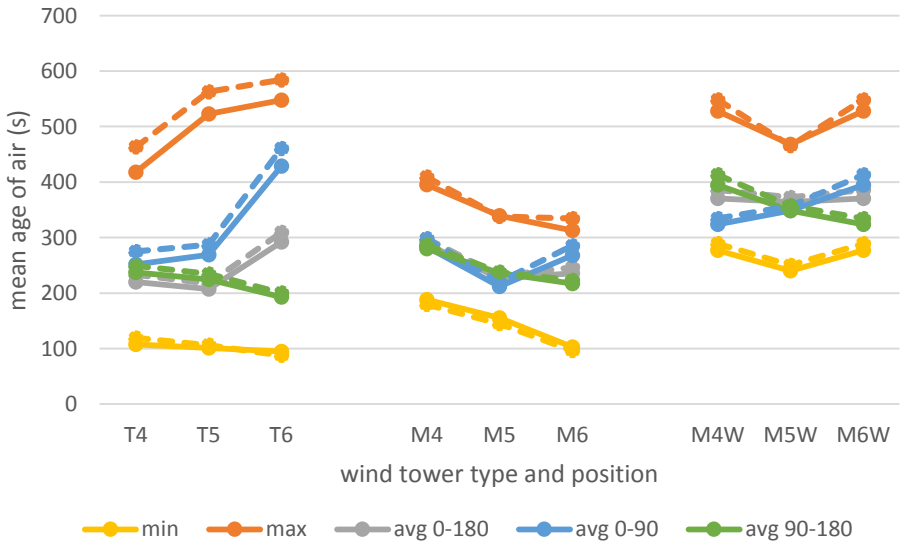


Figure 5.57. Volume-weighted (full-line) and area-weighted (dashed line) average mean age of air (s) at different wind tower positions

The average 0-180 mean age of air values for T and M groups are quite similar (see figure 5.57). Both groups show that the air in the room ventilated by a wind tower placed on the roof centre (position 5) is fresher. Contrarily, the stalest rooms are those ventilated only by windowless wind towers (MW group) followed by M4 and T6 in which the average mean age of air arrives to about 300 seconds. In wind direction 0-90 the M5 and M6 are those providing freshest air, while for wind angles 90-180, the all wind towers in T group are better in this regard. The T6 is wind directions 0-90 has the worst performance even compared to the windowless cases. This is despite the fact that the one-sided wind towers (T group) have the lowest minimum air ages. Four-sided wind towers with a window (M group) have the lowest maximum air ages.

For wind direction 0-90, 90-180 and 0-180, in a windowless space (MW group), the best placement of the wind tower is position 4, position 6 and position 5 respectively. The addition of a window can improve the freshness of the room's air in this case.

## 5.7.4 Air change efficiency

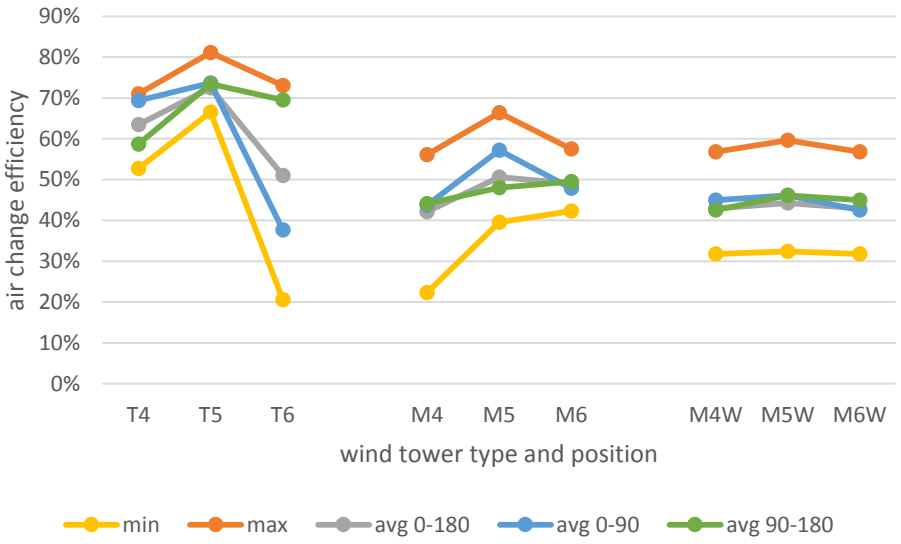


Figure 5.58. Air change efficiency (%) at different wind tower positions

According to the graph 5.58, the one-sided wind towers (T group) have a higher efficiency respect to the four-sided wind towers (M and MW groups) in wind directions 90-180 and 0-180. Even though, the least efficiency of all is provided by T6 wind tower in 0-90 wind angles. The four-sided wind towers working without a window (MW group) have an only slightly lower air change efficiency compared

to the four-sided wind tower with a window (M group) in wind directions 0-180 and 90-180. Though, for wind ranging between 0-90, the addition of a window to M5W can improve the air change efficiency almost by 10 per cent.

Finally, the placement of the wind towers on the roof center (position 6) is seen to be improving the air change efficiency on average in the three wind direction ranges.

## 5.8 Conclusion

Three case studies comprising 53 CFD simulations have been done to assess the effect of wind tower position on their performance at various wind incident angels. The parameters evaluated as part of this study include the volumetric airflow rate corresponding to the number of air changes, the velocity magnitude averaged in the whole room and on a surface placed at a height of 1.7 m, the mean age of air values averaged in the room volume and on a horizontal surface placed at a height of 1.70 m, and the air change efficiency. In order to derive the optimum positions, the maximum, minimum and average values of each parameter were calculated for each wind direction and for wind directions varying between 0-90, 90-180 and 0-180 degrees.

At many instances, an inconsistency is observed between the velocity magnitude, mean age of air and air change efficiency figures, meaning that higher velocities do not necessarily result in lower air ages (see M4W and M6W cases) and lower air ages do not guarantee an improved air change efficiency. In fact, at times a large air change efficiency happens in a room with very low induced air velocity and a high air age (see T5 at wind angle 90). Similarly, more air changes do not ascertain higher air change efficiencies (see M5 and M6 cases).

For this reason, in order to properly select the optimum position of a wind tower, it is essential to know which indicator is the most preferred one and for what purpose a wind tower is going to be utilized. The table 5.19 highlights the optimum positions considering highest air change efficiency ($\varepsilon_a$), lowest volume-weighted average mean age of air ($\bar{\tau}$), highest volume-weighted average velocity magnitude ($\overline{U}$), and highest volumetric airflow rate ($Q_v$) which correspond to the number of air changes. The colors orange, grey ad yellow utilized in the table to highlight the optimum positions of the wind tower according to each indicator, correspond to the colors used in the graphs and represent respectively positions 4, 5 and 6 of the wind tower on the roof (farthest, medium, and closest distance of the wind tower respect to the room's window).

As it is evident in the table, the wind direction can largely influence the choice for the wind tower position. The average performances for variable wind directions between 0-90, 90-180, and 0-180 are indicated in the table, too. For the rare conditions when the wind direction is variable between 0-180, the optimum wind tower position is the roof center. At this position and for all wind tower types, the average values of air change efficiency and the air freshness are at their maximum, even though the indoor air velocity and airflow rate values show a different trend. For wind direction between 0-90, the highest air change efficiency is provided by the centrally placed wind towers. For wind directions 90-180 the wind tower on top of the window induces highest airflow rates and lowest air ages.

Last but not least, this study shows that a four-sided wind tower ventilating a room individually can operate relatively well as its performance is only slightly worse than the cases with a window.

Table 5.19. The wind tower positions with optimal performances: highest air change efficiency, lowest mean age of air, highest indoor velocity, and highest airflow rate values (the colors orange, grey and yellow respectively represent the farthest, medium, and closest distance of the wind tower respect to the window)

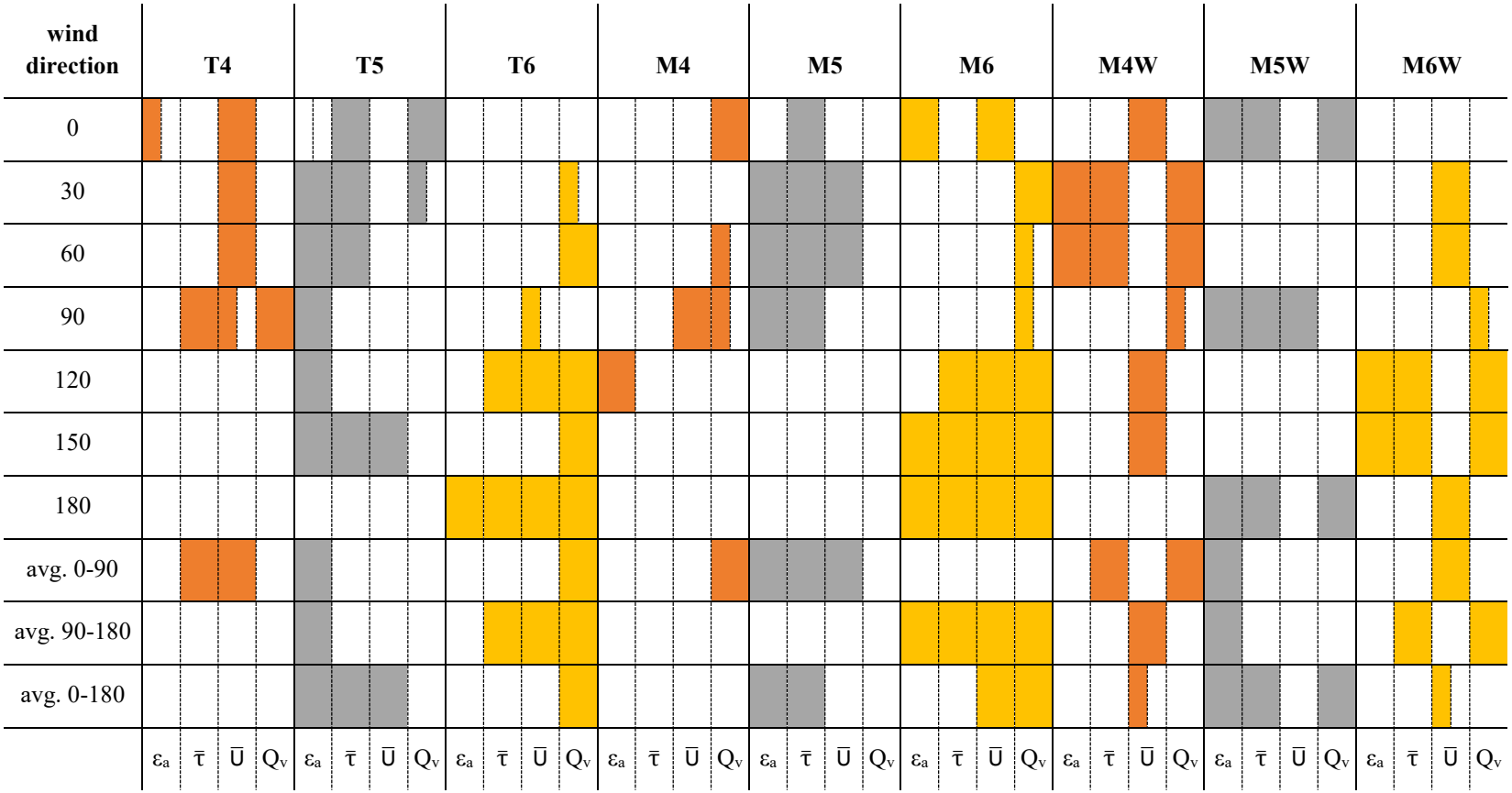

# Chapter 6

# Cross ventilation using two windows

## 6.1 Introduction

The simplest, most common and most familiar way of providing a cross ventilation in a room is by opening two windows on two opposite walls. In this thesis, the simulation on such a model has been done solely in order to illuminate how rooftop wind towers can function differently than windows at different wind incident angles and to highlight the extent of ventilation effectiveness of previously-assessed cases having wind towers.

## 6.2 Geometry and solver settings

This study consists of the previously-described room model lacking any wind towers and working solely with two window apertures placed on opposite walls. The length, width and height of the room are, as mentioned in preceding chapter, 8, 6 and 3 meters respectively and the windows placed in the centre of the smallest walls have square cross sections of 1 $m^2$ each (see figure 6.1). The new window added instead of the wind tower models is nominated as window B while the original window is called window A in the simulation results.

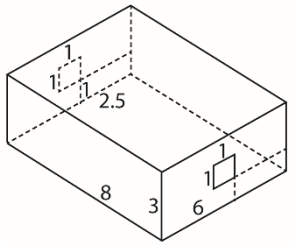


Figure 6.1. The room with two windows and their relative dimensions in meters.

The wind incident angles simulated in this chapter include 0, 30, 60 and 90 degrees as the symmetry of the model covers the angles between 120 and 180 degrees.

The domain size, the grid resolution, the boundary conditions and the solver settings are all identical with the previous cases, too. The choice to keep the boundary condition and solver settings equal to the previous cases is to eliminate the effect of computational parameters on the results of the simulation. However, according to the literature, for a cross-ventilation using two windows in a generic isolated building for which the experimental data is provided by Karava et al, 2008, the most appropriate turbulence model to use is SST k-ω (Ramponi & Blocken, 2012; Peren et al, 2015).

## 6.3 Results of the simulation

### 6.3.1 Reference values at zero incident angle

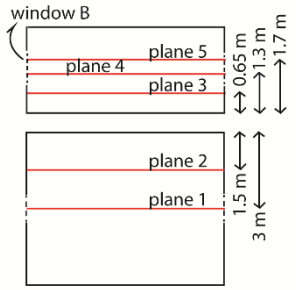


Figure 6.2. The vertical and horizontal planes on which the contours of pressure coefficient, velocity magnitude and mean age of air have been reproduced

At zero incident angle, the pressure coefficient, velocity magnitude and mean age of air distribution in and around the room are shown in tables 6.1, 6.2 and 6.3 respectively.

The average pressure coefficient value in the room ventilated by two windows when the wind blows perpendicularly to one of the windows, is 0.177 (see table 6.1). As evident in the picture, this value is homogenously spread in the room and the only slight variations are observed in front of the windows and below the leeward window. The windward roof edge is where the lowest pressure coefficient values are accumulated.

The velocity magnitude contours in table 6.2 show how the highest internal velocities (1 m/s) are formed in front of the windward window and how the air gets speedier as it is extracted from the leeward window aperture. The velocity in the

room reduces as we get distant from the windward aperture, however, except for the ceiling level, in the rest of the room on plane 1, the velocity is above 0.25 m/s.

The air age in the room (shown in table 6.3) increases as the distance from the windward window increases. In front of the windward window, the mean age of air value is less than 30 seconds, while it eventually increases to about 120 seconds on the leeward side of the room. The least fresh air in the room having mean age of air of above 150 seconds are observed in vicinity of the ceiling and floor around the windward window.

Table 6.1. Contours of pressure coefficient (-), velocity magnitude (m/s), and mean age of air (s) on the central vertical symmetry plane 1

| plane | pressure coefficient | velocity magnitude | mean age of air |
|---|---|---|---|
| | 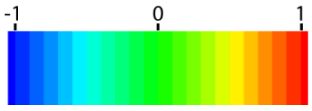  | 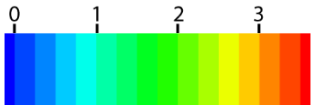  | 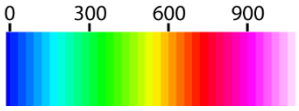  |
| 1 | 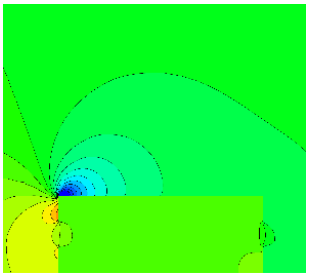 | 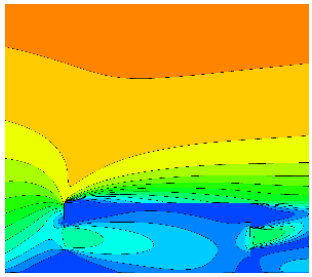 | 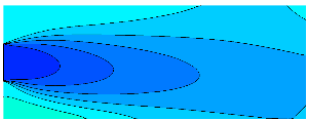 |

## 6.3.2 Volume flow rate and air change number

The induced volume flow rate and the corresponding air change number in a room ventilated by two opposite windows are shown in the graph 6.3. As it is evident, the highest volumetric flow rate of around 0.98 $m^3/s$ is induced when the wind blows perpendicularly to either of the windows. This corresponds to 24.4 air changes per hour. Contrarily, in 90 degrees wind angle, the two values reduce to the minimum values of 0.002 $m^3/s$ and 0.06 ACH.

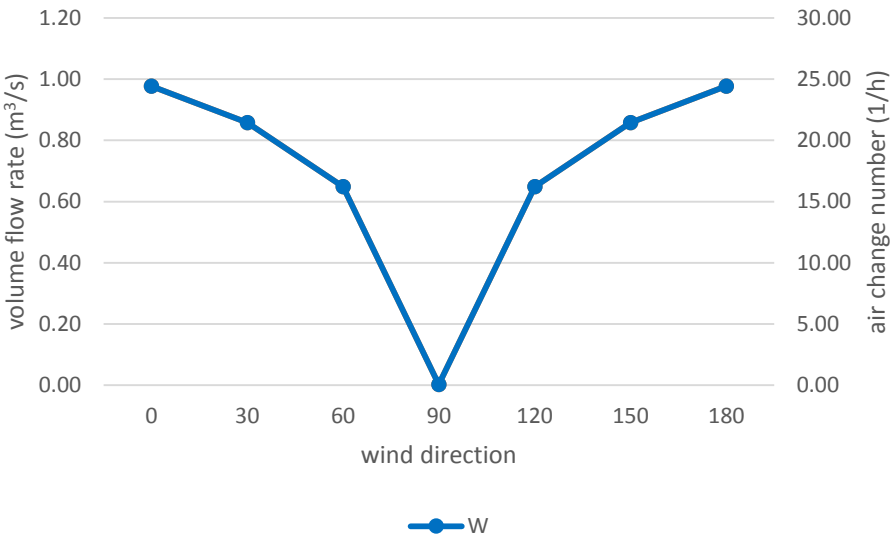


Figure 6.3. Volume flow rate ($m^3/s$) and air change number (1/h) by two windows at different wind directions

### 6.3.3 Pressure coefficient

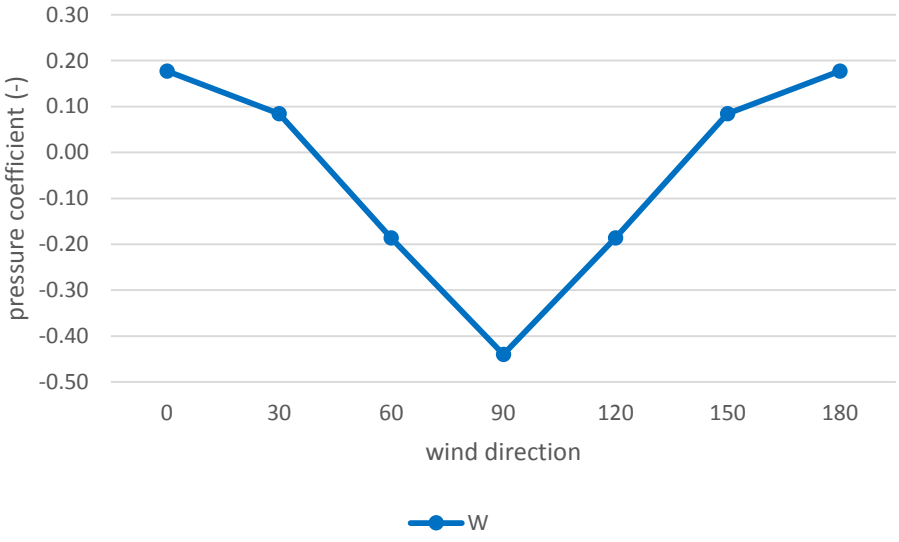


Figure 6.4. Volume-weighted average pressure coefficient (-) in the room

The graph 6.4 demonstrates the variation in the volume-averaged pressure coefficient values in the room by the change in wind incident angle. As evident in the graph, the lowest pressure coefficient value occurs at wind direction 90 where the Cp is -0.44. The Cp value increases as the wind direction deviates from 90

degrees towards 0 and 180. The pressure coefficient value is 0.18 wind directions 0 and 180.

The pressure coefficient values alter on each of the two windows as the wind direction changes (see figure 6.5). The highest positive Cp value of 0.32 is observed on the windward window when the wind blows perpendicularly to it (corresponding to window B at 0 degrees and window A at 180 degrees). This is followed by Cp equal to 0.21 on windward windows at 30 degrees incident angle. The lowest Cp occurs in wind incident angle 90 when both of the windows have an identical Cp value of -0.44. Finally, the pressure coefficient value of zero is obtained on the leeward window when the wind incident angle is 0.

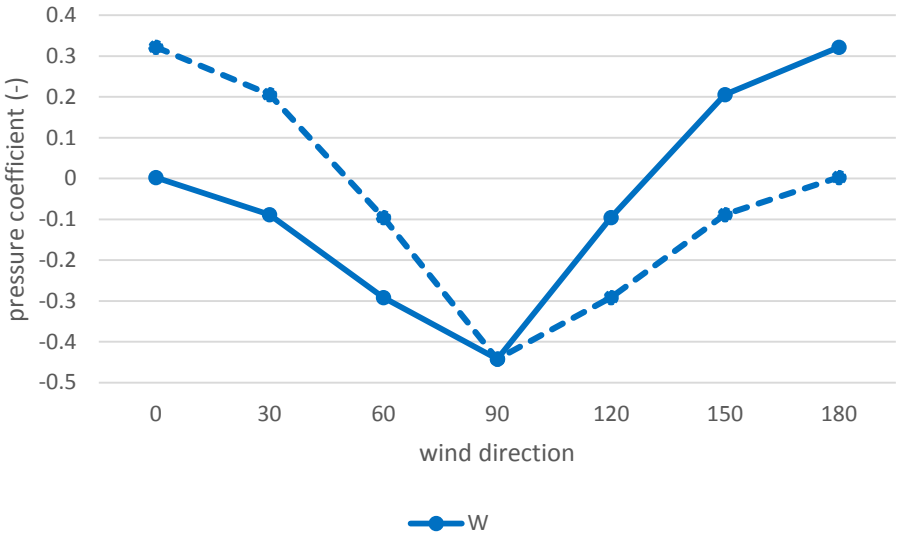


Figure 6.5. Area-weighted average pressure coefficient (-) on window A (full line) and window B (dashed line)

### 6.3.4 Velocity magnitude

On average, the highest indoor air velocity in the room provided by two opposite windows occur at wind directions 30 and 150. The volumetric average of this parameter stands at 0.28 m/s while the average on the horizontal surface at a height of 1.7 m is 0.32 m/s (see figure 6.6). These values reduce respectively to 0.24 and 0.28 m/s at wind angles 0 and 180 and reach to a minimum of 0.04 m/s at 90 degrees. The area-average velocity at all angles except for 90 degrees is higher than the volume-average figure, though this difference is less than 0.05 m/s (figure 6.6).

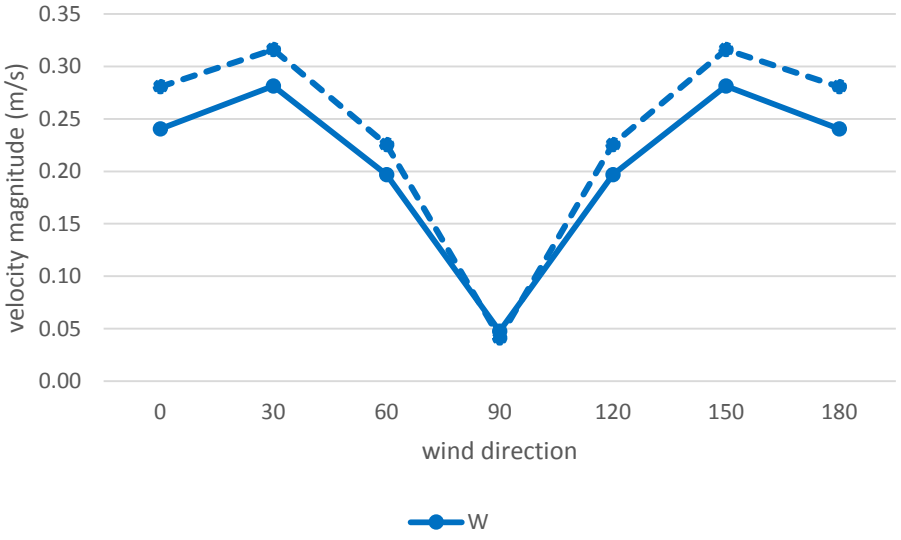


Figure 6.6. Volume-weighted (full-line) and area-weighted (dashed line) average velocity magnitude (m/s) in the room ventilated by two windows

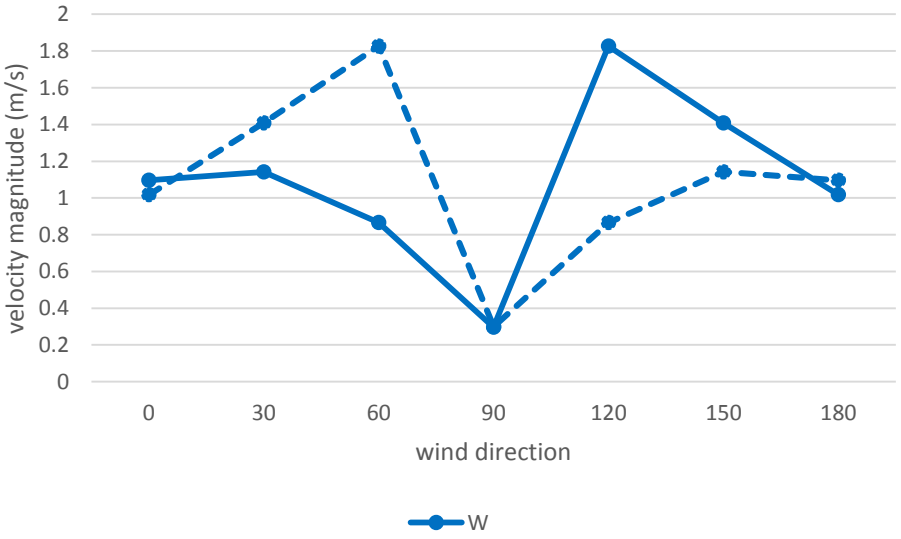


Figure 6.7. Area-averaged velocity magnitude (m/s) on window A (full line) and window B (dashed line)

The variation of the wind speed on each of the window surfaces are summarised in the graph 6.7. The wind on the windward window has a velocity of about 1 m/s at zero incident angle. This velocity eventually increases until it reaches a maximum of 1.83 m/s at 60 degree incident angle. This value drops to a minimum of 0.30 m/s

as the wind direction arrives to 90 degrees and gradually increases as the wind deviates further toward 180 degrees.

Table 6.2. Contours of velocity magnitude (m/s) on a horizontal surface placed 1.7 m above the ground

| **wind angle** | **W** |
|---|---|
| U (m/s) | 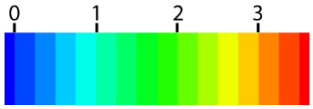  |
| 0 | 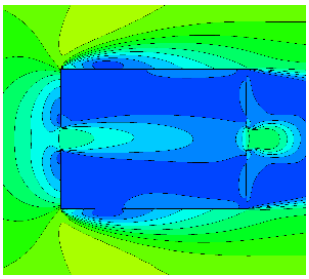 |
| 30 | 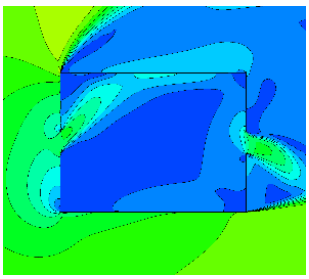 |
| 60 | 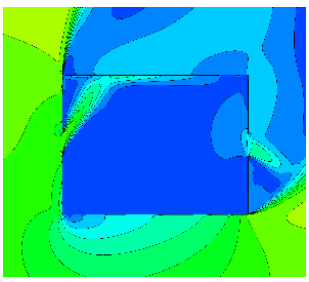 |

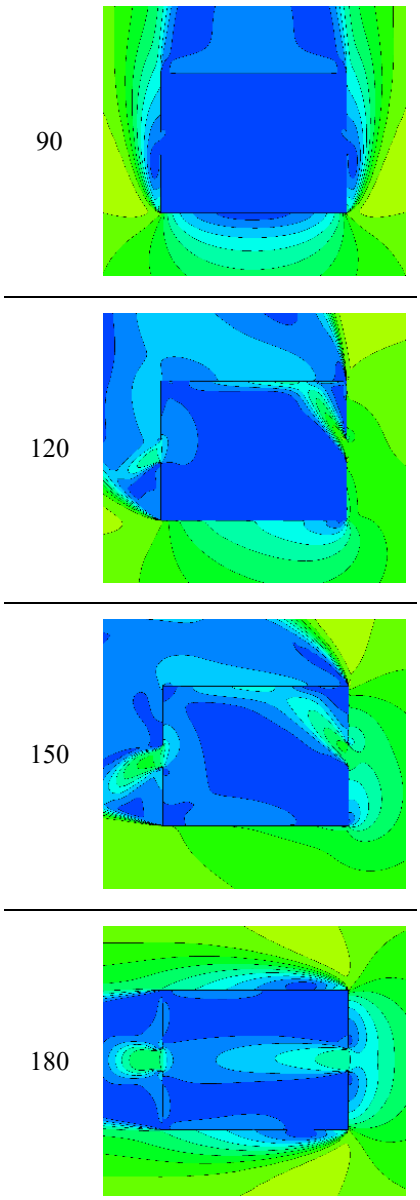


Contours of velocity magnitude on a horizontal surface positioned at a height of 170 cm from the ground representing a human height are shown in the table 6.2. According to the table, at zero incident angle the air enters to the room with a speed of about 1 m/s from the window B and it gradually loses its velocity as it travels toward to the leeward window. In vicinity of the leeward window, inside the room, the air velocity increases again and right after exiting the window it arrives to a speed of 1.25 m/s. At this wind angle, on this horizontal level, the two sides of the window has a speed range between 0 and 0.25 m/s and only in adjacency of the two

longer walls, the air movement is slightly speedier. The average velocity distributed on this height level is 0.28 m/s.

At 30 degree incident angle, the wind enters the room with a velocity of between 1.25 and 1.5 m/s. the airflow's speed gradually decreases once it is inside the room. Though, similar to the previous incident angle it becomes speedier once it gets close to the leeward window. A major portion of the room in the center has a speed of lower than 0.25 m/s, though in adjacency of the walls, the velocity is above 0.25 m/s. The velocity magnitude is better spread in the room compared to the previous wind direction and the average velocity on this horizontal level is also higher: 0.32 m/s.

At wind direction 60, the entering air velocity is more than 1.75 m/s. But as the airflow soon hits the internal wall of the room, it loses its velocity fast enough not to reach to the other room areas. At this angle, except for the leeward window and one of the internal walls vicinity, the other areas of the room has no air movement. In fact the area-average velocity magnitude for a standing person is 0.23 m/s.

When the wind blows to the room with a 90 degree angle, no air enters the room from either of the windows and the room remains still. The windows experience a very tiny amount of air movement with a velocity between 0 and 0.5 m/s. The area-average velocity magnitude at a height of 170 cm is 0.04 m/s.

Finally, the wind directions 120, 150 and 180 degrees are the horizontal reflections of the cases with 60, 30 and 0 incident angle.

### 6.3.5 Mean age of air

The freshness of the air in the room is at its optimum condition when the wind blows perpendicularly to either of the windows at 0 and 180. At these angles, the average mean age of air is 148 seconds in the whole room and 138 s for a standing person (as shown in figure 6.8). These values increase gradually until they arrive to 201-202 seconds at 60 and 120 wind angles and then sharply worsen until they reach respectively to 753 and 790 seconds at 90 degrees wind direction.

The distribution of mean age of air felt by a standing person are demonstrated in the table 6.3. At zero incident angle the average mean age of air at this level is 138 seconds (see dashed line in figure 6.8). The fresher portion of this air is accumulated in front of the windward window B while on each side of this window, the age of air has a value between 150 and 180 seconds. The other half of the room in front of the leeward window A has an air age ranging between 90 and 150 seconds. The stalest air in this wind direction has a mean age of 244 seconds.

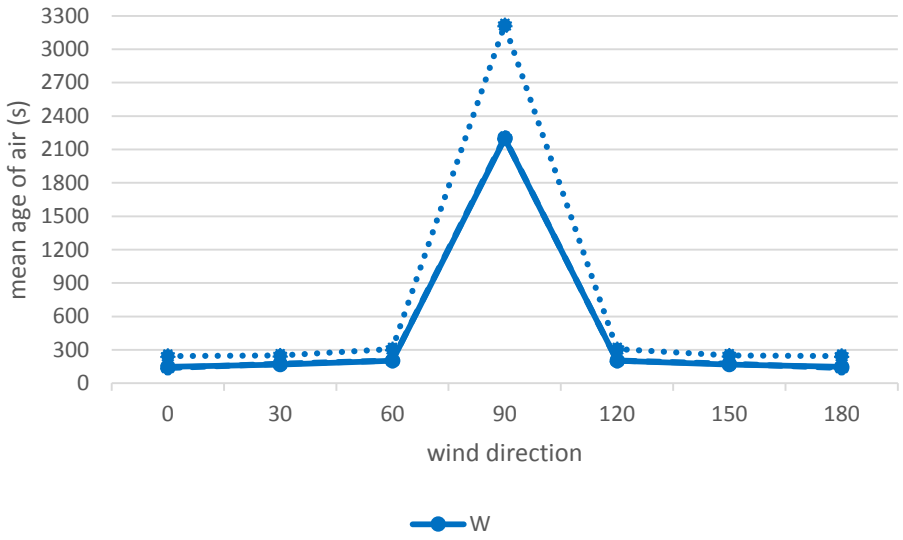


Figure 6.8. Volume-weighted average (full-line), area-weighted average (dashed line), and maximum (dotted line) mean age of air (s) in the room ventilated by two windows

When the wind direction arrives to 30 degrees, despite the improvement of velocity magnitude at this angle compared to zero degrees, and despite the fact that the maximum air age in this room is only 6 seconds higher than in the previous angle, the average mean age of air on the height of 1.7 m increases and reaches to 174 seconds (figure 6.8). The core of the room at 30 degrees wind direction has an air age of between 210 and 240 seconds (table 6.3). Only along the airflow through the windward window the air is fresher than 120 seconds, while around all other room walls, the freshness has a value between 120 and 180 seconds.

The air age in the room deteriorates even more at 60 incident angle. At this angle, on the left side of the windward window where the airflow is directed to, the air is fresh with an age of less than 120 seconds. In front of the leeward window in a 3-meter distance, the age of air ranges between 150 and 210 seconds. While, the remaining part of the room especially in front of the windward window the air has a higher age between 210 and 300 seconds. The area-average mean age of air at this height has a value of 202 seconds and the least fresh air has an age of 306 seconds (dotted line in figure 6.8).

Finally, a room ventilated by two windows when the wind direction is 90 degrees has the worst condition when it comes to air freshness, as the average mean age of air for a standing person arrives to a value of 2204 seconds! In this wind direction the highest mean age of air in the room is 3216 seconds (figure 6.8). The accumulation of the fresher airs is in vicinity of the window B and the internal side

of the windward façade. For clearer visibility of the contours in other cases, the limit value was set as 1080 seconds, this is why in table 6.3 in wind direction 90 the air ages above this value are shown as blank.

Table 6.3. Contours of mean age of air (s) on a horizontal surface placed 1.7 m above the ground.

| **wind angle** | **W** |
|---|---|
| τ (s) | 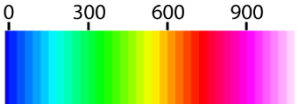  |
| 0 | 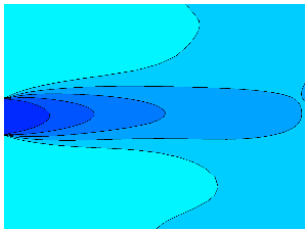 |
| 30 | 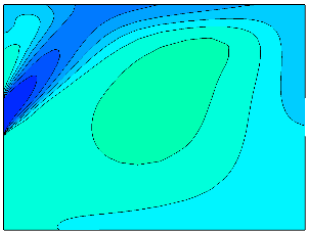 |
| 60 | 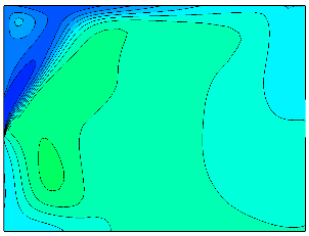 |
| 90 | 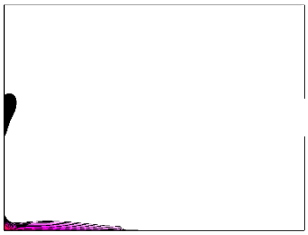 |

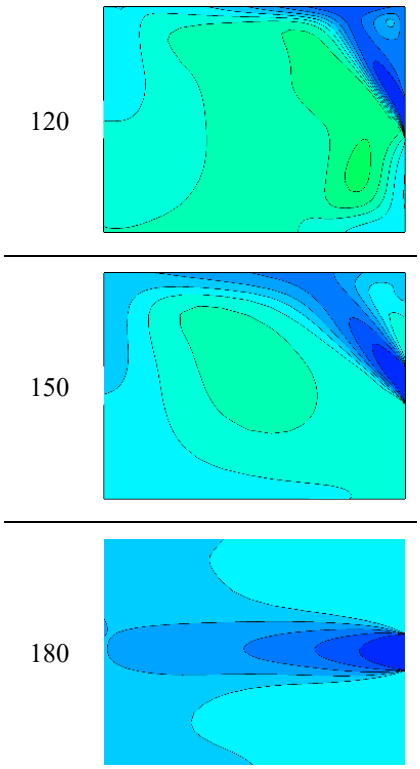


### 6.3.6 Air change efficiency

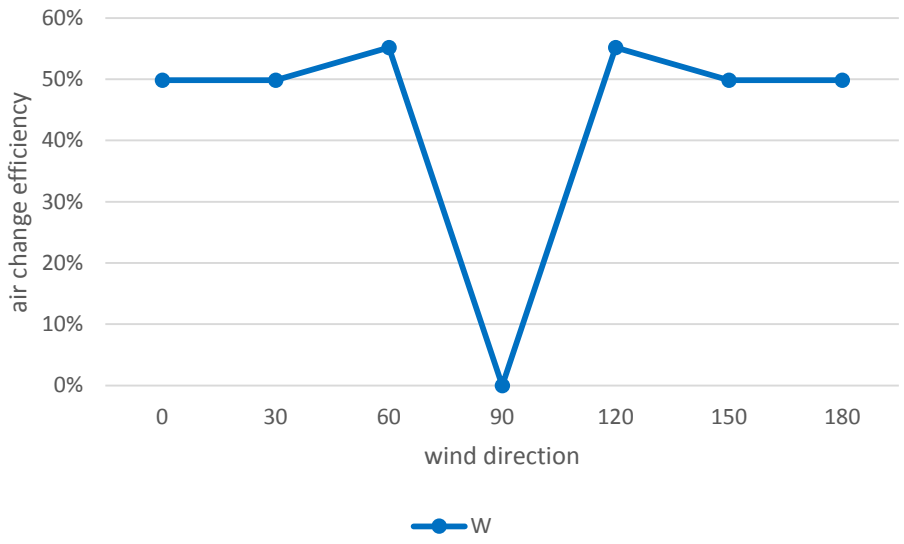


Figure 6.9. Air change efficiency (%) in the room ventilated by two windows

According to figure 6.9, the air change efficiency is at its highest value of 55.2% at wind incident angles 60 and 120 and its lowest value of 0% at wind direction 90. At the remaining four wind angles this figure is 49.8%.

## 6.4 Comparison with the wind tower cases

### 6.4.1 Volume flow rate

Comparing the wind tower cases in chapter 5 with the current case study in terms of volumetric air flow rate (shown in figure 6.10), it is noticeable that in majority of the wind directions the combination of a one-sided wind tower and a window can perform better than two windows. In fact, only at 0 and 60 degrees, the air flow rate provided by the two windows are better than the majority of the wind tower cases. Yet, at 0 incident angle T5 has a higher airflow rate and at 60 degrees M4, M5 and M6 have similar flow rates to the case with two windows. At 90 degrees incident angle where the T cases similar to the case W have no windward apertures, all three cases T4, T5 and T6 induce higher airflow rates than the case W. Furthermore, it is interesting to note that the four-sided wind tower cases M, only at 90 and 180 wind directions perform better than two windows, and at 60 degrees their induced volume flow rate is equal. A room having only one four-sided wind tower and no windows (MW) in all wind directions except 90 degrees induces lower airflows than two windows (W).

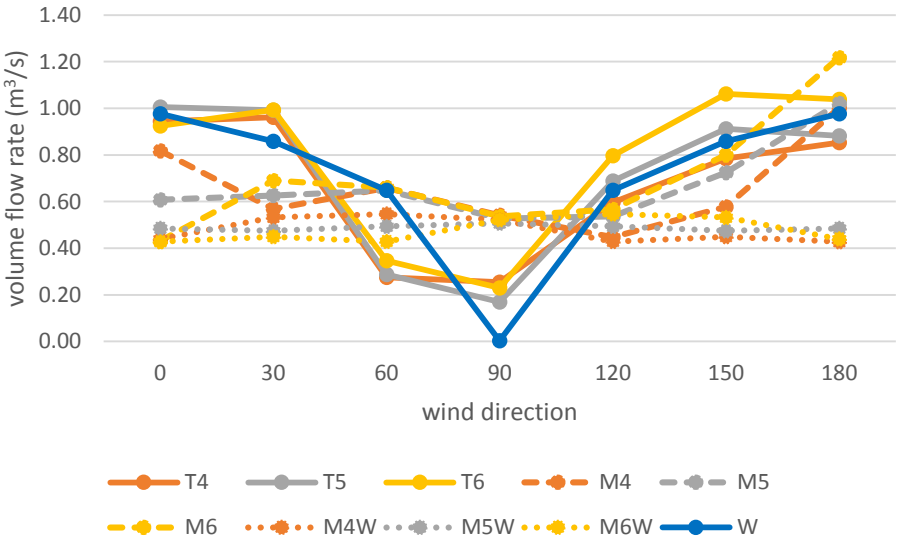


Figure 6.10. Comparison between the volume flow rate ($m^3/s$) in the rooms ventilated by the wind towers and/or windows

## 6.4.2 Velocity magnitude

Looking at the graph 6.11 of the volume-average velocity magnitude in different cases, it is remarkable that in all incident angles, there is at least one case with wind towers that induces higher speed than the case only with windows. Especially in leeward angles T5 and T6, and at 90 degrees all M and MW cases induce velocities of more than 0.1 m/s higher than the cases W. Among all cases with wind towers, the case T4 has the closest velocity figures to the case W.

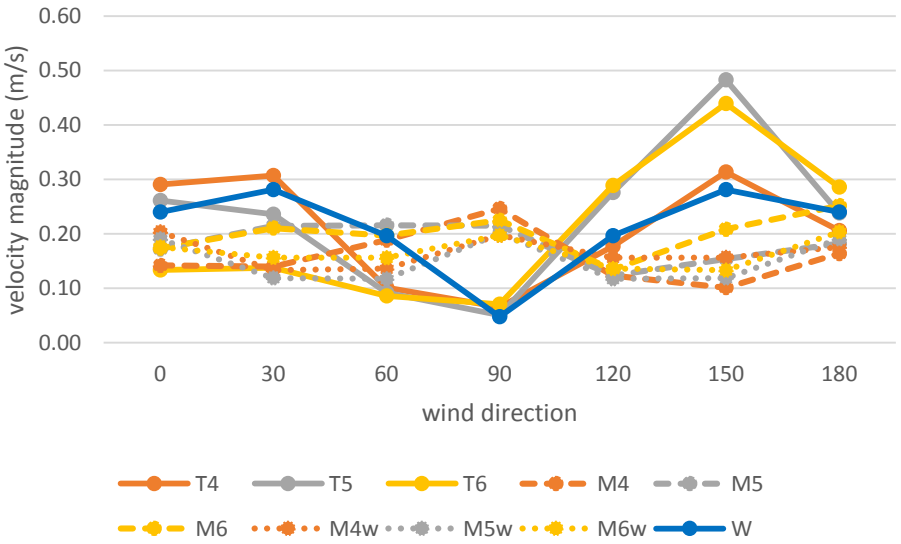


Figure 6.11. Comparison between the volume-average velocity magnitude (m/s) in the rooms ventilated by the wind towers and/or windows

## 6.4.3 Mean age of air

Observing the volume-average mean age of air values in figure 6.12, it is evident that except for 60 degrees incident angle, the one side wind tower T5 has a lower mean age of air in all other wind directions compared to the case W. in wind angles 0 and 30, T4 and T5 and in wind directions 120, 150 and 180, T5 and T6 provide fresher air in the room compared to W. At 60 degrees, the case W is preferred to all other cases but M5 which provides an air age of 5 seconds lower than the W case. In wind direction 90, the four-sided wind towers M and MW provide considerably fresher airs compared to the wind towers T and the two windows in case W.

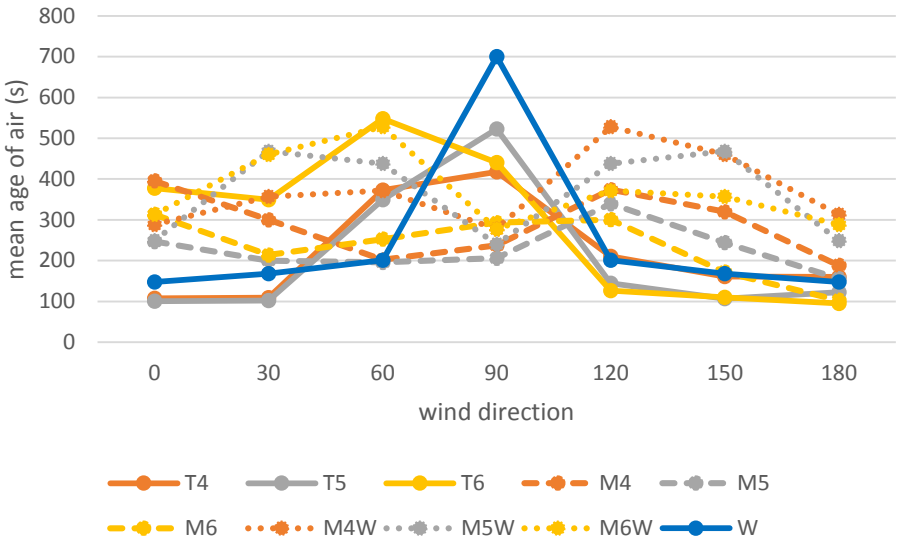


Figure 6.12. Comparison between the volume-average mean age of air (s) in the rooms ventilated by the wind towers and/or windows. For a better visibility, the air age of case W at 90 degrees is set as 700 s instead of the real value which is 2198 s.

### 6.4.4 Air change efficiency

The most notable point in the graph of air change efficiency (figure 6.13) having a zero value belongs to the case W at 90 wind incident angle. Other noticeable information in this graph is the superior performance of wind towers T5 respect to the W case and also respect to all other wind tower cases. T4 shows a similarly great performance in angles between 0 and 60, while T6 shows a big improvement and thus a very good performance in wind angles over 90 degrees. In wind angles 0-90, M5 performs either better or similar to W in terms of air change efficiency while its performance deteriorates as the wind deviates further toward 120 degrees.

Furthermore, it is interesting to note that the cases MW in which no window exists perform better than the two windows in case W in wind directions 0, 90 and 180 degrees.

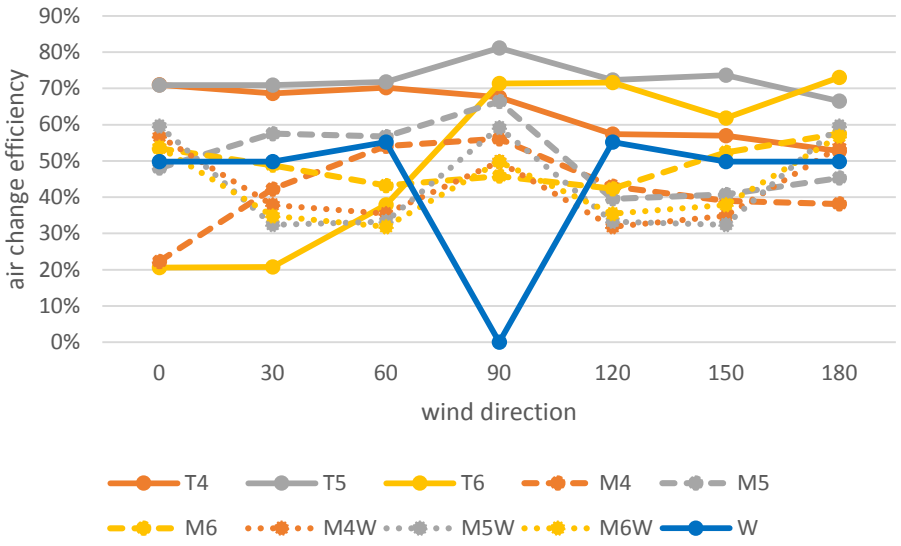


Figure 6.13. Comparison between the air change efficiency (%) in the rooms ventilated by the wind towers and/or windows

## 6.5 Conclusion

Cross ventilation through two windows is very different from cross ventilation using a wind tower-window combination. Deciding which is better is not straightforward as it is very much dependent on the wind direction, the type and position of the wind tower, and the parameter on which the comparison is based on.

The wind tower type that is expected to have the closest performance to the windows is the one-sided wind tower T4 as its aperture is right on top of window B with a 2.5-meter distance. Here a comparison between the two cases in terms of velocity and mean age of air distribution is given.

Even though the wind entering the wind tower T4 has a higher speed than the wind entering the window B, the contours of velocity on vertical and horizontal planes in case W are speedier. However, the volume-average velocity in the room ventilated by T4 is higher than in case W because the jet of air through the wind tower which is considerably speedier than that through the window does not distribute well in the room volume, rather it hits the room floor and distributes on that level. The same happens in wind directions 30. In wind direction 60 as there is a very small airflow through the wind tower, the W case is preferred. At 90 degrees there is no much difference between the cases and at the angles over that in both cases window A is the air supplier. At angles 120 and 180, the case W and at 150 degree, the case T4 provide better wind velocity distribution in the room.

The mean age of air contours show a slightly different behavior than the velocity ones. At 0 and 30 degrees, a standing person feels a fresher air in the T4 room rather than W room. At 60 degrees, W case has a substantially lower air age compared to T4 because the window B acts better as the air supply compared to T4 aperture. Perhaps the most interesting comparison in terms of air age is in 90 degrees. At this angle, the W case ceases to provide fresh air in the room. In fact, the mean air age values arrive to values of around 2200 seconds in the room volume and as area-average figure at a height of 1.70 meters. At T4 case, the situation is much better as the volume-average and area-average figures are 418 and 463 seconds respectively. The age of air contours at wind angles over 90 degrees are consistent with those of velocity, meaning that at 120 and 180 degrees where the case W provides higher velocities, and at 150 degrees where T4 induces speedier air, the air is fresher, too.

The charts 6.15-6.18 in the next two pages compare all cases by considering the average values for each parameter in wind directions 0-90, 90-180, and 0-180.

In wind directions 0-90, in terms of volume flow rate (figure 6.15), the case W performs slightly worse than M4, similar to all T cases, and better than M5, M6 and all MW cases. In terms of volume-average velocity (figure 6.16), the case W performs worse than M5 and M6, similar to T4, and better than T5, T6, M4 and all MW cases. In terms of volume-average mean age of air (figure 6.17), the case W performs worse than all other cases. And in terms of air change efficiency (figure 6.18), the case W performs worse than all cases except for T6.

In wind directions 90-180, in terms of volume flow rate (figure 6.15), the case W performs worse than T5, T6, all three M case, similar to T4, and better than MW cases. In terms of volume-average velocity (figure 6.16), the case W performs worse than T5, T6 and M6, similar to T4, and better than M4, M5 and all MW cases. In terms of volume-average mean age of air and air change efficiency (figures 6.17 and 6.18), the case W performs worse than all other cases.

In wind directions 0-180, in terms of volume flow rate (graph 6.15), the case W performs worse than T6, similar to T5 and M6, and better than T4, M4, M5 and all MW cases. In terms of volume-average velocity (figure 6.16), the case W performs worse than T5, similar to T4, and better than T6, all M and MW cases. In terms of volume-average mean age of air (figure 6.17), the case W performs worse than all other cases. And, in terms of air change efficiency (figure 6.18), the case W performs worse than M5, M6 and all T cases, similar to M5W, and better than M4, M4W and M6W.

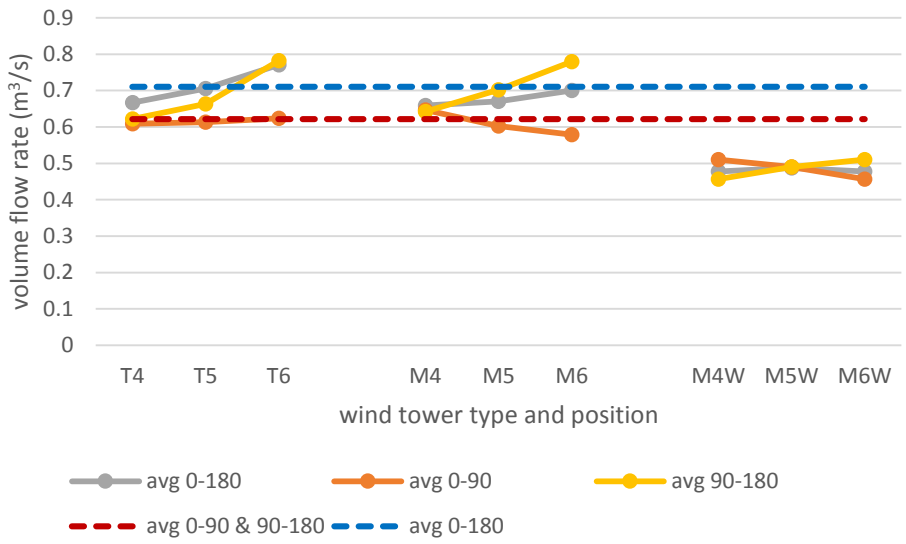


Figure 6.15. Volume flow rate ($m^3/s$) through different wind tower positions (full line) and the case with windows only (dashed line)

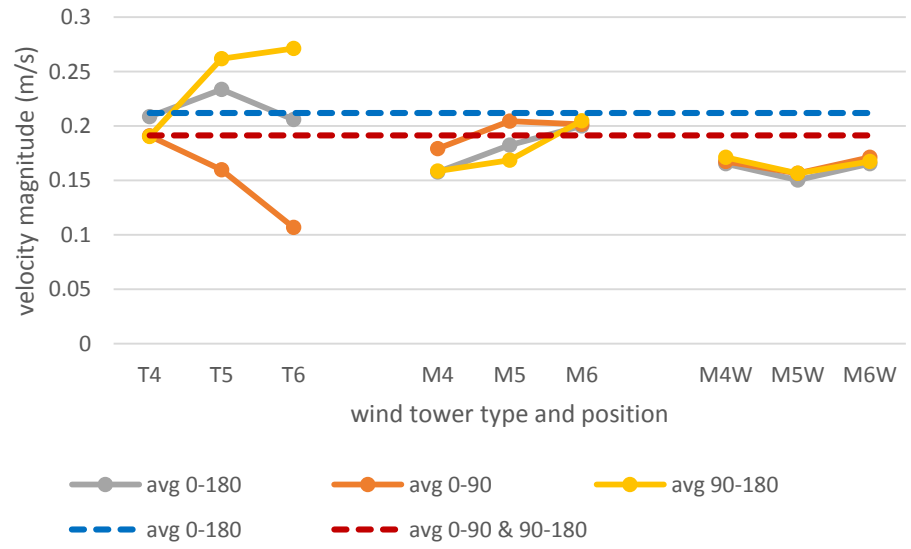


Figure 6.16. Volume-weighted average velocity magnitude in the room with different wind tower positions (full line) and the case with windows only (dashed line)

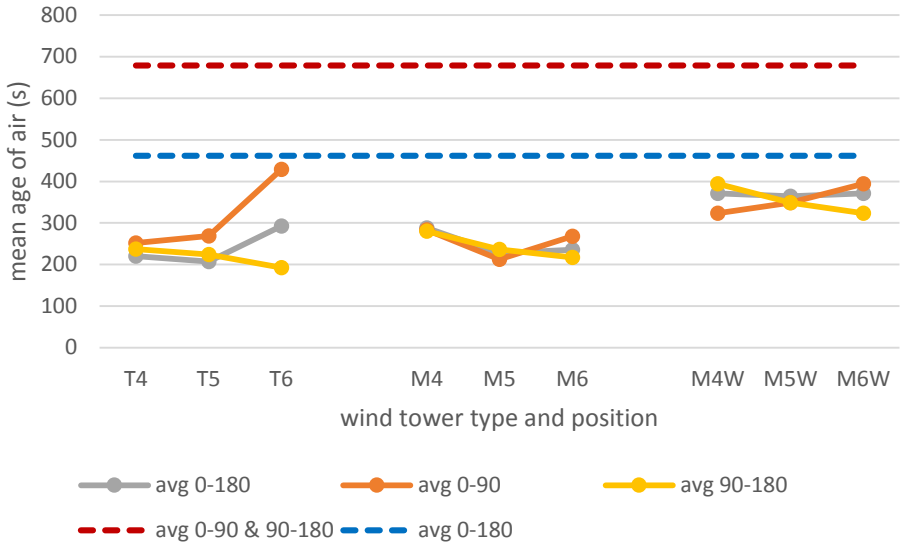


Figure. Figure 6.17. Volume-weighted average mean age of air (s) in the room with different wind tower positions (full line) and the case with windows only (dashed line)

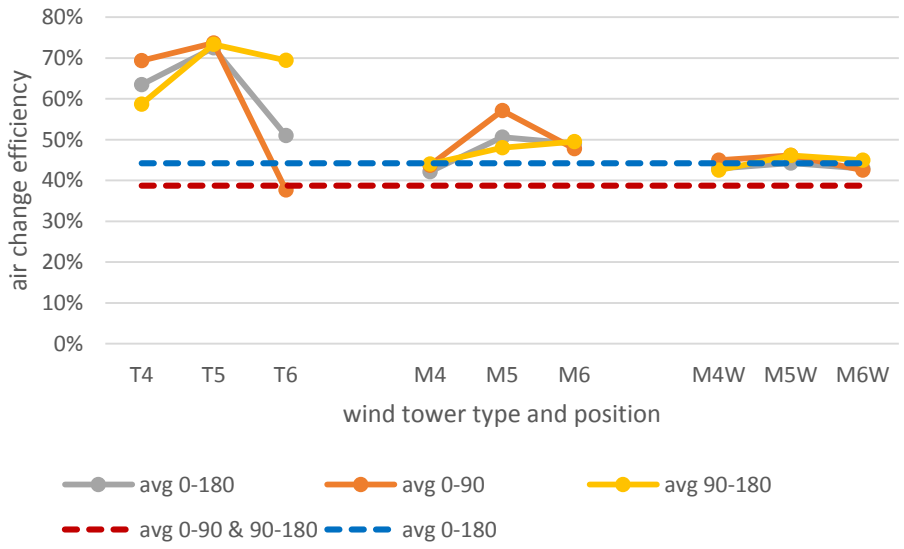


Figure 6.18. Air change efficiency (%) of different wind tower positions (full line) and the case with windows only (dashed line)

# Chapter 7

# Cross ventilation using wind towers in two-zone spaces

## 7.1 Introduction

As previously mentioned, almost all wind tower studies on up until this moment have been done on single zone spaces. Since no experimental data has ever been provided for multi-zone spaces, therefore, no numerical assessment has been done for such configurations either.

This final part of the thesis is prepared as an introduction to a possible future project about evaluating the effect of building layout on cross ventilation effectiveness where a one-sided wind tower works in combination with a window when either of them is placed in a different zone.

## 7.2 Geometry and solver settings

In order to be able to compare the results of this assessment with previous cases, the same room, wind tower and window with identical measurements have been utilized. The wind tower is the one-sided one placed at the farthest distance from the window (model T4). The internal partitions considered in this assessment were placed at either a 6-meter, 4-meter, or 2-meter distance from the window and they each have an opening as an empty door frame with a dimension of 1 in 2 m placed exactly in the center of the partition on the same axis as the wind tower and the window. The models are respectively nominated as R1, R2 and R3 (figure 7.1) and are made identically with structured meshes of 5,135,004 cells (figure 7.2).

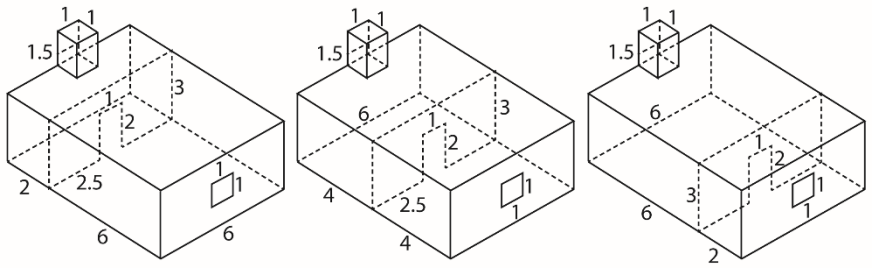


Figure 7.1. The room with a one-sided wind tower divided by partitions into two zones and their relative dimensions in meter, nominated as R1 (left), R2 (middle) and R3 (right)

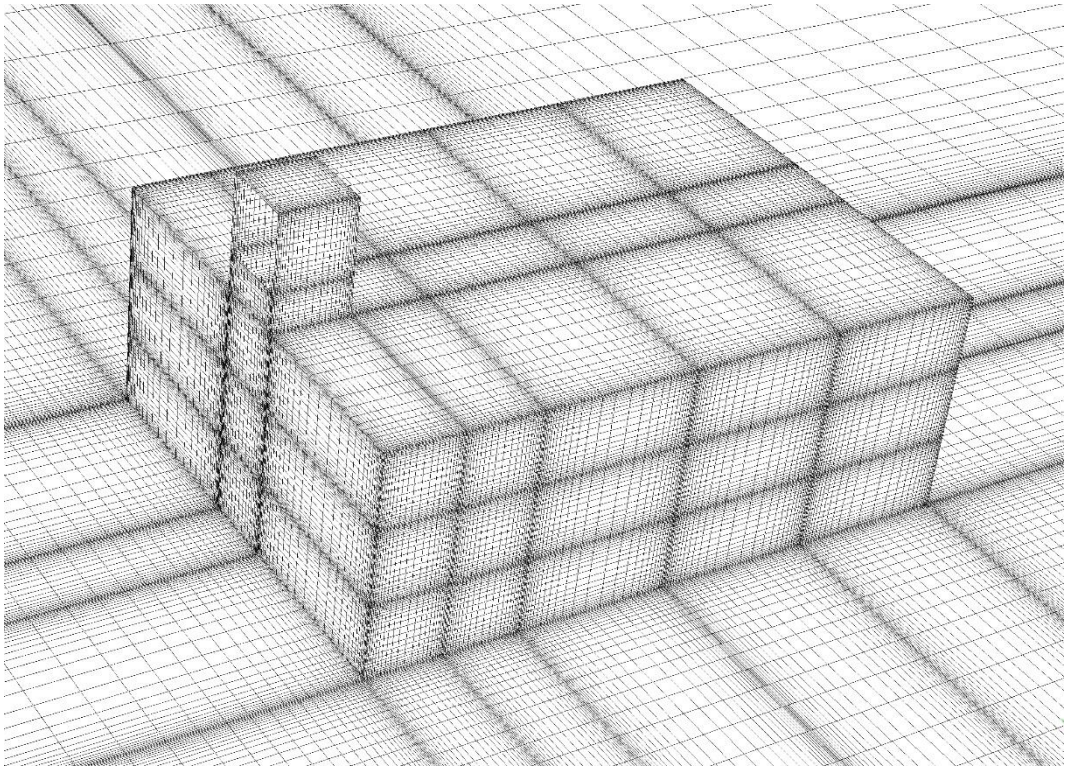

Figure 7.2. The mesh structure of the one-sided wind tower model divided by partitions into different zones

The wind incident angles simulated in this chapter are 0 and 180 degrees. The domain size, the boundary conditions, and the solver settings are all equal to the preceding studies in order to minimize the effect of computational parameters on the results of the simulations.

## 7.3 Results of the simulations

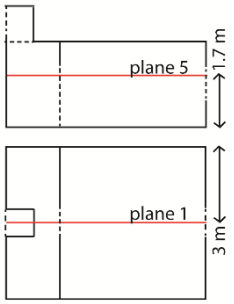


Figure 7.3. The vertical and horizontal planes on which the contours of pressure coefficient, velocity magnitude and mean age of air contours have been reproduced

### 7.3.1 Volume flow rate and air change number

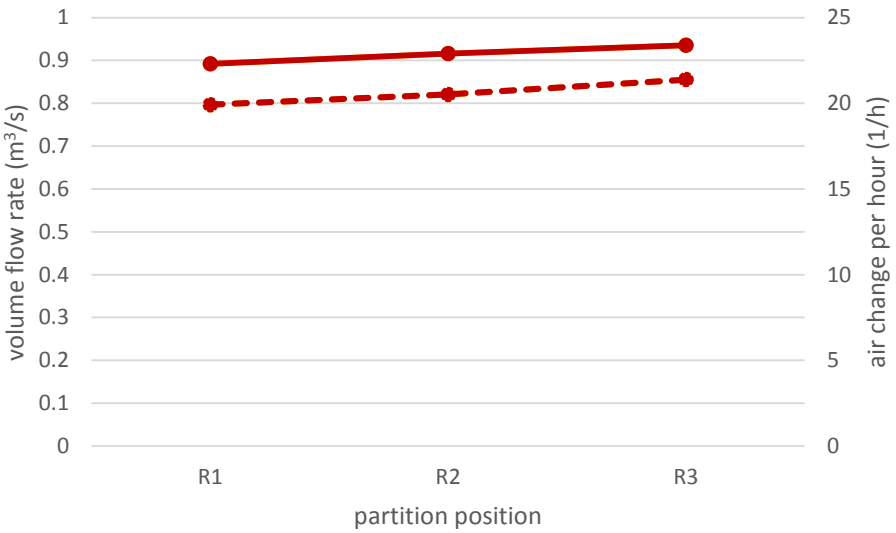


Figure 7.4. Volume flow rate ($m^3/s$) and air change number (1/h) in each model for wind directions 0 (full line) and 180 (dashed line)

As it is visible in the graph 7.4, the position of the internal partition does not majorly affect the induced volumetric air flow rate. The closer the partition is placed to the window, the higher is the airflow rate, but this variation is less than 0.08 $m^3/s$. Comparing the wind directions 0 and 180, however, it is notable that when the wind tower acts as the air supply at wind incident angle 0, the volume flow rate values are around 0.1 $m^3/s$ corresponding to 2.5 ACH higher than when the window supplies the air.

### 7.3.2 Pressure coefficient

The contours of pressure coefficient at wind incident angles 0 and 180 are represented in tables 7.1 and 7.2. As evident in table 7.1, the left part of the room, underneath the wind tower has a higher Cp than the right part when the wind angle is 0 and this difference is between 0.07 and 0.1. As it is summarized in the graph 7.5, the volume-average Cp value on the left side are 0.26, 0.29, and 0.24 for R1, R2 and R3 respectively. These figures change correspondingly to 0.18, 0.19, and 0.14 in the right side.

Table 7.1. Contours of pressure coefficient (-) on vertical plane 1 for wind incident angle 0

| plane | R1 | R2 | R3 |
|---|---|---|---|
| Cp (-) | 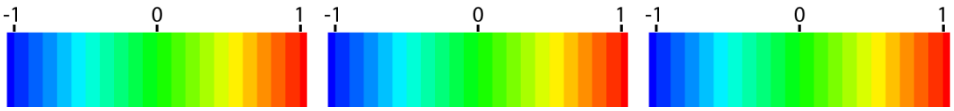  | | |
| 1 | 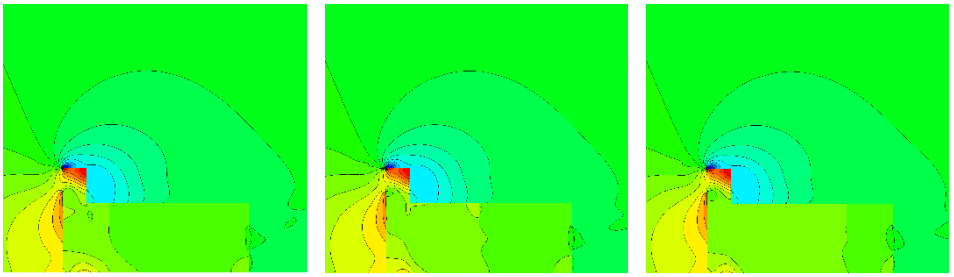 | | |

Table 7.2. Contours of pressure coefficient (-) on vertical plane 1 for wind incident angle 180

| plane | R1 | R2 | R3 |
|---|---|---|---|
| Cp (-) | 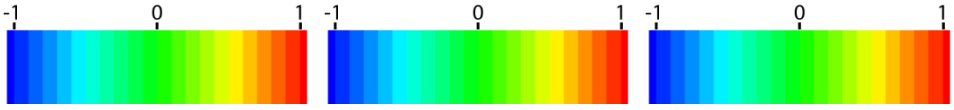  | | |
| 1 | 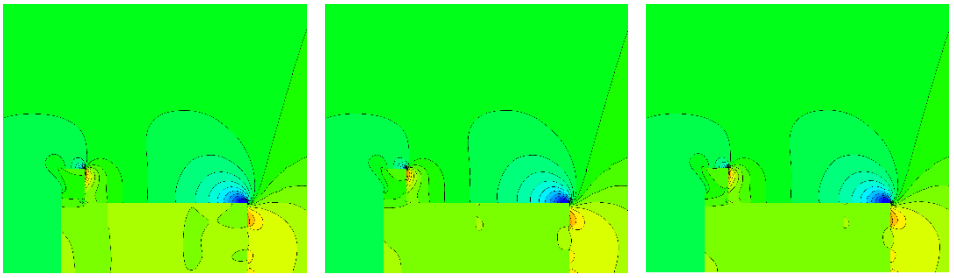 | | |

Looking at table 7.2, it is notable that the Cp variation is negligible comparing the R2 and R3 when the wind direction is 180, while the R1 has a higher Cp value. In fact, the average Cp in the volume of left side is 0.27, 0.28, and 0.28 in R1, R2, and R3 while on the right sides these figures are 0.31, 0.28, and 0.26 respectively.

What is furthermore noticeable in the graph of volume-average Cp (figure 7.5) is that while the Cp values on the left side are very close to each other in both wind directions, the Cp values on the right side are considerably lower in wind direction 0 compared to wind direction 180.

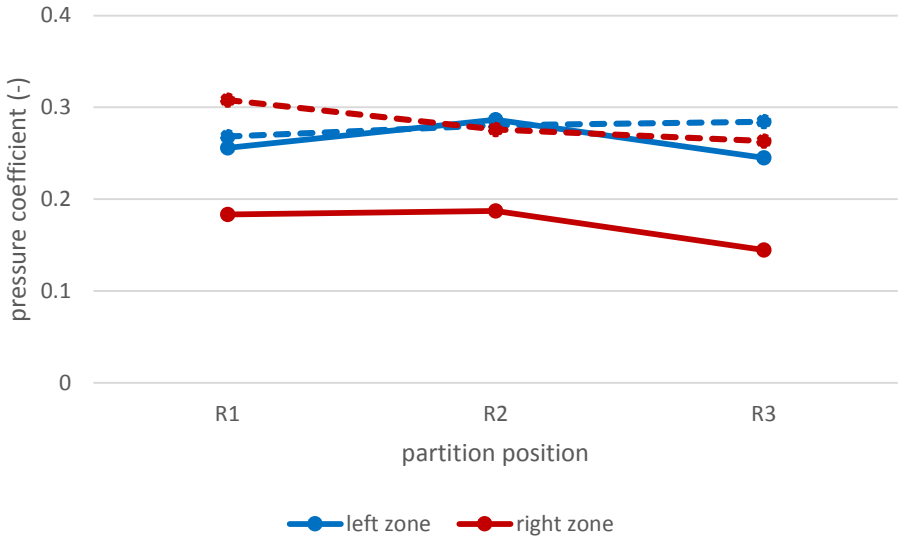


Figure 7.5. Volume-weighted average pressure coefficient (-) in each zone of the model for wind directions 0 (full line) and 180 (dashed line)

### 7.3.3 Velocity magnitude

The position of the internal partition seems to affect remarkably the distribution of the velocity magnitude in the room. As evident in table 7.3, when the wind blows perpendicularly to the wind tower aperture, the partition that is closer to the wind tower, R1, creates a high speed zone underneath the wind tower. In R1, after the air passes through the door, it is directed toward the ground and therefore, the major accumulation of the air velocity is lower than a height of 1 meter in the right side of the room. In fact, in R1, the left side of the room has an average velocity of 0.56 m/s while the air speed in the right side is 0.23 m/s (see figure 7.6). In R2 and R3 instead this condition is not seen. The jet of air is not influenced by the presence of the partition and the velocity is better spread in different parts of the room. The left and right side of the room have average wind speeds of 0.39 and 0.25 m/s in R2,

while in R3 these values are 0.33 and 0.29 m/s respectively (see figure 7.6). On plane 5 (table 7.2), the area-average velocity magnitude for the three wind towers are 0.52, 0.36, and 0.29 m/s in the left side of the room underneath the wind tower, while in the right side, these values are 0.14, 0.22, and 0.28 m/s in R1, R2 and R3 respectively (figure 7.6).

Table 7.3. Contours of velocity magnitude (m/s) on vertical plane 1 and horizontal plane 5 for wind incident angle 0

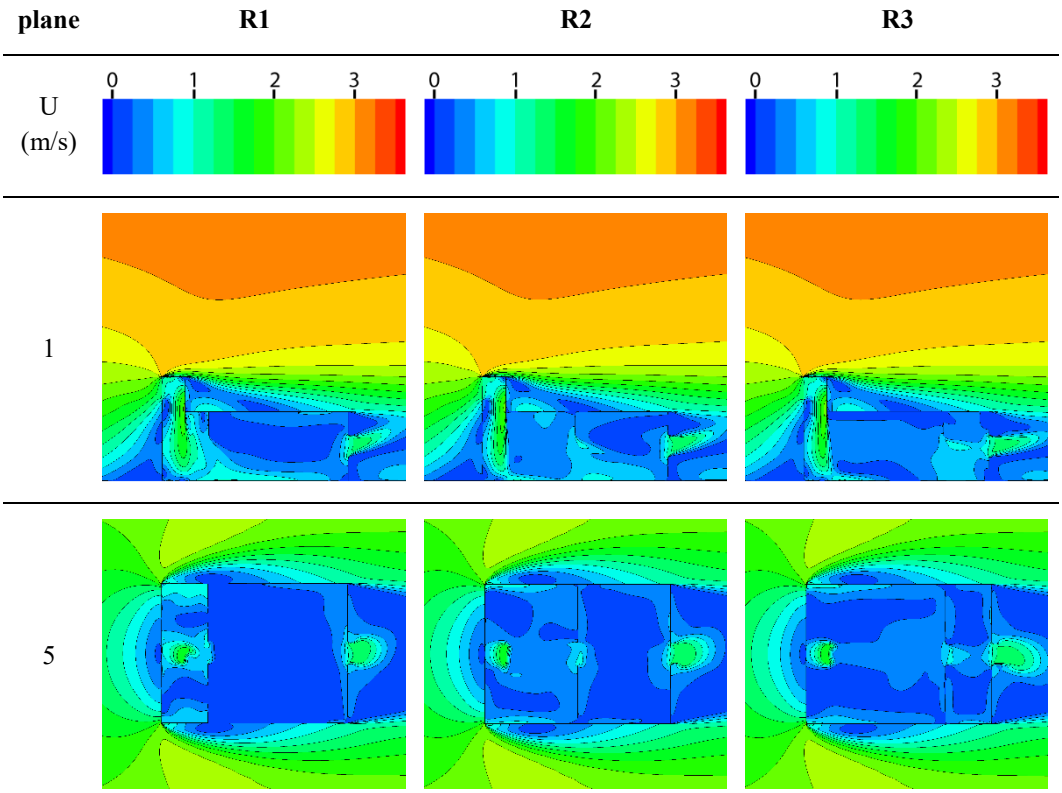


The contours of velocity in the three models for wind direction 180 are summarized in table 7.4. According to the table, R1 and R2 in which the internal partitions are more distant to the inlet aperture, which in this wind direction is the window, experience higher velocities in the room. In fact, the left side of the model R1 has the highest velocity of around 0.26 m/s as volume-average (figure 7.6). This figure on the left sides of the models R2 and R3 are 0.24 and 0.17 m/s respectively. On the right hand side, instead, R2 has a higher velocity of about 0.28 m/s compared to the R1 and R3 that both have a volume-average velocity of 0.21 m/s on this side. The area-average velocity figures on plane 5 representing a standing human on the left and right hand side of the room are respectively 0.25 and 0.24 m/s in R1, 0.23 and 0.32 m/s in R2, and 0.14 and 0.29 m/s in R3 model.

Table 7.4. Contours of velocity magnitude (m/s) on vertical plane 1 and horizontal plane 5 for wind incident angle 180

| plane | R1 | R2 | R3 |
|---|---|---|---|
| U (m/s) | 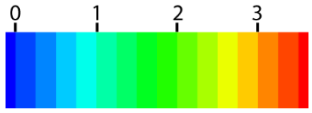 | 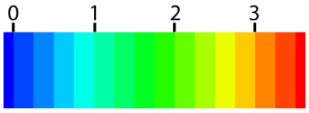 | 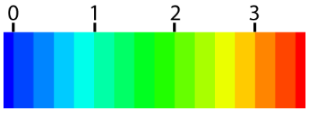 |
| 1 | 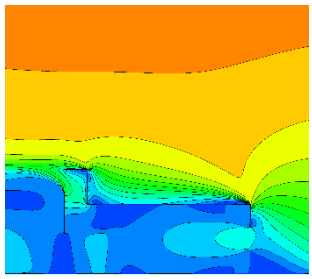 | 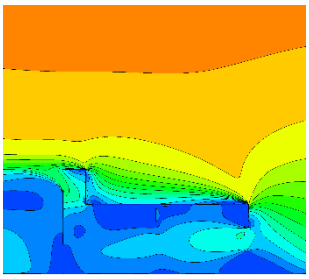 | 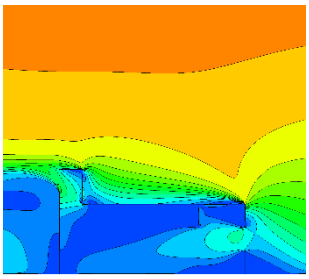 |
| 5 | 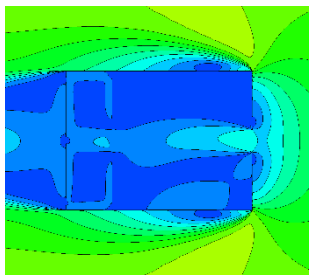 | 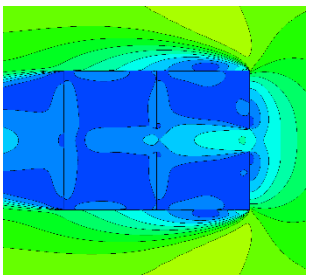 | 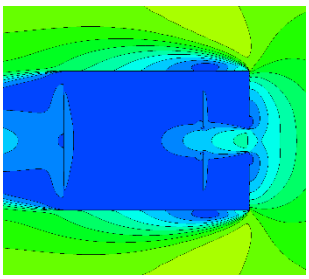 |

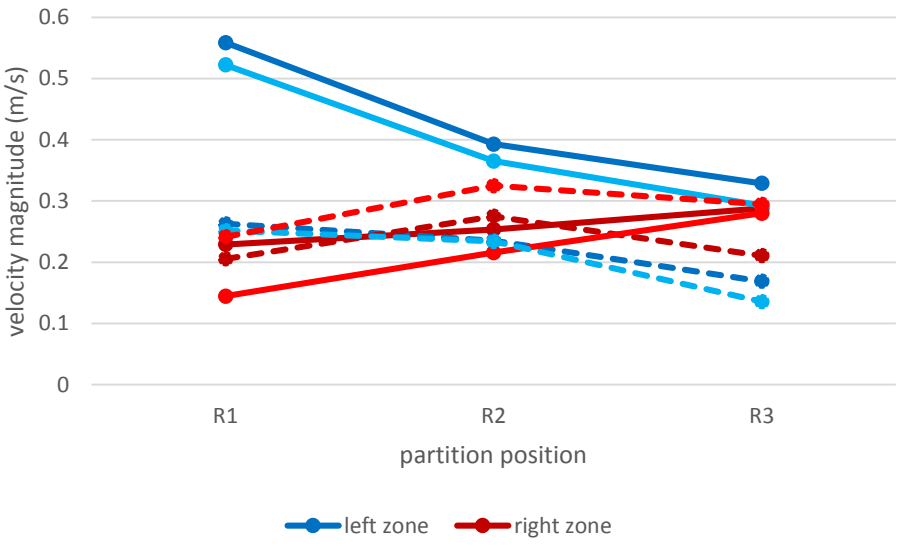


Figure 7.6. Volume-weighted (dark color) and area-weighted (light color) average velocity magnitude (m/s) in each zone of the model for wind directions 0 (full line) and 180 (dashed line)

Looking at the graph of volume-average and area-average velocity magnitude (figure 7.6), it is additionally notable that in wind direction 0 placing the internal partition closer to the window decreases the velocity magnitude in the left side and increases it on the right side. While, in wind direction 180 the trend is slightly different. In this wind direction, while placing the internal partition close to the window decreases the air velocity in the left side, but on the right side, the highest velocity is obtained with the middle position of the partition. Furthermore, it is also noticeable that the highest difference between the volume-average and area-average velocity figures happen always at the right side, in model R1 with wind direction 0, and in model R3 with wind direction 180.

### 7.3.4 Mean age of air

Table 7.5. Contours of mean age of air (s) on vertical plane 1 and horizontal plane 5 for wind incident angle 0

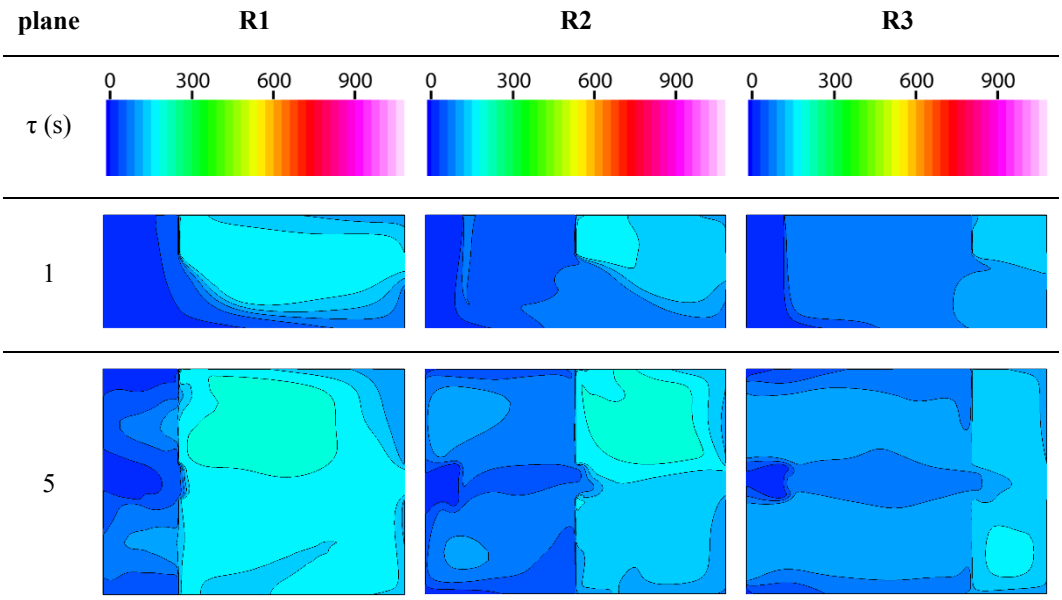


The air age contours are demonstrated in the two tables 7.5 and 7.6. As evident in table 7.5, the freshest air accumulation is obtained in the left side of the room in R1 model when the wind tower acts as an air supply. In this part of the room the volume average mean age of air is 44 seconds and for a standing person the area-average value stands at 55 seconds. Though, the close placement of the partition respect to the wind tower results in the right side of the room having the poorest freshness with volume- and area-average figures of 149 and 165 seconds

respectively. It is evident in the contours that a major portion of the right room side in R1 has an air age of between 150 and 180 seconds.

As the partition gets more distant from the wind tower, the freshness of the room decreases in the left side and increases in the right side of the room. The volume-average mean age of air values n R2 and R3 are 61 and 81 seconds on the left and 139 and 132 seconds on the right side of the room respectively. The area-average figures follow the same trend and are 68 and 90 seconds on the left and 150 and 136 seconds on the right side respectively in R2 and R3 models. However, quite interestingly, the maximum mean age of air value of the models R1 and R2 are both around 203 seconds, while this figure for R3 is 184.

Table 7.6. Contours of mean age of air (s) on vertical plane 1 and horizontal plane 5 for wind incident angle 180

| **plane** | **R1** | **R2** | **R3** |
|---|---|---|---|
| τ (s) | 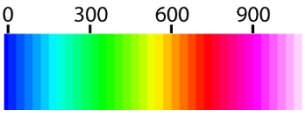 | 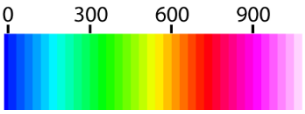 | 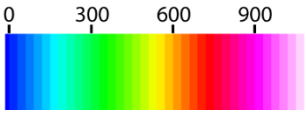 |
| 1 | 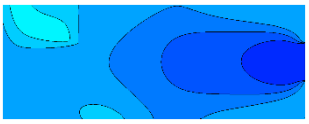 | 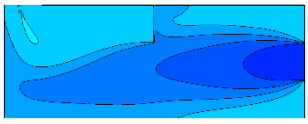 | 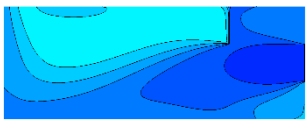 |
| 5 |  | 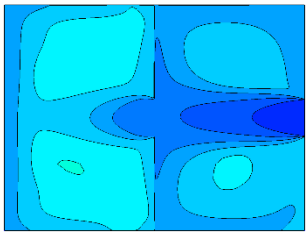 | 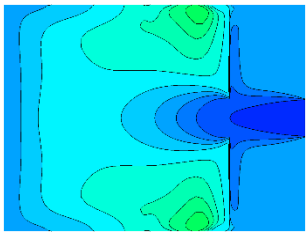 |

Comparing the mean age of air figures in wind incident angle 180 (table 7.6), it is notable that in R3 model, the left and right sides of the room experience very different air ages corresponding to 149 and 87 seconds respectively. In R2 and R1 the mean age of air volume-average figures are 137 and 144 on the left, and 117 and 121 seconds on the right side correspondingly.

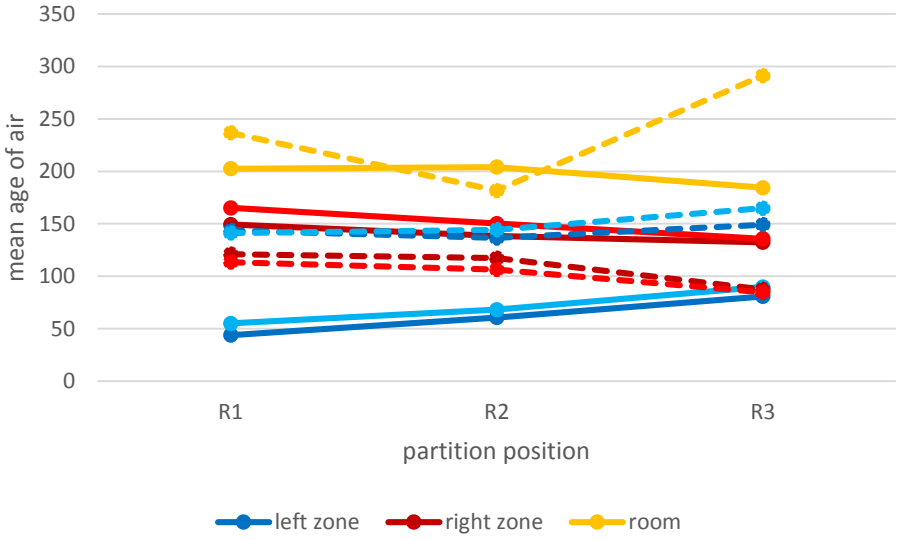


Figure 7.7. Volume-weighted (dark color) and area-weighted (light color) average mean age of air (s) in each zone of the model, and maximum mean age of air (s) in the room (yellow) for wind directions 0 (full line) and 180 (dashed line)

What is evident in the graph 7.7, the air freshness variation is less pronounced in the right part of the room when the wind direction is zero, and in the left part of the room when the wind direction is 180. The maximum mean age of air figures seem not to be very much affected by the internal partitions when the wind direction is zero, while in wind angle 180, the R3 model has a point in which the air age arrives to 291 seconds. The lowest maximum mean age of air value is seen in R2 at wind incident angle 180 with a value of 182 seconds.

## 7.4 Conclusion

Different placements of a partition with an empty door frame in its center was tested in the one-sided wind tower model T4 for wind incident angles 0 and 180 degrees. In wind angle zero, compared to the original T4 model in which no partition existed, the presence of the partitions has generally enhanced the velocity magnitude distribution especially in cases R2 and R3. In R1 the jet of air has better spread in the room compared to when there is no partition. Instead, in the right part of the room, where originally a low speed air movement was felt on the wind tower-window axis, after the placement of the partition, between the heights of 1 and 2 meters there is no air movement and all the major portion of the air speed is accumulated below the height of 1 m. Looking at the mean age of air contours in R1, it is notable how the freshness of air has deteriorated by placing the partition.

Contrarily in R3, the left side of the room underneath the wind tower has a fresher air compared to the model T4.

Looking at other indicators in wind incident angle 0, it is noticeable that the placement of partitions does not have a major impact on the volume flow rate values and the maximum difference between the volume flow rate in T4 and the same figure in R models is around 0.05 m3/s or 1.3 air change per hour. Interestingly, the volume-average velocity magnitude in the whole room, is only 0.1 m/s higher in R1 and around 0.03 m/s higher in R2 and R3. The volume-average mean age of air values are 8 and 14 seconds lower in R2 and R3 and 16 seconds higher in R1 compared to T4 model. And, the maximum mean age of air value in the whole room, in R1, R2 and R3 are 50, 52 and 32 seconds higher than the T4 model.

In wind direction 180, similar to wind direction 0, the closest partition to the inlet aperture which is the window has worsened the air velocity distribution compared to the original case T4. The partition in R3 model has inclined the airflow slightly toward to ground and has resulted in a reduction of air velocity felt by a standing person at a height of 170 cm. While, the R2 and R1 partitions have both helped in spreading the air velocity in the room. This is confirmed by the mean age of air contours, too. The near-window partition in R1, has deviated the fresh air toward to ground and compared to T4 has resulted in an even larger accumulation of air with an age of more than 150 seconds in the upper half of the room height. Furthermore, in R1, the left part of the room has a higher air age compared to model T4 with the worst air freshness accumulated on each side of the partition in the left part of the room.

Concerning other indicators in wind direction 180, it is observable that the volume flow rate values are similar with the highest difference seen in R1 model where the volume flow rate is 0.05 m3/s less than T4 model. The volume-average velocity figures are also similar to that in model T4 and the highest difference is experienced in R2 model in which the air speed is about 0.05 m/s higher than T4. The volume-average mean age of air in the whole room volume is lower for 33 seconds in R1 and R2 and 26 seconds in R3 model compared to T4. And finally, concerning the maximum mean age of air values, it is possible to understand that in T4 the least fresh point is 8 and 63 seconds staler than R1 and R2 respectively, while the stalest point in R3 is 46 seconds staler than T4 model.

To conclude, it is possible to state that dividing a room into two zones when a room is ventilated by a one-sided wind tower and a window can generally enhance the indoor air velocity and the distribution of the air freshness, with the condition that this internal divider is not placed close to the inlet apertures.

# Chapter 8

# Conclusion and recommendations

Wind towers are traditional architectural elements originated in Iran over 2000 years ago. They still exist in considerable numbers in historical parts of desert cities of Iran where the traditional architecture style was heavily influenced by the harsh climatic condition of those regions and so they now make up part of the architectural heritage of the country. Together with that particular and traditional style of architecture, wind towers have been eventually abandoned by the creation of new cities and the evolution of the living standards. Those big low density houses with several courtyards, seasonally occupied rooms, tall walls and narrow pedestrian alleyways in between this earth structures, were gradually substituted by an architecture that is now common almost all over the world, and consequently those bulky wind towers were replaced by different types of air conditioning devices which could more easily fit into the high rise buildings hosting a denser population.

Nevertheless, in modern times, wind towers are still occasionally constructed either as architectural features for ventilation or cooling purposes such as the wind towers in several buildings designed by Alan Short, or only as ornamental elements such as those in Doha University or those in Tehran's Museum of Contemporary Art reminding us of our roots. They are also built commercially, as installable products, by a handful of companies such as Monodraught ltd and Breathing Building ltd. and marketed in sustainable building industries especially in countries like UK where natural ventilation solutions can be more easily adopted because of the cool and windy weather. In spite of this occasional use, still not many architects and building engineers are convinced to employ such building component in their designs, perhaps on the one hand because of the difficulty of integrating it in modern especially high rise building designs, and on the other hand because not enough information is available about the efficiency of such component and its advantages compared to other more widespread natural ventilation devices such as windows are unknown.

However, it is important to note that obtaining a holistic conclusion about whether or not wind towers are effective ventilation/cooling elements in a real

building context, similar to researching the performance of any building with any ventilation system, is not an easy task because the variables in studying the real performance of such systems are many: from the larger scale parameters such as the ever-changing solar radiation, temperature and wind conditions, the specific geographical and topographical features, the surrounding urban morphology, and the amount of outdoor pollution, to the building scale variables such as the building dimension and geometry, building materials, the layout, the furniture, the indoor contamination sources, the number of occupants and the hours of occupancy among others, are all factors that could influence the effectiveness of a natural ventilation system such as a wind tower. For this reason, and considering the difficulty in obtaining reliable experimental data because of all the above-mentioned variabilities, the majority of the studies that have been done on the wind towers up until this moment consist of simplified modeling of room models out of any urban context, only aiming to obtain knowledge of the physics of the air flow.

Therefore, this study does not aim to justify the suitability of a wind tower as a natural ventilation component because that requires the inclusion of all other variables which at the end make the results very case-specific; this study rather aims to present a wind tower as a concept and an alternative way of providing airflow into a space. Thus, similar to the previous studies, this study has been done on a simplified model so that to remove the effect of all other variables affecting the air flowing in or out of the wind tower, thus making the results generalized enough to be applicable in different contexts.

For this purpose, through a thorough literature review, it has been highlighted that CFD is a proper tool for assessing natural ventilation problems using wind towers. In fact, CFD simulations validated by the experimental data obtained mainly from wind tunnel tests have been the most frequent methods in investigating wind towers. At a second step, the objective of each study, the wind tower characteristics such as its position, shape and number of openings, the wind information in each analysis were identified in order to find the gap in literature.

The objectives of the previous studies, regardless of the experimental, analytical or numerical research method employed, focus on several aspects: 1- understanding whether buoyancy or wind is the major force in providing more ventilation in buildings, 2- assessing the effect of various geometrical elements including wind tower's height, number of openings, internal partitions, shape of its walls or roof, and the addition of louvers and dampers, 3- investigating how the building configuration e.g. the building roof shape, the presence of other openings such as windows and their positions and sizes can alter the ventilation performance

of a wind tower, 4- evaluating the possibility of improving thermal behavior of wind towers by combining other passive techniques such as evaporative cooling, ground cooling, solar adsorption cooling, solar chimney, and heat transfer devices, and finally 5- weighing whether wind towers can be useful tools in urban scale issues e.g. for improving limited airflows in street canyons.

The wind towers in the literature were majorly three-dimensional structures coupled with a building and were either tall towers positioned next to the building connected to it through an outlet on the wall, or they were short structures positioned on the roof center or roof edge. Wind towers with different numbers of openings have been studied at various wind directions, but the most prevalent wind incident angle in previous studies was zero. Moreover, the utilization of atmospheric boundary layer wind has been limited to the more recent studies.

Even though the wind towers in the previous studies were placed in a variety of positions respect to the building, however, to date, there has been no study assessing how this variation in the position of a wind tower can alter its ventilation performance. This study, therefore, employs CFD and aiming to partly filling the gap in the literature, it evaluates how rooftop one-sided and four-sided wind towers with different positions may work differently at various wind directions. In this study the temperature effect has been ignored and the simulations have been performed in isothermal conditions.

Five groups of case studies and a total of 63 simulations have been done in this study consisting of: 21 simulations for three positions of a one-sided wind tower working with the room window at seven wind directions between 0 and 180, 21 simulations for three positions of a four-sided wind tower working with the room window at seven wind directions between 0 and 180, 11 simulations (excluding the symmetrical cases) for two positions of a four-sided wind tower working alone for wind directions between 0 and 180, 4 simulations (excluding the symmetrical cases) on a room that has no wind towers and is cross-ventilated using two windows for wind directions between 0 and 180 performed in order to understand in which conditions in terms of cross-ventilation wind towers can be preferred to windows as the simplest and most common means of providing cross-ventilation in a space, and finally 6 simulation for one position of the one-sided wind tower working with a room window at two wind directions 0 and 180 when there are three different partitions dividing the room into two zones.

The results of the simulations are assessed in terms of pressure coefficient, volume flow rate, velocity magnitude, mean age of air, and the ventilation effectiveness has been evaluated using the air change number as the most widely

used index in the standards and the air change efficiency index which ensures a rapid air exchange and is relevant at the design stage of a ventilation system where the placement and intensity of contaminant sources are unknown.

The findings of the thesis are summarised as follows.

- Obviously, the most important parameter that defines which case is superior respect to others, is the wind direction. The change in the wind incident angle hugely affects not only the performance of each case, but also the choice of the position of wind tower on the roof.
- Cross ventilation using two windows is different from cross ventilation using a one-sided wind tower-window combination and this difference is mainly in the distribution of the velocity and mean age of air in the room. Because the wind entering the building through a wind tower has a vertical form and thus in terms of velocity it does not distribute well in the room. In fact, when the wind direction is reversed and the wind tower starts acting as an exhaust aperture, the velocity distribution in the two cases becomes similar. The mean age of air values are however better spread in the case with wind tower. The only angle in which the case with windows perform substantially better than the case with one-sided wind tower is wind direction 60 which is close to the transition angle of the wind tower.
- In wind incident angle 90, cross-ventilation is not possible in a case that has only two windows. Therefore, for the spaces in which the orientation of the window on the façade is not favourable, keeping the window for daylight and adding a roof top wind tower, especially a four-sided one, could solve the cross-ventilation problem.
- Four-sided wind tower-window combination compared to one-sided wind tower-window combination and windows only show less variation by the change in wind direction. This is also valid for the four-sided wind towers working alone which show the least alteration compared to all other cases.
- The presence of the window in combination with a four-sided wind tower than can act both as inlet and outlet, improves its performance in terms of velocity and mean age of air, especially in wind directions between 0 and 90. While, in wind directions between 90 and 180, the volume flow rate values are majorly improved by the presence of the window as an air supply.

- The air change efficiency of one-sided wind tower-window combination is generally higher than the four-sided wind tower cases.
- The change in the position of the one-sided wind tower respect to the window has a bigger impact on its performance compared to the four-sided cases.
- In general, when the wind direction is between 0 and 90 and the one-sided wind tower is acting as an inlet, it should not be positioned on top of the window. This does not affect the volume flow rate through the wind tower but it reduces the velocity in the room and increases the air age which consequently decreases the air change efficiency. In wind directions between 90 and 180, when the window is the inlet, placing the one-sided wind tower at the farthest distance from the window induces the lowest air velocities, lowest volume flow rate, highest air age and consequently leads to the least efficiency compared to the other two wind tower positions.
- Considering the four-sided wind tower-window combination, in wind directions between 0 and 90, the wind tower that is placed on the centre of the roof induces slightly higher velocities, lower air ages and higher air change efficiencies. In wind direction 120, despite the induced velocities having the lowest values compared to the other two positions, the central wind tower still provides the freshest air and highest air change efficiency. While, in wind direction 150 and 180, the closer the wind tower is to the window, the better its performance is considering all indicators.
- It is possible to state that despite the different behaviours of the one-sided wind tower and four-sided wind tower when both are combined with a window, when the window is acting as the main air supply, placing either of the wind towers on top of the window is the best choice.
- Comparing the four-sided wind towers that provide cross-ventilation individually, it is notable that the change in the position of the wind tower does not affect its performance considerably. And in all wind direction, the wind tower that is placed closer to the windward edge of the roof has a better performance. Therefore, for the spaces where the windows are not operable and having an aperture on the façade is not possible, placing a four-sided wind tower with at least one of its aperture perpendicular to the wind, can guarantee an air change efficiency of around 50 per cent.

- Finally, the internal partitions in a cross-ventilated pace using a one-sided wind tower-window combination can enhance the indoor air velocity and the air freshness with the condition that this partition is not placed close to the inlet aperture.

Ideas for future projects are many. Some limitations were due to the assumptions in the thesis that could be addressed in the future as such is the inclusion of the temperature in the assessments. Using other indicators for evaluating the effectiveness of ventilation such as contaminant removal effectiveness index is recommended. Including the simulations at other wind incident angles, especially around transition angles for each case could be useful in order to better follow the pattern of the variation of each parameter. This could have been very helpful in understanding what really happens in a room with two windows when the wind direction is 90 degrees! Assessing the use of wind towers in more complicated layouts could be very beneficial and could better encourage the architecture community to consider the application of wind towers in buildings. Focusing on design issues related to the integration of wind towers' concept in several-story buildings and proposing some feasible ideas can be inspiring, too. Repeating similar projects within an urban context can better illustrate if and how wind towers can be advantageous to windows.

# References


Ahmadi, M., & Grosso, M. (2017). Potential cooling energy reduction by a wind tower model in Milan and Rome climate. In L. Brotas, S. Roaf, & F. Nicol (Eds.), *DESIGN TO THRIVE Proceedings of 33rd PLEA International Conference* (pp. 5206–5213). Edinburgh: NCEUB 2017.

Ahmadikia, H., Moradi, A., & Hojjati, M. (2012). Performance analysis of a wind-catcher with water spray. *International Journal of Green Energy*. https://doi.org/10.1080/15435075.2011.622019

Allard, F., & Ghiaus, C. (2006). Natural Ventilation in the Urban Environment. In M. Santamouris, & P. Wouters (Eds), *Building Ventilation: The State of the Art*. https://doi.org/10.4324/9781849770620

Ameer, S. A., Chaudhry, H. N., & Agha, A. (2016). Influence of roof topology on the air distribution and ventilation effectiveness of wind towers. *Energy and Buildings*. https://doi.org/10.1016/j.enbuild.2016.09.005

Anderson, J. (2009). Chapter 1- Basic Philosophy of CFD. In J. Wendt, *Computantional Fluid Dynamics: An Introduction* (3rd ed.). Rhose-Saint-Genese: Springer. https://doi.org/10.1007/978-3-540-85056-4

Ansys. (2009). Ansys fluent 12.0 Theory Guide. In *ANSYS Fluent*.

Arent, D. J., Tol, R. S. J., Faust, E., Hella, J. P., Kumar, S., Strzepek, K. M., … Ngeh, J. (2015). Key economic sectors and services. In *Climate Change 2014 Impacts, Adaptation and Vulnerability: Part A: Global and Sectoral Aspects*. https://doi.org/10.1017/CBO9781107415379.015

ASCE. (1996). Wind-tunnel studies of buildings and structures. *Journal of Aerospace Engineering.* https://doi.org/10.1061/(ASCE)0893-1321(1996)9:1(19)

Asfour, O., & Gadi, M. (2006). Effect of Integrating Wind Catchers with Curved Roofs on Natural Ventilation Performance in Buildings. *Architectural*

*Engineering And Design Management*, *2*(4), 289-304. https://doi.org/10.1080/17452007.2006.9684623

Attia, S., & Carlucci, S. (2015). Impact of different thermal comfort models on zero energy residential buildings in hot climate. *Energy and Buildings*. https://doi.org/10.1016/j.enbuild.2015.05.017

Awbi, H. B., & Elmualim, A. A. (2002). Full scale model windcatcher performance evaluation using a wind tunnel. In *Proceedings of the World Renewable Energy Congress VII*.

Bahadori, M. N., Mazidi, M., & Dehghani, A. R. (2008). Experimental investigation of new designs of wind towers. *Renewable Energy*. https://doi.org/10.1016/j.renene.2007.12.018

Bahadori, M. N. (1994). Viability of wind towers in achieving summer comfort in the hot arid regions of the middle east. *Renewable Energy*. https://doi.org/10.1016/0960-1481(94)90108-2

Bahadori, Mehdi N., Dehghani, A., & Sayigh, A. (2014). Wind towers: Architecture, climate and sustainability. In *Wind Towers: Architecture, Climate and Sustainability*. https://doi.org/10.1007/978-3-319-05876-4

Belarbi, R., Ghiaus, C., & Allard, F. (2006). Modeling of water spray evaporation: Application to passive cooling of buildings. *Solar Energy*. https://doi.org/10.1016/j.solener.2006.01.004

Ben-David, T., & Waring, M. S. (2016). Impact of natural versus mechanical ventilation on simulated indoor air quality and energy consumption in offices in fourteen U.S. cities. *Building and Environment*. https://doi.org/10.1016/j.buildenv.2016.05.007

Benkari, N., Fazil, I., & Husain, A. (2017). Design and performance comparison of two patterns of wind-catcher for a semi-enclosed courtyard. *International Journal of Mechanical Engineering and Robotics Research*. https://doi.org/10.18178/ijmerr.6.5.396-400

Blocken, B., Stathopoulos, T., & Carmeliet, J. (2007). CFD simulation of the atmospheric boundary layer: wall function problems. *Atmospheric Environment*. https://doi.org/10.1016/j.atmosenv.2006.08.019

Bolouhari, S. (2017). *Learning from the past in Today's Architectural Design Case Study: Architecture in hot and arid zone of Yazd in central Iran* (Ph.D.). Sapienza University of Rome

Bouchahm, Y., Bourbia, F., & Belhamri, A. (2011). Performance analysis and improvement of the use of wind tower in hot dry climate. *Renewable Energy*. https://doi.org/10.1016/j.renene.2010.08.030

Bowman, N., Lomas, K., Cook, M., Eppel, H., Ford, B., Hewitt, M., … Belarbi, R. (1997). Application of Passive Downdraught Evaporative Cooling (PDEC) to non-domestic buildings. *Renewable Energy*. https://doi.org/10.1016/0960-1481(96)00062-6

British Standards Institution (1991). Code of practice for ventilation principles and designing for natural ventilation. In *Bs 5925*. London: BSI

Building Research Establishment (1994). Natural Ventilation in Non-Domestic Buildings. *BRE Digest.* Garston: BRE

Calautit, J. K., & Hughes, B. R. (2014a). Measurement and prediction of the indoor airflow in a room ventilated with a commercial wind tower. *Energy and Buildings*. https://doi.org/10.1016/j.enbuild.2014.08.015

Calautit, J. K., & Hughes, B. R. (2014b). Wind tunnel and CFD study of the natural ventilation performance of a commercial multi-directional wind tower. *Building and Environment*. https://doi.org/10.1016/j.buildenv.2014.05.022

Calautit, J. K., & Hughes, B. R. (2016). A passive cooling wind catcher with heat pipe technology: CFD, wind tunnel and field-test analysis. *Applied Energy*. https://doi.org/10.1016/j.apenergy.2015.10.045

Calautit, J. K., Hughes, B. R., & Shahzad, S. S. (2015). CFD and Wind Tunnel Study of the Performance of a Uni-Directional Wind Catcher with Heat Transfer Devices. *Renewable Energy*. https://doi.org/10.1016/j.renene.2015.04.005

Calautit, J. K., O'Connor, D., & Hughes, B. R. (2014). Determining the optimum spacing and arrangement for commercial wind towers for ventilation performance. *Building and Environment*. https://doi.org/10.1016/j.buildenv.2014.08.024

Calautit, J. K., O'Connor, D., & Hughes, B. R. (2016). A natural ventilation wind tower with heat pipe heat recovery for cold climates. *Renewable Energy*. https://doi.org/10.1016/j.renene.2015.08.026

Campos-Arriaga, L. (2009). *Wind energy in the built environment: a design analysis using CFD and wind tunnel modelling approach* (Ph.D.). University of Nottingham.

Carlucci, S., Bai, L., de Dear, R., & Yang, L. (2018). Review of adaptive thermal comfort models in built environmental regulatory documents. *Building and Environment*, 73-89. https://doi.org/10.1016/j.buildenv.2018.03.053

Chen, Q. (2009). Ventilation performance prediction for buildings: A method overview and recent applications. *Building and Environment*. https://doi.org/10.1016/j.buildenv.2008.05.025

Chew, L. W., Nazarian, N., & Norford, L. (2017). Pedestrian-level urban wind flow enhancement with wind catchers. *Atmosphere*. https://doi.org/10.3390/atmos8090159

Chiesa, G., & Grosso, M. (2016). Breakthrough of natural and hybrid ventilative cooling technologies: models and simulations. *International Journal of Ventilation*. https://doi.org/10.1080/14733315.2016.1220701

Cruz-Salas, M. V., Castillo, J. A., & Huelsz, G. (2014). Experimental study on natural ventilation of a room with a windward window and different windexchangers. *Energy and Buildings*. https://doi.org/10.1016/j.enbuild.2014.08.033

De Dear, R. J., Brager, G. S. & Cooper D. J. (1997). Developing an adaptive model of thermal comfort and preference - Final Report on ASHRAE RP-884. *ASHRAE Transactions*. Sydney: MRL.

Dehghan, A. A., Kazemi Esfeh, M., & Manshadi, M. D. (2013). Natural ventilation characteristics of one-sided wind catchers: Experimental and analytical evaluation. *Energy and Buildings*. https://doi.org/10.1016/j.enbuild.2013.02.048

Dehghani Mohamadabadi, H., Dehghan, A. A., Ghanbaran, A. H., Movahedi, A., & Dehghani Mohamadabadi, A. (2018). Numerical and experimental performance analysis of a four-sided wind tower adjoining parlor and courtyard at different wind incident angles. *Energy and Buildings*. https://doi.org/10.1016/j.enbuild.2018.05.006

Elmualim, A. A. (2006a). Dynamic modelling of a wind catcher/tower turret for natural ventilation. *Building Services Engineering Research and Technology*. https://doi.org/10.1191/0143624406bse159oa

Elmualim, A. A. (2006b). Effect of damper and heat source on wind catcher natural ventilation performance. *Energy and Buildings*. https://doi.org/10.1016/j.enbuild.2005.11.004

Elmualim, A. A. (2006c). Verification of design calculations of a wind catcher/tower natural ventilation system with performance testing in a real building. *International Journal of Ventilation*. https://doi.org/10.1080/14733315.2005.11683717

Elmualim, A. A., & Awbi, H. B. (2002). Wind Tunnel and CFD Investigation of the Performance of "Windcatcher" Ventilation Systems. *International Journal of Ventilation*. https://doi.org/10.1080/14733315.2002.11683622

Elmualim, A. A., & Awbi, H. B. (2003). Post occupancy evaluation of a building employing windcatchers for summer ventilation. *Facilities*. https://doi.org/10.1108/02632770310507980

Fanger, P. O. (1970). *Thermal comfort*. Analysis and applications in environmental engineering. Mc Graw-Hill.

Ferziger, J. H., & Perić, M. (2002). Turbulent Flows. In *Computational methods for fluid dynamics* (3rd ed.). Berlin: Springer.

Ferziger, J. H., & Perić, M. (2002). Introduction to numerical methods. In *Computational methods for fluid dynamics* (3rd ed.). Berlin: Springer.

Ford, B., Patel, N., Zaveri, P., & Hewitt, M. (1998). Cooling without air conditioning: The Torrent Research Centre, Ahmedabad, India. *Renewable Energy*. https://doi.org/10.1016/S0960-1481(98)00150-5

Fountain, M. and Huizenga, C. (1997). A thermal sensation prediction software tool for use by the profession. *ASHRAE Transations 1997, Vol 103, Part 2*, Piedmont, California, USA.

Franke, J., Hellsten, A., Schlünzen, H., & Carissimo, B. (2007). Best practice guideline for the CFD simulation of flows in the urban environment. In *COST action*.

Ghadiri, M. H., Lukman, N., Ibrahim, N., & Mohamed, M. F. (2013). Computational analysis of wind-driven natural ventilation in a two sided rectangular wind catcher. *International Journal of Ventilation*. https://doi.org/10.1080/14733315.2013.11684002

Ghadiri, M. H., Ibrahim, N. L. N., & Dehnavi, M. (2011). The effect of tower height in square plan wind catcher on its thermal behavior. *Australian Journal of Basic and Applied Sciences*.

Ghadiri, M. H., Ibrahim, N. L. N., & Mohamed, M. F. (2013). Performance evaluation of four-sided square wind catchers with different geometries by

numerical method. *Engineering Journal*. https://doi.org/10.4186/ej.2013.17.4.9

Ghadiri, M. H., Lukman, N., & Mohamed, M. F. (2014). Applying computational fluid dynamic to evaluate the performance of four-sided rectangular wind catcher with different height. *Research Journal of Applied Sciences, Engineering and Technology*. https://doi.org/10.19026/rjaset.7.282

Ghobadian, V. (2009). *Sustainable traditional buildings of Iran, a climatic analysis*. Tehran: Islamic Azad University.

Grignon-Massé, L., Adnot, J., & Rivière, P. (2008). Towards Adaptive PMV/PPD Indices for European Climates. In *Scaling up: building tomorrow's solutions - Proceedings from the ACEEE 2008 Summer Study on Energy Efficiency in Buildings*. Pacific Grove CA: American Council for an Energy-Efficient Economy.

Grosso, M., Raimondo, L., Colombaro, L., & Deganutti, A. (2011). *SPERAVent – Programma di simulazione online per il calcolo della riduzione potenziale del fabbisogno di raffrescamento di un eificio da ventilazione naturale controllata* [Online simulation programme for calculating the potential reduction of cooling energy needs in a building due to controlled natural ventilation]; *User Manual*. Turin: Department of Science and Environmental Technology, Polytechnic University of Turin.

Grosso, M., & Ahmadi, M. (2016). Potential cooling energy reduction by a one-channel wind tower: case study modelling in south-Mediterranean climate. *International Journal of Ventilation*. https://doi.org/10.1080/14733315.2016.1214397

Haghighi, A. P., Pakdel, S. H., & Jafari, A. (2016). A study of a wind catcher assisted adsorption cooling channel for natural cooling of a 2-storey building. *Energy*. https://doi.org/10.1016/j.energy.2016.02.033

Haghighi, A. P., & Mohabbati, S. (2017). Performance analysis of wind catcher integrated with shower cooling system to meet thermal comfort conditions in buildings. *Journal Of Cleaner Production*, *148*, 452-466. doi: 10.1016/j.jclepro.2017.01.160

Halbe, R. (2007). *141 Housing in Carabanchel* [Image]. Retrieved from https://rolandhalbe.eu/portfolio/141-housing-by-morphosis-bdu/

Heidari, A., Sahebzadeh, S., & Dalvand, Z. (2017). Natural ventilation in vernacular architecture of Sistan, Iran; Classification and CFD study of

compound rooms. *Sustainability (Switzerland)*. https://doi.org/10.3390/su9061048

Heiselberg, P. (2004). Natural Ventilation Design. *International Journal of Ventilation*. https://doi.org/10.1080/14733315.2004.11683674

*Hodud al-Alam*. (1983). Tehran: Tahouri.

Hoffmann, K. A., Chiang, S. T. (2000). Chapter 7- Scalar Representation of the Navier-Stokes Equations. In *Computational Fluid Dynamics Volume I* (4th ed.). Wichita, KS, USA: Engineering Education System

Hosseini, S. H., Shokry, E., Ahmadian Hosseini, A. J., Ahmadi, G., & Calautit, J. K. (2016). Evaluation of airflow and thermal comfort in buildings ventilated with wind catchers: Simulation of conditions in Yazd City, Iran. *Energy for Sustainable Development*. https://doi.org/10.1016/j.esd.2016.09.005

Hosseinnia, S. M., Saffari, H., & Abdous, M. A. (2013). Effects of different internal designs of traditional wind towers on their thermal behavior. *Energy and Buildings*. https://doi.org/10.1016/j.enbuild.2012.10.058

Hughes, B. R., & Abdul Ghani, S. A. A. (2009). A numerical investigation into the effect of windvent dampers on operating conditions. *Building and Environment*. https://doi.org/10.1016/j.buildenv.2008.02.012

Hughes, B. R., Calautit, J. K., & Ghani, S. A. (2012). The development of commercial wind towers for natural ventilation: A review. *Applied Energy*. https://doi.org/10.1016/j.apenergy.2011.11.066

Hughes, B. R., & Ghani, S. A. A. A. (2010). A numerical investigation into the effect of Windvent louvre external angle on passive stack ventilation performance. *Building and Environment*. https://doi.org/10.1016/j.buildenv.2009.10.010

Hughes, B. R., & Mak, C. M. (2011). A study of wind and buoyancy driven flows through commercial wind towers. *Energy and Buildings*. https://doi.org/10.1016/j.enbuild.2011.03.022

International Energy Agency. (2013). World Energy Outlook: Executive Summary. *Paris: International Energy Agency*. https://doi.org/92-64-20131-9

Irving, S., Ford, B., & Etheridge, D. (2005). Natural ventilation in non-domestic buildings. *CIBSE Applications Manual AM10*.

Jomehzadeh, F., Nejat, P., Calautit, J. K., Yusof, M. B. M., Zaki, S. A., Hughes, B. R., & Yazid, M. N. A. W. M. (2017). A review on windcatcher for passive

cooling and natural ventilation in buildings, Part 1: Indoor air quality and thermal comfort assessment. *Renewable and Sustainable Energy Reviews*. https://doi.org/10.1016/j.rser.2016.11.254

Jones, W., & Launder, B. (1972). The prediction of laminarization with a two-equation model of turbulence. *International Journal of Heat and Mass Transfer*, *15*(2), 301-314. https://doi.org/10.1016/0017-9310(72)90076-2

Kalantar, V. (2009). Numerical simulation of cooling performance of wind tower (Baud-Geer) in hot and arid region. *Renewable Energy*. https://doi.org/10.1016/j.renene.2008.03.007

Kamal, M. A. (2012). An Overview of Passive Cooling Techniques in Buildings: Design Concepts and Architectural Interventions. *Civil Engineering & Architecture*.

Kang, D., & Strand, R. K. (2013). Modeling of simultaneous heat and mass transfer within passive down-draft evaporative cooling (PDEC) towers with spray in FLUENT. *Energy and Buildings*. https://doi.org/10.1016/j.enbuild.2013.02.039

Karava, P. (2008). *Airflow prediction in buildings for natural ventilation design: wind tunnel measurements and simulation* (Ph.D.). Concordia University.

Kazemi Esfeh, M., Dehghan, A. A., Manshadi, M. D., & Mohagheghian, S. (2012). Visualized flow structure around and inside of one-sided wind-catchers. *Energy and Buildings*. https://doi.org/10.1016/j.enbuild.2012.09.015

Klein, O., & Schlenger, J. (2008). Ventilation systems. In *Basics Room Conditioning* (1st ed.). Basel: Birkhauser Architecture.

Kirk, S., & Kolokotroni, M. (2004). Windcatchers in Modern UK Buildings: Experimental Study. *International Journal of Ventilation*. https://doi.org/10.1080/14733315.2004.11683904

Kobayashi, T., Chikamoto, T., & Osada, K. (2013). Evaluation of ventilation performance of monitor roof in residential area based on simplified estimation and CFD analysis. *Building and Environment*. https://doi.org/10.1016/j.buildenv.2013.01.018

Kool, R., Jørgensen, B., Greisberger, H., & Kurosawa, A. (2016). *Workshop on Space Cooling Summary Report*. Paris: IEA-EGRD. Retrieved from http://www.ieadsm.org/wp/files/EGRD_Workshop-on-Space-Cooling-final2.pdf

Larsen, T. S. (2006) *Natural Ventilation Driven by Wind and Temperature Difference* (Ph.D.) Aalborg University.

Launder, B. E., & Spalding, D. B. (1974). The numerical computation of turbulent flows. *Computer Methods in Applied Mechanics and Engineering, 3*(2), 269-289. https://doi.org/10.1016/0045-7825(74)90029-2

Li, L., & Mak, C. M. (2007). The assessment of the performance of a windcatcher system using computational fluid dynamics. *Building and Environment*. https://doi.org/10.1016/j.buildenv.2005.12.015

Linden, W. Van Der, Loomans, M., & Hensen, J. (2008). Adaptive thermal comfort explained by PMV. In Strom-Tejsen, P., Olesen, B. W., Wargocki, P., Zukowska, D., & Toftum, J. (Eds.) *Indoor Air 2008: Proceedings of the 11th International Conference on Indoor Air Quality and Climate*. Copenhagen: International Center for Indoor Environment and Energy, Technical University of Denmark.

Liu, S., Mak, C. M., & Niu, J. L. (2011). Numerical evaluation of louver configuration and ventilation strategies for the windcatcher system. *Building and Environment*. https://doi.org/10.1016/j.buildenv.2011.01.025

Loonen, R. C. G. M., Singaravel, S., Trčka, M., Cóstola, D., & Hensen, J. L. M. (2014). Simulation-based support for product development of innovative building envelope components. *Automation in Construction*. https://doi.org/10.1016/j.autcon.2014.05.008

Lucon, O., Ürge-Vorsatz, D., Zain Ahmed, A., Akbari, H., Bertoldi, P., Cabeza, L. F., … Vilariño, M. V. (2014). 2014: Buildings. *Climate Change 2014: Mitigation of Climate Change. Contribution of Working Group III to the Fifth Assessment Report of the Intergovernmental Panel on Climate Change*. https://doi.org/10.2753/JES1097-203X330403

Mahdavinejad, M., & Javanroodi, K. (2014). Natural ventilation performance of ancient wind catchers, an experimental and analytical study - Case studies: One-sided, two-sided and four-sided wind catchers. *International Journal of Energy Technology and Policy*. https://doi.org/10.1504/IJETP.2014.065036

Mahyari, A. (1996) *The Wind Catcher: A Passive Cooling Device for Hot Arid Climate* (Ph.D.). Sydney University.

Memarian, G.H. (1993). *Architecture of Yazd public cisterns* (in Farsi). Tehran: Iran University of Science and Technology.

Monodraught Ltd. (2019). *Windcatcher Classic* [Image]. Retrieved from https://www.monodraught.com/products/natural-ventilation/windcatcher-classic

Montazeri, H. , & Azizian, R. (2008). Experimental study on natural ventilation performance of one-sided wind catcher. *Building and Environment*. https://doi.org/10.1016/j.buildenv.2010.07.031

Montazeri, H., & Azizian, R. (2009). Experimental study on natural ventilation performance of a two-sided wind catcher. *Proceedings of the Institution of Mechanical Engineers, Part A: Journal of Power and Energy*. https://doi.org/10.1243/09576509JPE651

Montazeri, H. (2011). Experimental and numerical study on natural ventilation performance of various multi-opening wind catchers. *Building and Environment*. https://doi.org/10.1016/j.buildenv.2010.07.031

Montazeri, H., & Montazeri, F. (2018). CFD simulation of cross-ventilation in buildings using rooftop wind-catchers: Impact of outlet openings. *Renewable Energy*. https://doi.org/10.1016/j.renene.2017.11.032

Moujalled, B., Cantin, R., & Guarracino, G. (2008). Comparison of thermal comfort algorithms in naturally ventilated office buildings. *Energy and Buildings*. https://doi.org/10.1016/j.enbuild.2008.06.014

Mundt, E. (Ed.), Mathisen, H., Nielsen, P., & Moser, A. (2004). *Ventilation effectiveness*. Brussels: Rehva.

Nejat, P., Calautit, J. K., Majid, M. Z. A., Hughes, B. R., Zeynali, I., & Jomehzadeh, F. (2016). Evaluation of a two-sided windcatcher integrated with wing wall (as a new design) and comparison with a conventional windcatcher. *Energy and Buildings*. https://doi.org/10.1016/j.enbuild.2016.05.025

Nouanégué, H. F., Alandji, L. R., & Bilgen, E. (2008). Numerical study of solar-wind tower systems for ventilation of dwellings. *Renewable Energy*. https://doi.org/10.1016/j.renene.2007.03.001

Novoselac, A., & Srebric, J. (2003). Comparison of air exchange efficiency and contaminant removal effectiveness as IAQ indices. *ASHRAE Transactions*.

O'Connor, D., Calautit, J. K., & Hughes, B. R. (2014). A study of passive ventilation integrated with heat recovery. *Energy and Buildings*. https://doi.org/10.1016/j.enbuild.2014.05.050

Orme, M. (1999) *Applicable Models for Air Infilteration and Ventilation Calculations*, Technical Note 51, AIVC, Brussels

Perén, J. I., van Hooff, T., Leite, B. C. C., & Blocken, B. (2015). CFD analysis of cross-ventilation of a generic isolated building with asymmetric opening positions: Impact of roof angle and opening location. *Building and Environment*. https://doi.org/10.1016/j.buildenv.2014.12.007

Persily, A. K. (1985) *Ventilation effectiveness in mechanically ventilated office buildings (NBSIR 85-3208)* Gaithersburg: US Department of Commerce, National Bureau of Standards.

Poshtiri, A. H., & Mohabbati, S. M. (2017). Performance analysis of wind catcher integrated with shower cooling system to meet thermal comfort conditions in buildings. *Journal of Cleaner Production*. https://doi.org/10.1016/j.jclepro.2017.01.160

Ramponi, R., & Blocken, B. (2012). CFD simulation of cross-ventilation for a generic isolated building: Impact of computational parameters. *Building and Environment*. https://doi.org/10.1016/j.buildenv.2012.01.004

Ramponi, R. (2014) *Computational modeling of urban wind flow and natural ventilation potential of buildings* (Ph.D.). Eindhoven University of Technology.

Reyes, V. A., Moya, S. L., Morales, J. M., & Sierra-Espinosa, F. Z. (2013). A study of air flow and heat transfer in building-wind tower passive cooling systems applied to arid and semi-arid regions of Mexico. *Energy and Buildings*. https://doi.org/10.1016/j.enbuild.2013.07.032

Rezaeian, M., Montazeri, H., & Loonen, R. C. G. M. (2017). Science foresight using life-cycle analysis, text mining and clustering: A case study on natural ventilation. *Technological Forecasting and Social Change*. https://doi.org/10.1016/j.techfore.2017.02.027

Saadatian, O., Haw, L. C., Sopian, K., & Sulaiman, M. Y. (2012). Review of windcatcher technologies. *Renewable and Sustainable Energy Reviews*. https://doi.org/10.1016/j.rser.2011.11.037

Sadeghi, H., & Kalantar, V. (2018). Performance analysis of a wind tower in combination with an underground channel. *Sustainable Cities and Society*. https://doi.org/10.1016/j.scs.2017.12.002

Saffari, H., & Hosseinnia, S. M. (2009). Two-phase Euler-Lagrange CFD simulation of evaporative cooling in a Wind Tower. *Energy and Buildings*. https://doi.org/10.1016/j.enbuild.2009.05.006

Sandberg, M. (1981). What is ventilation efficiency? *Building and Environment*. https://doi.org/10.1016/0360-1323(81)90028-7

Schlichting, H. (1937). Experimental Investigation of the Problem of Surface Roughness. *NACA Techinical Memorandums*.

Sert, C. (n.d.) Governing Equations of Fluid Flow and Heat Transfer. *ME 582 Finite Element Analysis in Thermofluids*. Lecture, Middle East Technical University, Department of Mechanical Engineering.

Shahzad, S., Brennan, J., Theodossopuolos, D., Calautit, J. K., & Hughes, B. R. (2018). Does a neutral thermal sensation determine thermal comfort? *Building Service Engineering*. https://doi.org/10.1177/0143624418754498

Shih, T. H., Liou, W. W., Shabbir, A., Yang, Z., & Zhu, J. (1995). A new k-ε{lunate} eddy viscosity model for high reynolds number turbulent flows. *Computers and Fluids*. https://doi.org/10.1016/0045-7930(94)00032-T

Soutullo, S., Olmedo, R., Sánchez, M. N., & Heras, M. R. (2011). Thermal conditioning for urban outdoor spaces through the use of evaporative wind towers. *Building and Environment*. https://doi.org/10.1016/j.buildenv.2011.06.003

Soutullo, S., Sanjuan, C., & Heras, M. R. (2012). Energy performance evaluation of an evaporative wind tower. *Solar Energy*. https://doi.org/10.1016/j.solener.2012.02.001

Spentzou, E., Cook, M. J., & Emmitt, S. (2019). Modelling natural ventilation for summer thermal comfort in Mediterranean dwellings. *International Journal of Ventilation*. https://doi.org/10.1080/14733315.2017.1302658

Spiru, P., & Simona, P. L. (2017). A review on interactions between energy performance of the buildings, outdoor air pollution and the indoor air quality. *Energy Procedia*. https://doi.org/10.1016/j.egypro.2017.09.039

Su, Y., Riffat, S. B., Lin, Y. L., & Khan, N. (2008). Experimental and CFD study of ventilation flow rate of a Monodraught™ windcatcher. *Energy and Buildings*. https://doi.org/10.1016/j.enbuild.2007.10.001

Teodosiu, C., Ilie, V., & Teodosiu, R. (2015). Appropriate CFD Turbulence Model for Improving Indoor Air Quality of Ventilated Spaces. *Mathematical Modelling in Civil Engineering*. https://doi.org/10.2478/mmce-2014-0020

Tominaga, Y., Mochida, A., Yoshie, R., Kataoka, H., Nozu, T., Yoshikawa, M., & Shirasawa, T. (2008). AIJ guidelines for practical applications of CFD to pedestrian wind environment around buildings. *Journal of Wind Engineering and Industrial Aerodynamics*. https://doi.org/10.1016/j.jweia.2008.02.058

Vaziri, A., & Bastani Parizi, M. (Ed.) (2006). *Tarikh-e Kerman* (6th ed.) (In Farsi). Tehran: Elm.

Versteeg, H., & Malalasekera, W. (2007). *An introduction to computational fluid dynamics The Finite Volume Method* (2nd ed.). Essex, England: Pearson Education Ltd.

Villafruela, J. M., Castro, F., San José, J. F., & Saint-Martin, J. (2013). Comparison of air change efficiency, contaminant removal effectiveness and infection risk as IAQ indices in isolation rooms. *Energy and Buildings*. https://doi.org/10.1016/j.enbuild.2012.10.053

Walker, C. E. (2006). *Methodology for the Evaluation of Natural Ventilation in Buildings Usng a Reduced-Scale Air Model* (Ph.D.). Massachusetts Institute of Technology.

Yakhot, V., Orszag, S., Thangam, S., Gatski, T., & Speziale, C. (1992). Development of turbulence models for shear flows by a double expansion technique. *Physics Of Fluids A: Fluid Dynamics*, *4*(7), 1510-1520. https://doi.org/10.1063/1.858424

Yocom, J. E. (1982) Indoor-Outdoor Air Quality Relationships A Critical Review. *Journal of the Air Pollution Control Association*. https://doi.org/10.1080/00022470.1982.1046542

Zhang, X., Chen, B., & Fan, X. (2015). Different Fuel Types and Heating Approaches Impact on the Indoor Air Quality of Rural Houses in Northern China. *Procedia Engineering*. https://doi.org/10.1016/j.proeng.2015.08.1097

Zomarshidi, H. (1995). *Iranian Architecture: Building with Traditional Materials* (in Farsi). Tehran: Zomorrod.

# Appendix A

## Volume flow rate values

Table A.1. Volume flow rate through wind tower aperture

| wind direction | T4 | T5 | T6 |
|---|---|---|---|
| 0 | 0.94 | 1.01 | 0.93 |
| 30 | 0.96 | 0.99 | 0.99 |
| 60 | 0.28 | 0.29 | 0.35 |
| 90 | -0.25 | -0.17 | -0.23 |
| 120 | -0.60 | -0.69 | -0.80 |
| 150 | -0.78 | -0.91 | -1.06 |
| 180 | -0.85 | -0.88 | -1.04 |

Table A.2. Volume flow rate through wind tower apertures A

| wind direction | M4 | M5 | M6 |
|---|---|---|---|
| 0 | -0.39 | -0.47 | -0.43 |
| 30 | -0.35 | -0.36 | -0.39 |
| 60 | -0.28 | -0.25 | -0.26 |
| 90 | 0.15 | 0.12 | 0.16 |
| 120 | 0.18 | 0.27 | 0.28 |
| 150 | 0.33 | 0.40 | 0.42 |
| 180 | 0.37 | 0.40 | 0.40 |

Table A.3. Volume flow rate through wind tower apertures B

| wind direction | M4 | M5 | M6 |
|---|---|---|---|
| 0 | 0.30 | 0.22 | 0.14 |
| 30 | -0.22 | -0.26 | -0.30 |
| 60 | -0.38 | -0.39 | -0.40 |
| 90 | -0.54 | -0.53 | -0.54 |
| 120 | -0.31 | -0.31 | -0.30 |
| 150 | -0.02 | -0.09 | 0.03 |
| 180 | 0.31 | 0.31 | 0.41 |

Table A.4. Volume flow rate through wind tower apertures C

| wind direction | M4 | M5 | M6 |
|---|---|---|---|
| 0 | 0.21 | 0.17 | 0.12 |
| 30 | 0.20 | 0.22 | 0.12 |
| 60 | 0.27 | 0.25 | 0.12 |
| 90 | 0.15 | 0.12 | 0.16 |
| 120 | -0.11 | -0.13 | -0.18 |
| 150 | -0.24 | -0.22 | -0.21 |
| 180 | -0.31 | -0.36 | -0.30 |

Table A.5. Volume flow rate through wind tower apertures D

| wind direction | M4 | M5 | M6 |
|---|---|---|---|
| 0 | 0.31 | 0.23 | 0.14 |
| 30 | 0.29 | 0.26 | 0.12 |
| 60 | 0.24 | 0.17 | 0.12 |
| 90 | 0.03 | 0.02 | 0.05 |
| 120 | 0.27 | 0.26 | 0.29 |
| 150 | 0.25 | 0.32 | 0.35 |
| 180 | 0.32 | 0.31 | 0.41 |

Table A.6. Volume flow rate through the window

| wind direction | M4 | M5 | M6 |
|---|---|---|---|
| 0 | -0.43 | -0.14 | 0.03 |
| 30 | 0.08 | 0.14 | 0.46 |
| 60 | 0.16 | 0.23 | 0.42 |
| 90 | 0.21 | 0.26 | 0.18 |
| 120 | -0.03 | -0.09 | -0.08 |
| 150 | -0.32 | -0.42 | -0.59 |
| 180 | -0.70 | -0.66 | -0.92 |

Table A.7. Volume flow rate through wind tower apertures A

| wind direction | M4W | M5W | M6W |
|---|---|---|---|
| 0 | -0.44 | -0.48 | -0.43 |
| 30 | -0.33 | -0.29 | -0.30 |
| 60 | -0.22 | -0.16 | -0.12 |
| 90 | 0.21 | 0.17 | 0.20 |
| 120 | 0.18 | 0.27 | 0.29 |
| 150 | 0.21 | 0.21 | 0.23 |
| 180 | 0.14 | 0.13 | 0.04 |

Table A.8. Volume flow rate through wind tower apertures B

| wind direction | M4W | M5W | M6W |
|---|---|---|---|
| 0 | 0.20 | 0.19 | 0.14 |
| 30 | -0.20 | -0.18 | -0.15 |
| 60 | -0.33 | -0.33 | -0.31 |
| 90 | -0.52 | -0.51 | -0.52 |
| 120 | -0.31 | -0.33 | -0.33 |
| 150 | -0.15 | -0.18 | -0.20 |
| 180 | 0.14 | 0.19 | 0.20 |

Table A.9. Volume flow rate through wind tower apertures C

| wind direction | M4W | M5W | M6W |
|---|---|---|---|
| 0 | 0.04 | 0.13 | 0.14 |
| 30 | 0.23 | 0.21 | 0.21 |
| 60 | 0.29 | 0.27 | 0.18 |
| 90 | 0.20 | 0.21 | 0.21 |
| 120 | -0.12 | -0.16 | -0.22 |
| 150 | -0.30 | -0.29 | -0.33 |
| 180 | -0.43 | -0.48 | -0.44 |

Table A.10. Volume flow rate through wind tower apertures D

| wind direction | M4W | M5W | M6W |
|---|---|---|---|
| 0 | 0.20 | 0.16 | 0.14 |
| 30 | 0.30 | 0.26 | 0.24 |
| 60 | 0.26 | 0.22 | 0.25 |
| 90 | 0.11 | 0.13 | 0.11 |
| 120 | 0.25 | 0.22 | 0.26 |
| 150 | 0.24 | 0.26 | 0.30 |
| 180 | 0.14 | 0.16 | 0.20 |

Table A.11. Volume flow rate through the window 2

| wind direction | W |
|---|---|
| 0 | 0.98 |
| 30 | 0.86 |
| 60 | 0.65 |
| 90 | 0.00 |
| 120 | -0.65 |
| 150 | -0.86 |
| 180 | -0.98 |

Table A.12. Volume flow rate through wind tower aperture

| wind direction | R1 | R2 | R3 |
|---|---|---|---|
| 0 | 0.89 | 0.92 | 0.94 |
| 180 | 0.80 | 0.82 | 0.86 |

# Appendix B

## Pressure coefficient values

Table B.1. Volume-weighted average pressure coefficient in the room

| wind direction | T4 | T5 | T6 |
|---|---|---|---|
| 0 | 0.24 | 0.27 | 0.26 |
| 30 | 0.11 | 0.15 | 0.20 |
| 60 | -0.23 | -0.24 | -0.31 |
| 90 | -0.53 | -0.50 | -0.50 |
| 120 | -0.15 | -0.22 | -0.32 |
| 150 | 0.13 | 0.03 | -0.05 |
| 180 | 0.27 | 0.24 | 0.14 |

Table B.2. Area-weighted average pressure coefficient on the wind tower aperture

| wind direction | T4 | T5 | T6 |
|---|---|---|---|
| 0 | 0.55 | 0.28 | 0.34 |
| 30 | 0.46 | 0.36 | 0.48 |
| 60 | 0.00 | -0.06 | -0.11 |
| 90 | -0.55 | -0.52 | -0.52 |
| 120 | -0.31 | -0.45 | -0.60 |
| 150 | -0.20 | -0.43 | -0.54 |
| 180 | -0.05 | -0.17 | -0.34 |

Table B.3. Area-weighted average pressure coefficient on the window

| wind direction | T4 | T5 | T6 |
|---|---|---|---|
| 0 | 0.03 | 0.02 | 0.02 |
| 30 | -0.12 | -0.08 | -0.08 |
| 60 | -0.25 | -0.27 | -0.34 |
| 90 | -0.51 | -0.49 | -0.49 |
| 120 | -0.08 | -0.12 | -0.18 |
| 150 | 0.24 | 0.19 | 0.13 |
| 180 | 0.38 | 0.37 | 0.31 |

Table B.4. Volume-weighted average pressure coefficient in the room

| wind direction | M4 | M5 | M6 |
|---|---|---|---|
| 0 | -0.19 | -0.13 | -0.13 |
| 30 | -0.22 | -0.21 | -0.17 |
| 60 | -0.26 | -0.27 | -0.27 |
| 90 | -0.38 | -0.35 | -0.36 |
| 120 | 0.11 | 0.08 | 0.09 |
| 150 | 0.38 | 0.34 | 0.28 |
| 180 | 0.36 | 0.37 | 0.23 |

Table B.5. Area-weighted average pressure coefficient on the wind tower aperture A

| wind direction | M4 | M5 | M6 |
|---|---|---|---|
| 0 | 0.79 | 0.48 | 0.51 |
| 30 | 0.72 | 0.59 | 0.69 |
| 60 | 0.24 | 0.14 | 0.07 |
| 90 | -0.60 | -0.52 | -0.53 |
| 120 | -0.38 | -0.60 | -0.75 |
| 150 | -0.22 | -0.49 | -0.57 |
| 180 | -0.15 | -0.29 | -0.45 |

Table B.6. Area-weighted average pressure coefficient on the wind tower aperture B

| wind direction | M4 | M5 | M6 |
|---|---|---|---|
| 0 | -0.58 | -0.39 | -0.28 |
| 30 | 0.10 | 0.29 | 0.22 |
| 60 | 0.72 | 0.46 | 0.41 |
| 90 | 0.60 | 0.45 | 0.60 |
| 120 | 0.43 | 0.48 | 0.74 |
| 150 | 0.31 | 0.35 | 0.21 |
| 180 | -0.19 | -0.37 | -0.53 |

Table B.7. Area-weighted average pressure coefficient on the wind tower aperture C

| wind direction | M4 | M5 | M6 |
|---|---|---|---|
| 0 | -0.51 | -0.34 | -0.18 |
| 30 | -0.64 | -0.56 | -0.27 |
| 60 | -0.77 | -0.66 | -0.36 |
| 90 | -0.54 | -0.50 | -0.58 |
| 120 | 0.12 | 0.18 | 0.28 |
| 150 | 0.73 | 0.63 | 0.77 |
| 180 | 0.54 | 0.53 | 0.84 |

Table B.8. Area-weighted average pressure coefficient on the wind tower aperture D

| wind direction | M4 | M5 | M6 |
|---|---|---|---|
| 0 | -0.59 | -0.38 | -0.28 |
| 30 | -0.68 | -0.72 | -0.33 |
| 60 | -0.66 | -0.54 | -0.42 |
| 90 | -0.43 | -0.37 | -0.42 |
| 120 | -0.42 | -0.51 | -0.62 |
| 150 | -0.31 | -0.65 | -0.64 |
| 180 | -0.19 | -0.37 | -0.52 |

Table B.9. Area-weighted average pressure coefficient on the window

| wind direction | M4 | M5 | M6 |
|---|---|---|---|
| 0 | -0.17 | -0.13 | -0.13 |
| 30 | -0.22 | -0.22 | -0.23 |
| 60 | -0.27 | -0.29 | -0.32 |
| 90 | -0.39 | -0.38 | -0.38 |
| 120 | 0.11 | 0.09 | 0.08 |
| 150 | 0.40 | 0.37 | 0.33 |
| 180 | 0.44 | 0.45 | 0.37 |

Table B.10. Volume-weighted average pressure coefficient in the room

| wind direction | M4W | M5W | M6W |
|---|---|---|---|
| 0 | -0.51 | -0.20 | -0.11 |
| 30 | -0.15 | 0.08 | 0.22 |
| 60 | -0.02 | 0.02 | 0.09 |
| 90 | -0.25 | -0.24 | -0.25 |
| 120 | 0.09 | 0.02 | -0.02 |
| 150 | 0.22 | 0.08 | -0.15 |
| 180 | -0.11 | -0.20 | -0.51 |

Table B.11. Area-weighted average pressure coefficient on the wind tower aperture A

| wind direction | M4W | M5W | M6W |
|---|---|---|---|
| 0 | 0.77 | 0.48 | 0.51 |
| 30 | 0.72 | 0.60 | -0.27 |
| 60 | 0.26 | 0.17 | 0.12 |
| 90 | -0.55 | -0.48 | -0.50 |
| 120 | -0.38 | -0.60 | -0.75 |
| 150 | -0.26 | -0.55 | -0.63 |
| 180 | -0.17 | -0.33 | -0.54 |

Table B.12. Area-weighted average pressure coefficient on the wind tower aperture B

| wind direction | M4W | M5W | M6W |
|---|---|---|---|
| 0 | -0.66 | -0.39 | -0.27 |
| 30 | 0.12 | 0.32 | 0.27 |
| 60 | 0.74 | 0.48 | 0.43 |
| 90 | 0.61 | 0.46 | 0.61 |
| 120 | 0.43 | 0.48 | 0.74 |
| 150 | 0.27 | 0.32 | 0.12 |
| 180 | -0.27 | -0.39 | -0.66 |

Table B.13. Area-weighted average pressure coefficient on the wind tower aperture C

| wind direction | M4W | M5W | M6W |
|---|---|---|---|
| 0 | -0.54 | -0.33 | -0.17 |
| 30 | -0.63 | -0.55 | -0.26 |
| 60 | -0.75 | -0.60 | -0.38 |
| 90 | -0.50 | -0.43 | -0.55 |
| 120 | 0.12 | 0.17 | 0.26 |
| 150 | -0.27 | 0.60 | 0.72 |
| 180 | 0.51 | 0.48 | 0.77 |

Table B.14. Area-weighted average pressure coefficient on the wind tower aperture D

| wind direction | M4W | M5W | M6W |
|---|---|---|---|
| 0 | -0.66 | -0.43 | -0.27 |
| 30 | -0.67 | -0.69 | -0.31 |
| 60 | -0.63 | -0.51 | -0.42 |
| 90 | -0.42 | -0.35 | -0.42 |
| 120 | -0.42 | -0.51 | -0.63 |
| 150 | -0.31 | -0.69 | -0.67 |
| 180 | -0.27 | -0.43 | -0.66 |

Table B.15. Volume-weighted average pressure coefficient in the room

| wind direction | W |
|---|---|
| 0 | 0.18 |
| 30 | 0.08 |
| 60 | -0.19 |
| 90 | -0.44 |
| 120 | -0.19 |
| 150 | 0.08 |
| 180 | 0.18 |

Table B.16. Area-weighted average pressure coefficient on the window A

| wind direction | W |
|---|---|
| 0 | 0.00 |
| 30 | -0.09 |
| 60 | -0.29 |
| 90 | -0.44 |
| 120 | -0.10 |
| 150 | 0.21 |
| 180 | 0.32 |

Table B.17. Area-weighted average pressure coefficient on the window B

| wind direction | W |
|---|---|
| 0 | 0.32 |
| 30 | 0.21 |
| 60 | -0.10 |
| 90 | -0.44 |
| 120 | -0.29 |
| 150 | -0.09 |
| 180 | 0.00 |

Table B.18. Volume-weighted average pressure coefficient in left side of the room

| wind direction | R1 | R2 | R3 |
|---|---|---|---|
| 0 | 0.26 | 0.29 | 0.24 |
| 180 | 0.27 | 0.28 | 0.28 |

Table B.19. Volume-weighted average pressure coefficient in right side of the room

| wind direction | R1 | R2 | R3 |
|---|---|---|---|
| 0 | 0.18 | 0.19 | 0.14 |
| 180 | 0.31 | 0.28 | 0.26 |

# Appendix C

## Velocity magnitude values

Table C.1. Volume-weighted average velocity magnitude (m/s) in the room

| wind direction | T4 | T5 | T6 |
|---|---|---|---|
| 0 | 0.29 | 0.26 | 0.13 |
| 30 | 0.31 | 0.24 | 0.14 |
| 60 | 0.10 | 0.09 | 0.09 |
| 90 | 0.07 | 0.05 | 0.07 |
| 120 | 0.18 | 0.28 | 0.29 |
| 150 | 0.31 | 0.48 | 0.44 |
| 180 | 0.21 | 0.24 | 0.29 |

Table C.2. Area-weighted average velocity magnitude (m/s) on a horizontal plane placed at a height of 1.7 m

| wind direction | T4 | T5 | T6 |
|---|---|---|---|
| 0 | 0.27 | 0.25 | 0.13 |
| 30 | 0.28 | 0.23 | 0.13 |
| 60 | 0.09 | 0.09 | 0.08 |
| 90 | 0.05 | 0.05 | 0.06 |
| 120 | 0.19 | 0.28 | 0.32 |
| 150 | 0.33 | 0.52 | 0.46 |
| 180 | 0.21 | 0.27 | 0.33 |

Table C.3. Area-weighted average velocity magnitude (m/s) on tower aperture

| wind direction | T4 | T5 | T6 |
|---|---|---|---|
| 0 | 1.27 | 1.10 | 0.99 |
| 30 | 1.54 | 1.57 | 1.41 |
| 60 | 1.86 | 1.63 | 1.56 |
| 90 | 0.34 | 0.34 | 0.31 |
| 120 | 0.91 | 0.97 | 1.05 |
| 150 | 1.22 | 1.34 | 1.34 |
| 180 | 1.26 | 1.33 | 1.40 |

Table C.4. Area-weighted average velocity magnitude (m/s) on intersecting aperture

| wind direction | T4 | T5 | T6 |
|---|---|---|---|
| 0 | 1.07 | 1.01 | 0.93 |
| 30 | 1.15 | 1.13 | 1.13 |
| 60 | 0.85 | 0.74 | 0.80 |
| 90 | 0.30 | 0.20 | 0.28 |
| 120 | 0.72 | 0.83 | 0.95 |
| 150 | 1.04 | 1.16 | 1.34 |
| 180 | 0.97 | 1.07 | 1.23 |

Table C.5. Area-weighted average velocity magnitude (m/s) on the window

| wind direction | T4 | T5 | T6 |
|---|---|---|---|
| 0 | 1.15 | 1.22 | 1.58 |
| 30 | 1.20 | 1.18 | 1.68 |
| 60 | 0.33 | 0.37 | 0.44 |
| 90 | 0.47 | 0.40 | 0.55 |
| 120 | 1.79 | 1.87 | 2.01 |
| 150 | 1.37 | 1.45 | 1.58 |
| 180 | 0.88 | 0.91 | 1.10 |

Table C.6. Volume-weighted average velocity magnitude (m/s) in the room

| wind direction | M4 | M5 | M6 |
|---|---|---|---|
| 0 | 0.14 | 0.17 | 0.17 |
| 30 | 0.14 | 0.21 | 0.21 |
| 60 | 0.19 | 0.22 | 0.20 |
| 90 | 0.25 | 0.22 | 0.22 |
| 120 | 0.12 | 0.12 | 0.13 |
| 150 | 0.10 | 0.15 | 0.21 |
| 180 | 0.16 | 0.18 | 0.25 |

Table C.7 Area-weighted average velocity magnitude (m/s) on a horizontal plane placed at a height of 1.7 m

| wind direction | M4 | M5 | M6 |
|---|---|---|---|
| 0 | 0.13 | 0.16 | 0.16 |
| 30 | 0.12 | 0.20 | 0.20 |
| 60 | 0.17 | 0.19 | 0.19 |
| 90 | 0.23 | 0.20 | 0.21 |
| 120 | 0.11 | 0.13 | 0.13 |
| 150 | 0.10 | 0.16 | 0.21 |
| 180 | 0.16 | 0.21 | 0.28 |

Table C.8. Area-weighted average velocity magnitude (m/s) on tower aperture A

| wind direction | M4 | M5 | M6 |
|---|---|---|---|
| 0 | 0.68 | 0.89 | 0.71 |
| 30 | 1.11 | 1.24 | 1.07 |
| 60 | 1.83 | 1.49 | 1.37 |
| 90 | 0.59 | 0.32 | 0.53 |
| 120 | 0.79 | 0.92 | 0.97 |
| 150 | 1.20 | 1.29 | 1.29 |
| 180 | 1.31 | 1.28 | 1.22 |

Table C.9. Area-weighted average velocity magnitude (m/s) on tower aperture B

| wind direction | M4 | M5 | M6 |
|---|---|---|---|
| 0 | 0.75 | 0.40 | 0.27 |
| 30 | 1.76 | 1.65 | 1.64 |
| 60 | 1.21 | 1.20 | 1.14 |
| 90 | 0.92 | 0.98 | 0.91 |
| 120 | 1.09 | 1.14 | 1.17 |
| 150 | 1.40 | 1.56 | 1.53 |
| 180 | 0.67 | 0.61 | 0.92 |

Table C.10. Area-weighted average velocity magnitude (m/s) on tower aperture C

| wind direction | M4 | M5 | M6 |
|---|---|---|---|
| 0 | 0.64 | 0.43 | 0.39 |
| 30 | 0.79 | 0.72 | 0.40 |
| 60 | 0.81 | 0.73 | 0.55 |
| 90 | 0.54 | 0.46 | 0.59 |
| 120 | 1.29 | 1.41 | 1.77 |
| 150 | 0.99 | 1.16 | 1.06 |
| 180 | 0.64 | 0.82 | 0.61 |

Table C.11. Area-weighted average velocity magnitude (m/s) on tower aperture D

| wind direction | M4 | M5 | M6 |
|---|---|---|---|
| 0 | 0.63 | 0.52 | 0.27 |
| 30 | 0.86 | 0.70 | 0.41 |
| 60 | 0.78 | 0.65 | 0.51 |
| 90 | 0.27 | 0.27 | 0.27 |
| 120 | 0.89 | 0.87 | 1.02 |
| 150 | 0.91 | 1.21 | 1.21 |
| 180 | 0.67 | 0.61 | 0.91 |

Table C.12. Area-weighted average velocity magnitude (m/s) on intersecting aperture A

| wind direction | M4 | M5 | M6 |
|---|---|---|---|
| 0 | 1.59 | 1.88 | 1.72 |
| 30 | 1.55 | 1.62 | 1.64 |
| 60 | 1.24 | 1.15 | 1.12 |
| 90 | 0.92 | 0.90 | 0.88 |
| 120 | 1.11 | 1.66 | 1.67 |
| 150 | 1.60 | 1.89 | 2.00 |
| 180 | 1.53 | 1.68 | 1.71 |

Table C.13. Area-weighted average velocity magnitude (m/s) on intersecting aperture B

| wind direction | M4 | M5 | M6 |
|---|---|---|---|
| 0 | 1.44 | 1.11 | 0.85 |
| 30 | 0.92 | 1.24 | 1.25 |
| 60 | 1.70 | 1.67 | 1.67 |
| 90 | 2.16 | 2.11 | 2.14 |
| 120 | 1.31 | 1.36 | 1.43 |
| 150 | 0.45 | 0.51 | 0.60 |
| 180 | 1.60 | 1.68 | 1.98 |

Table C.14. Area-weighted average velocity magnitude (m/s) on intersecting aperture C

| wind direction | M4 | M5 | M6 |
|---|---|---|---|
| 0 | 1.20 | 0.95 | 0.52 |
| 30 | 1.20 | 1.21 | 0.63 |
| 60 | 1.47 | 1.30 | 0.65 |
| 90 | 0.85 | 0.70 | 0.94 |
| 120 | 0.57 | 0.68 | 0.82 |
| 150 | 1.11 | 1.06 | 1.05 |
| 180 | 1.27 | 1.49 | 1.27 |

Table C.15. Area-weighted average velocity magnitude (m/s) on intersecting aperture D

| wind direction | M4 | M5 | M6 |
|---|---|---|---|
| 0 | 1.50 | 1.12 | 0.85 |
| 30 | 1.47 | 1.42 | 0.82 |
| 60 | 1.29 | 1.06 | 0.85 |
| 90 | 0.58 | 0.47 | 0.61 |
| 120 | 1.42 | 1.43 | 1.48 |
| 150 | 1.46 | 1.69 | 1.70 |
| 180 | 1.62 | 1.68 | 1.98 |

Table C.16. Area-weighted average velocity magnitude (m/s) on the window

| wind direction | M4 | M5 | M6 |
|---|---|---|---|
| 0 | 0.55 | 0.32 | 0.07 |
| 30 | 0.12 | 0.29 | 0.75 |
| 60 | 0.32 | 0.31 | 0.92 |
| 90 | 0.34 | 0.34 | 0.80 |
| 120 | 1.21 | 1.39 | 1.44 |
| 150 | 1.06 | 1.10 | 1.22 |
| 180 | 0.71 | 0.67 | 0.97 |

Table C.17. Volume-weighted average velocity magnitude (m/s) in the room

| wind direction | M4w | M5w | M6w |
|---|---|---|---|
| 0 | 0.20 | 0.19 | 0.18 |
| 30 | 0.13 | 0.12 | 0.16 |
| 60 | 0.14 | 0.12 | 0.16 |
| 90 | 0.20 | 0.20 | 0.20 |
| 120 | 0.16 | 0.12 | 0.14 |
| 150 | 0.16 | 0.12 | 0.13 |
| 180 | 0.18 | 0.19 | 0.20 |

Table C.18. Area-weighted average velocity magnitude (m/s) on a horizontal plane placed at a height of 1.7 m

| wind direction | M4W | M5W | M6W |
|---|---|---|---|
| 0 | 0.19 | 0.17 | 0.16 |
| 30 | 0.12 | 0.12 | 0.15 |
| 60 | 0.13 | 0.10 | 0.14 |
| 90 | 0.18 | 0.18 | 0.18 |
| 120 | 0.14 | 0.10 | 0.13 |
| 150 | 0.15 | 0.12 | 0.12 |
| 180 | 0.16 | 0.17 | 0.19 |

Table C.19. Volume-weighted average velocity magnitude (m/s) in the room

| wind direction | W |
|---|---|
| 0 | 0.24 |
| 30 | 0.28 |
| 60 | 0.20 |
| 90 | 0.05 |
| 120 | 0.20 |
| 150 | 0.28 |
| 180 | 0.24 |

Table C.20. Area-weighted average velocity magnitude (m/s) on a horizontal plane placed at a height of 1.7 m

| wind direction | W |
|---|---|
| 0 | 0.28 |
| 30 | 0.32 |
| 60 | 0.23 |
| 90 | 0.04 |
| 120 | 0.23 |
| 150 | 0.32 |
| 180 | 0.28 |

Table C.21. Volume-weighted average velocity magnitude (m/s) in left side of the room

| wind direction | R1 | R2 | R3 |
|---|---|---|---|
| 0 | 0.56 | 0.39 | 0.33 |
| 180 | 0.26 | 0.24 | 0.17 |

Table C.22. Volume-weighted average velocity magnitude (m/s) in right side of the room

| wind direction | R1 | R2 | R3 |
|---|---|---|---|
| 0 | 0.23 | 0.25 | 0.29 |
| 180 | 0.21 | 0.27 | 0.21 |

Table C.23. Area-weighted average velocity magnitude (m/s) in left side of the room on a horizontal plane placed at a height of 1.7 m

| wind direction | R1 | R2 | R3 |
|---|---|---|---|
| 0 | 0.52 | 0.37 | 0.29 |
| 180 | 0.25 | 0.23 | 0.14 |

Table C.24. Area-weighted average velocity magnitude (m/s) in right side of the room on a horizontal plane placed at a height of 1.7 m

| wind direction | R1 | R2 | R3 |
|---|---|---|---|
| 0 | 0.14 | 0.22 | 0.28 |
| 180 | 0.24 | 0.32 | 0.29 |

# Appendix D

## Mean age of air values

Table D.1. Volume-weighted average mean age of air in the room

| wind direction | T4 | T5 | T6 |
|---|---|---|---|
| 0 | 107.39 | 100.95 | 377.83 |
| 30 | 109.14 | 102.42 | 349.45 |
| 60 | 372.57 | 349.42 | 547.79 |
| 90 | 417.97 | 522.74 | 440.29 |
| 120 | 210.12 | 144.76 | 126.14 |
| 150 | 161.22 | 107.07 | 109.67 |
| 180 | 160.15 | 122.73 | 94.84 |

Table D.2. Area-weighted average mean age of air on a horizontal plane placed at a height of 1.7 m

| wind direction | T4 | T5 | T6 |
|---|---|---|---|
| 0 | 119.27 | 107.71 | 408.03 |
| 30 | 121.39 | 110.64 | 372.64 |
| 60 | 396.02 | 366.79 | 584.01 |
| 90 | 463.13 | 562.62 | 476.47 |
| 120 | 213.06 | 153.49 | 127.79 |
| 150 | 167.19 | 106.20 | 108.85 |
| 180 | 152.15 | 115.80 | 87.62 |

Table D.3. Maximum value of mean age of air in the room

| wind direction | T4 | T5 | T6 |
|---|---|---|---|
| 0 | 152.10 | 137.87 | 477.35 |
| 30 | 176.12 | 149.65 | 488.15 |
| 60 | 475.82 | 458.91 | 875.98 |
| 90 | 765.65 | 952.44 | 806.54 |
| 120 | 362.03 | 182.51 | 210.49 |
| 150 | 264.87 | 144.01 | 227.49 |
| 180 | 244.77 | 198.02 | 139.34 |

Table D.4. Volume-weighted average mean age of air in the room

| wind direction | M4 | M5 | M6 |
|---|---|---|---|
| 0 | 395.29 | 246.84 | 313.09 |
| 30 | 299.94 | 199.91 | 213.68 |
| 60 | 202.05 | 195.90 | 252.50 |
| 90 | 237.19 | 205.89 | 293.12 |
| 120 | 374.04 | 339.35 | 300.44 |
| 150 | 319.87 | 243.82 | 171.96 |
| 180 | 188.39 | 155.66 | 102.83 |

Table D.5. Area-weighted average mean age of air on a horizontal plane placed at a height of 1.7 m

| wind direction | M4 | M5 | M6 |
|---|---|---|---|
| 0 | 409.13 | 254.06 | 334.22 |
| 30 | 314.36 | 207.34 | 229.41 |
| 60 | 216.79 | 205.81 | 267.78 |
| 90 | 251.72 | 212.96 | 310.17 |
| 120 | 387.38 | 337.98 | 303.11 |
| 150 | 327.97 | 254.73 | 182.70 |
| 180 | 179.49 | 144.93 | 96.45 |

Table D.6. Maximum value of mean age of air in the room

| wind direction | M4 | M5 | M6 |
|---|---|---|---|
| 0 | 568.36 | 300.22 | 387.98 |
| 30 | 442.76 | 258.87 | 296.50 |
| 60 | 281.15 | 293.14 | 328.50 |
| 90 | 294.73 | 280.89 | 353.13 |
| 120 | 517.04 | 460.76 | 422.74 |
| 150 | 478.54 | 318.85 | 267.59 |
| 180 | 287.39 | 233.22 | 183.56 |

Table D.7. Volume-weighted average mean age of air in the room

| wind direction | M4W | M5W | M6W |
|---|---|---|---|
| 0 | 288.53 | 249.12 | 312.89 |
| 30 | 357.18 | 468.10 | 460.22 |
| 60 | 371.50 | 437.90 | 528.07 |
| 90 | 277.22 | 240.04 | 277.22 |
| 120 | 528.07 | 437.90 | 371.50 |
| 150 | 460.22 | 468.10 | 357.18 |
| 180 | 312.89 | 249.12 | 288.53 |

Table D.8. Area-weighted average mean age of air on a horizontal plane placed at a height of 1.7 m

| wind direction | M4W | M5W | M6W |
|---|---|---|---|
| 0 | 303.20 | 257.20 | 334.17 |
| 30 | 372.61 | 465.64 | 480.46 |
| 60 | 372.89 | 455.36 | 548.44 |
| 90 | 289.16 | 250.15 | 289.16 |
| 120 | 548.44 | 455.36 | 372.89 |
| 150 | 480.46 | 465.64 | 372.61 |
| 180 | 334.17 | 257.20 | 303.20 |

Table D.9. Maximum value of mean age of air in the room

| wind direction | M4W | M5W | M6W |
|---|---|---|---|
| 0 | 344.34 | 318.98 | 387.12 |
| 30 | 552.22 | 630.71 | 675.71 |
| 60 | 618.39 | 552.7 | 761.14 |
| 90 | 367.20 | 309.33 | 367.2 |
| 120 | 761.14 | 552.70 | 618.39 |
| 150 | 675.71 | 630.71 | 552.22 |
| 180 | 387.12 | 318.98 | 344.34 |

Table D.10. Volume-weighted average mean age of air in the room

| wind direction | W |
|---|---|
| 0 | 147.86 |
| 30 | 168.41 |
| 60 | 200.94 |
| 90 | 2198.26 |
| 120 | 200.94 |
| 150 | 168.41 |
| 180 | 147.86 |

Table D.11. Area-weighted average mean age of air on a horizontal plane placed at a height of 1.7 m

| wind direction | W |
|---|---|
| 0 | 137.90 |
| 30 | 174.08 |
| 60 | 202.45 |
| 90 | 2204.36 |
| 120 | 202.45 |
| 150 | 174.08 |
| 180 | 137.90 |

Table D.12. Maximum value of mean age of air in the room

| wind direction | W |
|---|---|
| W 00 | 244.14 |
| W 30 | 249.67 |
| W 60 | 306.27 |
| W 90 | 3216.22 |
| W 120 | 306.27 |
| W 150 | 249.67 |
| W 180 | 244.14 |

Table D.13. Volume-weighted average mean age of air in left side of the room

| wind direction | R1 | R2 | R3 |
|---|---|---|---|
| 0 | 43.96 | 60.71 | 80.84 |
| 180 | 143.62 | 136.55 | 149.13 |

Table D.14. Volume-weighted average mean age of air in right side of the room

| wind direction | R1 | R2 | R3 |
|---|---|---|---|
| 0 | 149.31 | 138.54 | 132.43 |
| 180 | 121.13 | 117.28 | 87.51 |

Table D.15. Area-weighted average mean age of air in left side of the room on a horizontal plane placed at a height of 1.7 m

| wind direction | R1 | R2 | R3 |
|---|---|---|---|
| 0 | 55.12 | 68.24 | 89.84 |
| 180 | 141.23 | 144.29 | 164.88 |

Table D.15. Area-weighted average mean age of air in left side of the room on a horizontal plane placed at a height of 1.7 m

| wind direction | R1 | R2 | R3 |
|---|---|---|---|
| 0 | 165.15 | 150.23 | 135.73 |
| 180 | 113.54 | 106.41 | 84.64 |

Table D.16. Maximum value of mean age of air in the room

| wind direction | R1 | R2 | R3 |
|---|---|---|---|
| 0 | 202.53 | 204.08 | 184.37 |
| 180 | 236.67 | 181.68 | 291.15 |